INDIAN GEOPHYSICAL UNION

51st Annual Convention on

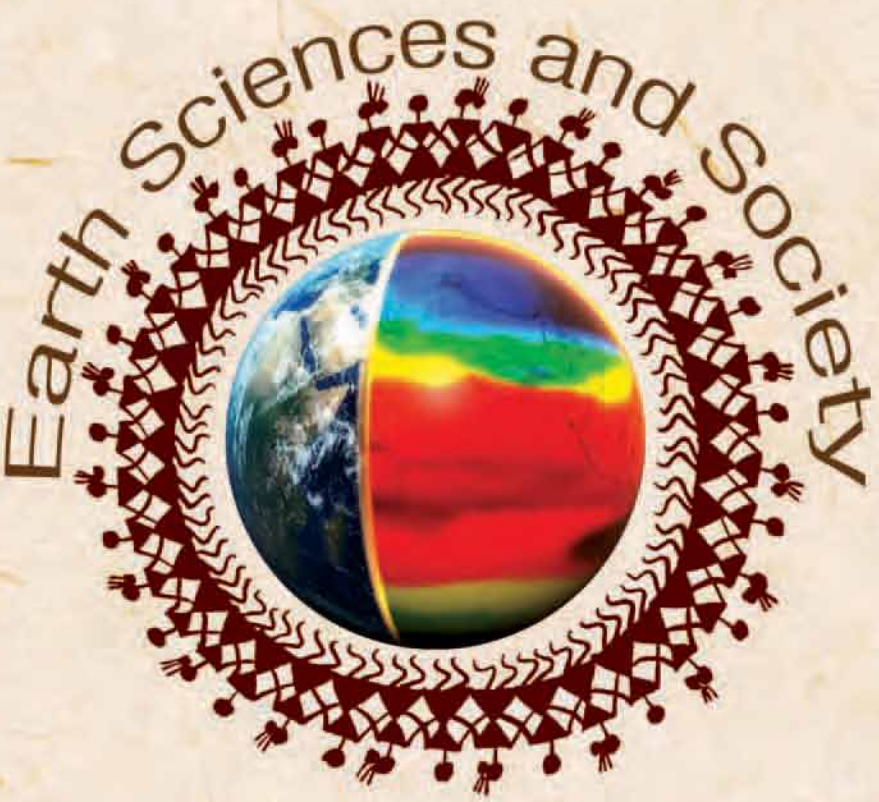

19-21 November 2014

Kurukshetra University,
Kurukshetra - 136119, Haryana, India

Organized Jointly By
Indian Geophysical Union
&
Department of Geophysics, Kurukshetra University

INCOIS Indian National Centre for Ocean Information Services

INCreasing the utility of the Ocean Information Spectrum

An Autonomous Society under the Earth System Sciences Organisation, the Ministry of Earth Sciences, Govt. of India, ESSO-INCOIS strives to fulfill its mission to provide ocean information and advisory services to society, industry, government and the scientific community through sustained ocean observations and constant improvements through systematic and focused research.

Key Activities

Early Warnings for Tsunamis and Storm Surges

Potential Fishing Zone Advisories for Fishermen

Ocean State Forecasts for Fishermen,
the Navy, the Coast Guard and Offshore Industries.

National and Regional Oceanographic Data Centre

Satellite Coastal and Oceanographic Research

Coastal Geospatial Applications

Ocean Modelling Studies

Ocean Observing System
(Member of the Indian Ocean Global Ocean Observing System)

Web-based Ocean Data, Information and Advisory Services

International Training Centre for Operational Oceanography

Public Outreach, User Interaction Workshops

Riding the Wave of Change ....

Indian National Centre for Ocean Information Services
(Earth System Sciences Organisation, Ministry of Earth Sciences)
Ocean Valley, Pragathi Nagar (BO), Nizampet (SO), Hyderabad - 500 090
Phone: 91-(0)40-23895000/23886000, Fax: 91-(0)40-23895001 | email: director@incois.gov.in,
URL: http://www.incois.gov.in

ABSTRACTS

51st Annual Convention

"Earth Sciences and Society"

19-21 November-2014

Venue:

Senate Auditorium, Kurukshetra University
Kurukshetra, Haryana, India

Sponsored by

Indian National Centre for Ocean Information Services (MoES-INCOIS)
National Centre for Antarctic and Ocean Research (MoES-NCAOR)
Oil and Natural Gas Corporation Limited (ONGC)
Indian Institute of Geomagnetism (IIG)
National Geophysical Research Institute (CSIR-NGRI)
CSIR- National Institute of Oceanography (CSIR-NIO)
National Remote Sensing Centre (NRSC)
Electrotek International Inc.-DMT
Aimil Ltd.
CGG
Nuclear Power Corporation of India Limited (NPCIL)
National Environmental Engineering Research Institute (CSIR-NEERI)

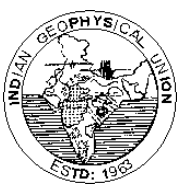

INDIAN GEOPHYSICAL UNION
HYDERABAD

November, 2014

Edited by

Kalachand Sain &
ASSSRS Prasad

Price: Rs. 150/-

For Copies

Write to:

Hon. Secretary
Indian Geophysical Union
NGRI Campus, Uppal Road
Hyderabad - 500 007
India

Printed by:

artworks
1-1-316/6, Chikkadpally,
Hyderabad - 500 020 India
Tel : (O) 27630690
email: myartworks@gmail.com

PREFACE

The Indian Geophysical Union has started in 1963 with the blessings of luminaries: Prof K.R. Ramanathan, Prof. S. Bhagavantham, Prof. M.S. Krishnan and Dr. S. Balakrishna continue to serve the Earth System scientists of India. Many scientists provided significant inputs to sustain its progress. We salute them for their contribution and support.The new executive committee has taken the job to conduct the Indian Geophysical Union works. We have been trying to enhance the visibility of the organization from April, 2014 onwards. Various developments have helped us to take appropriate steps for better output. We are fully aware that we can achieve better results only with the support of all those associated with IGU. The main objective of IGU is motivating young researchers in enhancing their research capabilities. The senior scientists are hereby requested by IGU to provide guidance to the young researchers, making use of their vast experience. The 51st annual convention of IGU is being held at Kurukshetra University, Kurukshetra, as in the past, is planned to provide a proper forum for presentation of latest works in various disciplines in earth system sciences. The disciplines cover Solid earth Geosciences, Marine Geosciences and Atmospheric, Space and Planetary Sciences. For this tear the special theme is "Earth Sciences and Society". This special theme assumes importance as we need to strengthen our society.

All the basic need soft the society-air, water, food, energy, shelter–are directly related to the optimal use of natural resources and knowledge of Earth system dynamics. The Earth and its inhabitants face different types of challenges today: development of new sources of energy; exploration of new sources of minerals and metals;change in climate; detail knowledge of surface and sub-surface water resources; preventive measures to face natural hazards such as the earthquakes, tsunamis, landslides, cyclones, floods, droughts, avalanches and volcanic activity etc. The deep understanding of different branches of Earth Science can help us in taking up apt measures to resolve many of these issues.

To encourage scientific measures in addressing various policy requirements, IGU wishes to closely associate for initiating developmental activities in several academic centers. It encourages the positive initiatives through close interaction of students/young researchers and senior scientists. Such a measure, being practiced by

IGU in the last 50 years, has yielded excellent results. Presently, to ensure a viable strategy to help the society in ensuring better quality of life, IGU has taken up the initiative to jointly organise its 51st annual convention at Kurukshetra University, which is known for its excellence in Earth Science education.

During the 51st Annual Convention, IGU would provide a platform to address the societal problems and guide the Indian Geo-scientific community to focus on the most relevant problems and respond effectively to the risks and challenges of presently witnessed global change that is directly affecting our society.

Besides the award lectures and invited talks, more than 145 papers are expected to be present during the three day convention. We have included 70 of them under poster session. This would help in better interaction between senior scientists and young researchers and students.

On behalf of IGU, I request the delegates to send full papers of their presentations, for publishing the same in the Journal of IGU, after proper reviewing process. I place on record the support extended by Dr. O.P. Mishra and Prof. RBS Yadav have motivated young researchers to participate and present their research work in the annual convention.

The three day convention is jointly organized by IGU, Kurukshetra University. The convention is co-sponsored by Indian National Centre for Ocean Information Services (MoES-INCOIS), National Centre for Antarctic and Ocean Research (MoES-NCAOR), Oil and Natural Gas Corporation Limited (ONGC), Indian Institute of Geomagnetism (IIG), CSIR- National Institute of Oceanography (CSIR-NIO), National Remote Sensing Centre (NRSC), Electrotek International Inc.- DMT, CGG, Nuclear Power Corporation of India Limited (NPCIL), National Environmental Engineering Research Institute (CSIR-NEERI) and National Geophysical Research Institute (CSIR-NGRI).

The IGU is thankful to all the co-organizers and sponsors for their support. We thank various organizations for accepting to participate in the exhibition. In addition to Krishnan Medal, Dr. H.N. Siddiquie Memorial Lecture, Prof. K.R.Ramanathan Memorial Lecture, IGU-ONGC Awards for the best poster presentation by PG Students & Research Scholars, Prof.Jagdeo Singh and Dr.S. Balakrishna Memorial grant for student's participation in the annual convention.

IGU - Harinarain Lifetime Achievement award in Geosciences and Prof. D. Lal best paper award, papers published in The Journal of Indian Geophysical Union four issues during 2014.

I place on record our Thanks to the Local Organizing Committee and Prof. Dinesh Kumar (LOC-Chairman) for their committed involvement and help in organizing the 51st Annual Convention. This hopefully, would ensure uninterrupted conduction of various technical sessions and better presence of delegates during the Award talks. We are organizing a special young research program session on first day afternoon for enhancing scientific capabilities of research scholars.

The Executive Committee of IGU is indebted to Prof. Shailesh Nayak, President of IGU, Prof. Harsh Gupta, Patron of IGU, Prof. V.P. Dimri, Former President-IGU, Lt. Gen. (Dr.) D.D.S. Sandhu, Vice-Chancellor, Kurukshetra University, Dr. Y.J. BhaskarRao, Dr. Sateesh C Shenoi, Dr. S.W.A. Neqvi, Dr. V.K. Dhahwal, the Vice- Presidents of IGU and Dr. P.R. Reddy for his unequivocal support and guidance. IGU is indebted to LOC-Kurukshetra University, Fellows and Members of IGU and Members of the Executive Committee for their continued support. We also thank the chair persons for technical sessions for accepting to conduct various sessions, as per suggested schedule. Finally, I wish to thank IGU office personals for their continued support in executing various works prior to and during the three day convention.

Kalachand Sain

CONTENTS

SESSION-I: "ATMOSPHERIC, SPACE AND PLANETARY SCIENCES"

SESSISON-II: "YOUNG RESEARCHERS PROGRAM"

POSTERS (YOUNG RESEARCHERS PROGRAM)

POSTERS (MARINEGEOSCIENCES)

POSTERS (SOLID EARTH GEOSCIENCES)

SESSION – I

ATMOSPHERIC, SPACE AND PLANETARY SCIENCES

AEROSOL GASEOUS INTERACTIONS: A CASE STUDY IN TRANS-YAMUNA AREA OF DELHI

Anshu Sharma*, Saumya Singh and U.C Kulshrestha
School of Environmental Sciences, Jawaharlal Nehru University, New Delhi 110067 INDIA
**sweetanshu28@gmail.com, umeshkulshestha@gmail.com*

INTRODUCTION

Air pollution is a major problem of most of the megacities due to continuously increasing traffic density and industrial activities. SO_2, NO_2 and particulate matter are the major pollutants contributed by the growing industries and vehicles. Dustfall deposition is an effective sink for acidic gaseous pollutants present in atmosphere (Singh et al., 2014, Kulshrestha et al., 2003). The reaction of alkaline $CaCO_3$ with H_2SO_4 and HNO_3 acids produces $CaSO_4$ and $Ca(NO_3)_2$.). The high values of pH of dustfall deposition, suggest the dominance of crustal components that add to alkalinity due to presence of carbonates and bicarbonates of Ca (Kulshrestha et al., 2003; Khemani, 1998, Kumar et al., 2014). The interaction of acidic gases with alkaline dust needs to be studied in order to understand the oxidation of these gases and their secondary products.

METHODOLOGY

The study was carried out at an urban residential site, Babarpur locality in Trans-Yamuna area of Delhi (28.68′N and 77.28′E) near Shahdara Industrial Area of North East Delhi (Fig.1). The sampling was carried out at the top floor of the building (about 10 meters from the ground surface). Gaseous (NO_2 and SO_2) samples were collected through the handy sampler (Envirotech, APM 821) at a flow rate of 1 LPM. A simple manual method was used to collect the dustfall samples in which a tray was exposed to the dustfall for a period of 6 days. The period of sample collection for both gaseous and dustfall was during October 2013-Feburary, 2014. Gaseous samples of NO_2 and SO_2 were analyzed by spectrophotometer and Ion chromatography respectively. The dust samples were analyzed using scanning electron microscope (SEM) and X-ray (EDX) for element analysis.

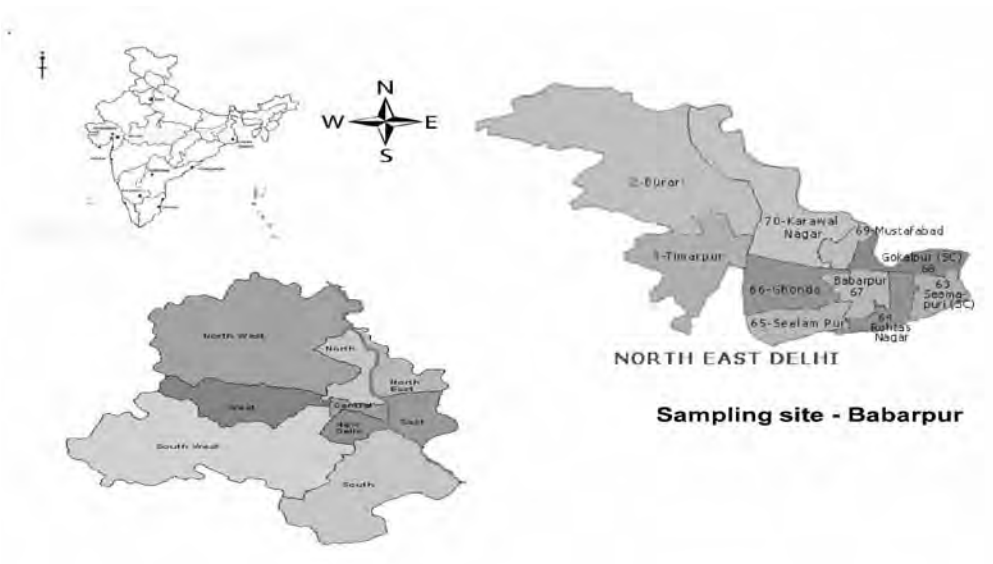

Fig. 1. Sampling site, Babarpur, Delhi.

RESULTS & DISCUSSIONS

The average concentrations of SO_2 and NO_2 were observed to be 18 $\mu g/m^3$ and 19 $\mu g/m^3$ respectively. Results showed that both SO_2 and NO_2 levels were found to be within permissible limit as defined by CPCB. The average pH of aqueous extracts was found to be 7.7 suggesting the alkaline nature of dust in Trans-Yamuna area which is similar to any other part of North India. Dust particles showed their predominance in size range more than 10 μm. Dust was found to be dominated by oxides of silicon, calcium, carbon, iron, aluminum, potassium, zinc, copper and sulfur. Such contribution indicates that dust is a mixture of natural as well as anthropogenic emissions. Presence of metals such as zinc and copper indicates the industrial contribution while presence of sulfur indicates the influence of diesel combustion. Presence of aluminum, silicon, calcium, iron, and potassium suggested the dominance of crustal sources. SEM results showed that dust particles had various shapes such as spherical, rectangular, platy and angular corroborating their origin from multiple sources. (Fig.2).

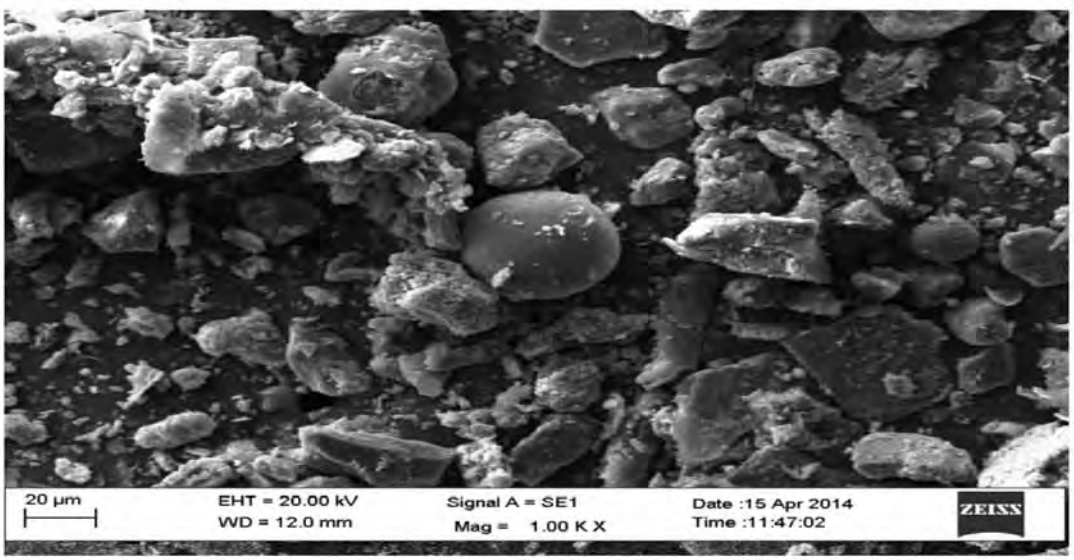

Fig.2. SEM images of dust particles

References

Khemani, L.T., 1998. Atmospheric aerosols and acidification of precipitation. In: Parashar, D.C., Sharma, C., Mitra, A.P. (Eds.), Global Environment Chemistry. Narosa Publishing House, New Delhi, pp. 251.

Kulshrestha, U. C., Kulshrestha, M. J., Sekar, R., Sastry, G. S. R. and Vairamani, M., 2003. Chemical characteristics of rainwater at an urban site of south-central India, Atmos. Environ., 37(21).

Kulshrestha, M.J., Kulshrestha, U.C., Parashar, D.C., Vairamani, M. (2003). "Estimation of SO4 contribution by dry deposition of SO_2 onto the dust particles in India". Atmospheric Environment 37, 3057–3063.

Kumar, B., Verma, K., and Kulshrestha, U. C., 2014. Deposition and mineralogical characteristics of atmospheric dust in relation to land use and land cover change in Delhi (India), Geography Journal.,2014,1-11.

Singh, S., Gupta, G. P., Kumar, B. and Kulshrestha, U. C.:, 2014. Comparative study of indoor air pollution using traditional and improved cooking stoves in rural households of Northern India, Energy Sustain. Dev., 19, 1–6.

MODIFIED CHEMICAL CHARACTERISTICS OF DUST AEROSOLS DUE TO URBAN ANTHROPOGENIC EMISSION IN DELHI

Kopal Verma*, Bablu Kumar and Umesh Kulshrestha
School of Environmental Sciences, Jawaharlal Nehru University, New Delhi 110067 India
**kopal38@gmail.com, umeshkulshestha@gmail.com*

INTRODUCTION

Dust aerosols play a very important role in determining their impacts on clouds, climate and health. The morphology, size, number and chemical composition of atmospheric aerosols are very specific to their sources, geographical area, season, transport, transformations, etc. These characteristics have their significant importance at local and regional scales (Khemani, 1989; Dentener et al., 2006; Kulshrestha et al, 2003). Soil-derived dust is abundant in the atmosphere in Indian region (Kulshrestha et al, 2009). Atmospheric dust has a complex mineralogical and chemical composition.Various atmospheric species react on the surface of dust particles and such reactions could cause modifications in the properties of dust. Hence, it becomes essential to find out the sources, composition, and content of dustfall as it can cause risk to human health, various ecosystem and atmospheric environment. Elements present in the dust can influence biogeochemistry of terrestrial and aquatic systems, vegetation, and rate and timing of snowmelt. Despite evidence of the ecological importance, the studies on chemical and morphological characterization of dust and soils are not extensively carried out in Indian region. Hence, the present study was carried out to highlight the modified properties of the soil-derived dust due to urbanization.

METHODOLOGY

The study was carried out in South Delhi inside the campus of Jawaharlal Nehru University (28°N 77°E)(Fig. 1). A simple manual method was used to collect dustfall samples in which a tray was exposed to the dustfall for a period of 3-5 days. The deposited dust was collected and weighed; hence the dustfall fluxes was calculated using the formula D=M/(AxT); where D is the dustfall flux, M is the mass of the dustfall collected, A is the area of the tray and T is the time period for which the dust was collected (Katz et al, 1969).

Mineralogy of the bulk samples of soil and dust was studied using a X-Ray Diffractometer (XRD) and their surface morphology was analyzed with the help of a Scanning Electron Microscope (SEM). Electron Dispersive X-Ray Spectroscopy (EDX) attached with the SEM instrument was used for the elemental analysis of the dust and soil samples.

RESULTSAND DISCUSSION

Results showed that the average pH (7.66) of aqueous extract of dust samples was very high typically representing the alkaline nature of atmospheric dust of this region. High pH at this site might be due to soil-derived particulate matter which is found to be rich in $CaCO_3$ content. Suspension of soil-dust, road dust and construction activities can contribute to high deposition fluxes of dustfall. In this study, average deposition flux was calculated as 35 g per m^2 per year which is relatively higher as compared to temperate regions. Such higher fluxes can be attributed to crustal sources. SEM analysis showed that the dust and soil particles were spherical, irregular, porous, long and prismatic, crystalline and rhombic twining in shape etc. Quartz, muscovite, and chlorite were identified as major minerals in soil and dust samples. EDX results showed that the dust samples had higher carbon concentration and calcium as compared to soils. This is probably due to the significant influence of urban sources such as industries, vehicular traffic and construction activities, etc. The study suggested that the

anthropogenic emissions significantly affect suspended soil modifying its chemical properties which might have significant importance for air quality and radiative forcing calculation.

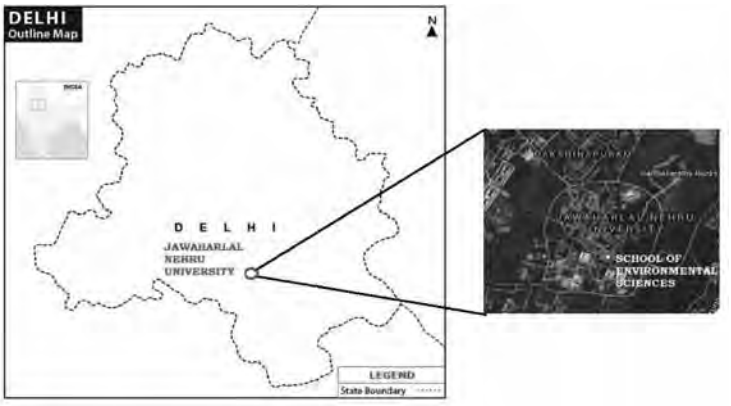

Fig 1: Sampling Site, Jawaharlal Nehru University, New Delhi.

REFERENCES

Dentener F, J. Drevet, J.-F.Lamarque, I. Bey, B. Eickhout, A.M. Fiore, D. Hauglustaine, L.W. Horowitz, M. Krol, U.C. Kulshrestha, M. Lawrence, et al. (2006). Nitrogen and sulphur deposition on regional and global scales: a multimodel evaluation. 2006. Global Biogeochemical Cycles, Vol 20, GB4003, doi:10.1029/2005GB002672.

Katz, M. (1969). "Measurement of Air Pollutants - Guide to Selection of Methods, World Health Organization, Geneva, Switzerland"

Khemani L.T. (1989). "Physical and chemical characteristics of atmospheric aerosols".Air Pollution Control. Vol. 2, Encyclopedia of Environmental Control Technology, Gulf Publ. Co., USA, p. 401 – 452.

Kulshrestha, M.J., Kulshrestha, U.C., Parashar, D.C., Vairamani, M. (2003)."Estimation of SO4 contribution by dry deposition of SO_2 onto the dust particles in India".Atmospheric Environment 37, 3057–3063.

Kulshrestha, U.C., Reddy, L.A.K., Satyanarayana, J. and Kulshrestha, M.J. (2009). "Real-time wet scavenging of major chemical constituents of aerosols and role of rain intensity in Indian region". Atmospheric Environment, 43, 5123-5127.

CHARACTERISTICS OF IONOSPHERIC SCINTILLATION AND ITS RELATION TO POST SUNSET HEIGHT RISE USING CADI IONOSONDE AT TIRUNELVELI

S. Banola, R.N.Maurya and S. Sripathi

Indian Institute of Geomagnetism, Navi Mumbai-410218, INDIA

sbanola@iigs.iigm.res.in

Plasma density irregularities in the ionosphere (associated with ESF, plasma bubbles and Sporadic E layers) cause scintillations in various frequency ranges. VHF radio wave scintillation technique is extensively used to study plasma density irregularities of sub-kilometre size. Indian Institute of Geomagnetism operated a ground network of 13 stations monitoring amplitude scintillations on 244/251 MHz (FLEETSAT 73°E) signals in India for more than a decade under AICPITS. At present VHF scintillation is being recorded at Mumbai by monitoring 251 MHz signal transmitted by geostationary satellite UFO2 (71.2° E).Statistical analysis is performed on VHF scintillations at Mumbai andionosonde observations of post sunset height rise over Tirunelveli, an equatorial station to understand their relationship to each other during ascending phase of solar cycle 24 (year 2011-12).The observations suggest that occurrence of scintillation at Mumbai and h'Fdata of ionosondeare correlated well only when the virtual height of h'F over equator reaches above 300 Km which seems to be necessarycondition to cause VHF Scintillationsat Mumbai. Occurrence of VHF scintillations at

Mumbai is lower as compared to equatorial spread F occurrence at Tirunelveli as seen by ionogram. Occurrence of range spread F is found to be higher in the pre-midnight period but frequency spread F is found to be dominant during post-midnight which is quite similar to the earlier reports. These observations are compared with occurrence of scintillations at Mumbai and detailed analysis of these results will be presented.

ROLE OF MAIN FIELD VERTICAL COMPONENT IN THE DEFORMATION OFSQ CURRENT SYSTEM

S. K. Bhardwaj*, P. B. V. Subba Rao and B. Veenadhari
Indian Institute of Geomagnetism, New Panvel, Navi Mumbai 410 218 India
**sandeep@iigs.iigm.res.in*

In the present study, we focus on how the vertical component (Z) of the Earth's main magnetic field that plays an important role in the deformation and modulation of the ionospheric Sq current system.

Examination of geomagnetic field variations at southern hemispheric stations; Crozet and Kerguelenreveal that the solar quiet daily (Sq) variations in this longitudinal sector do not show the expected V type or inverted V shaped variations in the horizontal component (H) but instead are marked by northern hemispheric type Dvariations i.e. easterly maxima in the forenoon and westerly minima in the afternoon hours.

It is found that Sq variation in three components for a chain of mid-latitude stations in the longitudinal band of 20° to 210° E shows the anomalous Sq variations. Z-component plays an important role in deformation of Sq current system along the longitudinal belt 30° to 90° E, which is fixed with Sun moving from Australian to African sector.A detailed study reveals that this anomalous deformation of Sq vortex, confined to narrow longitudinal sector, is characterized by anomalous pattern of main field vertical component (Z), a vital component in the generation of Sq current system through the dynamo mechanism. It is also shown that, the iso-magnetic field lines in vertical component (Z), instead of following the circle of latitude tend to align in N-S direction along this longitudinal sector (30° to 90° E) producing deformation in Sq current system.

PASSIVE REMOTE SENSING TECHNIQUES TO STUDY THE ANNUAL AND SEASONAL VARIATION OF THE AEROSOLS, PRECIPITABLE WATER CONTENT, AND TOTAL COLUMNAR OZONE IN LITTLE RANN OF KACHCHH AND RANN OF KACHCHH, GUJARAT, INDIA

C. P. Simha[1*], K. M. Rao[1], B. K. Rastogi[1], V. N. Sridhar[2], R. Prajapati[2] and A. K. Shukla[2]
[1] Institute of seismological research (I.S.R), Gandhingar, Gujarat-382009. [2] Space Application Centre (SAC), ISRO, Ahmadabad, Gujarat-382009.
simha.prasanna@gmail.com

This paper deals with the seasonal and annual variation of Aerosol Optical Thickness (AOT), Preceptible Water Content (PWC) and Total Columnar Ozone (TCO) in the Little Rann of Kachchh and Rann of Kachchh near the MPGO site, Desalpaur. The main objective of this paper is to study the AOT, TCO and PWC changes in Rann of Kachchh over winter and summer seasons and its influence on the monsoon cycle. We have followed standard protocol for field measurements such as 32 campaigns in little Rann of Kachchh (2012-13) and 32 campaigns in Rann of Kachchh (2013-14) in synchronization with some of the Indian satellites such as IRS-P6, IRS-RS2, OCM-2 of ISRO and

Land SAT 7+ of NASA satellite. For the above mentioned periods of satellite radiance, estimated radiance have been computed by compiling the 6S radiative transfer code (input as: Zenith Angle (θ), Azimuth Angle (φ), AOT, PWC, TCO and ground reflectance) in Fortran-77 within the limits of different band radiance of the satellites sensors (Green, Red, Nir and Swir bands). Passive remote sensing technique have been applied for our study and it works on the principle of beer-lamberts law and differential optical absorption techniques, portion of light which is coming from the sun after attenuating by scattering and absorption of water molecule, aerosols and gasses has taken at a certain zenith angle. Spectral analysis of the acquired data over two years in different seasons reveals the different species concentration such as AOT at 550nm, Preceptible water content(PWC), and Total columnar ozone(TCO) over the desert site. Influence of the desert aerosols radiative forcing over the study period has been done by computing the fraction of sunlight attenuated by aerosols and its influence for active and break monsoon over the study period. 10 to 20% high AOTs at lower wavelength have been observed at Rann Of Kachchh(2014) than Little Rann of Kachh(2013), which tells the more abundance of absorbing type aerosols due to accumulation of finer particle in the year of 2014 than 2013, IMD observatories also recorded rainfall of 777.33mm in 2013(excessive rainfall) and 463.9mm in 2014(normal rainfall) over Gujarat in monsoons.

VARIATIONS IN THE ATMOSPHERIC STRUCTURE AS OBSERVED DURING SECOND HALF PERIOD OF MONSOON 2011 BASED ON CAIPEEX DATA

S. G. Narkhedkar*, S. P. Ghanekar, Asha Nath, P. P. Leena, K. K. Dani, M. D. Chipade and Sunil Sonbawane

Indian Institute of Tropical Meteorology, Pune – 411 008, India.
narkhed@tropmet.res.in

Introduction

Integrated Ground Observation Campaign (IGOC) was carried out under the project Cloud Aerosol Interaction and Precipitation Enhancement EXperiment (CAIPEEX) over Indian region. Under this experiment, special radiosonde observations were taken at Mahabubnagar (16.73°N, 77.98°E) during the period 2 August to 31 October 2011 (study period). The station lies in the southwest sector of Hyderabad (17.45°N, 78.46°E) and in the rain shadow region with respect to southwest monsoon season. The experiment was designed to study all the atmospheric and thermodynamic parameters in context with the cloud seeding experiment around and in southwest sector of Hyderabad over the peninsular Indian region. With the availability of the special observations under this experiment, the present study investigates the variation in the atmospheric structure during the second half period of the monsoon of 2011 over Mahabubnagar. The study also brings out existence of atmospheric waves and attempts to investigate their characteristics and excitation sources based on the field data.

Data

Radiosonde balloon observations taken at Mahabubnagar (station) using Vaisala sounding system during the study period 02 August to 30 September 2011 under CAIPEEX program are used in the analysis. Synoptic weather data and various weather reports taken from the India Meteorological Department (IMD) website (http://www.imd.gov.in) are also used. Daily 2.5° X 2.5° Lat. / Lon. grid-point NCEP/NCAR reanalyzed wind data over the domain bounded by the latitudes Equator-30°N and longitudes 60°-100°E for the same period are also utilized.

Synoptic conditions observed during the study period

During 2011, the cross equatorial flow maintained its strength all through the month of August and in the first half of September. Various low pressure systems were formed during the same period. Most of these systems were either initially seen as an upper-air cyclonic circulation over the eastern part of the monsoon trough or formed over there. These systems further moved westward across the trough giving good rainfall activity over the country. The withdrawal of monsoon started from 23 September. For the Mahabubnagar district, the percentage departure rainfall for the months of August and September in 2011 are observed to be 6% & - 83 % respectively. The rainfall events (> 1 cm) at Mahabubnagar station occurred in the presence of various systems mentioned above. An isolated heavy rainfall event at the station on 21 August occurred during the period of an upper-air cyclonic circulation.

Results and Discussion

Monthly mean profiles of U, V, T and RH at Mahabubnagar

Monthly mean profiles of zonal (U) and Meridional (V) components of wind, Temperature (T) and Relative Humidity (RH) are studied to understand mean monthly features over the station (Figures not shown). It was noticed that U showed dominance of westerlies up to mid-tropospheric levels while strong easterlies were seen in the upper troposphere and lower stratosphere. V showed southerlies up to 900 hPa in August and northerlies in September in the lower troposphere, while southerlies were seen in mid-tropospheric levels in both the months. T did not show much significant change during the study period. RH showed relatively higher values (> 50%) up to mid-troposphere in August than that for September when they were noticed to be confined up to lower troposphere. The depth of moisture beyond 600 hPa in August is consistent with the frequent formation of synoptic scale systems as mentioned above. The mean tropopause height was estimated to be as 16.3 km.

Tropospheric wind shear based on NCEP/NCAR reanalysis data

Daily values of wind shear between the lower and upper tropospheric zonal components of wind (U_{850} - U_{200}) deduced based on NCEP/NCAR data over the study area are presented in Figure 1. The figure depicts Strong shears > 25 mps during 01-16 August and 25 August-11 September on most of the days. These are the periods around when monsoon disturbances were formed and good amount of rainfall occurred over the station. The shear is lowest on 20 August (11 mps). The highest/lowest values of shear are noticed to have repeated after about 30 days.

Atmospheric structure and wave activity at Mahabubnagar

The atmospheric structure and waves are investigated by analyzing daily observed and anomaly profiles of U and V for the study period. Figure 2 show the analysis of observed U and V over the station during the study period based on field data. High values of U > 10 mps are noticed during 2-14 August and from 26 August-10 September in the lower and middle troposphere (Figure 2a and b). While V shows repetitive occurrence of positive values with an interval of about 3-7 days during 1-23 August and with an interval of about 10-15 day during 1 - 26 September in the same layer of atmosphere (Figure 2c and d). Such high values are in accordance with the formations of synoptic systems and their movements. In the upper levels, around the tropopause height (16 km), high negative values of U (> |-30| mps), persisting for few days are noticed up to about 20 September, indicating the presence of Tropical Easterly Jet (Figure 2a and b). Such high values are seen to reappear after about 10-15 days. The variations of U and V fields are found in good agreement with that observed based on NCEP/NCAR reanalyzed data (Figures not shown).

The anomaly plots of U and V are given in Figure 3. The anomaly plot of U (Figure 3a and b) shows positive anomalies (anomalous westerlies) for 2-13 August, 25-31 August and 01-10 September up to mid-troposphere, intercepted by negative anomalies (anomalous easterlies) during 14-25 August. Around tropopause level, alternate pockets of negative/positive anomalies are noticed appearing after about 10-15 days. The anomaly plot of V (Figure 3c and d) shows alternate pockets of positive and negative anomalies up to mid-tropospheric levels, reappearing after about 3-7 days in August and 10-15 days in September in consistent with the prevailing synoptic weather situations. While around tropopause level, negative (positive) values are noticed in the first (second) fortnight of September.

The anomaly plots show various wave activities especially from tropopause level with certain periodicity propagating either upwards in stratosphere or downwards to surface layer. Since the wave structure is clear and systematic in the case of U, in this analysis, the tropospheric waves in the U field over the station are only looked into. Preliminary results of U anomaly plots show downward propagation of waves from tropopause level up to surface during the period of about 2-25 August and 1-15 September. This is noticed under conditions of good monsoon activity witnessed through the formation of synoptic systems in presence of strong wind shear between 850 and 200 hPa levels. The further analysis is being carried out to test the significance of the wave progression and to understand their characteristics.

Concluding Remarks

The analysis of upper-air radiosonde observations taken under CAIPEEX at Mahabubnagar during 02 August to 30 September of 2011 well captures the features of evolution of monsoon from established to withdrawal phase and found in good agreement with the analysis of synoptic weather data and NCEP/NCAR data.

Based on the field data, the tropopause is estimated at a height of about 16.3 km. Vertical time anomalies of U depict wave propagation originating from around tropopause height (level of Tropical Easterly Jet: TEJ) and descending (propagating) down (up), up to the surface (lower stratosphere). The results suggest that, the tropospheric waves are found to be generated under prevalence of stronger winds associated with TEJ and strong vertical wind shear in the troposphere and acted as excitation source for these waves. The propagation of wave is seen to follow a near 30 day low frequency oscillation, in accordance with the vertical wind shear and prevailing monsoon conditions. Anomalies of V however depict a mixed wave structure in the troposphere showing influence of 5-7 day and 10-15 day oscillations over the location. For this the transient synoptic systems (convective) moving across the monsoon trough may be playing a role as the source. Further analysis is being carried out to test the significance of the wave progression and also to study their characteristics.

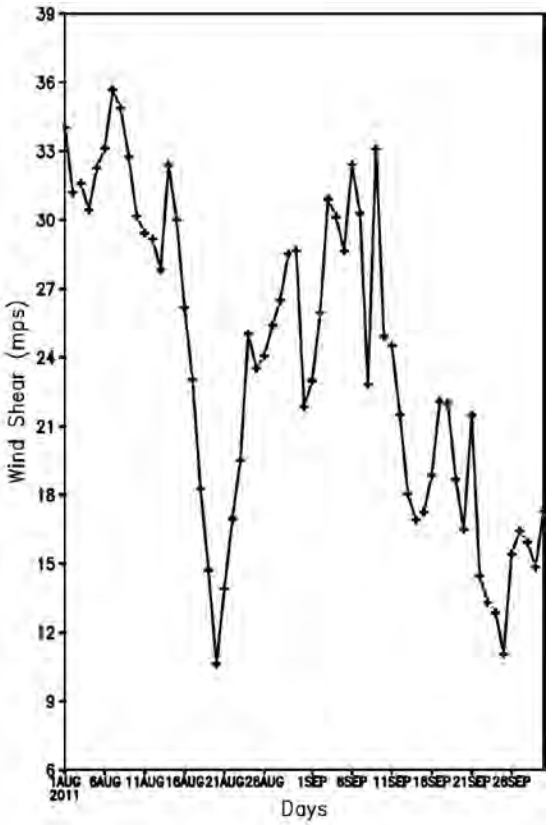

Figure 1. *Wind shear over the study domain (16°-17°N and 77°-78°E) between lower and uppertroposphere (850-200 hPa) during 1 August to 30 September 2011.*

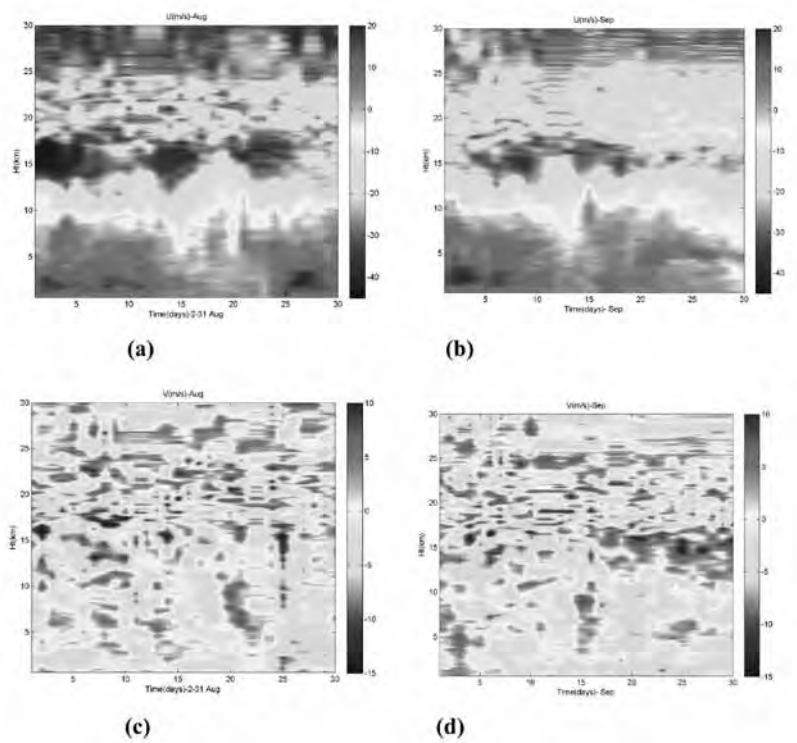

Figure 2 Vertical Time sections of U (a and b), V (c and d) both in mps for the months of August and September respectively.

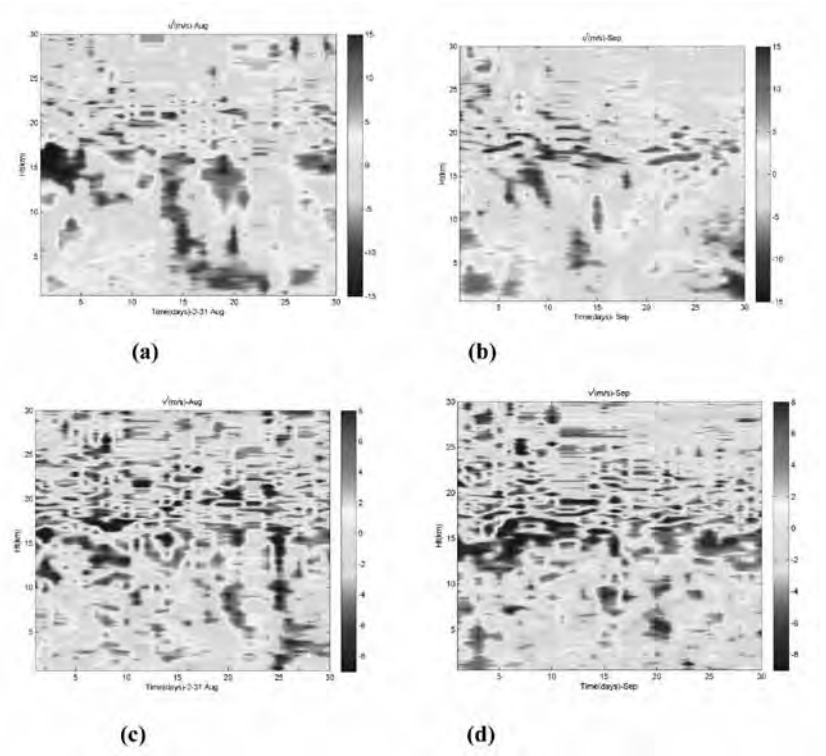

Figure 3 Vertical Time sections of anomalies of U (a and b), V (c and d) both in mps for the months of August and September respectively.

ON THE ROLE OF PHOTO-CHEMISTY VIS-A-VIS- ELECTRODYNAMICS IN CONTROLLING SUNRISE UNDULATION OF THE F REGION PEAK ALTITUDE AT THE DIP – EQUATOR

K M Ambili* and R K Choudhary

Space Physics Laboratory, VSSC, Trivandrum, India

**ambilisadasivan@gmail.com, rajkumar_choudhary@vssc.gov.in*

The discovery of the ionosphere was not less than a boon for mankind as it facilitated the wireless transmission of radio signals and paved ways for the High Frequency (HF) radio communication. Then came the advent of Global Positioning System (GPS) based technologies with numerous applications in the fields of communication, navigation, education, agriculture, medicine etc making life easier and the world a smaller place to be in. But it did not take too long to realize that what supported the HF communication and the wireless transmission of radio signals now posed to afflict the propagation of radio waves. Its evolution from being boon to bane is solely because it has not been understood properly. As modern day activities are increasingly dependent on GPS radio signals, the need for understanding the ionosphere and processes affecting the radio signals is immensely felt. Over the last six decades, several attempts have been made to understand ionospheric features. There are however still several critical issues which have remained unresolved. The aim of the present study is to understand how the equatorial ionospheric system responds during sunrise period using the help of experimental facilities and theoretical models. This paper shows that, during sunrise time, there is an enhancement of peak height of F region (hmF2) and contrary to previous explanations, the apparent undulating motion of the equatorial F region peak at sunrise is produced mainly by photochemistry rather than dynamics. Our study is based on an investigation of the behaviour of the early morning

ionosphere observed by a Digital Ionosonde at Trivandrum, India, and an In-coherent backscatter radar measurements at Jicamarca, Peru. Electrodynamics is not responsible for the sunrise undulation, but plays an indirect role in the detection of the sunrise effect by simultaneously lowering during the night the peak height and decreasing the density.

Introduction

The equatorial region is rich in ionospheric phenomena observed exclusively at low latitudes. A primary example is the steep climb in the peak height of the F-region during local sunset hours at the dip equator [Balsley, (1969)]. Studies based on incoherent scatter radar observations have shown the PRE phenomenon to be clearly related to a reversal in the sign of the zonal electric field [Woodman ,(1970); Fejer, (1981)] . A less documented but similar undulation in the altitude of the F region peak has also been reported shortly after sunrise. Given the similarities of the F peak motion with the evening PRE undulation and the fact that the zonal electric field changes sign around sunrise, it has been assumed that the sunrise undulation is also the result of an electrodynamic phenomenon [Woodman ,(1970); Aggson et.al., (1995); Nayar et.al., (2009)] .

Here we have used observations from Digisonde systems, and incoherent backscatter radar located at the dip-equator to perform a more detailed study of the F region undulation at sunrise. We have focused on data obtained in March 2010 at a time when the sunrise undulation in the F region was particularly clear and repeatable. We show that chemistry explains not only the sudden increase in the F region peak altitude after sunrise, but also a previously unnoticed F peak density increase during the undulation. The main role played by the electrodynamics is to remove, prior to sunrise, F region plasma produced on the previous day.

Data and Method of Analysis

F region electron density information was retrieved from Digisondes installed at Trivandrum (8.47^0 N, 76.92^0E, 0.17^0S dip-latitude) and Jicamarca (12.0^0 S, 75.2^0 W, 0.17^0S dip-latitude) and electron density profiles obtained from an incoherent backscatter radar at Jicamarca. We compared measurements from these instruments with calculations from a time-dependent one-dimensional numerical ionospheric model that solved the ions and electron continuity equations. The model was limited to a computation of O^+, NO^+, $N2^+$ and $O2^+$ densities based on the photo-ionization of O, O_2, and N_2, the conversion of O^+ to molecular ions via charge exchange reactions, and the subsequent dissociative recombination reactions of molecular ions. Details on model used in this study can be found in *Ambili et al,* [2012]. The model also incorporates the effects of vertical electrodynamic drifts resulting from zonal electric fields. It does not, however, include diffusion as the altitudes of interest are well below 400 km, where the magnetic field lines are horizontal, the time scale for diffusion to operate was assumed to be long compared to the time scales of interest.

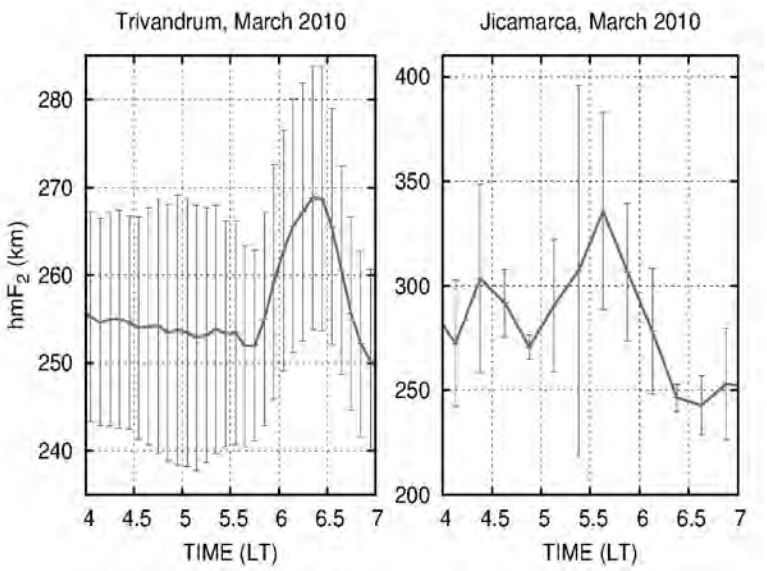

Figure 1. *Temporal variations in monthly averaged hmF_2 during sunrise period at Trivandrum (left) and Jicamarca (right) during March 2010.*

Results and Discussion

FIGURE 1 presents the temporal evolution of the F-region peak height (hmF2) derived from the Digisonde observations during March 2010 at Trivandrum, and Jicamarca. The plots represent the monthly averaged value in 5 minutes intervals (at Trivandrum, left panel), and in 15 min intervals (at Jicamarca, right panel), along with the standard deviations at each bins during sunrise (04:00 to 07:00 LT) periods. The peak height of the F region shows uplift and then a descending motion (more clearly at Trivandrum than at Jicamarca) during morning hours. As discussed in the introduction, such undulation in the F region is frequently seen during evening hours and is well known as the Pre Reversal Enhancement (PRE) associated with a reversal in the sign of the zonal electric field. It should be clear from FIGURE 1 that there is a strong trend at Trivandrum around 06:30 LT for a descending F peak that becomes detectable around 300 km altitude. Within a half hour the peak comes down to 250 km only to move back after 07:30 LT. A similar undulation in hmF_2 at Jicamarca can also be identified from FIGURE 1 where the F-region peak appears to jump from 260 km at 4:45 LT to 335 km at 05:45 LT and thereafter moves swiftly down to 240 km by 06:30 LT. *Ambili et al,* [2012] have shown that the apparent jump in the F-region altitude is a result of two separate factors: an erratic remnant from the night before, which is typically found below 260 km altitude, and a fast descending component that starts at an altitude far in excess of the `remnants' mean altitude.

In order to study the roles of residual ions from the prior night on the observations of sunrise undulations, we compare in FIGURE 2 the observations on March 11, 2011 (blue curves) with the numerical model results by initializing the model under two different set of conditions, namely, [Case 1, red curves] with negligible density so that only the newly produced plasma and hence the evolution of the ionosphere with time could be tracked, and [Case 2, green curves] with the plasma density matching the ISR observations at the pre sunrise time. March 12 was a special day a moderate geomagnetic storm with Dst ~ -90 nT had started on 11 March 2011 at 03:00 UT, and was in its recovery phase on March 12. A double hump structure was observed in the electron density profile which had remained unexplained till date.

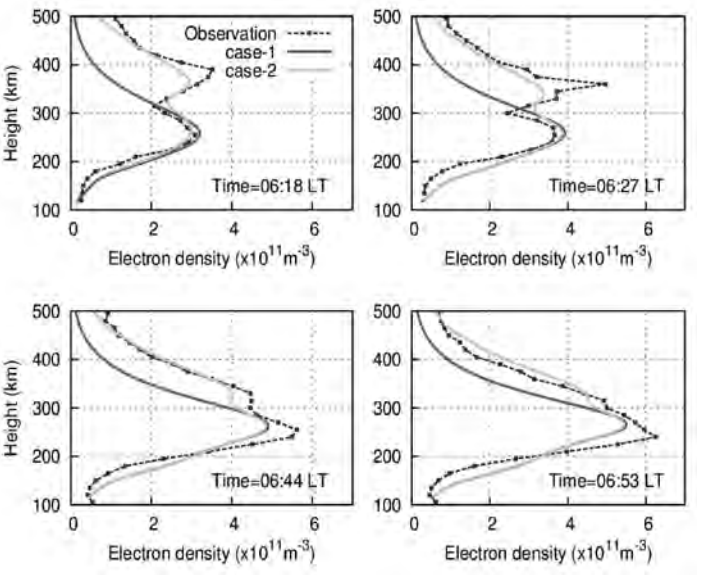

Figure 2. *Comparison of model derived electron density profiles with densities derived from Incoherent backscatter radar measurements at Jicamarca on March 11, 2011 [after Ambili et al., (2013)].*

As the Fejer model output could not represent actual electric field conditions prevailing during March 12, in our model run for Case 2, we initialized the model with ISR- measured plasma density at 03:00 AM and applied a modest up drift of 5 m/s till 06:15 LT (there was no drift data from the ISR itself). Afterwards, we used the Fejer drift in the calculations..While the agreement with observations may not be perfect, our model calculations can clearly be used to emphasize that the lower peak in the density profile was associated with the SU effect while the other peak came from remnant plasma that had been lifted up to unusually high altitudes and had undergone little, if any, recombination. This upper peak descended near dawn because of the downward motion seen after 06:15 LT. The motion of the upper peak therefore had nothing to do with the chemical processes associated with the plasma produced through the SU mechanism. It just so happened that the remnant plasma was high enough and had a large enough density to be seen in tandem with the photo chemically produced plasma, even as late as 06:53 LT. Therefore, even though there was an initial rise in altitude followed by a downslide after sunrise, the temporal variations in hmF2 on March 12, 2011 was entirely due to an unusual electrodynamical effect.

Conclusions

The behaviour of the ionosphere shortly after sunrise has been characterized using high time resolution observations from a Digital Ionosonde (Digisonde) at Trivandrum, India and incoherent backscatter measurements at Jicamarca. Our study makes it clear that the hmF2 jump after the upper F region sunrise, and its subsequent downward excursion afterwards is entirely explicable by chemical effects associated with the production of new plasma after sunrise. Our chemical calculations not only predict the right altitudes at the right time for the F peak, but also, very near the right densities. The up and down oscillations that follow sunrise are therefore not due to an oscillating vertical drift. Using incoherent backscatter measurements we have also shown that the peak in plasma density due to its fresh production during morning hours can be easily identified even in the case when background density is high. A double hump structure in the electron density in the morning of a geomagnetically disturbed day was also explained with the upper peak due to remnant plasma and lower due to pure chemistry.

References

K. M. Ambili, J.-P. St. Maurice and R. K. Choudhary (2012). On the sunrise oscillation of the F region in the equatorial ionosphere, Geophys. Res. Lett., 39: L16102.

K. M. Ambili, R. K. Choudhary, J.-P. St. Maurice and J. L. Chau (2013). Night-time vertical plasma drifts and the occurrence of sunrise undulation at the dip-equator: A study using Jicamarca Incoherent backscatter radar measurements, Geophys. Res. Lett., 40: 5570-5575.

T. L. Aggson, F. A. Herrero, J. A. Johnson, R. F. Pfaff, H. L. Kso, N. C. Maynard and J. J. Moses (1995). Satellite observations of zonal electric fields near sunrise in the equatorial ionosphere, J. Atmos. Terr. Phys., 57: 19-24 .

B. B. Balsley (1969). Some characteristics of non-two-stream irregularities in the equatorial electrojet, J. Geophys. Res., 74: 2333-2347.

B. G. Fejer (1981), Low- latitude electrodynamic plasma drifts: A review, J. Atmos. Terr. Phys., 53: 677-693 .

S. R. P. Nayar, T. J. Mathew, C. V. Shreehari, S. G. Sumod, C. V. Devasia, S. Ravindran, V. Sreeja, T. K. Pant and R. Sridharan (2009). Electrodynamics of the equatorial F region ionosphere during pre-sunrise period, Ann. Geophys., 27: 107-111 .

R. F. Woodman (1970). vertical drift velocities and east-west electric fields at the magnetic equator, J. Geophys. Res., 75: 6249-6259.

PLANETARY WAVE OSCILLATIONS IN THE EQUATORIAL ELECTROJET DURING SUDDEN STRATOSPHERIC WARMING EVENTS

C. Vineeth and T. K. Pant

Space Physics Laboratory, Vikram Sarabhai Space Centre, ISRO, Trivandrum, India.
cnvins@gmail.com

This study presents the impact of polar Stratospheric Sudden Warming (SSW) event of January 22, 2006 on the dip equatorial upper atmosphere through the intensification of planetary wave activity. The noteworthy observations as far as the dip equator ionosphere is concerned are (i) amplification of the quasi 16-day wave in the equatorial mesopause temperature and the EEJ induced magnetic field prior-to, during and after the SSW period (ii) regular occurrence of Counter Electrojet (CEJ), with a periodicity of ~16 days (iii) diminishing CEJ strength concurrent with the damping of the amplitude of wave oscillation with time. These results are discussed in context of the changes in large-scale circulation during the SSW.

Introduction

The energetics/dynamics of the upper atmosphere is primarily controlled by tides, planetary and gravity waves in addition to the photochemistry. Over the dip equator, these waves and tides significantly influence the background wind in the lower ionospheric heights leading to the generation and modulation of the global dynamo electric field. The variability of the Equatorial Electrojet (EEJ) and Counter Electrojet (CEJ) are the consequence of such modulation. The Planetary Waves (PWs) and their interactions with the prevailing wind in the dip equatorial upper atmosphere could impose significant changes in the EEJ and CEJ. Though, PW oscillations of periodicities 2, 5, 10 and 16 days have been identified in the EEJ current [1], the quasi 16-day wave is found to have a major role modulating the EEJ region during certain winter months especially when polar SSW occurs.

The present study discusses the impact of one such polar SSW event that occurred on January 22, 2005 on the dip equatorial upper atmosphere. The important observations as far as the equatorial upper atmosphere is concerned are (i) the intensification of the PW of quasi 16-day periodicity in mesopause temperature and the EEJ induced magnetic field (ii) the modulation of tidal components

by the amplified PW and (iii) occurrence of Counter Electrojet (CEJ) events on consecutive days with a quasi periodicity ~16 days. These observations directly demonstrate importance of the vertical and lateral coupling of different atmosphere regions during SSW events.

Experiments

The equatorial Mesopause Temperature (MT) over Trivandrum (8.5°N, 77°E, 0.5°N diplat.) was estimated using the daytime intensity measurements on two emissions in the OH Meinel (8-3) band using the ratio method. The EEJ induced magnetic field at the surface was measured using a co-located Proton Precession Magnetometer (PPM).

Observations

The daymean values of the MT during the period December 01, 2005- March 31, 2006 are analyzed and depicted in Figure 1. The temperature exhibited both long and short period fluctuations during this period. In addition, the MT showed an overall enhancement during this period (dashed line in Figure 1). The shaded portion indicates the period when the polar stratospheric temperature showed a major enhancement from the annual mean.

The EEJ induced surface magnetic field also exhibited some interesting features during this period as evident from Figure 2. The ΔH values show clear-cut enhancements during noontime, at around day number 50, 64 and 78. The enhancements seen after day number 80 are found to be due to the geomagnetic disturbances. Further, CEJs are occurred on consecutive days around day numbers (45, 46, 47), (59, 60, 61) and (71, 72, 73) and those days are highlighted using the ovals. The negative excursions observed on days other than these were identified as geomagnetically disturbed. The occurrence of the these bunches of CEJs exhibited a periodicity of quasi 16 days. The strongest CEJ was observed on day number 45 and the strength of the subsequent CEJs decreased linearly coinciding with the decrease of the amplitude of the quasi 16-day wave. In addition, the occurrence time of the CEJ is found to be shifting towards evening as the event progresses.

In order to find the nature of the quasi 16- day wave in MT and EEJ induced magnetic field, the 'Morlet' wavelet analysis has been performed and the power spectra hence obtained (not shown here) clearly showed that the most dominant wave in both the parameters is the quasi 16-day wave. Further, the wave in both the parameters exhibited amplification between day 25 and 75.

Results and Discussion

Studies in the past have shown that the quasi 16-day wave of the mesosphere in the winter hemisphere has large amplitude, especially during the SSW years [2]. The enhancement of the averaged amplitude in the upper mesosphere and lower thermosphere occurs when the amplitude in the stratosphere becomes large [4]. The present paper discusses the impact of the polar SSW on the equatorial upper mesosphere and lower ionosphere during the SSW event of January 22, 2006.

The major changes observed over the equatorial region are, an overall enhancement in MT and presence of amplified quasi 16-day waves prior to and during the SSW event. In the ionosphere, the occurrence of consecutive CEJ events of same periodicity was observed during the same period. It is proposed that, the changes in prevailing wind pattern at stratospheric and mesospheric altitudes play an important role in the propagation of the lower atmospheric waves and tides upward. Such changes in the background circulation observed during the SSW events allow the westward propagating PWs to reach upper mesospheric altitudes unlike in the normal years.

The PWs at upper mesospheric heights interact with the tides nonlinearly such that they generate a group of secondary waves, resulting in significant modulation of the tidal amplitudes [5]. The modified tides can change the temperature at mesospheric altitudes as high as 20 K as observed in the present study. At lower thermosphere altitudes, such a modification in the tidal components significantly affect the EEJ since it is driven essentially by the diurnal tide wind dynamo. Perhaps, in this study it has been observed that when the phase of the quasi 16-day wave was positive, the tidal amplitudes were enhanced and when it was negative they got weakened. The CEJs were observed on all the days where tidal components were weakened and strong EEJs were observed when the amplitude of the tidal components strengthened. It clearly shows that the changes in lower atmospheric circulation during the SSW facilitate easy upward propagation of lower atmospheric waves from stratospheric altitudes to lower thermosphere-ionosphere heights.

Conclusion

The presents study discusses the influence of polar SSW events in modulating various parameters of the equatorial upper atmosphere. It has been observed over the equatorial mesospheric region are as well as lower ionospheric region respond significantly to the changes in the dynamics during the SSW events.

References

Forbes, J. M., and S. Leveroni, Quasi 16-day oscillations in the ionosphere, *Geophy. Res. Lett*., 19, 981– 984, 1992 .

Chau J. L, Goncharenko L. P, Fejer B. G, Liu H L Equatorial and Low Latitude Ionospheric Effects During Sudden Stratospheric Warming Events Ionospheric Effects During SSW Events, *Space Sci. Rev.*, 2011, doi 10.1007/s11214-011-9797-5.

Vineeth, C, T. K. Pant, K. K. Kumar, G. Ramkumar and R. Sridharan, Signatures of Low latitude-High Latitude Coupling in the Tropical MLT Region during Sudden Stratospheric Warming, *Geophy. Res. Lett*., 36, 2009, L20104, doi: 10.1029/2009GL040375.

Forbes J. M, M. E. Hagan et al., Quasi 16-day oscillation in the mesosphere and lower thermosphere, *J. Geophys. Res.*, 100, 9149-9163,1995.

Mitchell, Mitchell, N. J., H. R. Middleton et al., The 16-day planetary wave in the mesosphere and lower thermosphere, *Ann. Geophys.*, 17, 1999, 1447-1456.

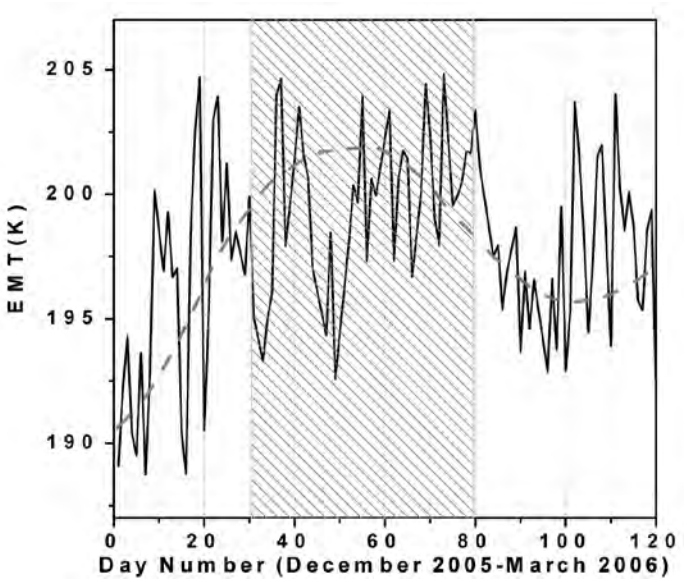

Figure 1: -*Day to day variation of MT over Trivandrum during December 01,2005-March31, 2006.*

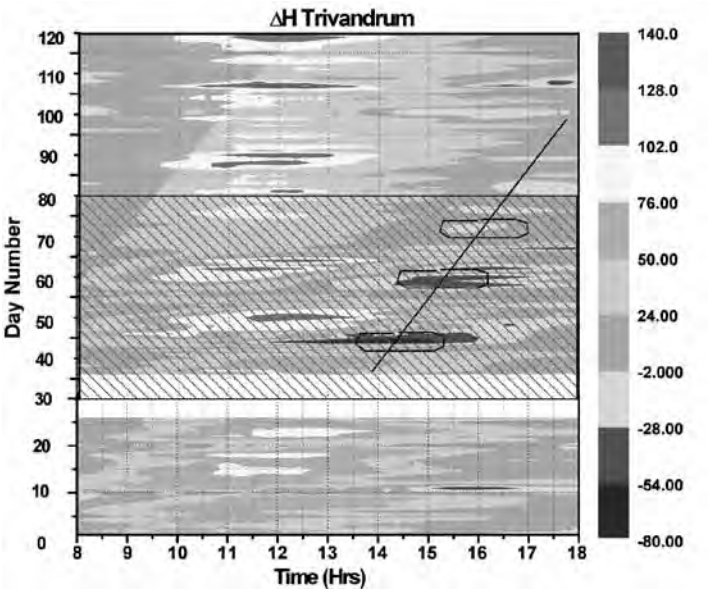

Figure 2: - *Daily variation of EEJ induced magnetic field (ΔH) during the same period.*

SPATIAL AND TEMPORAL VARIATIONS IN THE MAGNITUDE OF GHAGGAR RIVER FLOODS IN HARYANA AND PUNJAB: 1990-2013

Dinesh Kumar[1] and *Omvir Singh[2]

Department of Geography, Kurukshetra University, Kurukshetra, Haryana, India
**ovshome@yahoo.com; dineshgeographer@gmail.com*

In this paper a comprehensive flood frequency and severity study of Ghaggar river basin has been attempted on the basis of Gauge and Discharge data of 13 sites using 24 years data between 1990 to 2013. A close examination of basin flood data revealed that a maximum of 18 floods occurred during the year 1995. However, the basin experienced maximum floods in the month of July (56) followed by August (50). The highest flood discharge of 5430 m^3/s was recorded at Ambala-Chandigarh Road Crossing site on September 12, 1999. Khanauri on the main Ghaggar and Jansui on the Tangri (a tributary) are the worst flood hit sites and experienced about 37 floods out of the total 145 floods that occurred during the 24 years period in the basin. Moreover, the magnitude of the flood deviation from the Danger Level was observed to be highest at Ambala-Chandigarh Road Crossing Site (11.3 m) on September 12, 1999. It was also observed from the flood data that Khanauri site experienced six floods during 1995 flood season which is the highest occurrence for any recorded site in Ghaggar river basin during the study period. The enormity of floods in Ghaggar river basin may be attributed to a host of related causes such as natural, hydro-meteorological and anthropogenic. The present research will be valuable for water resource engineers and administrators for taking up the remedial measures against recurrent floods in the basin.

STUDY ON ZENITH TOTAL DELAY (ZTD)VARIATIONS RELATED TO ATMOSPHERIC STORMS AND DEPRESSIONS: GPS OBSERVATIONS AT TIRUNELVELI AND HYDERABAD STATIONS OF SOUTH INDIA DURING THE YEAR 2010

A.Akilan[1*], K.K Abdul Azeez[1],S.Balaji[2], H. Schuh[3] and Y. Srinivas[4]

CSIR-National Geophysical Research Institute, Uppal Road, Hyderabad- 500 007, India

[2]Department of Disaster Management, Pondicherry University, Port Blair-744112, India

[3]GFZ, German Research Centre for Geosciences, Potsdam, Germany

[4]Manonmaniam Sundaranar University, Tirunelveli-627012, India

akilan@ngri.res.in

Global Positioning System (GPS) monitoring of Zenith Total Delay (ZTD)of the troposphere which is related to water vapor is important as it may help us in weather forecasting.The atmospheric water vapor variesaccording to the season and it also varies quickly on short temporal and spatial scales during stormy periods, and thus plays a crucial role in meteorology. GPS is one of the relatively inexpensive tools available to monitorthe water vapor content in the atmosphere. In the present study, the importance of GPS meteorology is demonstrated by observing the perturbations in ZTD during various atmospheric events. An attempt has been made to utilize the GPS derived meteorology parameters for weather forecasting oftwo storms occurred between 25th October, 2010 and 11th December, 2010 that hit the Southeast coast of India. The ZTDwas estimated for this period at the NGRI operated GPS stations at Hyderabad (HYDE) and MS University, Tirunelveli (MSUN) andthe corresponding power spectrawereprepared. During thestormyperiodthere wasa strong variation in ZTD. The average ZTD was found to behigher near the coastal station at MSUN and less at the HYDE inland station. This meteorological anomaly helped us to understand and forecast the rainfall during the stormy weather conditions in South India and the Equatorial Indian Ocean region. The GPS derived higher ZTD value with quick changes and the corresponding spectral analysis of ZTD enable usto predict that there was a possibility of rainfall expected at MSUN approximately within 32 hours and 50 minutes.Therefore, the GPS meteorology can be effectively used in weather forecasting and as a precursor of rainfall prediction.

Introduction

The GPS radio wavestravelling from satellites in space to the receiver on ground undergo significant delay induced by the ionosphere and troposphere (Hogg et al., 1981). The delay due to the troposphere is known as Zenith Total Delay (ZTD), which is the combined effect of delay caused by the wet Zenith Delay (ZWD) and Zenith Hydrostatic Delay (ZHD) components in the troposphere (e.g. Nilsson and Elgered, 2008).Thus, the relation between Zenith Total Delay (ZTD) experienced by the GPS signal and the atmospheric water content (Bevis et al., 1992) opened a useful application of GPS monitoring in meteorological studies (Businger et al., 1996). Atmospheric events such as storms and deep depressions bring sudden change of atmospheric water content, and the dynamic perturbations in the atmospheric water vapor content would get reflected in the ZTD values, which can be obtained from GPS data (e.g. Rocken et al., 1993).In this study, we demonstrate the correlation between the ZTD values estimated from continuous GPS monitoring and atmospheric storms affected the East coast of South India during the year 2010.

The Data

In the year 2010, Eastern margin of Indian peninsula has seen a few severe weather conditions, which were originated in the Eastern Indian Ocean(IMD report, 2010). The prominent events among them were the very severe cyclonic storm 'GIRI' (20-23 October, 2010), severe cyclonic storm 'JAL'

(4-8 November, 2010), and another deep depression during 7-8 December, 2010. We usedhere about two and half months (17thOctober – 27thDecember, 2010,a period equivalent to the 288-358 GPS day period) of GPS data recorded at the Hyderabad (HYDE) and Tirunelveli (MSUN) stations to estimate the ZTD perturbations over these locations, and study their correlation with the atmospheric events.

Analysis and Results

The raw GPS data in RINEX format were processed using the Bernese 5.0 softwareZTD values over Hyderabad and Tirunelveli stations. The variation in the hydrostatic delay that contributes 90% to the total ZTD value is a slow process and hence is negligible.Thus the observed variations in ZWDthat contribute about 10% to the absolute ZTD value might represent the changes in water vapor content in the troposphere. Our GPS derived ZTD timeseries shows peaks and lows corresponding to the atmospheric water vapor changes associated with the severe weather periods. To verify the reliability of GPS derived ZTD in establishing its relation with atmospheric weather changes, we compared our results with numerical weather models from http://ggosatm.hg.tuwien.ac.at/.The comparison carried out for the Hyderabad station data showed a remarkably good agreement of ZTD between the GPS derived and the numerical prediction values. This exercise was not possible forMSUN site as this is not an IGS station and NWMdata arenot readily available for this location. We also tested the good consensus shown between the GPS and NWM data using two other IGS GPS stations,Cocos Island (COCO) and Diego Garcia (DGAR),located in the equatorial Indian Ocean region.The rainfall data for the Hyderabad and Tirunelvelistations were also compared with the ZTD estimates to understand the correlation between the two phenomena. For theTirunelveli station the ZTD peak values are relatively higher (> 2.6 m) and show correlation with the atmospheric events noted in the South India region. No rainfalls are reportedfrom this location during the major events GIRI and JAL. But, higher ZTD values were observed in the atmosphere during the GPS days 327 to 330 and significant rains were reported from this location.

Discussions

The comparison of the ZTD variations between the stations in onshore and offshore regions showed spatial variation of ZTD values and suggested the weakening of ZTD towards the shore. This indicates that stations close to the ocean or inside the ocean are more affected by storms than stations located inland. The ZTD value decreases as one moves to the interior of land, as confirmed by the lower value observed at HYDE against the station near the coast, i.e. MSUN. The increase in ZTD may be an indication for a precursor of rain. The overall analysis shows that during the onset of a rainy day the ZTD is significantly higher atstations MSUN, HYDE, COCO, and DGAR.Sometimes during rainfall, ZTD may come down if the atmosphere is not dynamic. It is difficult to predict the place of rain since atmospheric dynamics depends on various other factors that are beyond the scope of this paper.The inland station HYDE shows less variability in ZTD, but the station near the coast, MSUN, exhibitshigher variability.The stations which are located around the equatorial Indian Ocean region (DGAR and COCO),in particular show large abrupt changes in ZTDvariation.

The power spectrum of the ZTD time series shows a number of peaks and drops, which are interpreted to represent charging of water vapor and discharging of water vapor, respectively. The spectral analysis indicated that the rainfall was expected within 32 hours and 50 minutes at MSUN and as predicted heavy rainfall resulted. The station in the land and away from the equator i.e. HYDE and MSUN, happen to take longer duration to charge water vapor but discharge quickly. On the other side, the stations in the ocean that are close to the equator, i.e. DGAR and COCO, took shorter time to charge and longer time to discharge.

References

Bevis, M.,Businger, S., Herring, T. A., Rocken, C., Anthes, R. A., Ware, R. H., 1992. GPS meteorology: Remote sensing of atmospheric water vapor using the Global Positioning System. Journal of Geophysical Research97, 15787-15801.

Businger, S., Chiswell, S. R., Bevis, M.,Duan, J.,Anthes, R. A.,Rocken, C., Ware, R. H.,Exner, M.,VanHove, T.,Solheim, F. S., 1996.The promise of GPS in atmospheric monitoring. Bulletin of the American Meteorological Society 77, 5-17.

Hogg, D. C., Guiraud, F. O., Decker, M. T., 1981. Measurement of excess transmission length on earth-space paths. Astronomy and Astrophysics 95, 304-307.

IMD [Indian Meteorological Department] report, 2010.(http://www.imd.gov.in/section/nhac/dynamic/RSMC-2010.pdf).

Nilsson, T., Böhm, J., Wijaya, D. D., Tresch, A., Nafisi, V.,Schuh, H., 2013. Path delays in the neutral atmosphere, in:J. Böhm, H. Schuh (Eds.), Atmospheric Effects in Space Geodesy,Springer-Verlag Berlin Heidelberg, doi: 10.1007/978-3-642-36932-2_3.

Rocken, C, Ware, R., Hove, T. V.,Solheim, F.,Alber, C. Johnson, J., Bevis, M.,Businger, S., 1993. Sensing atmospheric water vapor with the Global Positioning System.Geophysical Research Letters 20, 2631-2634.

INVITED TALK

RECENT ADVANCEMENTS IN THE UNDERSTANDING OF COUPLING OF ATMOSPHERES

D. Pallamraju[1], F. I. Laskar[1], R. P. Singh[1], D. K. Karan[1], K. Phadke[1], T. Vijaya Lakshmi[1], and M. Anji Reddy[1]

[1]Physical Research Laboratory, Navrangpura, Ahmedabad, 380009
[2]Jawaharlal Nehru Technological Universtity, Hyderabad.
raju@prl.res.in

Coordinated investigations using optical emissions at multiple latitudes and multiple wavelengths revealed several interesting aspects of vertical and horizontal coupling of atmospheres present during both day and night times in the mesosphere - thermosphere regions. High spectral resolution echelle and grating spectrographs have been fabricated for carrying out these measurements. High cadence data over a large field-of-view is obtained from low-latitude observational sites at JNTU, Hyderabad and PRL's Optical aeronomy observatory at Gurushikhar, Mt. Abu. Daytime optical oxygen emissions at 557.7 nm, 630.0 nm, and 777.4 nm that originate at 130 km, 230 km, and peak height of the F-region, respectively, and nighttime mesospheric temperatures derived from the rotational band structure of OH and O2 molecules originating at 87 km and 94 km, respectively, are used in this study. Satellite-based temperature and wind data are used to complement the high-cadence ground-based optical data. These set of data obtained over long periods show several features that reveal new features on various aspects of coupling of atmospheres during varying geophysical conditions. Some of these include variation of the effect of small-scale waves (e.g., gravity waves) and large-scale waves (e.g., planetary waves, semi-annual, etc.) at different altitudes that vary as a function of solar activity, sudden stratospheric warming events, and geomagnetic disturbances. Large-scale transfer of energy along latitudes in terms of temperature variations, wind changes, etc., are also seen on global-scales. These new findings advance our understanding on the behaviour of the mesospheric to thermospheric regions and their coupling under varying inputs of energy from above (solar) and from below (lower atmosphere). Highlights of some of the results obtained in the recent past will be presented.

SESSION – II

YOUNG RESEARCHERS PROGRAM

ESTIMATION OF HORIZONTAL COMPRESSIVE STRESS OF INDIAN CONTINENTAL PLATE

***Radheshyam Yadav and Virendra M. Tiwari**
Gravity and Magnetic Studies Group, CSIR-National Geophysical Research Institute, Hyderabad, India
shamgpbhu@gmail.com

In situ measurements of maximum horizontal stress (S_{max}) of Indian continent using well Breakouts, Hydrofractures and Focal mechanisms are sparse. The observed orientation of S_{max} varied considerably and often do not follow the plate velocity direction. We have made an attempt to simulate orientation and magnitude of S_{max} to understand the variability of S_{max}, using finite element solver (Abaqus CAE) and incorporating heterogeneities in elastic property of Indian continent. With plane stress approximation, we made simulation for four different scenarios (i) homogenous plate with fixed north and east Himalayan boundary (2) homogeneous plate with applied boundary conditions at north and east Himalayan boundary (3) heterogeneous plate with fixed north and east Himalayan boundary condition (4) heterogeneous plate with applied boundary condition at north and east Himalayan boundary. The estimated orientation and magnitude of S_{max} with heterogeneous plate with applied boundary conditions at north and east Himalayan boundary better correlate with measured maximum horizontal stress.

SEISMIC STRUCTURE OF THE LITHOSPHERE AND UPPERMANTLE NEAR THE MID-OCEANIC RIDGES

Chinmay Haldar[1,2], Prakash Kumar[1] and M. Ravi Kumar[1]
1,National Geophysical Research Institute (CSIR), Uppal Road, Hyderabad-500007, India
2,AcSIR-NationalGeophysical Research Institute, Hyderabad-500007, India
chinmay.haldar@gmail.com

The Mid-Oceanic Ridges (MOR) are the largest sources of magma on the earth. Being the locus of new lithosphere generation and accretion to the existing ones, their study assumes importance in understanding the dynamics of plate tectonics. These linear features on the ocean floor control the rheology of oceanic lithosphere, ridge topography, the style of oceanic crustal accretion and also affect the earth's deeper discontinuities. New oceanic lithosphere created at the mid-oceanic ridges undergoes cooling and thickening as it subsequently spreads away. Deciphering the seismic character of the young lithosphere near the MOR is a challenging endeavor. In this study, we determine the seismic structure of the oceanic plate beneath the oceanic islands located near the MORs, using the P-to-s conversions for data recorded at 5 broadband seismological stations situated on the ocean Islands in their vicinity.

Estimates of the crustal and lithospheric thickness values from waveform inversion of the P-receiver function stacks at individual stations reveal that the Moho depth varies between ~10±1 km and ~20±1 km with the depths to the lithosphere-asthenosphere boundary (LAB) varying between ~40±4 and ~65±7km. We found evidence for an additional low-velocity layer below the expected LAB depths at stations on Ascension, Sao Jorge and Easter Islands. The layer probably relates to the presence of a hotspot corresponding to a magma chamber. The shear velocity drop across LAB is sharp in nature, implying presence of partial melt in the asthenosphere. Inclusion of little more than 1% melt in the asthenosphere, in addition to the temperature contrast, provides a realistic explanation of the large velocity drop. Further, thinning of the upper mantle transition zone suggests a hotter mantle transition zone due to the possible presence of plumes in the mantle beneath the stations. All the stations show a delay in both the discontinuities with respect to the global average values predicted by the IASP91 model.

DE-NOISING AND DATA GAP FILLING OF 2D AND 3D SEISMIC DATA: A NEW SPATIO- TEMPORAL DOMAIN SINGULAR SPECTRAL APPROACH

***Rajesh Rekapalli[1,2] and R.K.Tiwari[1,2]**
[1]AcSIR-NGRI, Uppal Road, Hyderabad
[2]CSIR-NGRI, Uppal Road, Hyderabad
**rekapalli@gmail.com*

The seismic data suffers from random and coherent noises that arise due to nonlinear interaction among different seismic waves and unwanted processes. The distorted signal amplitudes due to thepresence of such noise mislead the physical interpretations.In particular, correlated and colourednoises createserious problems in recognizing the geological features. Various signal processing techniques have been employed using the frequency domain singular spectral approaches for random noise suppression and data gap filling. However, the more acute problem of correlated and colourednoise suppression and artefacts arise due to domain conversionare not well addressed. Here, we employed SpatialSingular Spectrum Algorithm (SSSA) to recover the true reflection amplitudes by exploiting the Eigen properties of the data in time domain. We have tested the robustness of algorithm on synthetic data contaminated with correlated and coloured noises and have presented comparison with Multi-channel SSA/ FXSSA algorithms. Further the method was applied to the 2D seismic reflection filed data. The structural features observed from the SSSA stack sections are verified using the borehole data anddiscussed with reference to the geological inferences. Finally, we also demonstrate the application SSSA method on 3D seismic synthetic data.

INVERSION OF GRAVITY ANOMALY OF SEDIMENTARY BASIN USING PARTICLE SWARM OPTIMIZATION

Kunal K. Singh* and Upendra K. Singh
Department of Applied Geophysics, Indian School of Mines, Dhanbad-826004, India
kunalkishoresingh0@gmail.com

Inversion of gravity anomalies of sedimentary basin mimics a mathematical process of trying to fit observed anomalies to calculated ones for obtaining basin parameters. The mathematical geometry used for sedimentary basin modeling is stacked prism model of Bott (1960). A Matlab code is developed based on the Particle swarm optimization to estimate the depth to the bottom of the sedimentary basin where density varies parabolically with depth. The PSO simultaneously estimates regional background in addition to depth parameters. The PSO algorithm is tested on synthetic data by calculating the depth of the basin.

Introduction

Negative anomalies are observed over sedimentary basins having a large thickness of lower density rocks. Rama Rao and Murthy (1978) opined that the ambiguity in gravity anomalies can be overcome by assigning a mathematical geometry to the anomaly causing body with a known density contrast. The cross-section of the basin is described by the stacked prism model of Bott (1960). The Marquardt inversion by Chakravarthi and Sundararajan (2007) solved simultaneously the structure of a sedimentary basin as well as estimating regional background from observed gravity anomalies. Kennedy and Eberhart (1995) first conceived the idea of implementing the social behavior of birds into optimization problems and called the resulting technique particle swarm optimization PSO. PSO is an extremely simple algorithm that dispenses with the need for mimicking the complex processes of gene transfer and mutation from one generation to another, as required in GA, and for finding

computational analogs of thermodynamic processes, as in SA (Sen and Stoffa, 1995). Instead, PSO has a memory component for each particle in the swarm so that both the cognitive knowledge and social behavior of the particles are used simultaneously in deciding the excursion of the solution in model space. A Matlab code in PSO is used to interpret the gravity anomalies of sedimentary basin.

Theory

In the Bott's approach, sedimentary basin is described by a series of 2.5-D vertical prisms (Figure 1a), each with equal width, 2b, but having different strike lengths, 2S. The gravity

anomaly at any point, , on the profile, in the presence of regional background, A +B, of a sedimentary basin is given by Chakravarthi and Sundararajan (2006a) as

$$g_{basin} = \sum_{i=2}^{N-1} g_i(x_k, 0) + Ax_k + B. \qquad (1)$$

N is the number of observations on the profile, A and B are coefficients of regional background and $g_i(x_k,0)$ is the gravity effect of the *i*th prism at any point, P (x_k, 0), expressed (Fig. 1b) by Chakravarthi and Sundararajan (2006a) as

$$g(x_k, 0) = \int_{w=d_1}^{d_2} \int_{v=-s}^{s} \int_{u=-b}^{b} \frac{G\,\Delta\rho(w)\,w\,du\,dv\,dw}{[(u-x_k)^2+v^2+w^2]^{3/2}}, \qquad (2)$$

Here G is the universal gravitational constant and dudvdw is the volume of an elementary mass, b is half width of the prism, are depths to the top and bottom of the prism (Fig. 1b), respectively. Δ and α are constants of the parabolic density function at any depth, w, as expressed by Chakravarthi and Sundararajan (2006a)

$$\Delta\rho(w) = \frac{\Delta\rho_0^3}{(\Delta\rho_0 - \alpha w)^2}. \qquad (3)$$

After integration, Eq. (2) changes to

$g(x_k, 0) =$

$$-2G\,\Delta\rho_0^3\{(\frac{\alpha x_k S}{t_4} ** \left(\frac{1}{t_2}+\frac{1}{t_3}\right)\ln\frac{t_5}{t_6} + \frac{S}{2t_2} * \ln\frac{(R+x_k)}{(R-x_k)} + \frac{x_k}{2t_3}\ln\frac{(R+S)}{(R-S)} + \frac{\Delta\rho_0}{\alpha}[\frac{1}{t_2}\tan^{-1}\left(\frac{SR}{wx_k}\right) +$$

$$\frac{1}{t_3}\tan^{-1}(\frac{x_k R}{wS})] - \frac{1}{\alpha t_5}\tan^{-1}(\frac{Sx_k}{wR}))_{x_k-b}^{x_k+b}\}_{d_1}^{d_2} \qquad (4)$$

Here

$$R = (x_k^2 + S^2 + w^2),$$

$$t_1 = x_k^2 + S^2,$$

$$t_2 = S^2\alpha^2 + \Delta\rho_0^2,$$

$$t_3 = x_k^2\alpha^2 + \Delta\rho_0^2,$$

$$t_4 = \sqrt{(t_1\alpha^2 + \Delta\rho_0^2}),$$

$$t_5 = \Delta\rho_0^2 - \alpha w,$$

and

$$t_6 = -2(\alpha R t_4 + t_1\alpha^2 + \Delta\rho_0\alpha w).$$

The theoretical gravity anomaly obtained from eq. (4) is made at the respective centers of each prism but not on the profile, CC´. In order to calculate anomalies on the profile, CC´, eq. (4) has to be estimated twice by substituting S-s and S+s for S and taking its average (Chakravarthi and Sundararajan, 2006a).s is the offset of the profile, CC´, from their corresponding centers of each prism.

The algorithm begins by calculating initial depths of the basin assuming that the observed gravity at each observation on the profile, CC´, is being generated by an infinite horizontal slab along which the density contrast decreases parabolically with depth as expressed by Chakravarthi and Sundararajan (2006a) as

$$z_i = \frac{g_{obs}(x_i)\Delta\rho_0}{41.89\Delta\rho_0^2 + \alpha g_{obs}(x_i)} \qquad i = 2,3,\ldots\ldots,N-1$$

with $z_1 = 0$ and $z_N = 0$

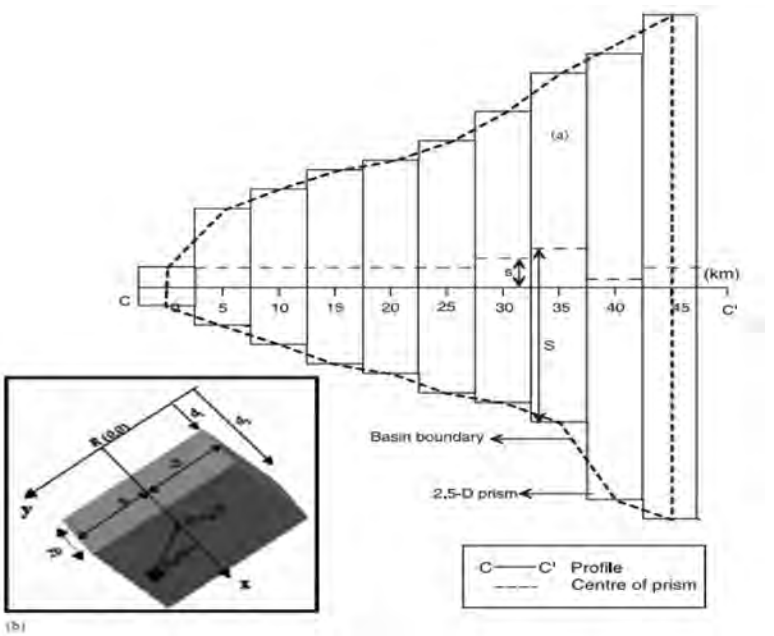

Figure 1. *(a) Plain view of a 2.5-D sedimentary basin and its approximation by juxtaposed prisms. S is half-strike length of a prism and s is offset of profile, CC´, center of a prism (b) Geometry of a 2.5-D vertical prism in Cartesian coordinate system (Chakravarthi and Sundararajan, 2007).*

Kennedy and Eberhart (1995) first conceived the idea of implementing the social behaviour of birds into optimization problems and called the resulting technique particle swarm optimization (PSO) PSO is initialized with a group of random particles (solutions) and then searches for optima by updating generations. In every iteration, each particle is updated by following two "best" values. The first one is the best solution (fitness) it has achieved so far. (The fitness value is also stored.) This value is called pbest. Another "best" value that is tracked by the particle swarm optimizer is the best value, obtained so far by any particle in the population. This best value is a global best and called gbest. When a particle takes part of the population as its topological neighbors, the best value is a local best and is called lbest.

After finding the two best values, the particle updates its velocity and positions with following equation (6) and (7).

v[] = w * v[] + c1 * rand() * (pbest[] - present[]) + c2 * rand()*(gbest[]-present[]) (6) present[] = present[] + v[] (7)

v[] is the particle velocity, present[] is the particle position (solution). pbest[] and gbest[] are defined as stated before. rand() is a random number between (0,1). c1, c2 are positive learning factors which controls the maximum step length. Usually c1 = c2 = 2. w is the inertial weight factor which controls the speed of the particles.

Synthetic Example

10 juxtaposed vertical prisms each with equal width 2 km but different strike lengths are used to approximate the cross-section of the sedimentary basin. Here synthetic anomaly is generated with parabolic density function using the values of and g/ /km (Chakravarthi and Sundararajan, 2005). PSO best result is found with 500 iterations and with 50 numbers of models. The RMS Error is 0.0011. Regional Coefficients are A=0.0015 mgal/km and B= -2.0466 mgal. The upper part of figure 2 shows the variation of synthetic and calculated gravity anomalies of a synthetic model of a 2.5-D sedimentary basin obtained from PSO algorithm and the lower part show the inferred structure obtained from PSO.

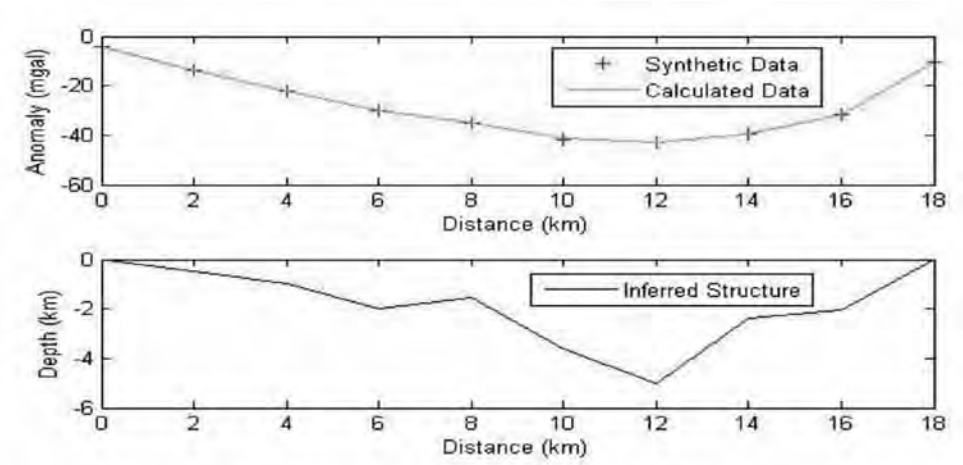

Figure 2. *Synthetic and Calculated gravity anomalies with parabolic density function due to a synthetic model of a 2.5-D sedimentary basin and Inferred structure obtained from PSO.*

Conclusions

PSO is very simple to apply and is controlled by only one operator i.e. velocity updating. PSO makes few or no assumptions about the problem being optimized and can search very large spaces of candidate solutions. We have implemented PSO algorithm on synthetic data with regional background. We found good and reliable result.

References

Bott, M.H.P., 1960. The use of rapid digital computing methods for direct gravity interpretation of sedimentary basins. Geophysical Journal of the Royal Astronomical Society 3, 63–67.

Chakravarthi, V., Sundararajan, N., 2005. Gravity modeling of 2.5-D sedimentary basins-a case of variable density contrast. Computers and Geosciences 31, 820-827.

Chakravarthi, V., Sundararajan, N., 2006a. Gravity anomalies of 2.5-D multiple prismatic structures with variable density: a Marquardt inversion. Pure and Applied Geophysics 163, 229–242.

Chakravarthi, V., Sundararajan, N., 2007. INV2P5DSB-A code for gravity inversion of 2.5-D sedimentary basins

using depth dependent density. Computers and Geosciences 33,449-456.
Kennedy, J., Eberhart, R., 1995. Particle Swarm Optimization. Proceedings of IEEE International Conference on Neural Networks. IV 1942-1948.
Rama Rao, B.S.R., Murthy, I.V.R., 1978. Gravity and Magnetic Methods of Prospecting. Arnold-Heinemann Publishers, New Delhi, India, 390pp.
Sen, M.K., Stoffa, P.L., 1995. Global Optimization methods in geophysical inversion. Elsevier Scientific Publishing Company pp. 1-281.
Shaw, R., Srivastava, S., 2007. Particle Swarm Optimization: A new tool to invert geophysical data. Geophysics, 72(2), 75-83.

DOES BOTTOM WATER OXYGEN CONCENTRATION AFFECT ARAGONITE COMPENSATION DEPTH IN THE SOUTHEASTERN ARABIAN SEA?

D.P. Singh, D.K. Naik, R. Saraswat and R. Nigam
Marine Micropaleontology Laboratory, National Institute of Oceanography, Goa, India

Enhanced anthropogenic greenhouse gas emission induced ocean acidification will affect aragonite compensation depth (ACD). Therefore, precise estimates of ACD from different parts of the world oceans are required to understand the effect of ocean acidification on ACD. Here we report the ACD from the southeastern Arabian Sea, by using pteropod preservation in the surface sediments. A total of 80 spade core-top samples along seven latitudinal transects (T1-T7) at 1 degree interval, covering the continental shelf, slope and abyssal region of the southeastern Arabian Sea were analyzed to document aragonite compensation depth. Pteropods were picked from coarse fraction ($\geq$63 μm). Pteropods are dominated by *Limacina inflata* in this area as earlier reported from the Indian Ocean. Based on the pteropod preservation, we report that in the southeastern Arabian Sea, ACD lies at a water depth of 720-1040 m. We further report that the ACD decreases from north to south in the southeastern Arabian Sea. These ACD estimates are deeper than so far reported from the rest of the Arabian Sea (off Oman 500$\pm$200 m; off Pakistan 250-400 m). On the basis of the comparison of pteropod abundance with the dissolved oxygen, we suggests that low dissolved oxygen favours better pteropod preservation.

REVISITING THE LAST GLACIAL-INTERGLACIAL PRODUCTIVITY PARADOX IN THE EASTERN ARABIAN SEA

D.K. Naik[1⋆], Rajeev Saraswat[1#], R. Nigam[1], David W. Lea[2], S.R. Kurtarkar[1] and D.P. Singh[1]
[1] *Micropaleontology Laboratory, Geological Oceanography Division, National Institute of Oceanography, Goa, India.*
[2] *Department of Earth Science, University of California, Santa Barbara, USA.*
⋆ *dineshkumarnaikdu@gmail.com;* # *rsaraswat@nio.org*

Changes in marine primary productivity are suggested as a major factor that affects atmospheric CO_2 concentration during glacial-interglacial periods. Past primary productivity estimates, however, vary from region to region, with enhanced primary productivity during glacial intervals being mainly reported from the Southern Ocean while diminished glacial productivity in the monsoon affected Arabian Sea. The primary productivity estimates from the eastern Arabian Sea, however, are in contrast to those from the rest of Arabian Sea, suggesting a unique role for this region in carbon cycle changes. This study reconstructs paleo-productivity changes from a well-characterized eastern Arabian Sea core spanning the past ~32 kyr, using absolute abundances of planktic and benthic foraminifera, relative abundances of *Globigerina bulloides,* and angular asymmetrical benthic foraminifera (AABF). and measurements of total organic carbon (C_{org}), $CaCO_3$, and $\delta^{18}O$. A close correspondence between *G. bulloides* abundance and ice-volume corrected $\delta^{18}O$ (a salinity proxy) throughout the sequnce

suggests that productivity changes in this region were driven by changes in monsoon strength. The high relative abundance of *G. bulloides* during MIS3 and last glacial maximum (LGM) suggests that productivity in the southeastern Arabian Sea was high during these time intervals, as also supported by high absolute abundance of planktic foraminifera, as well as coarse fraction percentage. The $\%C_{org}$ was also higher during MIS 3 and the LGM, although much lower than that during the late Holocene, suggesting that the water was well oxygenated. An abrupt decrease in *G. bulloides* abundance as well as planktic foraminifera, C_{org} and coarse fraction percentage during the early deglacial transition, suggests a decrease in productivity. The productivity was uniform during the later part of the glacial-interglacial transition. The coarse fraction, $CaCO_3$, C_{org} and AABF, however, further decreased, suggesting a combination of well oxygenated waters and poor carbonate preservation. Increase in *G. bulloides* abundance, planktic abundance, $CaCO_3$, coarse fraction and C_{org} during the early Holocene until ~5 kyr, suggests increased productivity as a result of early Holocene monsoon optimum. The AABF abundance during early Holocene was high which indicates oxygen depleted waters. The *G. bulloides* abundance is uniform throughout the last ~5 kyr suggesting no change in productivity during the Late Holocene. An abrupt and continuous increase in C_{org} is noted during this interval, which is attributed to better preservation as a result of oxygen depletion, as also suggested by a simultaneous increase in AABF. A drop in bottom water oxygen over the last 5 kyr is further supported by a decrease in coarse fraction, attributed to increased dissolution susceptibility of biogenic carbonate in CO_2-rich, oxygen-depleted waters. Although the productivity changes inferred from proxy records in the Malabar core resemble records from other cores collected from similar depths, the pattern is not consistent throughout the eastern Arabian Sea, suggesting a regional pattern of high productivity and subsequent $CaCO_3$ and C_{org} deposition in a narrow zone along the continental slope.

SOURCE PARAMETERS OF REGIONAL EARTHQUAKES IN INDIA AND THE 11THMAY 1998 POKHRAN NUCLEAR EXPLOSION

Bandana Baruah[1,2], Prakash Kumar[1] and M. Ravi Kumar[1]

CSIR - National Geophysical Research Institute, Hyderabad-500007
AcSIR- National Geophysical Research Institute, Hyderabad-500007
mailbandanabaruah@gmail.com

Parameterizing the nature of an earthquake source enables an understanding of the physics of the source process and seismic hazard. The key source parameters are seismic moment, stress drop and corner frequency, whose determination assumes importance for prediction of ground motion, aftershock patterns and propagation of seismic waves. Spectral analysis of body waves and source parameter estimation was performed by various workers in various parts of the Indian shield and Himalaya. However, a comprehensive study of the earthquakes sources using the recent digital data from the Indian shield stations is not attempted so far. Here, we analyze the P- and S-wave amplitude spectra of regional earthquakes in and around the Indian subcontinent to estimate the source and attenuation parameters, employing a grid search method developed by us. The regional earthquakes show corner frequencies are lesser than 10Hz, while the moment magnitudes are all within the range of 1013 to 1018 (Nm). Further, the crack radii for these sources are less than 5km. We utilize the path characteristics discerned from the regional passive source data to constrain the source characteristics of the Pokhran nuclear explosion recorded by broadband stations at regional distances. We compare the estimates of the moment, stress drop and body wave magnitude of the explosion to those of an earthquakes in its vicinity, in order to obtain clues about the strength of the nuclear explosion and the estimated yield, which is a key parameter in monitoring of nuclear explosions. We feel that calibration of the nuclear explosions based on various uncertain source and path parameters is not a straight forward task; however, a comparison with earthquake source parameters may place tighter

constraints on the possible strength of these explosions. Further, the source dynamics for both the energy sources will be discussed

INTEGRATED SEISMIC AND WELL LOG STUDY IN A PART OF SOUTH ASSAM SHELF

Sujata Gogoi and Subrata Borgohain

Department of Petroleum Technology, Dibrugarh University

The present study covers the correlation of the well logs mainly by the lithostratigraphic principles and use of seismic to understand the structural features at the time of Bokabil deposition. Further the thin section studies have been carried out for the better understanding of the petrography of the reservoirs and have a fair idea about the reservoir characteristics. The preliminary log correlation is used for the preparation of various maps like structure contour, isopach and sand percentage. Moreover the seismo-geological cross sections are also prepared. The ultimate objective that is to decipher the hydrocarbon prospectively of the Lower Bokabil Formation in the Nambar & Khoraghat area of South Assam Shelf can be achieved

SOURCE PARAMETERS AND SCALING RELATIONS FOR SMALL EARTHQUAKES IN NATIONAL CAPITAL (DELHI) REGION

Manisha Sandhu, Dinesh Kumar and S.S. Teotia

Department of Geophysics, Kurukshetra University, Kurukshetra 136119, India
sandhu.manisha553@gmail.com

The National Capital Region (NCR) of India lies in the geological realm of the Peninsular India and is about 200 km from the India plate boundary (Himalaya). The seismotectonic set up of NCR and its position in the neighbourhood of Himalaya makes it vulnerable to high seismic hazard zone. Since historical past, the NCR have experienced earthquakes of magnitude 6.0 and above which cause severe damages in the Delhi region and collapsed the whole the physical systems as well as the loss of human lives. The occurrence of such an event in a densely populated city with several old and weak structures such as Delhi can be devastating.

The locally recorded accelerograms carry rich information about the source parameters, which may be used for testing models of sources and develop scaling relations, which are useful for the evaluation of seismic hazard in the region. For the analysis of the source parameters in the region, we have used the accelerograms of 15 events with the magnitude range of 2.3-4.7, recorded by the network set up by IIT, Roorkee. The source spectra obtained from the accelerograms have been modeled in the terms of Brune Spectra to estimate source parameters (moment, magnitude, stress drop, source dimension) and attenuation parameter Q. a grid search procedure has been adopted for this purpose. The estimated moment magnitude of the earthquakes lie in the range 2.46-4.47, seismic moment is 5.708×10^{19} to 6.134×10^{22} N-m, and the source radius vary from 0.14 to 0.5 km. The scaling relations have been developed using the estimated source parameters.

ESTIMATION OF SOURCE PARAMETERS AND SCALING RELATIONS FOR MODERATE SIZE EARTHQUAKES IN NORTH-WEST HIMALAYA

***Vikas Kumar[1], Dinesh Kumar[2], Sumer Chopra[1]**
[1] Seismology Division, Ministry of Earth Sciences, New Delhi
[2]Department of Geophysics, Kurukshetra University, Kurukshetra
vickypu05@gmail.com

The earthquake source parameter of small, moderate and large earthquakes are interrelated to each other in systematic and predictable way. The dependence of earthquake parameters with each other gives scaling relations. These relations is helpful to understand the physics of earthquakes and the rupture process. The significance of these relations is that the stress drop is approximately constant over a wide range of earthquakes.These scaling relations is also used in simulation of ground motion, which is an important study in seismic hazard assessment methods. In our study we adopted the method developed by Aki (1967) and Brune's (1970, 71) which is based on the ω-2 model of the source spectrum. The corner frequency fc is calculated by Andrew's approach.

The scaling law is established between the source parameter of 34 earthquakes having 217 accelerograms andwhose magnitude rangevaries between $3.4 \leq M \leq 5.8$. In this study, the source parameters are found by the spectral analysis of P and S wave separately. The average corner frequency of P wave, fc (p) varies from 0.81 to 4.86 and that of S wave, fc(s) varies from 0.43 to 3.23 Hz, which shows that the P wave corner frequencies are greater than that of S wave frequencies. The average seismic moment varies from 7.65 X 1014 N-m to 2.26 X 1017 N-m and average stress drop varies from 12 to 92 bars. By Zuniga parameter, ε, we found that the partial stress drop mechanism is present in NW Himalayan region. Similarly, the average seismic energy varies from 1.48 X 1010 J to 1.91 X 1013 J. The linear regression analysis between the seismic moment (Mo) and corner frequency (fc) gives the scaling relation M0fc3 = 3.49 × 1016 N-m/s3, which is similar to the relationsobtained from other seismically active regions of the world.

POSTER

EOF ANALYSES OF GRACE SATELLITEGRAVITY DATA: IMPLICATIONS ONWATER STORAGE VARIABILITY OVER INDIA

Harika Munagapati and Virendra M. Tiwari
CSIR-National Geophysical Research Institute, Hyderabad
hmunagapati@gmail.com,

Terrestrial water storage (TWS) variability at large spatial scales can now be derived from Satellite gravity data recorded by the Gravity Recovery and Climate Experiment (GRACE). Major part of variance in temporal gravity is contributed by hydrological mass interaction in the absence of anylargesignals from tectonic event(e.g. earthquake).To deconvolve the signal to identify spatio-temporal variability of hydrological mass over India, we utilized Empirical Orthogonal Functions(EOF).This approach is based on the principle that a continuous stochastic process can be expressed as a combination of linear orthogonal functions, where each linear function accounts for one contributing variable to the total variance. For a spatio-temporal dataset $d(\lambda, \Phi, t) = \mu_k (\lambda, \Phi)\ e_k (t)$where, μ is the EOF, representing spatial variation and e is Principal component(PC), representing temporal variation. EOF and PC occur in associated pairs and eachsuch pair is called as a mode and signifies the spatial and temporal structures of each variable. We calculate EOFs of GRACE data,GRACE corrected for soil moisturefrom

GLDASglobal model, and accumulated rainfall. We observe that storage in the total terrestrial water (TWS) component and ground water is continuously decreasing, irrespective of rainfall pattern in the northern India. However there are periodic acceleration and deceleration to the depletion depending on rainfall pattern. In a rainfall deficient year, the amplitude of variance is higher because of the deficit caused by less input andfollowing an excess year, depletion is stabilized for a certain period. Also we find an anomalous reservoir induced storage pattern, which increases the storage seasonally. But over a longer time scale anthropogenic depletion is dominant over northern India. We alsonoticed contrasting storage patterns in northern and southern India which also differ considerably in their hydrological setups. To validate our results of groundwater component, we compare its EOF with EOF of normalized groundwater levels. A good match between the two is found, establishing the authenticity of finding.

HAS THE INDIAN MONSOON STRENGTHENED SINCE THE INDUSTRIAL REVOLUTION?

Manasa M., R. Saraswat and R. Nigam

Micropaleontology Laboratory, Geological Oceanography Division, National Institute of Oceanography, Goa, India

manumalenki@gmail.com

Food grain production drives the economy of several countries in the Indian subcontinent. For irrigation, a large part of the arable land in this part of the world, still depends on monsoon. Even minor deviations in rainfall cause large change in food grain production. Therefore, it is important to understand the factors which affect monsoon. The past records of monsoon can help us in understanding the monsoon dynamics, especially its relationship with some key climate components. The high resolution monsoon records of the common era, can further help us to understand the effect of climatic changes as a result of industrial revolution, on monsoon. Here we reconstruct, sub-decadal scale changes in monsoon intensity from a core collected from the northwestern Bay of Bengal, by using marine microfossil based proxies. The chronology of the core was established from accelerator mass spectrometer radiocarbon ages. The core covers, the last ~250 years. Previous studies documenting recent foraminiferal distribution suggest the presence of a benthic foraminifera, namely *Asterorotalia trispinosa*, in the hyposaline regions of the Bay of Bengal. On the basis of the previous reports, we have used variations in the relative abundance of *A. trispinosa* as a proxy for past salinity changes. We studied temporal changes in the relative abundance of *A. trispinosa* in the core and observed a remarkable increase in its abundance since ~1900 A.D. The increase in relative abundance of *A. trispinosa* is inferred as the prevalence of hyposaline condition. The hyposaline environment is attributed to increased runoff as a result of strengthened monsoon. The strengthening of the monsoon coincides with the increase in atmospheric carbon-di-oxide and associated changes as a result of industrial revolution. Therefore, we propose that the monsoon in the Indian subcontinent has strengthened in response to changes associated with industrial revolution.

IDENTIFICATION OF HIGH YIELDING POTENTIAL GROUND WATER AQUIFER BEARING ZONE UNDER DALDAL-SENOI, RAIPUR, CHATTISHGARDH(CG)

K.C.Mondal[1], S.C Singh[1], D.C Jhariya[2] and H.S.Mandal[3]

[1]Rajiv Gandhi National Ground Water Training & Research Institute, Raipur (CG)
Email- mondalkamalesh13@gmail.com
[2]National Institute of Technology, Department of Geology, Raipur(CG)
E-mail- dcjhariya@hotmail.com
[3]Earthquake Risk and Hazard Assessment, Centre for Seismology, New Delhi
Email-himangshu1970@gmail.com

The multi-geo-electrical survey were conducted over an area of 45.95 acre of land at village Daldal Seoni, Raipur in the state of Chattisgardh to meet the require consumption of potable ground water for the Rajiv Gandhi National Ground Water Training & Research Institute (RGNGWTRI). The study area fall under the Survey of India Topo Sheet No.64G/11 bounded by latitude 21^0 17′49″ N and longitude 81^0 40′ 42″ E of surroundings. There are 56 vertical electrical sounding (VES) and 7-gradient resistivity profiling (GRP) were conducted at 43 locations to outline the sub surface hydro-geological setting for potential ground water aquifer bearing zone and recommendation for drilling site.

From the inversion study of resistivity values and correlation with 7-borehole drilling logs, the study area is demarcated into four horizontal layers up to 100 meter below the ground level. The top thin layer resistivity value is found varied from 5 to 15 Ohm-m, indicating topsoil of thickness varying from 1.0 to 2.5 m. Second layer which is just below topsoil is the weathered sandstone of thickness varies from 4m to 9 m of low resistive in the order of 3 ohm-m -10 Ohm-m. The third and fourth layer are in general found relatively higher increasing order resistivity values which are varies from 30-150 Ohm-m of thickness 20 – 30 m and 150 - 600 Ohm-m below down are indicated dry shell or clay and compact rock formation limestone respectively. After pump test conducting it observed that all boreholes drilled by Central Ground Water Board are high yielding with reasonably good quality of water with salinity varies up to 890ppm. More interestingly the fracture patterns bellow 5-10m are identified through repetitive GPR survey which provides pinpointing the borehole locations and good yielding of ground water.

INDIAN SUMMER MONSOON CHARACTERIZATION USING SPELEOTHEMS: INSIGHTS INTO ABRUPT CLIMATE CHANGE AND ITS DRIVING MECHANISMS

***Mahjoor Ahmad Lone[1], Syed Masood Ahmad[1], Joyanto Routh[2], Vikash Kumar[3], Kalpana M. Singamshetty[1], Ravi Rangarajan[4], Prosenjit Ghosh[4] and Chuan Chou Shen[5]**

[1]CSIR-National Geophysical Research Institute, Uppal Road, Hyderabad 500007, India
[2]Department of Water and Environmental Studies, Linköping University, Sweden
[3]National Centre for Antarctic and Ocean Research, Goa, India
[4]Center for Earth Sciences, Indian Institute of Sciences, Bangalore 560012, India
[5]HISPEC, Dept. of Geosciences, National Taiwan University, Taiwan, ROC
**lonemahjoor@gmail.com*

Indian summer monsoon (ISM) variability is critical in understanding regional and global climate because it is the primary source of rainfall for the most densely populated sub-continent andregulates the socio-economy of South Asia. Abrupt changes in ISM have been cited as a dominant factor in the rise and fall of ancient civilizations like Harappans – a Bronze Age urban civilization. ISM variability has been widelystudied using marine and lake sediments and sporadically speleothems. However, high-resolution centennial-millennial scale climatic records from the terrestrial core monsoon zone

are rare. Here, we report the last deglacial(1 ka) and Mid-Late Holocene (~5 ka) ISM variability recordgenerated from $\delta^{18}O$ time series of speleothems from Valmiki Cave in Kurnool (South India) and Syndai and Rupasor Caves in Jantia Hills, Meghalaya (NE India).High amplitude $\delta^{18}O$ variations in these records reflect abrupt changes in ISM activity with decadal to multi-decadal and centennial scale phases. Our records archives significant global climatic events like Termination 1a (T1a), 4.2 ka cold event, Roman Warm Period (RWP), Medieval Warm Period (MWP) and Little Ice Age (LIA) and their dynamics in Indian sub-continent. Comparison of our record with other Asian speleothem records and Ice core (NGRIP) reveals strong tropical climatic changes vis-à-vis synchronous multidecadal to centennialscale variability between ISM and East Asian monsoon (EAM). Spectral analysis of $\delta^{18}O$ time series in these records reveal important cycles that modulate ISM dynamics which are ~220 yr (Suess/ de Vries cycle), 156-184 and 95 yr (High frequency Gleissberg cycle), 65, 57 and 49 yr (Low frequency Gleissberg cycle), 32 yr (unnamed)11 yr (Schwabe/ sunspot-cycle).Notably, the 65 and a 32 yr cycle has been attributed to Atlantic (Pacific) Multi decadal Oscillation and quasi-periodic variation in the sunspot cycle amplitudes. These cycles therefore reveal strong control of solar forcing and Ocean-atmospheric circulation on ISM variability.

DELINEATION OF MOHO DISCONTINUITY OVER DHARWAR CRATON: A 3D INVERSION OF GRAVITY DATA USING MATLAB ENVIRONMENT

Ravi Roshan[1], Pramod Kumar[2]
[1]Department of Applied Geophysics, ISM, Dhanbad-826004, India.
[2]ONGC, Dehradun, India
roshanravi.sinha@gmail.com

3DINVER.M is a highly efficient MATLAB inversion program which inverts gravity data to compute three dimensional geometry of horizontal density interface. This advance code is capable of handling large volume of gravity data-sets and is able to produce satisfactory density interface geometry. The algorithm uses gridded gravity anomaly by Parker- Oldenburg iterative method. The procedure is based on a relationship between the Fourier transform of the gravity anomaly and the sum of the Fourier transform of the interface topography. The mean depth of the density interface and the density contrast between the two media should be known. The iterative process is terminated when either the RMS error between two successive approximations is lower than a pre-assigned value—used as convergence criterion, or until a pre-assigned maximum number of iterations are reached. A high-cut filter in the frequency domain has been incorporated to enhance the convergence in the iterative.

Methodology

The equation described by Parker (1973) is used in the inversion procedure to calculate the gravity anomaly caused by an uneven, uniform layer of material by means of a series of Fourier transforms. This expression is defined as

$$F(\Delta g) = -2\pi G\rho e^{-kZo} \sum_{n=1}^{\infty} \frac{h^{n-1}}{n!} F[h^n(x)] \qquad (1)$$

Where F (Δg) is the Fourier transform of the gravity anomaly,
G is the gravitational constant,
ρ is the density contrast across the interface,
k is the wave number,
h(x) is the depth to the interface (positive downwards) and

Z0 is the mean depth of the horizontal interface.

Oldenburg (1974) rearranged this equation to compute the depth to the undulating interface from the gravity anomaly profile by means of an iterative process and is given by

$$F[h(x)] = -\frac{F[\Delta g(x)]e^{(-kZo)}}{2\pi G\rho} - \sum_{n=2}^{\infty}\frac{h^{n-1}}{n!}F[h^n(x)] \qquad (2)$$

Above expression uses to determine the topography of the interface density by means of an iterative inversion procedure. In this procedure first of all we have assume the mean depth of the interface, Zo and the density contrast associated with two media. Firstly we demeaned the observed data which will give regional gravity anomaly. Then, the first term of Eq. (2) is computed by assigning h(x) =0 and its inverse Fourier transform provides the first approximation of the topography interface, h(x). This value of h(x) is then used in Eq. (2) to evaluate a new estimate of h(x). This process is continued until a reasonable solution is achieved.

Following Oldenburg (1974) the process is convergent if the depth to the interface is greater than zero and it does not intercept the topography. Further, the amplitude of the interface relief should be less than the mean depth of the interface. As the inversion operation (Eq. (2)) is unstable at high frequencies, a high-cut filter, HCF (k) is included in the inversion procedure to ensure convergence of series. This filter is defined by

$$HCF(K) = \frac{1}{2}[1 + COS(\frac{K - 2\pi WH}{2(SH - WH)})]$$

for WH<k<SH,
HCF (k) =0 for k>SH,
and HCF (k)=1 for K<WH

The iterative process is terminated when a certain number of iterations has been accomplished or when the difference between two successive approximations to the topography is lower than a pre-assigned value as the convergence criteria. Once the topographic relief is computed from the inversion procedure, it is desirable to compute the gravity anomaly produced by this computed topography.

The inversion of a gravity anomaly over Brittany (France) is presented by author David Go´ mez-Ortiz & Bhrigu N.P. Agarwal (2005) and same code has used to compute the Moho depth of Dharwar crustal province (India). Over Brittany (France), the maximum depth of 32.4 km, located at the NW related to a NW–SE trend direction and minimum depth is 27.4 km, located at the NW corner of the area. Over Dharwar crustal province (India), the thickest moho of 43 km is beneath the Dharwar craton and thinnest of 34 km beneath the Eastern Ghat.

The Dharwar crustal province is one of the earliest formed preserved crustal areas of the world. Dhrawar craton is oldest in India with age of 3.6-3.7 Gyr. It is delimited on the west, south and east by the present day coastline.

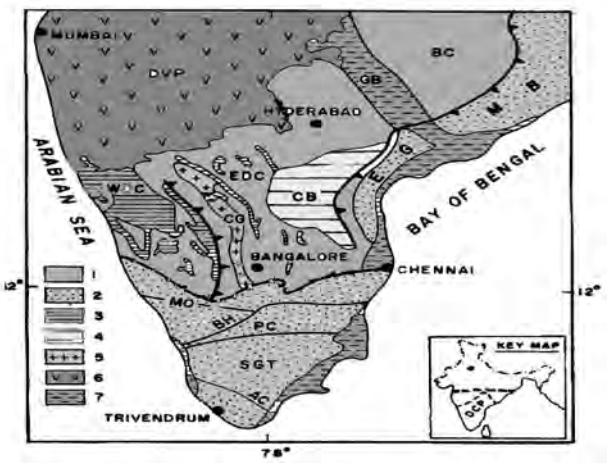

Fig. 1 Generalized geological map of Dharwar Crustal Province (India)

Matlab code used:

The flow chart of Matlab code which is used in this work to calculate moho depth is shown in following figure. The algorithm first loads the gridded data values of the gravity anomaly and the parameters used in the process, viz. number of rows and columns, data spacing, density contrast, mean interface depth, convergence criterion

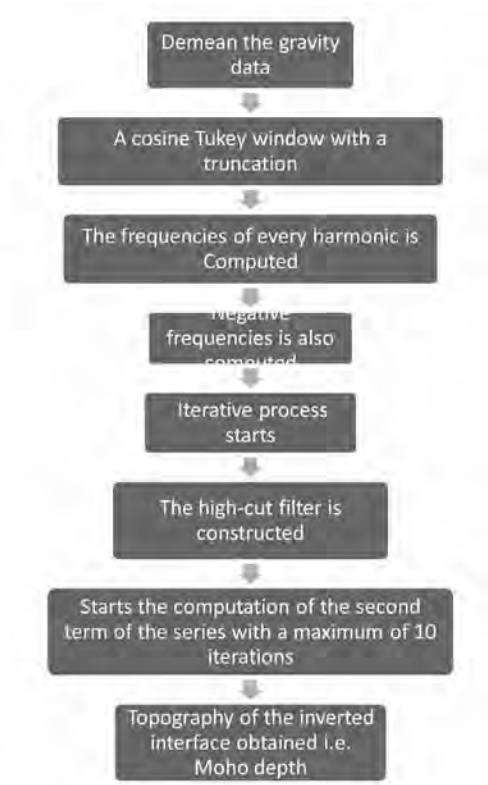

Regional anomaly map and determined Moho depth map:

The map shows the regional anomaly map over the Dharwar crustal province (India). As shown in the map, the west coast where the average elevation is near the mean sea level, a

negative gravity anomaly in the isostatic regional reflects mass deficiency. In fact the negative anomaly over the Western Ghats spreading over the low-lying coastal plains indicates a regional overcompensation through un-dissipated crustal root in the mantle.

Contour interval is taken 10 mGal

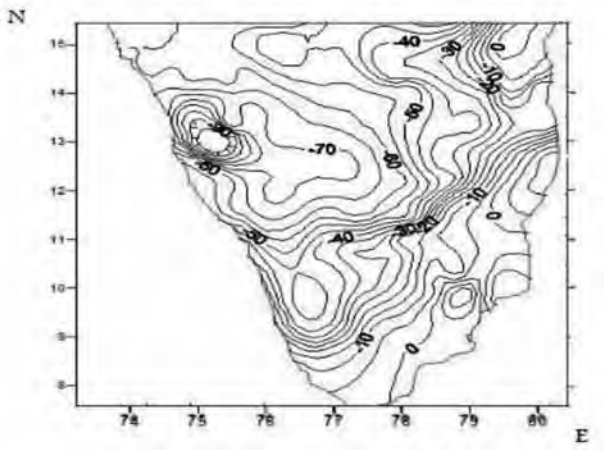

Fig.2 Isostatic gravity anomaly map of Dharwar Crustal Province (India)

Parameter used to evaluate Moho depth:

Mean depth z0 is taken here 36 km.

Density contrast is taken 0.6 gm/cc

The filter cut-off parameters have been chosen as WH = 0.01 and SH=0.012, as per frequency intervals determined for the Moho

Truncation window data length established for the cosine taper window is selected as 10% of the extended data length. Convergence criterion =0.02 km. Area of extent is 710x710km2

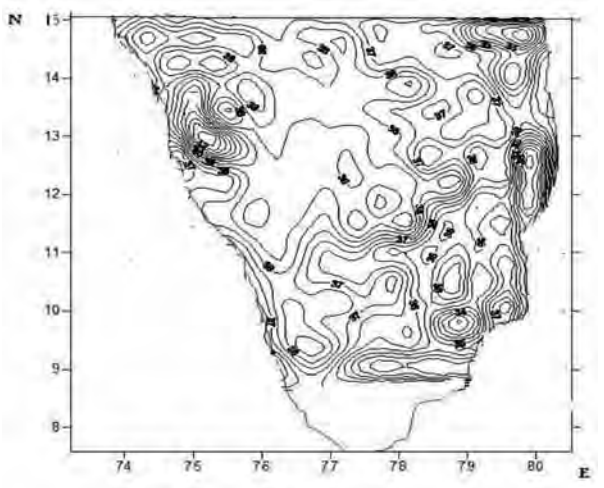

Fig.3 The Moho relief map (in km) of Dharwar Crustal Province (India)

Fig.3 shows the results (i.e. Moho depth) obtained from the application of the Matlab code on above observed gravity anomaly. Convergence of the iterative procedure has been achieved at the second iteration, with a RMS error of 0.0147km. Moho undulation found to vary between 34km beneath the eastern Ghat mobile belt to 43km maximum beneath the western Dharwar craton, which is matching with other published Moho depth.

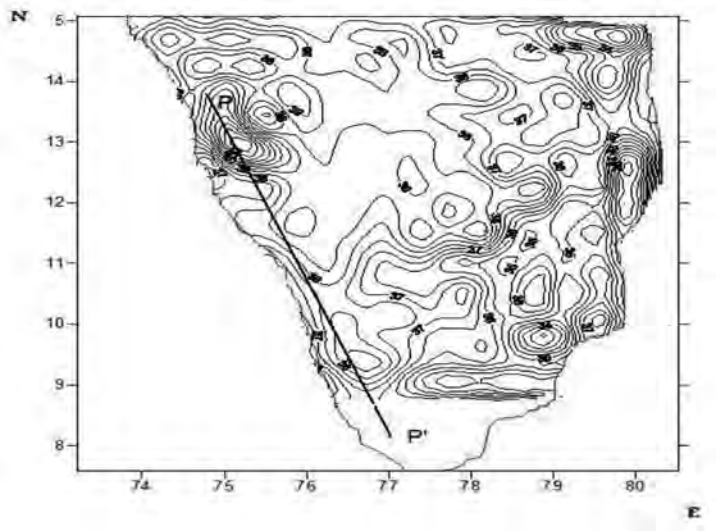

Fig. 4 *Moho relief map with profile line PP'*

Finally, Moho depth model is created by using gravity modelling software (GM-SYS from Geosoft), One gravity profile, marked PP′ has been selected as shown in fig.4. Fig.5 shows the results obtained for the profile PP′.

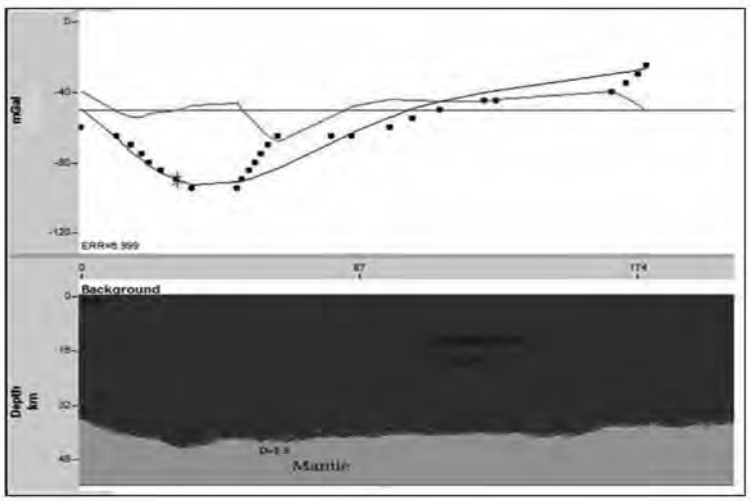

Fig. 5 Gravity modelling along a profile line PP' of Dharwar Crustal Province (India)

It can be observed from this figure that the Moho relief obtained from the GM–SYS software produces a gravity anomaly very similar in shape to the observed anomaly, but with slightly greater amplitude. Moho relief obtained from the GM–SYS software produces a gravity anomaly very similar in shape to the observed anomaly. The error between both curves is only about 6.99%.

Conclusion

An inversion of gravity data with the help of Matlab and Geosoft to compute three-dimensional geometry of a density interface using the Parker–Oldenburg method has been presented. The program requires a previous knowledge of two parameters, viz. the mean depth and the density contrast of the interface. Gravity modelling has revealed that all methods provide a very similar geometry, with small differences related to the amplitude of the interface. Moho depth varies from 34km to 43km over Dharwar Crustal province, India and Moho depth vary from 27.4km to 32.4km over Brittany France as shown by author.

References

Singh,A.P., Mishra,D.C., Laxman,G., 2003. Apparent density mapping and 3-D gravity inversion of dharwar crustal province. J. Ind Geophys. Union Vol.7 No.1.pp.1-9.

Chakraborty, K., Agarwal, B.N.P., 1992. Mapping of crustal discontinuities by wavelength filtering of the gravity field. Geophysical Prospecting 40, 801–822.

Mishra,D.C., Chandra Sekhar,D.V., Venkata Raju,D.Ch., Vijaya Kumar,V., 1999. Crustal structure based on gravity–magnetic modelling constrained from seismic studies under Lambert Rift, Antarctica and Godavari and Mahanadi rifts, India and their interrelationship. Earth and Planetary Science Letters 172 (1999) 287–300. [*]

Mishra,D.C., Gupta,S.B., Venkatarayudu,M.,1989. Godavari Rift and its extension towards the east coast of India, Earth Planet. Sci. Letters. 94 (1989) 344–352.

Gomez-Ortiz, D., Agarwal, B.N.P. 2005. 3DINVER.M: a matlab program to invert the gravity anomaly over a 3D horizontal density interface by Parker–Oldenburg's algorithm. Computers & Geosciences 31 (4), 513–520.

Nagendra, R., Prasad, P.V.S., Bhimasankaram, V.L.S., 1996. Forward and inverse computer modeling of a gravity field resulting from a density interface using Parker–Oldenburg method. Computers & Geosciences 22 (3), 227–237.

Oldenburg, D.W., 1974. The inversion and interpretation of gravity anomalies. Geophysics 39 (4), 526–536.

Parker, R.L., 1973. The rapid calculation of potential anomalies. Geophysical Journal of the Royal Astronomical Society 31, 447–455.

Radhakrishna Murthy. I. V., Rama Rao, P., Jagannadha Rao, 1990. The density difference and generalized programs for two- and three-dimensional gravity modelling. Computers & Geosciences. v. 16. 277-287.

Syberg, F.J.R., 1972. A Fourier method for the regional residual problem of potential fields. Geophysical Prospecting 20, 47–75.

Vicki Langenheim, Viki Bankey, 1997. Introduction to Potential fields: Gravity. Pat Hill U.S. Geological Survey, FS-239-95

APPLICATION OF SELF-POTENTIAL METHOD FOR COAL FIRE DETECTION OVER JHARIA COAL FIELD

Abhay Kumar Bharti, S.K.Pal* and Jitendra Vaish

Department of Applied Geophysics, Indian School of Mines, Dhanbad – 826 004, India

sanjitism@gmail.com

Underground coal fires of Jharia coal field pose a great threat to Indian national economy. Coal fires results to the loss of valuable economic resources, emission of greenhouse gases, toxic gases and vegetation deterioration. The present study deals with the mapping and understanding of coal fire of Jharia coal field, India on the basis of the self-potential anomalies derived from two aspects: one is the redox potential generated by the oxidation of coal and the other is the Thomson potential caused by temperature gradients.

Most of the SP anomaly corroborated with coal fire and non coal fire regions subsequent to their surface characteristic with better agreement. The relatively high SP anomalies with short wavelength

indicate shallowly buried coal fire and the temperature near the ground surface is high. Whereas, the relatively low SP anomalies with longer wavelength indicate the fire is of deep source and temperature anomalies may not exist on the ground surface.

Conversely, if negative anomalies are measured, that means the fire is deeply buried, and temperature anomalies may not exist on the ground surface.

Introduction:

Coal-seam fire is a generic name given to in situ burning coal. The ignition of coal-seam fire can be (1) spontaneous, e.g., due to lightning, grass or forest fires, or through the direct influence of oxygen through exothermic reactions, or (2) anthropogenic (DeKok, 1986; Pone et al., 2007; Carras et al., 2009). Jharia coal-field has been burning underground for nearly a century and hosts the maximum number of uncontrollable surface and subsurface coal fires in India (Chatterjee et al., 2006). The self-potential method has been qualitatively used to identify the location of coal seam fires (Corwin and Hoover, 1979; Shao et al.,2014 ; Revil et al., 2013, Karaoulis,2014).

Theory

Self-potential is a non-invasive geophysical method that measures the natural potential of the earth (Nyquist and Corry, 2002). This method is called non-invasive because it does not cause any disturbance to the earth. Potential measurements are made between two points on the surface of earth's surface. The self-potential method was initially proposed by Robert Fox in 1830 (Reynolds, 2011) by using a copperplate electrode with a galvanometer measuring device for detecting the copper-sulfide deposits in Cornwall, England. The self-potential method has been used since 1920 as a complementary application in the exploration of metal deposits. The self-potential anomalies in coal fire areas derive from two aspects: one is the redox potential generated by the oxidation of coal; the other is the Thomson potential caused by temperature gradients. Violent oxidation reactions (combustion of coal) occur between underground coal and oxygen that penetrates into coal seams. The coal looses the electrons and becomes positively charged, forming an oxidation zone around the burning coal. Some of the electrons from the burning coal will migrate to the ground surface, resulting in the formation of a relative reduction zone near the ground surface, which is negatively charged. Consequently, a redox potential field is formed between the burning coal and the ground surface.

Further, the combustion of underground coal releases a large amount of heat. The temperature of the rock and coal around the burning center is high, which is generally several hundred degrees Celsius and may even exceed one thousand degree Celsius. However, due to the high heat capacity and low thermal conductivity of sedimentary rocks, it is difficult for heat to transfer to the ground surface. Therefore, the temperature of the ground surface is much lower than the burning center. The temperature difference between two points in a conductor or a semiconductor results in a voltage difference between those two points. A schematic model is shown in Fig.1 explaining the mechanism of self-potential anomalies in the coal fire area (Shao et al., 2014). The electrons at the hot end are more energetic and therefore have greater velocities than those at the cold end. Consequently, there is a net diffusion of electrons from the hot end toward the cold end, which causes the hot end to be positively charged and accumulates electrons at the cold end. This situation prevails until an electric field develops between the positive ions in the hot region and the excess electrons in the cooler region, preventing further electron motion from the hot to the cold end. Therefore, a voltage called Thomson potential is developed between the hot and the cold ends.

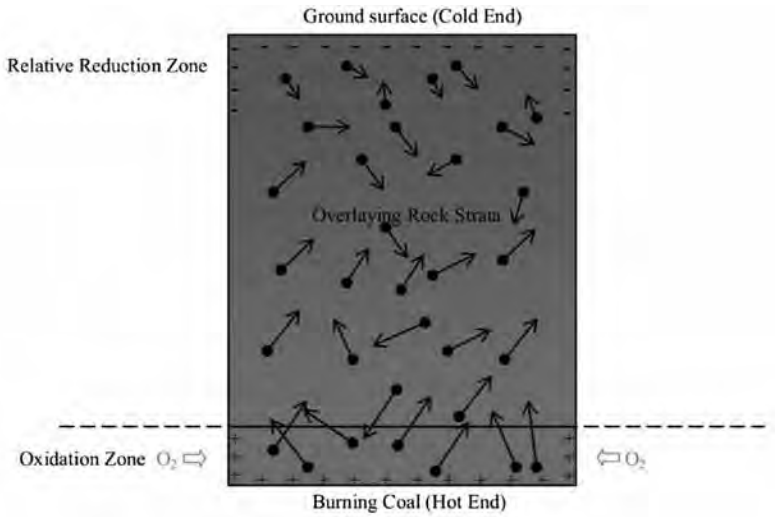

Fig.1 *Schematic model explaining the mechanism of self-potential anomalies in the coal fire affected area. The red and blue color means the hot and cold regions, respectively (Shao, et al.2014).*

Results and discussion:

Self Potential anomaly variation along a profile of 130m length over a region of coal fire affected in Sudamdih colliery, Jharia coal field, India is shown in Fig.2. From Fig.2 total three two coal fire affected regions have been delineated. The **locations-1** and 2 are characterized by shallow coal fire activity with depth of about 6m and 8m, respectively. Whereas, the location-3 is characterized by deep source coal fire activity with depth of about 60m.

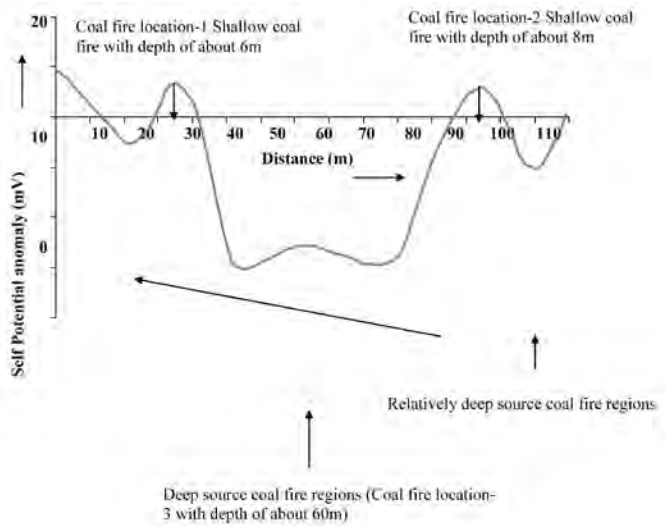

Fig.2 *Self Potential anomaly variation along the profile showing different zone of shallow and deep source coal fire regions*

Conclusion:

The redox potential and Thomson potential, resulting from the combustion of coal and high temperature, lead to self-potential anomalies in coal fire areas. Positive anomalies indicate a shallowly buried fire, and negative anomalies indicate a deeply buried fire.

Acknowledgements:

The authors wish to thank to the Director, ISM and HOD, Department of Applied Geophysics, ISM, Dhanbad for their keen interest in this study. Authors are thankful to DST for funding a project (SB/S4/ES-640/2012) on geotechnical characterization of Jharia coal field area using Geophysical techniques.

References

Carras, J. N., S. J. Day, A. Saghafi, and D. J. Williams, 2009, Greenhouse gas emissions from low temperature oxidation and spontaneous combustion at open-cut coal mines in Australia: International Journal of Coal Geology, 78, 161–168, doi: 10.1016/j .coal.2008.12.001

Corwin, R. F., and D. B. Hoover, 1979, The self-potential method in geothermal exploration: Geophysics, 44, 226–245, doi: 10.1190/1.1440964.

DeKok, D., 1986, Unseen danger: A tragedy of people, government, and the Centralia mine fire: University of Pennsylvania Press, http://daviddekok .com/.

Karaoulis, M., Revil, A., and Mao, D.,2014 Localization of a coal seam fire using combined self-potential and resistivity data. International Journal of Coal Geology 128–129, 109–118.

Nyquist, J.E., Corry, C.E., 2002. Self-potential: the ugly duckling of environmental geophysics. Lead. Edge 21 (5), 446–451.

Pone, J. D., N. Hein, K. A. A. Stracher, G. B. Annegarn, H. J. Finkleman, and D. R. Blake, 2007, The spontaneous combustion of coal and its byproducts in the Witbank and Sasolburg coalfields of South Africa: International Journal of Coal Geology, 72, 124–140, doi: 10.1016/j .coal.2007.01.001.

Reynolds, J.M., 2011. An Introduction to Applied and Environmental Geophysics [M]. Wiley. com.

Revil, A., Karaoulis, M., Srivastava, S., and Byrdina, S., 2013.hermoelectric self-potential and resistivity data localize the burning front of underground coal fires. Geophysics, 78(5), B259–B273.

Shao, Z., Wang , D., Wang, Y., Zhong, X., 2014. Theory and application of magnetic and self-potential methods in the detection of the Heshituoluogai coal fire, China. Journal of Applied Geophysics, 104, 64–74.

AUDIOMAGNETOTELLURIC (AMT) RESULTS OVER BAKRESWAR HOT SPRING (BHS)

Anurag Tripathi*, Shalivahan, Ved Prakash Maurya, Shailendra Singh and Ashishkumar Bage

Applied Geophysics Department, ISM Dhanbad, 826004, India

** anuragtripathiism@gmail.com*

An Audiomagnetotelluric (AMT) study has been carried out to identify the source of geothermal reservoir of the Bakreswar Hot Spring (BHS). The Geothermal Province of Bakreswar is located in Birbhum district of West Bengal belongs to the Chotanagpur gneissic complex in the eastern part of Peninsular India. The main hot spring is located at Bakreswar 23°52′48″ N; 87°22′40″ E. The Hot spring are located on or close to major fault/shear zones within Precambrian crystalline and the rock types vary from granite gneiss to migmatite and even graded to granulites and charnokites at some places. An Audiomagnetotelluric (AMT) studies carried out by Sinharay et al. (2010) in the western part of Bakreswar geothermal region. AMT survey shows that the NS fault close to Bakreswar, there is no deep geoelectrical structure (≤ 300 m), which cannot act as the source of Bakreswar hydrothermal system. The subsurface information below the fault zone is resistive up to a great depth which indicate the absence of a heat source. They further, suggested that source may be ~15 km to NW of BHS. Thus a 20 km N-S profile taken perpendicular to BHS which is ~ 15 km away from BHS. Which contain seven AMT soundings was taken to delineate possible geothermal reservoir. The apparent resistivity and phase response were calculated for each AMT sites. Measured field components (E and H) are used to calculate Impedance tensors (Z) for each frequency of a particular site. The impedance tensor matrix was used to find out the geoelectric strike direction and the dimensionality of the subsurface

structure from skew, ellipticity, and tipper. These analysis shows the skew values are generally less than 0.1 and tipper values are less than 0.5 indicating the area is mainly 2-D in nature. Some site shows higher tipper and skew value. Therefore, 2D Non-linear conjugate gradient (NLCG) inversion technique used for the electrical conductivity over geothermal province. 2D modelling shows that source of BHS is not exactly below the hot springs. The geothermal reservoir is about 15 km to the NW of BHS. The N-S profile indicates the presence of geothermal reservoir about 15 km from west of BHS at a depth of about 1km.

References

Majumdar, S. K., 1988, Crustal evaluation of Chotanagpur gneiss complex and mica belt of Bihar: Memor., Geo. Surv. Ind., 8, 49-84.

Majumdar, R.K., Majumdar, N. and Mukherjee, A.L., 2000, Geoelectric investigations in Bakreswargothermal area, West Bengal, India: Journal of Applied Geophysics,45,187-202.

Majumdar, R. K., Majumdar, N., and Mukherjee, A.L., 2000, Geoelectric investigations in Bakreswar geothermal area, West Bengal, India: J. Appl. Geophys., 45, 187-202.

Mukherjee, A. L., and Majumdar L. K., 1999, Hydrology and convective heat flow of Bakreswar thermal spring area, Birbhum district, West Bengal in Proc. Golden Jubilee Seminar on Exploration Geophysics: Geol. Surv. Ind., Spec. Pub., 49, 219-228.

Mukhopadhyay, D. K., 1996, Geothermal parameters and thermal energy potential of Bakreswar, Tantloie group of hot springs in Birbhum district, West Bengal and Dumka district, Bihar, in U. L. Pitale and R. N. Padhi, eds., Geothermal energy in India: Geological Survey of India, Special Publication 45, 87–98

Narula, P.L., Acharya, S. K., and Banerjee, J., 2000, Seismotectonic atlas of India and its environs: Geo. Surv. of India, Kolkata, India.

Sinharay, Rajib K., Shalivahan, and Bhattacharya, Bimalendu B., 2001, An anlysis of magnetotelluric (MT) data over geothermal region of Bakreswar, West Bengal: Journal of Geophysics,**XXII**,31-39.

Sinharay, Rajib K., Shalivahan, and Bhattacharya, Bimalendu B., 2010, Audiomagnetotelluric studies to trace the hydrological system of thermal fluid flow of Bakreswar Hot Spring, Eastern India: A case history, Geophysics, 75, 187-195.

HYDROGRAPHIC SURVEY FOR ARCHAEOLOGICAL AND GEOLOGICAL EVIDENCES

R. Shyam, M. Dixit and S. K. Aggarwal

Institute of Seismological Research, Gandhinagar (Gujarat)

radhekr1990@gmail.com

The hydrographic survey is a tool, which is mainly applied for various marine services, such as for oil and gas sector, offshore renewable energy sector, environmental impact monitoring, dredging of marine constructions, etc. The survey is based on the principle of acoustic seismic sounding. The hydrographic survey deals with side scan sonar, sub bottom profiler, eco sounders and magnetometer instruments. These instruments provide high resolution images of the sub-surface, sea bed data and information. The hydrographic survey generally carried out before offshore construction because of precise pipe line laying, platform construction, jacket installation, sub-sea installation etc. With the help of hydrographic images we can find the sea water depth, nature of sea-bed, nearby environmental condition, to propose the suitable construction location under sea.

The first author performed the hydrographic survey in gulf of Persia in a region of 1.0 square km profile during his M. Tech. dissertation at Daniel Surveying Ltd. Sharjah (UAE). The objective of the survey was to collect Geophysical data in the survey areas, to enable engineering, designing and installation of platforms, sub-sea structures, pipelines and to locate potential hazards within the survey area. We had taken 10 profiles along the tracks in N-S directions with 100 m spacing and 5 across

the tracks in E-W direction with 200m spacing with sample interval 2 mille second. We performed the survey navigation using GPS / DGPS (Positioning) system in gulf.

The main aim of the survey was to achieve different objectives and we have recognized the sub-sea features, such as ferrous material, sea morphology, and presence of pipelines, telecommunication cables, bathymetric and depth of first reflector. We found the bathymetric range 55 to 70 meter and feature of some ferrous material which could be the presence of pipelines, the sinking-ship and demolish platforms. We identify the depth of first reflector which varies from 15 to 25m. We also demarcate pock marks of about 2 to 3m dimension.

The side scan sonar identifies the nature of the soil, types of sea-floor and features present on the sea bed which are shown in **Figure 1**. The sub bottom profiler identifies Sub- sea morphology and subsurface information as shown in **Figure 2**. The magnetometer provides the information about the magnetic material in vicinity of the site as shown in **Figure 3**. The echo sounder identifies the depth of the sea-bed and imaging of the sea-bed. By processing and correlation of all these data we marked various anomalous features as shown in **Figure 4**, like ferrous material and pock marks etc. We can also estimate the physical property of sea water like conductivity, density, temperature, salinity at a point from these datasets.

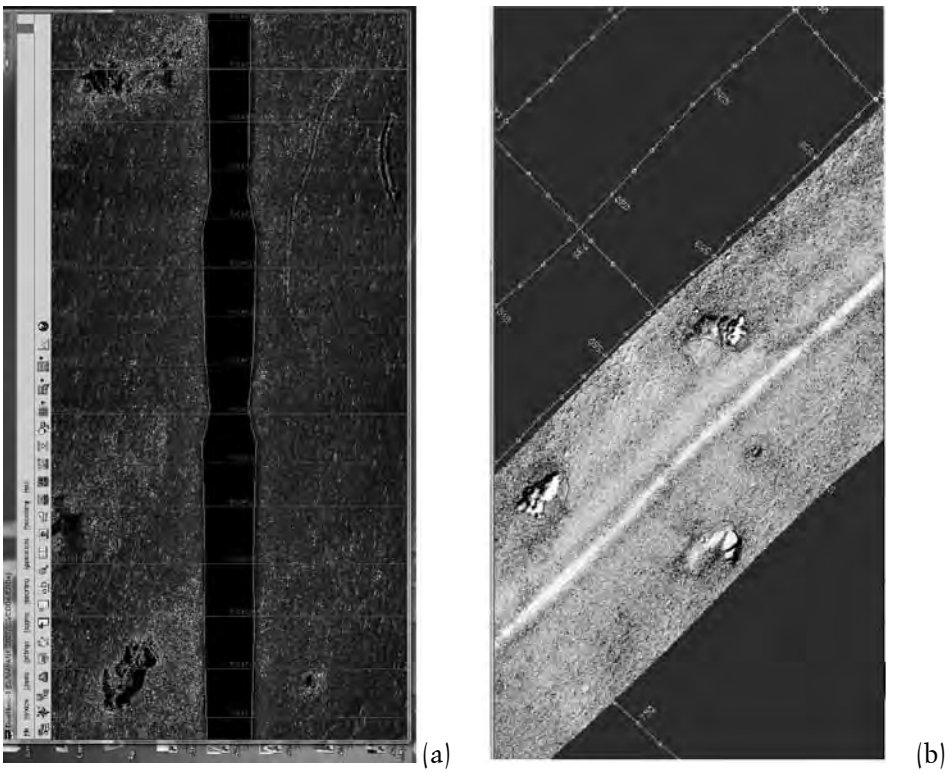

(a) (b)

Figure1: (a) *Shows a processed image of single track of side scan sonar in survey profile* **(b)** *Interpretation of same track using AutoCad software to locate anomaly.*

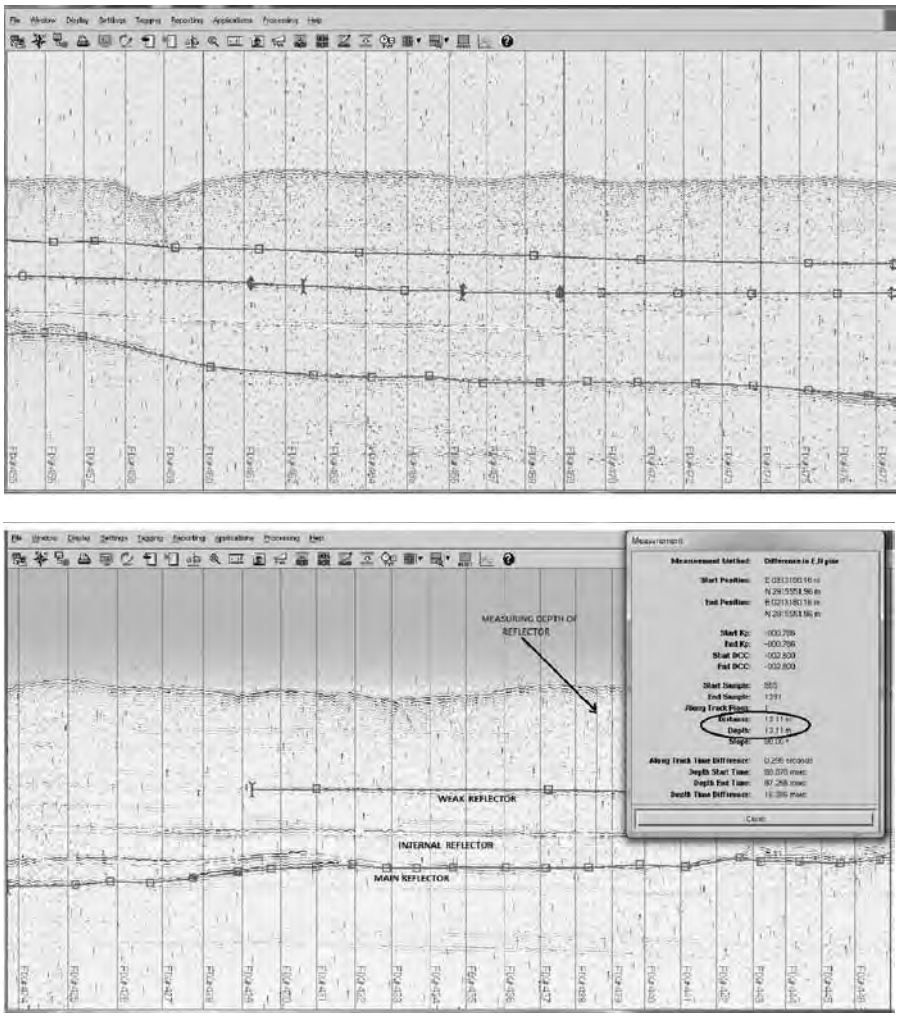

(a)

(b)

Figure2: (a) *Shows a processed image of sub surface sea bed from sub bottom profiler in single track.* **(b)** *Interpretation of same track to identify depth of week and strong reflectors.*

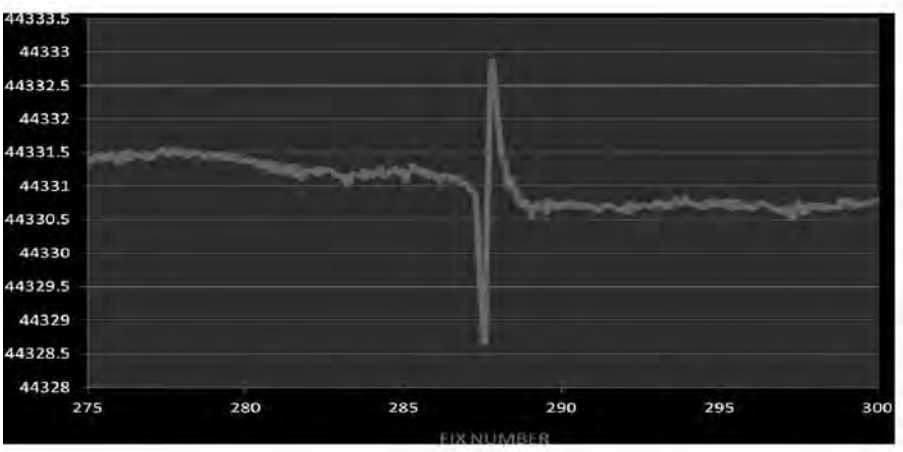

Figure3: *Shows the image of ferrous material identify by strong spike using Magnetometer data in a track.*

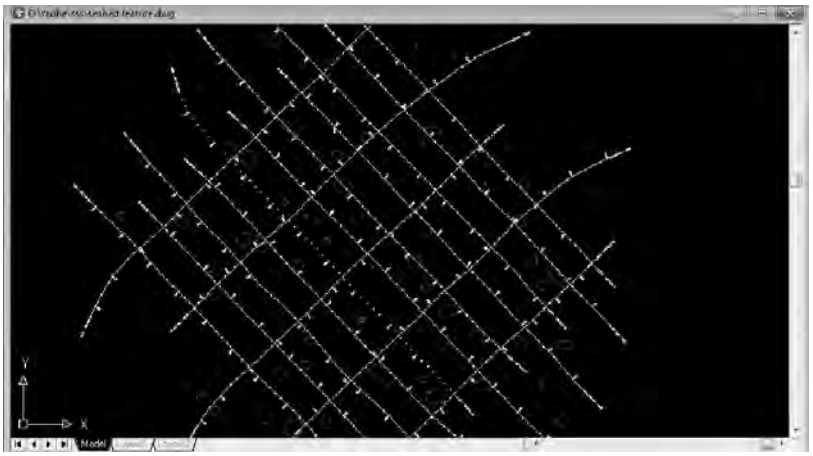

Figure4: Represents the AutoCad image of complete survey area anomalies using side scan sonar.

INTRODUCTION OF ROBOTICS IN OIL WELL LOGGING AND ITS APPLICATIONS

***Nitin Lahkar and Rishiraj Goswami**

Petroleum Engineering, Dibrugarh University Institute of Engineering and Technology (DUIET)
Dibrugarh University
**nitinlahkar@gmail.com*

The hour at hand calls for rapid innovation and drastic introduction of new technology to minimise problems in Oil and Gas Industry and to meet the growing need for Petroleum in all parts of the world. "Oil Well Logging" or the practice of making a detailed record (a well log) of the geologic formations penetrated by a borehole is an important practice in the Oil and Gas industry. Although a lot of research has been undertaken in this field, some basic limitations still exist. One of the main arenas or venues where plethora of problems arises is in logistically challenged areas. Accessibility and availability of efficient manpower, resources and technology is very time consuming, restricted and often costly in these areas. So, in this regard, the main challenge is to decrease the Non Productive Time (NPT) and Huge Mechanical Requirements involved in the conventional logging process. The thought for the solution to this problem has given rise to a revolutionary concept called the "Robotic Logging Technology". Robotic logging technology promises the advent of successful logging in all kinds of wells and trajectories. It consists of a wireless logging tool controlled from the surface. This eliminates the need for the logging truck to be summoned which in turn saves precious rig time and in turn also reduces Bulk Mechanical Requirements by introduction of Robotics and Automation in the Oil Well Logging Technology.The robotic logging tool here, is designed such that it can move inside the well by different proposed mechanisms and models listed in the full paper as TYPE A, TYPE B and TYPE C. These types are classified on the basis of their operational technology, movement and conditions/wells in which the tool is to be used. Thus, depending on subsurface conditions, energy sources available and convenience the TYPE of Robotic model will be selected.

Advantages over Conventional Logging Techniques-Reduction in Non Productive time

Lesser energy requirements

Very fast action as compared to all other forms of logging

Can perform well in all kinds of well trajectories (vertical/horizontal/inclined)

SESSION – III
MARINE GEOSCIENCES

SEAFLOOR SEDIMENT CLASSIFICATION USING AN INTEGRATED APPROACH OF NEURAL NETWORKS AND FUZZY ALGORITHM

***Ratan Srivastava, Abhishek Tyagi and John Kurian P.**
National Centre for Antarctic and Ocean Research, Headland-Sada, Goa-403804
ratan@ncaor.gov.in

Acoustic characterization studies of seafloor sediments in western continental shelf of India has been undertaken by using the artificial neural network and fuzzy approach. The Self Organizing Maps (SOM) and Gath Geva fuzzy clustering methods are applied to Multibeam bathymetry and backscatter data collected in the study area Off-Marmugao, Goa. The features having the most discriminating characteristics are used to classify the seafloor sediments. Backscatter and roughness are the input features for classification of seafloor sediments. Backscatter is found to be the most discriminating feature for sediment classification and roughness (extracted from bathymetry), when used along with backscatter, increases the spatial resolution and preserves angular information on the data. The technique of SOM is applied to backscatter data and roughness to unravel the maximum possible number of classes of various shape and sizes contained in the datasets, where a priori knowledge of sediment type is not available. The output of SOM is used as an initial partition matrix for Gath Geva input. The technique of Gath Geva clustering along with validation techniques is further utilised to cross verify the results of SOM and to identify the sediments of distinct, overlapping classes and map the sediment distribution along the tracklines in the study area. Comparison of results with ground truth revealed that this integrated approach of SOM and Gath Geva clustering is useful for classification of seafloor sediments without having a priori knowledge of sediment type of that area.

WAVE FIELD SEPARATION OF OBS DATA TO ENHANCE THE SIGNAL TO NOISE RATIO (SNR)

N.Satyavani and Kalachand Sain
Gas Hydrate Group, CSIR-National Geophysical Research Institute, Hyderabad, India.
satyavani_nittala@yahoo.com

The multi-component Ocean Bottom Seismometer (OBS) data captures the entire wave field by employing 3 (Z,X,Y) component geophone and one hydrophone (P). However, this recording includes the free surface multiples that interfere with the up/down going wavefield and need to be removed before further processing. The hydrophone sensors are pressure dependent and direction independent while the geophones are particle motion and direction dependent. This discerning aspect can be utilized to eliminate the free surface multiples by simple summation of the P and Z components. PZ summation is very effective in removing all the receiver side multiples (ghost) arrivals, while it does not effectively remove the source side multiples. In order to remove the source side multiples, we have to separate the full wavefield into the constituent up and downgoing fields and this can be achieved by combining the P and Z components. Once the components are separated, the deconvolution of the upgoing field with the downgoing field is carried out which results in obtaining the multiple free (source and receiver) wave field (PP reflectivity). Similarly the PS reflectivity can also be extracted by deconvolution of the radial (X) component of the OBS data with the downgoing wavefield. This procedure increases the SNR to a significant level and the efficacy of this method is illustrated in the present work, using the OBS data acquired in the Mahanadi basin. In addition to the noise free P wave field, we have also obtained the converted (PS) wave field using the above approach. A remarked increase in the SNR is noticed in the PP reflectivity while there is a an increased level of resolution in the PS wavefield compared to the radial component.

SATURATION OF GAS HYDRATE FROM 2-D P-WAVE VELOCITY MODEL USING OBS DATA IN MAHANADI BASIN

Soumya Jana*, Maheswar Ojha and Kalachand Sain
CSIR- National Geophysical Research Institute, Uppal Road, Hyderabad-500007
soumya.jana89@gmail.com

Multi channel seismic (MCS) and ocean bottom seismic (OBS) data were acquired in 2010 in Mahanadi basin, eastern Indian offshore showing wide spread occurrences of bottom simulating reflector (BSR) which indicate presence gas hydrate. In this paper, we have derived P-wave velocity using reflection travel time inversion algorithm based on the ray path tracing. For travel time inversion, both MCS and OBS data have been used. To avoid the trade-off between depth and velocity in travel time inversion, depth is kept fixed and only velocity is inverted to match the calculated travel time with observed travel time picked from the OBS data. Depth of each layer in the velocity model is selected from depth section of MCS data. Initially a forward modelling is performed to match observed and calculated travel time and later, a damped least square inversion is used to update the model parameters with uncertainty ±10 m in depth and ±20 m/s in velocity. The stopping criterion for inversion algorithm is based on the root-mean-square travel time residual, chi-square distribution and ability to calculate travel time at all observed points. From this derived velocity, we have estimated hydrate saturation using three phase Biot-type equation. Here we have considered five 2-D MCS lines at ~1.5km spacing, where five OBSs are situated at ~ 1.5km spacing along each MCS line.

GEOCHEMICAL FRACTIONATION OF NI, CU AND PB IN DEEP SEA SEDIMENTS FROM CENTRAL INDIAN OCEAN BASIN

Simontini Sensarma[1,*], Parthasarathi Chakraborty[1], Ranadip Banerjee[1], Subir Mukhopadhyay[2]
[1]*Geological Oceanographic Division, National Institute of Oceanography (CSIR), Dona Paula, Goa - 403004*
[2]*Department of Geological Sciences, Jadavpur University, Kolkata, India (700032)*
**ssensarma@nio.org*

Sequential extraction protocolwas used to investigate distribution and chemical speciation ofNi,Cu and Pb in deep sea sediments, collected from four environmentally different locations (terrigenous, terrigenous-siliceous transition,siliceous and red clay sediments) of Central Indian Ocean Basin (CIB). This study showed that the highest fractions of all the metals were associated with Fe-Mn oxyhydroxide phase, followed by the residual phase (which is mainly associated with the structurally bound silicate minerals) in all the studied sediment.

Further speciation study (by using sequential extraction protocol proposed by Poulton and Canfield to investigate the speciation of these metals in Fe/Mn oxyhydroxide phase) showed that maximum concentration of all the elements was mainly associated with "easily reducibleoxide phase" (which is mainly Mn-oxides) in the sediments.

Major element chemistry of these sediment showed that the major part of manganese has an "excess" source(i.e. non-terrigenous in nature) with strong positive correlation with Ca, P, Ni and Cu, but not with Pb. Whereas, the "excess" part of iron, which is marginally lower than the detrital part, showed excellent positive correlation with Pb but none with Ni and Cu.

These results show an increased tendency of Cu and Ni to get incorporated into the deep sea sediment via non-detrital Mn-oxidefraction whereas, Pb gets incorporated via amorphous Fe-oxide into the sediment.

VARIATION OF S AND SR ISOTOPES IN HYDROTHERMAL BARITE CHIMNEY FROM FRANKLIN SEAMOUNT: CONSTRAINTS ON FLUID COMPOSITION

***Durbar Ray[1], Ranadip Banerjee[1], S. Balakrishnan[2], Anil L. Paropkari[1] and Subir Mukhopadhyay[3]**

[1] CSIR-National Institute of Oceanography, Dona Paula, Goa-403004, India.
[2] Department of Earth Sciences, Pondicherry University, Puduchery-605014, India.
[3] Department of Geological Sciences, Jadavpur University, Kolkata-700032, India.

Isotopic composition of strontium and sulfur in six layers across the horizontal section of a hydrothermal barite chimney, from the Franklin seamount, Woodlark Basin has been investigated. Sr-isotope ratio (i.e., $^{87}Sr/^{86}Sr$) in all layers varies within an interval between 0.70478 - 0.70493. Less radiogenic Sr-isotopic composition in bulk sample, relative to seawater ($^{87}Sr/^{86}Sr$ = 0.70917) likely indicate considerable leaching of subsurface magma or rocks characterized with lower isotope ratio is involved in formation of this chimney. Sulfur isotope fractionation in these samples ($\delta^{34}S$) range between 19.5 - 20.6‰, which was lighter than seawater sulfate ($\delta^{34}S \geq 21‰$). Results of both the isotopes and absence of H_2S in fluid suggest disproportionation of magmatic volatiles (e.g. SO_2) rather than oxidation of dissolved sulfide, as major sources of sulfate for this barite deposit. Moreover, distribution of isotopic composition showed systematic changes across this chimney section, possibly indicating temporal change in the physiochemical nature of the end-member fluid throughout the growth history of the chimney. The outermost rim of the chimney, containing maximum amount of Sr (0.7%), also has maximum enrichment of heavy S and Sr-isotopes ($\delta^{34}S$ = 20.58‰, $^{87}Sr/^{86}Sr$ = 0.70493). More abundance of heavy S-isotope probably indicates more contribution of seawater sulfate in hydrothermal fluid during initial stage of chimney development. Further gradual thickening of inner portion of chimney wall, due to precipitation hydrothermal barite, causes gradual depletion in bulk Sr content (0.42 - 0.49%) and enrichment in lighter isotopes. Thus, intermediate layers, between outermost rim to inner orifice of chimney section, representing the active phase of the chimney showed a steady drop in heavy Sr ($^{87}Sr/^{86}Sr$ = 0.70491 to 0.70478) and S-isotope ($\delta^{34}S$ = 20.42 to 19.48‰). Steady upward flow during active phase carried more magmatic components in hydrothermal fluid. In contrast, silica-rich layer surrounding the fluid conduit showed increase in Sr (0.63%) and heavy S- isotope ($\delta^{34}S$ = 20.3‰) and this suggest increasing influence of percolating seawater during late stage paragenetic shift towards the waning phase of this extinct chimney. Thus, present isotopic investigation corroborates the three stage growth model of this chimney which was developed earlier on the basis of basic mineralogy and major element composition.

MERCURY PROFILES IN SEDIMENT CORES FROM THE MARGINAL HIGH OF ARABIAN SEA: INFLUENCES OF REDOX MEDIATED REACTION AND ATMOSPHERIC MERCURY DEPOSITION

Parthasarathi Chakraborty*, Krushna Vudamala, Kartheek Chennuri, Kazip A, Linsy P., Darwin Ramteke, Tyson Sebastian, Saranya Jayachandran, Chandan Naik, Richita Naik, B. Nagender Nath

National Institute of Oceanography (CSIR), India, Dona Paula, Goa, 403004, India,
**pchak@nio.org*

Total Hg distributions and its speciation was determined for two sediment cores collected from the western continental marginal high (under anoxic condition) of the Indian Ocean. Total Hg content in the sediment cores was found to gradually increase (by ~ 2 times) towards the surface of both the cores. The evidence suggests that redox mediated reactions (Fe (II)/Fe (III) and Mn (IV)/Mn(VI) cycling) had no effect on the Hg profiles in the sediment cores collected from the anoxic environments. Mercury was preferentially bound to sulphide in the sediments down the core. This study suggests that increasing atmospheric Hg deposition attributed to the increasing Hg concentration on the surface sediment of both the cores.

METHANE-DERIVED AUTHIGENIC CARBONATES - A PROXY FOR GAS HYDRATE EXPLORATION: A COMPARATIVE STUDY FROM THE CONTINENTAL MARGINS OF INDIA

M. Kocherla and Surabhi Pillai

CSIR-National Institute of Oceanography, Dona Paula, Goa-403004, India

˙kocherla@nio.org

We report the abundant occurrence of authigenic Fe-rich carbonates, high Mg-calcite (HMC) nodules/precipitates from 17 long cores recovered from the Krishna-Godavari Basin (K-G Basin), Bay of Bengal. The cores were collected as part of our gas hydrate exploration program on board R/V Marion Dufresne (MD-161: May, 2007) under various geological environments, including mud diapirs, mass flows, and hemipelagic sediments over a water depth range of 740-2080 m from K-G Basin. Authigenic carbonates are distributed at different depths (5-29 mbsf) within the sediment section ranging from 1 mm to 12 cm in diameter and display irregular shapes and exhibit clear vertical zonation. From the cores, 173 carbonate samples have been investigated for their depth distribution, mineralogy, geochemical and stable isotopic composition.Bulk mineralogical compositions by X-ray diffraction (XRD) revealed that the carbonates are predominantly soft friable Fe-rich carbonates nodules with inclusions of strontianite, witherite, cerussite and occasionally high-mg calcite (HMC) at specific sub-surface depths but rarely aragonite or low-Mg calcite (LMC) with trace amounts of pyrites and barites. The stable carbon isotopic composition of the carbonates (around -50 ‰) allows the differentiation into methane-related carbonates (HMC), especially at Sites 8 and 15, but also in low abundance at Sites 1, 5, 9 and 12. Results indicate that the carbonates at Site 8 and 15 represent paleo methane seepage locations. The Fe-rich carbonates occur abundantly at many sites in the K-G Basin. Their varying carbon isotopic composition indicates that probably not only organic sulphate reduction but also methanogenesis are the responsible processes for their formation.Different types of carbonate morphologies ranging from finely dispersed crystals to massive nodules and chimneys are the products of two different fluids migration systems of dispersive to diffusive respectively and the occurrence of similar age carbonate deposits associated with methane seepage throughout the K-G Basin indicate a regional supply of methane.Although the presence of gas charged sediments and sub-surface gas-escape features has been inferred from shallow seismic studies and possible occurrence of gas hydrates by BSR's, but evaluation of pore-fluid chemistry and stable carbon isotope signatures of authigenic carbonates are not indicative of enhanced methane flux in this region and argue against a precipitation of carbonates due to AOM and refute the possible connection of methane from the shallow gas charged sediments to the observed carbonates or suspected BSR's in the Western continental margin of Inida.

Introduction

Methane-derived authigenic carbonates are indirect indicators of high methane flux region (such as gas seepages and pore fluid venting) which are common in areas overlying gas hydrate deposits. Precipitation and consequent preservation of authigenic carbonates is mainly due to increase in pore water bicarbonate (HCO_3^-) ion concentration and anaerobic oxidation of methane (AOM) from gas hydrate system and concomitant sulfate reduction process in the sediment sequence. Authigenic carbonates can also be formed due to degradation of organic matter during early diagenesis. These processes increase pore water alkalinity by the production of bicarbonate (HCO_3^-) thus favouring precipitation of authigenic carbonate minerals in the shallow sub-surface. Determining which of the above two processes is responsible for the authigenic carbonate precipitation is very essential as it provides definite evidence for high methane fluxes either due to localized diagenetic processes or due to the presence of gas hydrates beneath. In marine sediments, methane migrates upward and reacts with sulfate at SMTZ and results in the formation of various authigenic minerals depending on the

fluids, gases and composition of the host sediments. The variety of authigenic minerals that are formed in cold seep environments provide diagnostic information on the chemistry of the diagenetic fluids, and therefore their mineralogy, morphology can be used to indicate the magnitude of methane flux and the depth of SMTZ and consequently the presence of underlying methane gas hydrate deposits.In the northern Indian Ocean occurrences of methane-derived authigenic carbonates are reported from the Krishna-Godavari basin, eastern continental margins of India and Makran accretionary prism off Pakistan in the Arabian Sea. Western continental margin is characterized by shallow gas charged sediments and several gas escape features. Geophysical studies in the western continental margin of India revealed the presence mud-diapirs and bottom simulating reflectors (BSRs) & vent-like features representing gas escape features from the sea floor. Recent drilling work carried out on-board JOIDES Resolution Leg-3A confirmed the presence of massive authigenic carbonate nodules/concretions along with more than 100 m thick accumulation of gas hydrates in Krishna-Godavari offshore basin, Bay of Bengal. Since occurrence of authigenic carbonates can help to decipher the source of gas seepages in an area we undertook a comparative study of authigenic carbonates from the both Eastern and Western continental margins of India (Fig.1).

Geological Settings

Eastern Continental Margin of India (ECMI): The study area in the K-G Basin lies in the middle of Eastern continental Margins of India (ECMI) which is a pericratonic rift basin (Rao, 2001) that evolved after the breakup of Gondwanaland around 130 Ma years ago (Powell et al., 1988; Scotese et al., 1988; Ramana et al., 1994). Onshore extension of K-G Basin is ~28,000 km^2 and its offshore extension is ~1, 45,000 km^2 (Ojha and Dubey, 2006). Much of the detrital influx into the K-G Basin is brought by the two major river systems: Krishna and Godavari Rivers. The sediment thickness ranges from 3-5 km in onshore region to ~8 km in the offshore portion of the basin (Prabhakar and Zutshi, 1993; Basti, 2007) with several cycles of deposition, ranging in age from late Carboniferous to Pleistocene. The sediment in the study area consists of silty clay with negligible amount of sand (Kocherla et al., 2006). The dominant clay fraction is montmorillonite with traces of illite and kaolinite.

In the K-G Basin, widespread presence of gas hydrate is manifested in the multi-channel seismic data in the form of bottom simulating reflectors (BSRs). Drilling and coring in the K-G Basin has confirmed the presence of gas hydrate (Collett et al., 2008). Several acoustic features related to fluid and/or gas migration have been reported in the shallow subsurface (Ramana et al., 2007; Ramana et al., 2009; Dewangan et al., 2010) suggesting active migration of methane in the study area. The geological and geochemical analyses of long sediment cores, acquired on-board the R/V *Marion Dufresne*, have confirmed paleo-methane seepage in the study area (Mazumdar et al., 2009). Slumping/sliding of slope sediments, associated with fluid and/or gas migration, has led to mass transport deposits in the K-G offshore basin (Ramprasad et al., 2011). Several bathymetric mounds formed due to shale tectonics are heavily faulted and show acoustic signatures of fluid and/or gas migration through the fault system (Dewangan et al., 2010). The analysis of available geophysical datasets such as multi-channel seismic, high resolution seismic, sub-bottom profiler, and multibeam bathymetry has divided the study area into distinct deposition environments, including mid-slope mini basins, in the north-east and south-west directions, bathymetry mounds, toe-thrust sedimentary ridges, and deep oceanic basin (Ramana et al., 2007; Ramana et al., 2009; Dewangan et al., 2010; Ramprasad et al., 2011). The sediments are nano fossil bearing clays with sand silt beds and terrigenous organic carbon content. The accumulation of total organic carbon (TOC) content of the sediments along ECMI has been enhanced as a consequence of the uplift and erosion of the Himalaya (Meyer and Dickens, 1992). The high sedimentation and the consequent rapid burial in the K-G Basin have resulted in preserving the TOC in the sediments. The environment shows dominance of carbonates mostly Fe-rich carbonates, occurring as nodules, crusts, hard grounds and fine grained bands.

Western Continental Margin of India (WCMI): The western continental margin of Indiais a passive margin and characterized by (i) NW-SE trending shelf more than 200 km wide in the north and about 50 km in the south near Cape Comorin, (ii) a straight outer edge limited by 200m isobaths, (iii) a narrow continental slope bounded by 200 and 2000m isobaths, (iv) deep sedimentary basins viz., Western Arabian Basin, Eastern Arabian Basin, Kori-Komorin Basin and Kerala-Konkan Basin and (v) several structural features such as Chagos-Laccadive Ridge, Laxmi Ridge, Pratap Ridge(east of Chagos Laccadive Ridge). Geographically Goa offshore (Eastern Arabian Basin) lies between the eastern end of Laxmi-Laccadive Ridge and the adjacent western continental slope of India (Biswas 1982; Kolla and Coumes 1987; NIO (2005). The depth in this basin ranges from 1800 to 3600m. Approximately 2.9 km thick sediments overlie the basement. The Indus River is the primary source of detrital sediment to this region. Average sedimentation rate in this region is 2-6 cm/ky over last 100 ky (Banakar et al 2005). The study area in the eastern Arabian Sea has oxic bottom waters (2665-3210 m) and overlain by the well-established OMZ in mid-depths (200 to 1500 m) (Parpokari et al., 1993). The sediments are characterised by low organic carbon content and abundance of nano fossils/ foram-rich nano-ooze. The inorganic carbon content is diluted by terrigenous input and ocean productivity. The sediments show illite as the dominant clay mineral. Authigenic carbonates are microscopic and inferred as being diagenetic in origin. Few large pyrites and mono sulphides are also observed at bottom depth of 130-190m. The occurrence of gas charged sediments and the presence of BSR's (possible gas hydrate horizons) have been detected along the western continental margin of India based on shallow seismic records (Veerayya et al 1998; Satyavani et al., 2005; Ramana et al., 2006; Dewangan and Ramprasad., 2007).

Samples and Methods

A total of 17 long cores (23-35 m long) were recovered over a water depth range of 740-2080 m from regions of elevated methane in the K-G Basin from the R/V Marion Dufresne using a Giant Calypso piston corer. A suite of authigenic carbonate nodules/precipitates from the sediment subsamples (5 to 29 mbsf) were isolated and washed with water to remove the salts and then washed in an ultrasonic bath for 15 min and dried and cleaned. Mineralogy, TIC, $CaCO_3$ and stable carbon isotopic compositions have determined for the carbonate precipitates. Typical carbonate nodules/precipitates were selected and powdered with an agate mortar and pestle for XRD analysis and stable isotope measurements. Bulk mineralogy of carbonate precipitates was carried out on randomly oriented samples using a Regaku X-ray diffractometer (Ultima-IV). All the carbonate samples were run from 25 to 35 °2θ at 1°/min scan speed using CuKα radiation (λ = 1.541838Å) at the National Institute of Oceanography, Goa India. The $MgCO_3$ (mole %) was calculated using an $MgCO_3$ content (mole %) - d-spacing standard curve in Hardy and Tucker (1988). Dried and disaggregated sediment samples were first examined under the binocular microscope (Nikon, SMZ-1500) and some selected grains/samples were examined under scanning electron microscope (JEOL-JSM 5800 LV1 at the National Institute of Oceanography, Goa India for their morphological studies. Several freshly broken surfaces of the carbonates have been investigated using Scanning Electron Microscopy (SEM) and Energy-dispersive X-ray spectroscopy (EDS) to understand textural, morphological characteristics and their mutual association. Carbon and oxygen isotope ratios of authigenic carbonate samples were determined with a Thermo Finnigan Delta plus XP continuous flow isotope ratio mass spectrometer attached to a GASBENCH II and equipped with a PAL auto sampler at the National Geophysical Research Institute, Hyderabad, India. The carbon isotope ratios are reported in standard $\delta^{13}C$ formats relative to VPDB standard. A sample reproducibility of 0.1‰ for both carbon and oxygen is reported here.

Results and Discussion

The down-core carbonate size distribution along with carbonate mineralogy shows that mostly carbonate nodules are confined to 5-29 mbsf within the sediment sequence ranging from 1 mm to 12 cm in diameter and display irregular shapes (Fig.2). The average thickness of the carbonate concretions range between 1 mm - 12 cm in diameter with a minimum being at stations 3,7,13,14,16 and17 (Fe-rich carbonates) and maximum at stations 8 and 9 HMC and LMC respectively. The $\delta^{13}C$ and $\delta^{18}O$ values for the Fe-rich carbonate nodules vary from -35.4 to +6.42 ‰ and -0.1 to 6.1 ‰ VPDB respectively. Whereas for the HMC nodules $\delta^{13}C$ and $\delta^{18}O$ range from -52.42 to -27.8 ‰ and 0.3 to +5.4 ‰ VPDB. Highly depleted carbon isotope ratios of HMC nodules indicate anaerobic oxidation of methane (AOM) as the primary source of bicarbonate ions and show characteristic finger printing isotopic composition for HMC and Fe-rich carbonates. The AOM is very evident at shallow depths of 5-29mbsf.A possible mechanism for widespread methane seepage in the Krishna-Godavari Basin could be a glacial sea level lowering shifting the bottom of the gas hydrate stability zone into shallower depths followed by gas hydrate decomposition in deeper sediments. This enhanced decomposition of gas hydrates may then generate an increase in methane outflow.

For the Western region the $\delta^{13}C$ values of the authigenic carbonates range between –0.63 and –8.12‰, and is attributed to a contribution of isotopically light CO_2 derived from the oxidation of sedimentary organic matter in the surficial sub-oxic Fe reduction and the bacterial sulphate reduction zone during early diagenesis. The observed CH_4 concentration does not show an appreciable increase with depth indicating that the contribution of CH_4 from the shallow sediments to authigenic carbonate formation is negligible. Although the presence of gas charged sediments and sub-surface gas-escape features in and around the study area has been inferred from shallow seismic studies and possible occurrence of gas hydrates by BSR's.But mineralogy morphology and stable carbon isotope signatures of authigenic carbonates and evaluation of pore-fluid chemistry are not indicative of enhanced methane flux in the region and argue against a precipitation of carbonates due to AOM and refute the possible connection of methane from the shallow gas charged sediments to the observed carbonates or suspected BSR's. The recent drilling carried by JOIDES Resolution (NGHP-Leg1) in the study area rules out the occurrence of BSR's due to gas hydrates and supports our contention. In the present study we report on the occurrence of different types of authigenic carbonates in sedimentary cores from both the Eastern and Western continental margins of India and discuss their origin based on their mineralogy, morphology and stable carbon isotopes signatures.

ConclusionsA variety of authigenic carbonates from 17 long cores (23-35 m long) were recovered at numerous locations in K-G Basin in the gas hydrate bearing sediments with wide variety of morphologies, predominantly as nodules followed by chimneys, tubules, bone-like structures, individual slabs, thinly lithified pavements, fine grained carbonate bands micro-nodules and as dispersed crystal aggregates. The carbonate size distribution along with their mineralogy show that they are confined to 5-29 mbsf within the sediment sequence ranging from 1 mm to 12 cm in diameter and display irregular shapes. The average thickness of the carbonate precipitates are minimum at sites 3, 7,13,14,16 and 17 (Fe-rich carbonates) and maximum at stations 5 (Fe-rich carbonates) 8 (HMC) and 9 (LMC), 12 (Fe-rich carbonates) and 15 (Fe-rich carbonates) and most of sites with massive carbonate nodules are associated with topographic mounds.

Highly depleted isotopic ratios of HMC advocate AOM as the primary source of bicarbonate ions and unambiguously indicate that the carbonates are predominantly derived from sedimentary methane via AOM. The carbon source for the formation of authigenic carbonates is attributed to gas

hydrates below and the carbonates were formed from the flow of methane-enriched fluids through fracture network formed because of shale diapirism reported in this region.

Different types of carbonate morphologies ranging from finely dispersed crystals to massive nodules and chimneys are the products of two different fluids migration systems of dispersive to diffusive respectively and the widely distributed methane seep carbonates suggest that they are related to similar age throughout the K-G Basin pointing to a large supply of methane and more regional acting mechanism rather than the site specific attributes. The detailed genetic framework is under investigation.

Dispersed authigenic carbonates are reported from five sediment cores from Goa offshore region central continental margin of western India between water depths 2665 to 3070 m. Morphological evidences such as euhedral carbonate crystals, slender radiating aragonite crystals and $\delta^{13}C$ values suggest that these carbonates are formed authigenically. The $\delta^{13}C$ values of the authigenic carbonates range between–0.63 and –8.12‰, and is attributed to a contribution of isotopically light CO_2 derived from the oxidation of sedimentary organic matter in the surficial sub-oxic Fe reduction and the bacterial sulphate reduction zone during early diagenesis.

Although the presence of gas charged sediments and sub-surface gas-escape features in and around the study area has been inferred from shallow seismic studies and possible occurrence of gas hydrates by BSR's, but mineralogy morphology and stable carbon isotope signatures of authigenic carbonates and evaluation of pore-fluid chemistry are not indicative of enhanced methane flux in the region and argue against a precipitation of carbonates due to AOM and refute the possible connection of methane from the shallow gas charged sediments to the observed carbonates or suspected BSR's. The recent drilling carried by JOIDES Resolution (NGHP-Leg1) in the study area rules out the occurrence of BSR's due to gas hydrates and supports our contention. Further studies are in progress for comprehensive understanding of the process involved.

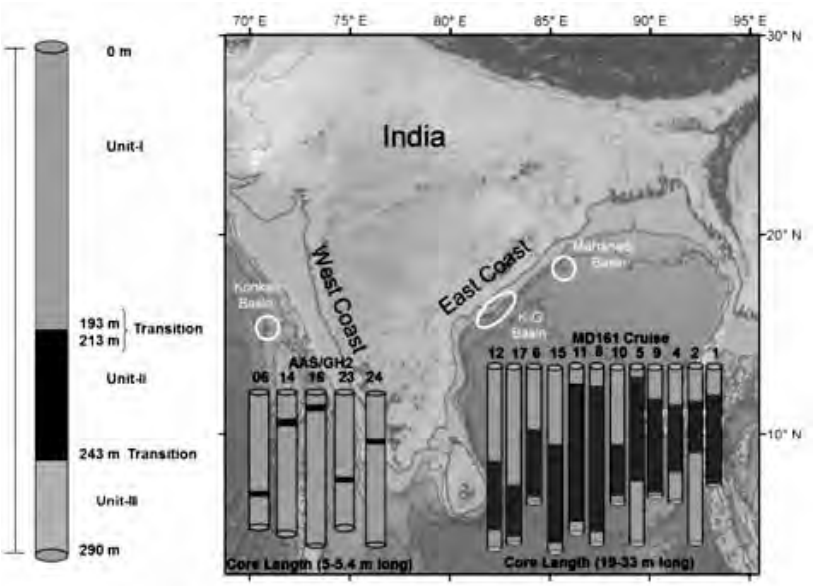

Figure-1. Map showing the core locations in the Eastern and Western Continental margins of India: 5 cores (5 m long from AAS/GH2 cruise and 290 m long ODP core from NGHP-01 Leg-1 and 17 cores (19-33 m long) from MD-161 cruise).

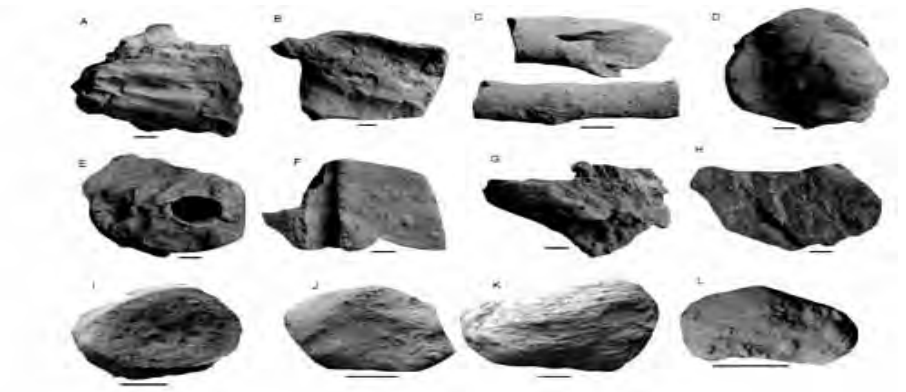

Figure-4. Morphology of authigenic Carbonate concretions: (A) tree trunk-like; (B) Chimney-like structures with conduits; (C) High-Mg calcite tubules with conduits; (D) Massive; (E) Chimney; (F) Slab with conduits (F) Fractured; ((H) Layered; highly lithified Fe-rich carbonates nodule; (J, K,) moderately lithified Fe-rich carbonatess nodules; (L) soft Fe-rich carbonates nodule. Scale bar represents 1cm (A-from site 8 at1656 cmbsf; B- from site 8 at 1650 cmbsf; C- from site 8 at 1752 cmbsf; D-from site 9 at 8800 cmbsf; E-H from site 15 at 2902 cmbsf; I- from site 2 at 8250 cmbsf; J-K from site 9 at 1625 cmbsf; L- from site 12 at 2225 cmbsf).

Acknowledgements

We thank Directors of CSIR-NIO, CSIR-NGRI, NCAOR, NIOT and secretary MoES, India, for supporting the study, facilities and permission to publish this work. H. Leau, head of the Oceanography Department, and P. Sangiardi, in charge of on-board operations of IPEV on board *RV Marion Dufresne* (MD-161) is thanked for providing on-board technical support and facilities. The authors also thank T. Ramprasad A. Mazumdar, P. Dewangan, M.J Gonsalvesand M. Joao for their valuable inputs. Mr.GirishPrabhu and Mr. Vijay Khedekar are thanked for their help during XRD and SEM operation and data acquisition respectively.

References

Banakar, V K., Oba, T., Chodankar, A. R., Kuramoto, T., Yamamoto, M., Minagawa, M., Monsoon related changes in the sea surface productivity and water column denitrification in the Eastern Arabian Sea during the last glacial cycle. Mar. Geol, 219, 99-108.

Bastia., 2007. Geologic settings and petroleum systems of India's east coast offshore basins, Concepts and Applications. Technology Publication, Dehradun, India.

Biswas 1982; Biswas, S.K., Rift basins in the western margin of India and their hydrocarbon prospects. AAPG Bulletin., 66,1497-1513.

Collet T., Riedel, M., Cochran, J., Boswell, R., Presley, J., Kumar P., Sathe, A., Sethi, A., Lall, M. and Sibal, V., 2008. Results of the Indian National Gas Hydrate Program Expedition 01 initial reports, Dir. Gen. of Hydrocarbons, Min. of Pet. and Nat. Gas, New Delhi.

Dewangan, P., Ramprasad, T., Ramana, M.V., Mazumdar, A., Desa, M. and Badesab, F.K., 2010. Seabed morphology and gas venting features in the continental slope region of Krishna-Godavari basin, bay of bengal: Implications in Gas-Hydrate Exploration. Mar. Pet. Geol., 27(7),1628-1641.

Kocherla M., Mazumdar, A., Karisiddaiah, S.M., Borole D.V. and RamalingeswaraRao., B., 2006. Evidences of methane derived authigenic carbonates from the sediments of the Krishna – Godavari Basin, eastern continental margin of India. Curr. Sci., 91, 318-323.

Kolla, V. and Coumes, F., 1987. Morphology, internal structure, seismic stratigraphy, and sedimentation on the Indus Fan – AAPG Bulletin, 71, 650-677.

Mazumdar A., Dewangan, P., Joa¨o, H. M., Peketi, A., Khosla, V. R., Kocherla, M., Badesab, F. K., Joshi, R. K., Roxanne, P., Ramamurty, P. B., Karisiddaiah., S. M., Patil, D. J., Dayal, A. M., Ramprasad, T., Hawkesworth, C. J. and Avanzinelli, R., 2009. Evidence of paleo–cold seep activity from the Bay of Bengal, offshore India. Geochem. Geophys. Geosys., 10(6),1-15.

Meyers, P. A. and Dickens, G. R., 1992. Accumulations of organic matter in sediments of the Indian Ocean: A synthesis of results from scientific deep sea drilling. In: Duncan, R. A., et al., (eds.) Synthesis of Results From Scientific Drilling in the Indian Ocean, Geophys. Monogr. Ser., 70, 295-309.

Ojha and Dubey., 2006. Gaint hydrocarbon fields of offshore Krishna-Godavari Basin. Petroview 1, published by Directorate General of Hydrocarbons, New Delhi , 26-30.

Powell C.M., Roots, S.R. and Veevers, J.J.,1988. Pre-breakup continental extension in east Gondwanaland and the early opening of the eastern Indian Ocean. Tectonophysics, 155, 261-283.

Prabhakar and Zutshi, 1993. Evolution of southern part of Indian east coast basins. J. Geological Society of India, 41, 215-230.

Ramana, M.V, Ramprasad, T., Desa, M, Sethi, A.K., Sathe, A.V., 2010. Gas hydrate related proxies inferred from multidisciplinary investigations in the India off-shore areas. Curr.Sci.., 91, 183 –189.

Ramana, M.V, Ramprasad, T., Paropkar A.L, Borolei, D.V. RamalingeswaraRao B., Karisiddaiah, S.M., Desa, M., Kocherla, M., Joao, H.M., Lokabharati .P., Maria-Judith Gonsalves., Pattan, J.N., Khadge, N.H., PrakashBabu, C., Sathe, A.V., Kumar, P., Sethi, A.K., 2009. Multidisciplinary investigations exploring indicators of gas hydrate occurrence in the Krishna–Godavari Basin offshore, east coast of India. Geo-Marine Lett., 29, 25-38.

Ramana, M.V, Ramprasad, T, KameshRaju., K.A. and Desa., M 2007. Occurrence of gas hydrates along the continental margins of India, particularly the Krishna-Godavari offshore basin. Int. J. Environ. Stud., 64, 675-693.

Ramana M.V., Nair, R.R., Sarma, K.V.L.N.S., Ramprasad, T., Krishnaa, K.S., Subrahmanyam, V., D'Cruza, M., Subrahmanyam, C., Paul, J., Subrahmanyam, V. D. and Chandra Sekhar, V., 1994. Mesozoic anomalies in the Bay of Bengal. Earth Planet. Sci. Lett., 121,469–475.

Ramprasad, T., Dewangan, P., Ramana, M.V., Mazumdar, A., Karisiddaiah, S.M., Ramya, E.R. and Sriram, G., 2011. Evidence of slumping/sliding in Krishna-Godavari offshore basin due to gas/fluid movements. Mar. Petrol. Geol., 28,1806-1816.

Rao, 2001. Sedimentation, stratigraphy, and petroleum potential of Krishna-Godavari Basin, East Coast of India. AAPG Bulletin, 85, 1623-1643.

Satyavani, N., Thankur, N.K., Arvind Kumar , N., Reddy, S.I., Migration of methane at the diapiric structure of the western continental margin of India- Insights from seismic data. Mar. Geol., 219,19-25.

Scotese C. R., Gahagan, L.M. and Larson, R.L., 1988. Plate tectonic reconstructions of the Cretaceous and Cenozoic ocean basins. Tectonophysics, 155, 27-48

Veerayya, M., Karisiddaiah, S. M., Vora, K. H., Wagle, B. G., Almeida, F., Detection of gas charged sediments and gas hydrate horizons in high resolution seismic profiles from the western continental margin of India. In Gas Hydrates, Relevance to World Margin Stability and Climate (edHenriet, J. P. and Mienert, J.), Spec. Publ. Geological Society of London., 137, 239–253.

DISSEMINATED SULPHIDES IN BASALTS FROM NORTHERN CENTRAL INDIAN RIDGE: IMPLICATIONS ON LATE-STAGE HYDROTHERMAL ACTIVITIES

Ranadip Banerjee* and Dwijesh Ray[1]

Geological Oceanography Division, CSIR-National Institute of Oceanography, Dona Paula, Goa 403004, India

[1]PLANEX, Physical Research Laboratory, Ahmedabad 380009, India

**ocean1@rediffmail.com*

Investigations on mineralogy and mineral chemistry of disseminated sulphides (mainly chalcopyrite-pyrite) in partly altered basalts from northern Central Indian Ridge (NCIR), Indian Ocean, indicate Pyrites and chalcopyrites are associated with the oxide phases namely magnetite and often ilmenite. Close association of sulphide and oxide minerals suggests paragentically they are not far away from each other. Sulphides also occur within the late impregnated veins cutting through the basaltic hosts. Chemical composition of pyrite (avg. Fe: 46.3 wt% and S: 53.7 wt%) and chalcopyrite (avg. Cu: 34.4 wt%; Fe: 30.7 wt% and S: 34.7 wt%) are almost uniform, while the secondary ilmenite often shows MnO-enrichment (up to 3-3.4 wt%). The associated altered minerals typically resemble the greenschist facies mineral assemblages e.g. chlorite±epidote. Evidences of albitisation and silicification refer to low

temperature hydrothermal alteration processes. This is further supported by the bulk Au content (up to 60 ppb) of host altered basalts with pyrite mineralization. Au enrichment is usually associated with late stage pyrites and thus related with low temperature hydrothermal activities. The tectonic activities around Vityaz megamullion, appearing close to the present sampling location, might have helped in generating the hydrothermal circulation and subsequent alteration of the mineral constituents in basalts, finally inducing the formation of the late-stage disseminated sulphide minerals in these rocks.

GEOCHEMICAL AND SR-ND ISOTOPIC INVESTIGATIONS OF FERROMANGANESE ENCRUSTATIONS FROM CENTRAL INDIAN RIDGE AT $6^0$38.5'S

Ranadip Banerjee[1*], George K. Devasia[2] , Durbar Ray[1] and S. Balakrishnan[2]

[1]National Institute of Oceanography, CSIR, Dona Paula, Goa 403004

[2]Department of earth sciences, Pondicherry University, Kalapet, Puducherry 605014

Geochemical and isotopic (Sr and Nd) studies of fourteen ferromanganese (Fe-Mn) encrustations on basaltic substrates from central Indian ridge at 6^0 38.5′ S indicate that except two (NC3 and NC4) remaining samples are of typical hydrogenous type. The inter-element relationships in these Fe-Mn samples indicate a strong positive correlation exists between Mn and Ni (r =0.89), Co and Pb (r = 0.87), Fe and Pb (r = 0.78), Ni and Cu (r =0.6), Fe and Co (r =0.5) and Mn and Cu (r =0.43). The Fe and Ni (r = -0.68) and Fe and Cu (r= - 0.18) are strongly negatively correlated with each other confirming their nil association with Fe Phase. A good positive correlation of Co and Pb with Fe (r=0.51 and r=0.69, respectively) indicate their association with Fe phase.NC3 and NC4 have a slightly higher growth rate (1.15 and 3.28 mm/Myr, respectively, while average growth rate of other samples is 0.91mm/Myr), lower bulk trace metal content and low ∑REE (specially in NC4).They have a lower content of High Field Strength (e.g. Hf, Ta, Zr, Nb), incompatible (e.g. Pb, Th and U) and LIL elements (e.g. Sr and Ba), than others. In addition, NC3 has a lower $^{87}Sr/^{86}Sr$ ratio (0.708825) than remaining samples (range 0.709149-0.709253) and higher $^{143}Nd/^{144}Nd$ ratio (0.512296) than others (range 0.512258-0.512279). Both NC3 and NC4 have relatively higher radiogenic component indicated by their low ε_{Nd} value (-6.67) than remaining samples (range -7.00 to -7.41). All these evidences together indicate a possible contribution of trace metals by a local mixed source of hydrothermal and hydrogenous origin during the growth history of NC3 and NC4, while remaining samples have grown purely hydrogenetically.

THE SCIENCE OF GAS HYDRATE EXPLORATION: GEOCHEMICAL PERSPECTIVE

Aninda Mazumdar

Gas Hydrate Research Group, Geological Oceanography

CSIR-National Institute of Oceanography, Donapaula, Goa-403004

maninda@nio.org

Dwindling petroleum reserves and high consumption of petroleum products and gas have given birth to the hydrate exploration program globally. The primary aim is to search for alternative hydrocarbon fuel to fulfill the need of ever increasing population. On the other hand hydrate exploration program has brought to light many more aspects of marine science e.g., link between methane seepage events and paleoclimate, benthic life in sulfidic sediment water interface, hydrate destabilization and sea bed instability, deep biosphere and microbial ecology linked to methanogeneseis and methanotrophy. Discovery of Gas hydrates in the Bay of Bengal has placed India prominently on the global hydrate map. Methane hydrate in India are distributed in Krishna-Godavrari, Mahanadi and Andaman basins having distinct geological and geochemical properties. Here I present an overview of geochemical

aspects of gas hydrate exploration and sediment chemistry linked to methane emission and sulfate methane interface processes. Hydrate exploration is an expensive venture, hence it is important to innovate methods using shorter sediment cores and accoustic data. A coupled study of the physical and geochemical parameter can be of great help in hydrate exploration.

The Krishna-Godavari basin (K-G basin) is a pericratonic rift basin with onshore and offshore extensions. The rift basin extends offshore along the eastern continental margin of India (ECMI). The K-G basin covers an area of 28,000 km^2 onshore and 145,000 km^2 offshore (Rao, 2001; Bastia, 2007). Geographically, it lies between Kakinada in the northeast and Ongole in the southwest of Andhra Pradesh. The Mahanadi offshore basin is a well known petroliferous basin located along the East coast of India (Singh, 2008). Mahanadi Basin extends from Jagannathpur in the north to Chilka Lake in the south and further extends offshore into the Bay of Bengal. It is a passive pericratonic basin covering an area of 2,60,000 km^2 with water depth exceeding 3000 m (including deep offshore) (Singh, 2008).

Seismic data of the Krishna-Godavari (K-G), Mahandi and Andaman Basins show the regional presence of gas hydrates manifested in the form of a bottom simulating reflector (BSR). BSRs represent a phase boundary where low-velocity gas-charged sediments occur below the hydrate stability zone. Drilling and logging activities on-board JOIDES Resolution in the Indian margin under the aegis of Indian National Gas Hydrate Program (NGHP) have proved the existence of massive methane hydrate deposits in the K-G Basin (Ramana et al.,2007). Methane hydrate, a crystalline, ice-like form of methane and water (molar ratio 1:6) exists within the marine sediments at suitable temperature-pressure conditions (Kvenvolden, 1988).

Sediment cores collected from the K-G and Mahanadi basin (Collett et al., 2008; Mazumdar et al., 2012, 2014) reveal variable pore water sulfate, alkalinity, methane and chloride concentration profiles (Fig.1). Organoclastic degradation and anaerobic oxidation of methane (AOM) are known to influence sulfate, methane and bicarbonate concentrations of sediment pore-waters. C1/C2+C3 ratios and $\delta^{13}C_{CH4}$ of headspaces gases in sediments recovered from K-G and Mahanadi basins indicate biogenic origin of methane. Our findings show both shallow and deep biogenic methane sources in the K-G basin. Distinctly different sulfate profiles are identified from two basins. A range of different sulfate profiles have been reported from the K-G and Mahanadi basins and correlated with the occurrence of gas hydrates and shallow gas sources. The S and kink type sulfate profiles represent transient states compared to the steady state quasi-linear profiles. The transient nature of sulfate profiles suggests recent enhancement of methane flux possibly from the neotectonic activities in K-G basin which results in opening of fault/fracture conduits allowing migration of methane. Apparently, the kink type sulfate profile in areas without evidence of slide block movement may indicate the occurrence of deep methane source possibly associated with gas hydrate deposits. The quasi-linear sulfate concentration profile and a shallow SMTZ suggest high methane flux likely originating from the young and rapidly deposited sediments. These finding may help to short list locations of hydrate occurrence with the help of short cores (20-30 m). The complex nature of alkalinity profiles to organo-clastic degradation, variation in methane flux, transition of SMTZ and alkalinity consumption via precipitation of carbonates and possibly silicate weathering

Occurrence of authigenic carbonates, chemosynthetic clam shells suggest paleo-methane emission events in the K-G basin possibly triggered by passive tectonics induced faulting or fracturing. The methane emission event resulted in proliferation of chemosynthetic benthic communities. Activities of these benthic communities are recorded as bioturbation casts and faecal pellets (Mazumdar et al., 2011). A high resolution record of Fe-S-Mo sytematics also show the influence of methane seepage

on anaerobic methane oxidation (AMO), sulfate reduction and high sulfide flux in sediment (Peketi et al., 2012).

Chloride (Cl^-) concentrations in porewater show remarkable variation due to thawing or formation methane hydrate in sediments. Thus the Cl^- concentration change can be used as a proxy for quantifying hydrate content in sediment by comparing with the ambient sea water values (550 mM). Hydrate thawing releases fresh water resulting in lowered porewater salinity and vice versa. $\delta^{18}O_{H2O}$ of porewater can also indicate hydrate presence due to marked difference in oxygen isotope ratios in hydrate bound water and ambient pore water.

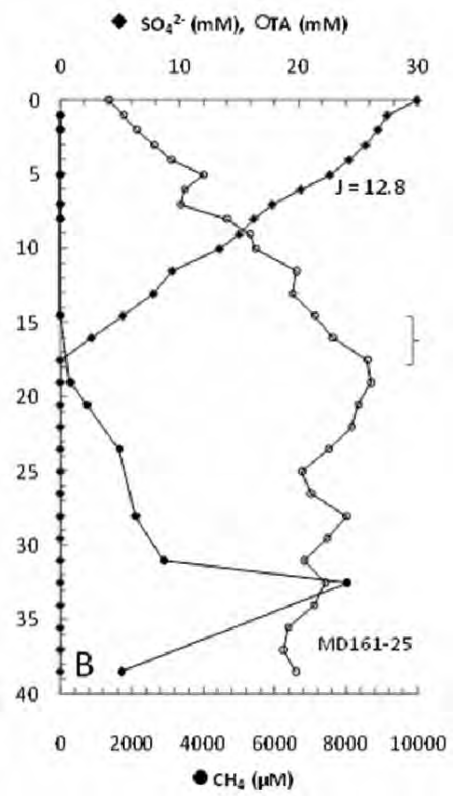

Figure-1 Sulfate, total alkalinity and methane concentration profiles from Mahanadi basin. The bracket indicates the approximate location of the sulfate-methane transition zone (SMTZ) (Mazumdar et a., 2014)

References:

Bastia, R., 2007. Geologic Settings and Petroleum Systems of India's East Coast Offshore Basins: Concepts and Applications: Eastern Book Corporation, 204p.

Collett, T., Riedel, M., Cochran, J., Boswell, R., Presley, J., Kumar, P., Sathe, A., Sethi, A., Lall, M., and Sibal, V., 2008. The NGHP Expedition 01 Scientists. Indian National Gas Hydrate Program Expedition 01 Initial Reports.

Kvenvolden, K. A.,1988. Methane hydrate—a major reservoir of carbon in the shallow geosphere?. Chemical Geology, 71, 41-51.

Mazumdar, A., Joao, H.M., Peketi, A. Dewangan, P., Kocherla, M., Joshi, R.K., Rarnprasad, T., 2012. Geochemical and geological constraints on the composition of marine sediment pore fluid: Possible link to gas hydrate deposits. Marine and Petroleum Geology 38, 35-52.

Mazumdar, A., Joshi, R. K., Peketi, A., & Kocherla, M.,(2011. Occurrence of faecal pellet-filled simple and composite burrows in cold seep carbonates: A glimpse of a complex benthic ecosystem. Marine Geology, 289, 117-121.

Mazumdar, A. Peketi, A. Joao H.M, Dewangan, P. Ramprasad , T. 2014, Pore-water chemistry of sediment cores

off Mahanadi Basin, Bay of Bengal: Possible link to deep seated methane hydrate deposit. Marine and Petroleum Geology, 2014, 49, 162-175

Peketi, A., Mazumdar, A., Joshi, R.K., Patil, D.J., Srinivas, P.L. and Dayal, A.M., 2012, Tracing the Paleo sulfate-methane transition zones and H_2S seepage events in marine sediments: An application of C-S-Mo systematics . Geochemistry Geophysics Geosystems, V. 13, 1-11.

Rao, G.N., 2001. Sedimentation, stratigraphy, and petroleum potential of Krishna-Godavari basin, east coast of India. AAPG Bull. 85, 1623-1643.

Ramana, M.V., Ramprasad, T., Kamesh Raju, K.A., Desa M., 2007. Occurrence of gas hydrates along the continental margins of India, particularly the Krishna-Godavari offshore basin. International Journal of Environmental Studies 64, 675–693.

Singh, L., 2008. Mahanadi Basin (Mahanadi -NEC basin) Oil and gas fields of India, Indian Petroleum publishers, Dehradun, India. 325-346.

EFFECT OF SALINITY INDUCED PH/ALKALINITY CHANGES ON BENTHIC FORAMINIFERA: A LABORATORY CULTURE EXPERIMENT

Sujata Kurtarkar, Rajeev Saraswat, Mamata Kouthanker, , Rajiv Nigam, S.W.A. Naqvi and V.N. Linshy

Micropaleontology Laboratory, National Institute of Oceanography, Goa, India

The salinity of coastal waters in the vicinity of seasonally fresh water fed estuaries changes tremendously and reportedly affects the living calcite secreting organisms like foraminifera as well as their dead remains. The precise mechanism of adverse effect of such seasonal salinity changes on calcite secreting organisms is, however not clear. The seasonal fresh water influx from the estuaries also affects the pH and alkalinity of the coastal seawater. Therefore, to understand the effect of salinity induced pH/alkalinity variations on benthic foraminifera, living specimens of *Rosalina globularis* were subjected to different salinity. Additionally, water samples were collected from an estuary during both monsoon and post monsoon season to understand the relationship between salinity, pH and total alkalinity (TA). The pH decreased with decreasing salinity during both the seasons. A similar decrease in TA with decreasing salinity was also observed but only till 20 salinity, below which the TA increased with decreasing salinity. The maximum growth was reported in specimens kept at 35 salinity while the rest of the specimens maintained at salinity higher or lower than 35, showed comparatively lesser growth. Specimens kept at 10□□ and 15 salinity became opaque within two days of lowering the salinity and later on their tests dissolved within 24 and 43 days, respectively. No specimen reproduced at 10 and 15 salinity while only a few specimens (3%) reproduced at 20 salinity. As compared to 10-20 salinity, ~60 % reproduction was observed in specimens subjected to 25-40 salinity. The specimens maintained at 20 salinity took twice the time to reach maturity than those subjected to 25-40 salinity. Since a big drop in pH was observed at 10-15 salinity (pH 7.2 and 7.5, respectively), while the alkalinity was still higher, we suggest that fresh water influx induced drop in pH adversely affects calcification and reproduction in benthic foraminifera. The response is, however not linear as beyond a certain limit, a further increase in pH does not affect benthic foraminifera; rather they respond to salinity as per their salinity tolerance range. It is further inferred that the time required to reach reproductive maturity increases at the extreme salinity tolerance limits. Dissolution of calcareous foraminifera below 20 salinity, suggests that salinity induced changes control the carbonate inventory in the coastal regions subjected to seasonal fresh water influx.

EVIDENCE OF HYDROTHERMAL CIRCULATION IN AN OLDEST OCEANIC CRUST: NUMERICAL MODELING CONSTRAINED WITH HEAT FLOW DATA

Ray Labani [1], Yoshifumi Kawada[2], Hideki Hamamoto[2,3], Makoto Yamano[2]
CSIR-National Geophysical Research Institute, Hyderabad, 500 007, India[1]
Earthquake Research Institute (ERI), University of Tokyo, Japan[2]
Center for Environmental Science in Saitama, Japan[3]
labani@ngri.res.in

On the outer slope and the outer rise of the Japan Trench, where the old oceanic Pacific plate (130-135 Myr) subducts beneath the continental Eurasian plate, anomalous high heat flow has been observed along three profiles perpendicular to the trench axis with 150-200 km long and 100 km apart. There exist regional anomalies with a spatial scale of a hundred of kilometers; the heat flow values range between 42 and 114 mW m^{-2} with a mean of 67 mW m^{-2}. They also have sharp peaks with a spatial scale of a few kilometers. The multiple-scale heat flow anomalies can be explained by different mechanisms associated with subduction-zone related phenomena. Plausible sources that are individually or jointly responsible for the observed multi-scale heat flow anomalies are: (i) young volcanic intrusions, (ii) heat conduction in the presence of topography of sediment / basalt interface, (iii) hydrothermal circulation in the presence of the topography, and (iv) hydrothermal circulation in the presence of faults penetrating near to the seafloor. To evaluate the effects of these sources, numerical simulations with different complexities are carried out, considering the transport of heat and fluid. The combined results indicate that hydrothermal circulation plays an important role in causing the heat flow anomalies. In a spatial scale of few hundreds of kilometers, the heat flow anomaly could be due to processes associated with subduction; in a spatial scale of a few tens of kilometers, it could be due to hydrothermal circulation in the presence of the topography; in a spatial scale of a few kilometers, it could be due to the high-permeable faults. Thus, this study indicates that hydrothermal circulation in very old oceanic plate also plays an important role on the heat transportation near subduction zones.

GAS HYDRATES SATURATION FROM SEISMIC AND LOG DATA IN THE MAHANADI BASIN

Uma Shankar* and Kalachand Sain
CSIR-National Geophysical Research Institute, Uppal Road, Hyderabad – 500007, India
umashankar_ngri@yahoo.com

Well log down holedata was acquired from Mahanadi Basin,off the East Coast of India during NGHP Expedition-01 for gas hydrate exploration and assessment in 2006. Initial analyses of the acquired well log data suggested that there were no significant gas hydrate occurrences at Site NGHP-01-19. However, Infrared imaging of recovered core confirmed gas hydrate occurs predominantly in discrete layers. Electrical resistivity and pore water chemistry data analysis shows considerable amount of gas hydrate at site NGHP-01-19. Gas hydrate saturations were calculated based on rock-physics modeling utilizing P-wave velocity log measurements through the gas hydrate stability zone shows good correspondence with the gas hydrate saturation directly measured from the pressure core, which is 2.4% of the pore space at site NGHP-01-19. Acoustic impedance inversion was then performed around the well sites for regional extrapolation of the borehole data. Estimated gas hydrate saturation varies maximum up to 5.0% of pore space along seismic profile and shows good agreement with the well log and pressure core gas hydrate concentration estimates.This paper documents the first gas hydrate saturation along a seismic line rather than a single log position which can give confidence on areal extent of gas hydrate in MahanadiBasin.

AN APPRAISAL OF TSUNAMI RECURRENCE IN THREE MAJOR TSUNAMIGENIC ZONES OF WESTERN PACIFIC OCEAN REGION

Amardeep*, Anchal Mehra, Mamta and Vishal
Department of Geophysics, Kurukshetra University, Kurukshetra -136119
**amar7080@gmail.com; amardeeprao80@gmail.com*

West Pacific Ocean is the most Tsunamigenic region of the world,which has experienced several large to great earthquakes resulting destructive tsunamis. Most of the earth's seismic energy is released along the subduction zone of the Pacific Ocean Rim.In this research work, probabilities of occurrence of large Tsunami intensities I≥3.0(*Soloveiev-Imamura Intensity Scale*) with average height H ≥5.66m, are calculated during a specified time interval using Weibull Stochastic Model.Tsunami Recurrence are calculated for the in three major regions namely, Japan-Karil-Kamchatka(JAP-KK), Philippines-Indonesia-New Guiana(PHI-IND-NGS) and New Zealand (NZT) in thePacific Ocean. For this purpose, a reliable, homogeneous and complete Tsunami catalog with Tsunami intensity I≥3.0 during the period of 1500-2011 has been used. The Tsunami hazard parameters are estimated using the method of maximum likelihood function. For this purpose logarithm of likelihood function (lnL) are estimated and used to test the suitability of models in the examined region. The Weibull model is observed to be the most suitable model to estimate Tsunami recurrence in the region. The sample mean interval of occurrence of Tsunami with intensity I≥3.0 is also calculated for observed data as well as for Weibull model. Thus, with the help of this data and estimated model parameters,the cumulative and conditional probabilities in the three major Tsunamigenic zones of Pacific Ocean region are calculated. The estimated probabilities of occurrences of large tsunamis can be further used for long term Tsunami hazard assessment in this region.

NUMERICAL SIMULATION OF MARINE MAGNETOTELLURIC RESPONSE ACROSS 85^0E RIDGE, BAY OF BENGAL, INDIA

***K. Sivannarayana Murthy, K. Veeraswamy and Prasanta K. Patro**
MT-DRS Group, CSIR - National Geophysical Research Institute, Hyderabad, India
**snmurthykudupudi@gmail.com*

Electromagnetic (EM) induction technique is one of the most important geophysical techniques in understanding the subsurface structure and it plays a pivotal role where there is a geological complexity of the subsurface layers in terms of resistivity. It is well known that the land natural source electromagnetic data acquired will be affected by the sea water near to it, in the same way data acquired in the marine environment will also get affected by the land near to it (Key and Constable, 2011; ; Worzewski et al., 2012). The large conductivity contrast between the ocean and adjacent land causes a large distortion in magneto-telluric measurements and it is called coast-effect. In order to estimate how much data gets distorted by the coast, an attempt has been made here, to simulate the Marine Magneto-telluric (MMT) response by considering vertical coast and a single host with variable resistive body.

Modeling has been initiated by considering a simple sea-land boundary with a view to estimate the distortion in MMT response at different distances from the coast line in the offshore region. In order to derive this response, we have taken the initial model which cuts across the coast with -800km (land) to +800km (ocean) and down to 600 km depth with a water column of 4 km, because actual

sea bathymetry in general won't exceed 4 km. First model includes water (0.25 Ohm-m) with vertical slope and a single resistive half space with minimum resistive value about 50 Ohm-m as shown in Fig.1. We have computed the response for it. Simultaneously to check the distortion in MMT response the host resistivity has been considered as 500 Ohm-m and 1000 Ohm-m. The results are shown in Fig.1 in the form of apparent resistivity, phase, horizontal electric & magnetic fields and tipper.

It has been observed that the response characteristics have been strongly affected by the coast. The TE mode and Tipper responses at several locations with frequency show significant changes that might be due to the coast. Rho-a gets distorted when the station is located at <100 km while Tipper attains maximum between 300 and 3000 sec. Similarly, phase also gets distorted when the station is located at <100 km, while Tipper phase is +ve when the station is at >100km and it is –ve when the station is at <60 km. From fig.1 it is evident that the apparent resistivity and tipper phases are +ve when the station is located at >100 km and it is –ve for stations <30 km. Interestingly, when the station lies between 30-100 km the phase reversal takes place (i.e. +ve at 100 sec and -ve at 1000 sec). The coast effect produces increased TE mode apparent resistivities at longer periods where skin depth of the host becomes large. Magnitude of the Ex component decreases with distance, while Hy magnitude is maximum between 30 and 3000 sec (Fig.2). The maximum coast effect is related to the minimum in the magnitude of Horizontal magnetic field component (Hy) and there is no change in the horizontal electric field (Ex) at the same location. In the minimum resistive body (50 Ohm-m) setting the maximum magnitude with smallest half width occurs at 30 km with corresponding response of phase. Similar response has been noticed for higher resistive bodies (500, 1000 Ohm-m), however the maximum coast affect position has been moved to longer distances. For higher resistive body setting the tipper component, in general, decreases towards the ocean, but there is an increase in magnitude at distances 30 km to 100 km for periods between 100 sec and 10000 sec when the body has low resistivity. The corresponding response is observed in the phase component of the tipper.

As the resistivity of the host increases, the apparent resistivity shows progressive increase with variable characteristic distances where the coast effect is maximum in the period range of 40-60secs. The phase reversal in both (Ex and Hy) components takes place in the period range of 20-50sec.

85^0E ridge in the Bay of Bengal region is one of the interesting geotectonic features in the Indian off-shore due to surprisingly low gravity anomalies over it (Krishna, 2003). Keeping this in view the MMT response has been simulated across this ridge to estimate the resolvability of layer parameters like thickness and resistivity followed by period band where it shows maximum response and amount of data required (in terms of no. of days) to penetrate the signal to the desired depth. On the basis of geodynamical history of this region, it appears that the orientation and alignment of 85^0E ridge matches with the trace of the Crozet hotspot (Curray and Munasinghe, 1992; Raval and Veeraswamy, 2014). In such a case the ridge structure is likely to show conductive signature. Accordingly, different resistivity values have been assigned to estimate the influence of ridge structure on MMT measurements.

Acknowledgements

The authors are thankful to the Director, CSIR-NGRI for his kind permission to present this study. This activity is supported by CSIR, New Delhi under GEOSCAPE project.

References

Curray, J.R. and Munasinghe, T., 1991. Origin of the Rajmahal traps and the 85^0E ridge: Preliminary reconstructions of the trace of the Crozet hotspot. Geology, 19, 1237-1240.

Key, K. and Constable, S., 2011 Coast effect distortion of marine magnetotelluric data: insights from a pilot study offshore northeastern Japan, Phy. Earth and Planet. Inter., 184, 194-207.

Krishna, K.S., 2003. Structure and evolution of the Afanasy Nikitin seamount, buried hills and 85^{0}E ridge in the northeastern Indian ocean. Earth and Planet. Sci. Lett., 209, 379-394.

Raval, U. and Veeraswamy, K., 2014 Energy resources and mid-continental (SCR) earthquakes over India: Association with mantle plume affected regions. Current Science (in Press).

Worzewski, T., Jegen, M. and Swidinsky, A., 2012. Approximations for the 2-D coast effect on marine magnetotelluric data. Geophy. J. Int., 189, 357-368.

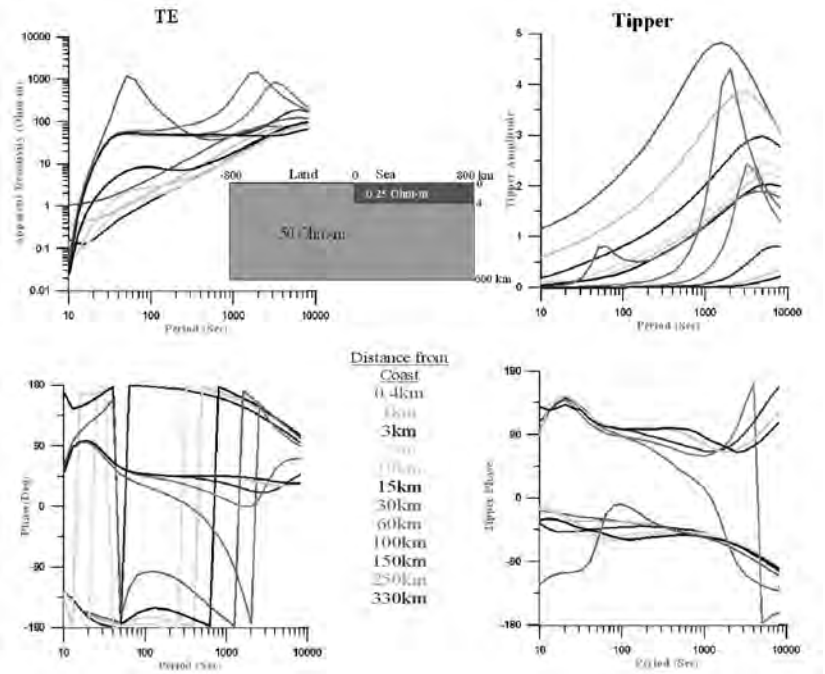

Fig.1 Variation in Rho-a, Phase (TE mode) and Tipper responses with period at different sites in the offshore.

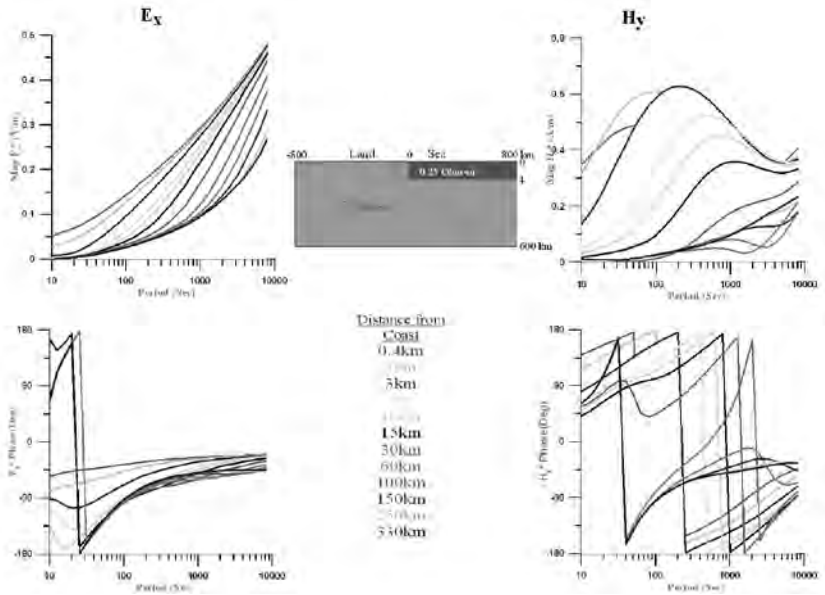

Fig.2 Variation in magnitude and phase of Ex and Hy components with period at different sites in the offshore.

FORAMINIFERAL AND SEDIMENTOLOGICAL STUDIES TO UNDERSTAND RECENT ENVIRONMENTAL CHANGES AT ARAMDA DOCKYARD, GULF OF KUTCH, GUJARAT

J.P. Bhardwaj[1], R. Nigam[2], R. Saraswat[2], Sundaresh[2] and A.S. Gaur[2]
1 Kurukshetra University, Kurukshetra
2 Micropaleontology Laboratory, National Institute of Oceanography, Goa
rsaraswat@nio.org

Aramda Dockyard is an artificial rectangular structure (~103×38 m) with ~5 m depth lying at the northwestern indented coast of Saurashtra Peninsula near Dwarka and Okhamandal Coast. The region is characterized by an inter-tidal regime and is analogous to a microenvironment and gets frequently inundated by tidal upheavals. A series of field visits and remote sensing images revealed that prior to the current stage wherein it is almost fully covered by mangroves and cut-off from the main sea, the dockyard was extensively used till the late 90s. The change in the status of Aramda dockyard is a prelude to the fate of famous Lothal dockyard, also discovered from near coastal regions of Gujarat and suggested to be the oldest known dockyard. The current study focuses on understanding the multitude of processes that synergistically culminated in the unabated growth of mangroves and associated siltation at Aramda Dockyard, Gulf of Kutch, Gujarat, during the last two decades, and can help in understanding the processes which lead to the demise of Lothal dockyard.

A 15 cm long core (AD-2, Aramda Dockyard, Landside) was collected from the dockyard and processed for foraminiferal and sedimentological studies. The data helped to understand the energy regime and the dominant processes that affected the site in the past and eventually led to sedimentation and proliferation of mangroves in the region. The increase in coarse fraction from the bottom of the core till ~8 cm, indicates high energy environment, and is also supported by a decrease in clay fraction. The coarse fraction percentage is constant in the top ~8 cm of the core, whereas the clay fraction increases in this section indicating reduced tidal intensity and a stable depositional medium. Quinqueloculina percentage also decreases in the top section of the core indicating a decrease in intertidal environment. The increase in relative abundance of agglutinated foraminifera towards the top correlates and verifies the carbonate under-saturated, hyper-saline regime. Such an environment is favorable for mangrove productivity. Therefore, we suggest that this zone (~8 cm depth) may be a transformation zone, marked by decrease of intertidal activity, conducive for the growth of mangroves in the region. The study suggests that a significant environmental change occurred during the time covered by the top ~8 cm section of the core, which rendered the dockyard unsuitable for boats and fit for mangrove growth.

APPLICATION OF AVO ATTRIBUTE ANALYSIS FOR GAS HYDRATE IDENTIFICATION IN THE ANDAMAN REGION, INDIA.

***A.Prasanti and Kalachand Sain**
CSIR-National Geophysical Research Institute, Hyderabad- 500 007.
**prasanti.ngri@gmail.com*

The most important characteristic parameter in gas hydrate identification is the acoustic impedance, which is generated when the gas hydrate layer is underlain by free-gas /brine saturated sediments. This configuration produces a strong reflection, which runs roughly parallel to the sea floor and termed as Bottom Simulating Reflector (BSR). The BSR lies at depths of a few hundred meters below the sea floor guided by the local temperature and pressure conditions. Marine gas hydrates are commonly associated with a bottom-simulating seismic reflector (BSR) that is evident on low-frequency seismic reflection sections.

The reflections associated with some reservoirs for gas-bearing rocks increase in amplitude with offset. The P and S wave characteristics as a function of offset in the presence of gas-saturated sediments led to Amplitude versus Offset (AVO) analysis. This is one of the few exploration methods used widely for the direct detection of hydrocarbons. The AVO responses of free gas, bottom simulating reflector (BSRs), and gas hydrates are discussed and the AVO attributes in relation to gas hydrates are analyzed.

In this study, we have discussed the changes observed in the attributes like intercept, gradient, fluid factor and Poisson's ratio with respect to gas hydrates and free gas layers. The cross-plotting of the AVO attributes helps us to interpret anomalies in the context of lithology and pore fluids. It is also can be observed that there is a background trend for reflections from non-hydrocarbon related interfaces.

A MAGNETIC STUDY EAST OF THE CHAGOS LACCADIVE RIDGE COMPLEX, NORTHERN INDIAN OCEAN

Maria Ana Desa, T. Ramprasad and K. A. Kamesh Raju
National Institute of Oceanography Dona Paula, Goa India
mdesa@nio.org

About 20,000 line km of magnetic data collected in the 1980's under the Polymetallic Manganese Nodules (PMN) project has been studied in the region east of the Chagos Laccadive Ridge (CLR) complex, Northern Indian Ocean. This area (15°S to 15°N latitude; 73°E to 81°E longitude) has a complex structure and tectonics due to the influence of the CLR in the north. Oceanic crustal age of more than 60 Ma and N-S trending fracture zones have been inferred in this region (Mckenzie and Sclater, 1971; Norton and Sclater, 1979; Schilch, 1982; Kamesh Raju and Ramprasad, 1989; Royer et al., 1989). DSDP and ODP sites on the CLR complex suggest the presence of volcanics of age 57.5 Ma to 49.6 Ma resulting from the Reunion hotspot activity (Duncan, 1990). The trace of the Indian Triple Junction has also been inferred in the study area (Patriat and Segoufin, 1988; Dyment, 1993). But the nature and age of the underlying crust has been debated, and the fine scale tectonic evolution of the region has remained unknown.

Synthetic seafloor spreading model study facilitated the identification of magnetic anomalies 34 to 24 in the study area (Cande and Kent, 1995). Half-Spreading Rate (HSR) is low (2.5 cm/yr) initially between chrons 34 and 33, while the rates are higher and variable (4.5 to 7.5 cm/yr) between chrons 33 to 24.

The downward continued gravity signature facilitated the demarcation of the earlier identified major fracture zones (FZ). The prominent FZ signature seen immediate east along the CLR complex belongs to the La Boussole FZ (Patriat and Segoufin, 1988). This FZ separates the CLR complex which is characterized with high frequency and high amplitude magnetic anomalies from the oceanic crust on the east. Towards south, this FZ is seen bifurcating/relocating to FZ-A towards east. NNW-SSE trending lineations are seen in the south close to India-Sri Lanka. Approximately E-W to ENE-WSW trending lineations are the imprints of the periodic deformation in the study area (Krishna et al., 1998). The FZ-A causes a major right lateral offset of upto 150 km of the magnetic isochrones. The central region in the study area depicts minimum offsets of the magnetic isochrones. Further east, the major FZs such as L'Astrolabe and Indira FZs are seen running ~N-S and depict right lateral offsets.

The study suggests that the oceanic crust south of 3°N is younger to chron 34 (83.5 Ma) upto 52 Ma and was formed by an ~E-W trending spreading center. The CLR ridge may have emplaced over the pre-existing oceanic crust of Middle to Late Cretaceous age. Further, the study suggests that the La Boussole FZ combined with FZ-A may be the trace of the Indian triple junction from chron 34 to 24 (83.5 to 52 Ma) and is a major boundary separating the older oceanic crusts off the west and east coasts of India.

References:

Cande, S. C. and Kent D. V., 1995. Revised calibration of the geomagnetic polarity time scale for the Late Cretaceous and Cenozoic, *J. Geophys. Res*., **100**: 6093-6095.

Duncan, R.A. 1990. The volcanic record of Reunion hotspot, *Proc. ODP, Sci. Res.*, **115**: 3-10, College Station, TX (Ocean Drilling Program).

Dyment J. 1993. Evolution of the Indian Triple Junction between 65 and 49 Ma (Anomalies 28 to 21). *J. Geophys. Res*., **98**: 13863-13877.

Kamesh Raju, K.A. and Ramprasad, T., 1989. Magnetic lineations in the Central Indian Ocean for the period A24-A21: A study in relation to the Indian Ocean Triple Junction trace, *Earth Planet. Sci. Lett*., **95**: 395-402.

Krishna, K.S., Ramana, M.V., Rao, D.G., Murthy, K.S.R., Rao, M.M.M., Subrahmanyam, V. and Sarma, K.V.L.N.S., 1998. Periodic deformation of oceanic crust in the central Indian Ocean, *J. Geophys. Res.*, **103:** 17859-17875.

McKenzie, D. and Sclater, J. G. 1971. The evolution of the Indian Ocean since the Late Cretaceous, *Geophys. J. R. Astr. Soc*., **25**: 437-528.

Norton, I. O. and Sclater, J. G. 1979. A model for the evolution of the Indian Ocean and the breakup of Gondwanaland, *J. Geophys. Res*., **84**: 6803-6830.

Patriat, P. and Segoufin, J., 1988. Reconstruction of the Central Indian Ocean, *Tectonophysics*, **155**: 235-260.

Royer, J. Y., Sclater, J. G. and Sandwell, D. T., 1989. A preliminary tectonic fabric chart of the Indian Ocean, In: Brune, J. N., (Ed.), *Proc. Ind. Acad. Sci., Earth Planet. Sci.,* **98**: 7-24.

Schlich, R., 1982. The Indian Ocean: aseismic ridges, spreading centers and ocean basins, In: Nairn, A. E. and Stehli, F. G. (Eds.), *The Ocean Basins and Margins*, Plenum, New York, **6**: 51-147.

UNDERSTANDING THE NATURE AND EVOLUTION OF THE GULF OF MANNAR BASIN DERIVED FROM GEOPHYSICAL METHODS

Goverdhan. K*, John Kurian. P and Abhishek Tyagi

National Centre for Antarctic & Ocean Research, Headland Sada, Goa-403 804, India.

**goverdhan@ncaor.gov.in, john@ncaor.gov.in*

The breakup of Gondwanaland since the cretaceous period and the subsequent rifting and drifting of continental masses led to the present day configuration of the northern Indian Ocean. During the spreading of these continental masses and their subsequent movements, Sri Lanka always remained geographically close to India. Even though the geological correlations between the South Indian shield and Sri Lanka have been well established, contrasting views exists about their post break-up transit to the present location because of the limited perceptive about the nature and crustal configuration of the Mannar Basin. The objective of the present study is to develop a better understanding about the Mannar basin, which separates Indian landmass from Sri Lanka. Analysis of a few multi-channel seismic reflection (MCS) profiles in the area reveals the presence of four sequences of late Jurassic to recent sediments in the basin, the oldest sequence is being inferred as deposited during the initial synrift phase of basin development. Integrated analysis of the bathymetry, gravity and seismic data have been attempted to decipher the morpho-tectonic set-up of the region. Two-dimensional crustal modeling of the gravity data by incorporating constraints from MCS data revel thin crust flooring the basin. Preliminary analysis of the results indicate that Mannar basin may have been evolved by extensional tectonics between India and Sri Lanka, but underlined by relatively thin continental crust.

FACTORS CONTROLLING PLANKTONIC FORAMINIFERA SHELL CALCIFICATION IN NORTHERN INDIAN OCEAN

Sushant S. Naik, Shital P. Godad and Priya Kolwankar
CSIR-National Institute of Oceanography
sushant@nio.org

Shell weights of various species of planktonic foraminifera were measured from sediments cores and traps from the northern Indian Ocean in order to understand the controlling factors on shell calcification. The downcore study from the eastern Arabian Sea reveals that variation in shell weights of *Globigerinoidessacculifer* during the Holocene and the last glacial period are mainly related to the variation in surface water [$CO_3^=$] through time in response to changing atmospheric CO_2. On the contrary, in the intense upwelling region of the western Arabian Sea it was seen that foraminifera shell weights of *Globigerinabulloides* and *Globigerinoidesruber* cannot be utilized as a proxy of surface water [$CO_3^=$].This was also seen to be the case on seasonal timescales. It was seen that shell calcification varies from region to region. Further comparisons will be made with *G. ruber* shell weights from the Bay of Bengal sediment core SK218/1 the results of which will be presented in the talk.

IMPROVED HIGH RESOLUTION CAPABILITIES OF MULTIBEAM ECHOSOUNDING SYSTEM TOWARDS GEOLOGICAL ASPECTS OF OCEAN MAPPING

Mahale V.P., Afzulpurkar S., Ranade G.H.
National Institute of Oceanography, Goa, India
vmahale@nio.org

In the recent past, there have been major advancements in the capabilities of echosounder equipments utilized in ocean mapping. To be specific, charting the depths of the seafloor have been a basic, yet most crucial aspect of ocean mapping. Oceanographic or hydrographic surveys undertaken to accomplish this task is simply referred to as bathymetric mapping. Evolution in echosounder's instrumentation as well as software and digital electronics in the past few decades, has initiated improvement in spatial resolution and precision in depth information to the hydrographic community.

Based on these advancements the concept of swath bathymetric mapping of the seabed was introduced.

Swath bathymetric system is also commonly referred to as Multi-Beam Echo-Sounder (MBES). As these systems acquire a swath of soundings approximately 4 time the water depth the digital bathymetric data increase rapidly. Further, the spatial resolution and accuracy of the systems is also increasing leading to a voluminous data. The products from the seafloor mapping include standard contour maps, shaded relief bathymetry, beam amplitude, and acoustic backscatter imagery. This form of high resolution information provides new perspectives and deeper understanding about the morphology of the seafloor. One such geomorphic feature that is of importance to marine geo-scientists are the Seamount, which provide a means to investigate the volcanic, tectonic and sedimentological processes operating in the region. Further, mapping the morphology of the seabed with high resolution plays an important role in its characterization and classification. In the present study, Ramman seamount along the Laxmi basin in the eastern Arabian sea have been investigated from the resolution perspective of the mapping sonar. An attempt has been made here to demonstrate the importance of the spatial as well as depth resolution of the present day MBES system as compared to the older MBES systems. In this study, a comparative analysis of the MBES system data acquired over the seamount have been investigated and reported. Analysing the two data sets revels that the resolution and accuracy capabilities of the MBES system on-board the National Institute of Oceanography's new vessel R/V

Sindhu Sadhana, is much higher. This revels the fact that higher resolution data indeed helps better understanding of the seabed morphology and in-turn deeper understanding of the geological settings. Hence it concludes that the new tool on-board the oceanographic research vessel possesses a great potential to marine geoscientists for further investigations in marine geophysical research.

INTERNAL STRUCTURE OF THE 85°E RIDGE, BAY OF BENGAL – EVIDENCE FOR MULTIPHASE VOLCANIC CONSTRUCTION OF THE RIDGE

K. Srinivas[a],[*],[**] , K.S. Krishna[a], M. Ismaiel[a], J. Mishra[b], D. Saha[b]

[a] *CSIR – National Institute of Oceanography, Dona Paula, Goa-403004, India*

[b] *ONGC-Keshava Deva Malavia Institute of Petroleum Exploration, 9, Kaulagarh Road, Dehradun*

[*] *Corresponding author*

[**] *Present Address: National Institute of Oceanography Regional Centre, 176, Lawsons Bay Colony, Visakhapatnam-530017, Andhra Pradesh*

The 85°E Ridge is an enigmatic structure that possesses variable geophysical anomalies throughout its length. Newly identified fracture zones west of the ridge and internal time marker (Q1) of Cretaceous Superchron and magnetic anomalies (C33, C34) in the central basin adjacent to the ridge suggest that the ridge was emplaced over a young oceanic crust. Modeled regional flexure at Moho level in the vicinity of the ridge is attributed to the ridge load on a young oceanic crust. The geometry of internal structure of the ridge consisting of volcanic plug like feeders, lava deltas, volcanic clinoforms and fissure eruptions at different stratigraphic levels suggest that the ridge is a volcanic structure and was built on multiple phases of volcanism. Inferred wave-cut terraces at different stratigraphic levels suggest that volcanic phases were separated by time gaps and the ridge remained either sub-aerial or in shallow waters post ~23 Ma age. The ridge became a sub-surface feature during early Miocene period due to higher sedimentation rates. Both morphology and internal structure of the 85°E Ridge are found to be varying considerably along the ridge track. Lava deltas have been mapped in the areas (~16°N, 85°E) where the ridge observed to be subdued. The shallow water conditions during Eocene- Oligocene facilitated formation of wide-spread carbonate sequence over the ridge. The microsedimentary basins on the top and carbonate sedimentation over the ridge are inferred to be good source and reservoir rocks. We infer that the ridge was formed by Kerguelen Hotspot and independent of Rajmahal volcanism.

INVITED TALK

MY FIFTY YEARS OF ADVENTURES WITH MEASURING GRAVITY OVER THE OCEANS (AND ON THE MOON)

Manik Talwani

Department of Earth Science, Rice University, Houston, Texas

manik@rice.edu

During a span of more than five decades, I have made measurements of gravity at sea from a number of vehicles. These include a fishing boat, a world war II submarine, and a number of oceanographic research ships. These measurements were made in all the oceans of the world. In addition I have madegravity gradiometer measurements from an airplane, and (by proxy) gravity measurements on the moon.

In this talk, I will primarily confine myself to two topics. One, what was the unforeseen problem faced by the first surface ship gravimeters, and how it was overcome? The second topic deals with some human aspects of making the measurements. How some very smart people made some very serious mistakes which had to be pointed out by beginners? And how commercial considerations sometimes clouded scientific ethics?

SESSION – IV
SOLID EARTH GEOSCIENCES

ON EXPLORATION AND MANAGEMENT OF GROUNDWATER RESOURCES IN AND AROUND GRANITIC TERRAINS OF HYDERABAD USING ELECTRICAL RESISTIVITY TOMOGRAPHY

S.N. Rai[1]*, S. Thiagarajan[2] and M. Sateesh Kumar [2]
1Department of Earth Sciences, Indian Institute of Technology Roorkee, Roorkee-247667
2. CSIR-National Geophysical Research Institute, Hyderabad-7
**snrai_ngri@yahoo.co.in*

A major part of Andhra Pradesh, Telangana, Karnataka and Tamil Nadu states is occupied by crystalline granitic rocks. Granites like other hard rock formations possess negligible primary porosity and groundwater occurs in limited quantity in secondary porosity generally developed due to weathering, fracturing and faulting. Because of sporadic nature of distribution of these water bearing geological formations/structures, their delineation is a challenging task. If geological formations/ structures are saturated with groundwater, a noticeable contrast between the water saturated fractured/faulted rock's units and compact rock units would be observed. The former will be showing lower resistivity than the compact unit of hard rock which is devoid of grounwater. Because of this phenomenon, resistivity method is found to be most suitable method among all geophysical methods in delineation of groundwater bearing zones in hard rock terrains. Hyderabad is a growing city with explosive population growth and increase in industries. A considerable share of water supply demand in Hyderabad city is met from groundwater resources. Due to ever increasing exploitation of groundwater resources in excess to their replenishment has led to continuous declining of water table to a deeper level year by year. As a result finding their exact locations is a challenging task. This paper discuses the efficacy of newly developed 2-D electrical resistivity tomography (ERT) in delineation of groundwater bearing zones in complex hydrogeological environs of granitic terrains with the help of case studies from some regions in and around Hyderabad city. From management point of views, ERT results have been analysed to identify suitable sites for managing aquifer recharge. These sites can be developed for enhancing recharge to the aquifers, which in turn will be helpful in maintaining their sustainability of water supply. Some corrective measures over existing practices of bore well design have been also suggested to increase yield of the bore well and its sustainability. This study has helped in establishing some general criterion about the selection of potential groundwater resources in similar geological environs.

SEISMIC SOURCE INTERFERENCE NOISE ATTENUATION USING VELOCITY FILTERING: A CASE STUDY

Amrinder Sharma, D S Manral, GVJ Rao, P K Paul
Oil India Limited, Duliajan, Assam
amrindersharma19@gmail.com

The increasing demand of hydrocarbons worldwide imposing immense pressure on the E & P companies of the upstream sector to explore/exploit every yard of the subsurface in order to hunt / extract every drop of hydrocarbons present in the subsurface. Unfortunately, sometimes one E & P company while acquiring the seismic data in their area of interest found themselves to be working in the vicinity() of the other E & P company's area acquiring seismic data for their own interest. In these circumstances ,no doubt we have to be extra conscious while recording the data but the quality of the data is at risk because every time one recording the data there is possibility of data being deteriorated by the simultaneous data recording of the other. The noise recorded in such circumstances is called as ''source interference or cross source noise''. In field such type of noise is unavoidable and can totally destroy the data recorded for both the E&P companies.

In this paper it is shown that how while processing the data this noise can be minimized/ attenuated to a great extent by applying velocity filtering or f-k filtering. As the recorded wave field {u(x, y, t)} is a function of space and time. So by analyzing data spectrum in two dimensions the source interference noise can be attenuated.

Introduction: in the year of 2010-2011, Oil India Limited (an upstream E & P Company) assigned to carry out seismic survey operations in OIL's operational area of Assam Arakan Basin. While carrying out the seismic survey, ONGCL (an upstream E & P Company) was also found to be carrying out seismic survey in the vicinity of OIL's area operations. Which had given rise to the situation of source interference and generation of cross noise.

The affected data with SIN has very poor S/N ratio and it cannot be used for seismic imaging directly because it will deteriorate the final imaging output. So it is necessary to attenuate sin first by applying velocity filtering or f-k filtering to enhance the quality of the data and thereby increasing signal to noise ratio.

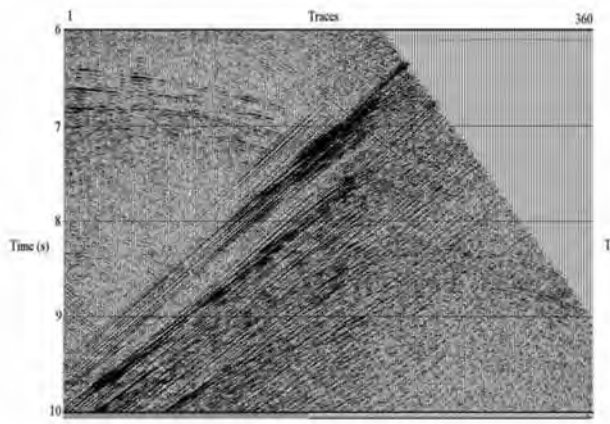

SIN affected

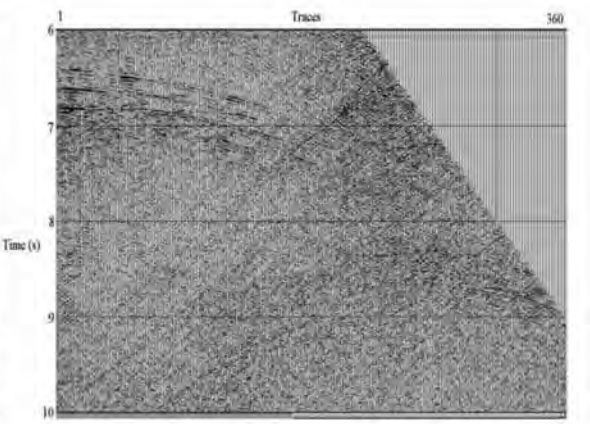

Sin corrected.

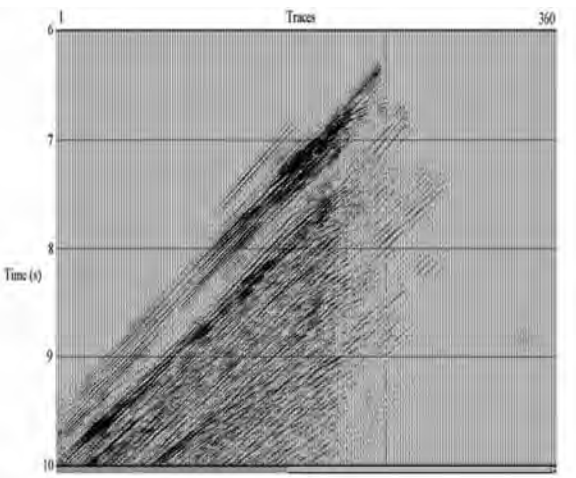

Filtered SIN

Note: here the data examples shown are taken from published text but during the final presentation author will be showing real data analysis and its results based on the real seismic data.

GEOCHEMISTRY AND GEODYNAMIC SETTING OF THE PROTEROZOIC VOLCANIC ROCKS OF THE MAHAKOSHAL FOLD BELT, CITZ, CENTRAL INDIA: IMPLICATIONS FOR PLUME-ARC INTERACTION PROCESSES

D.V Subba Rao, M. Sathyanarayanan and V. Rajachaitanya Kumar
(CSIR-National Geophysical Research Institute, Hyderabad-7, India)
dvsubbarao3s@rediffmail.com;dvsubbarao@ngri.res.in

The Central Indian Shield contain continental scale tectonic feature of Proterozoic age represented by the Central Indian Tectonic Zone (CITZ), which divides Indian Continental Shield into two tectono-magmatic provinces *viz.*, the northern cratonic province comprising Bundelkhand-Aravalli cratons and the southern cratonicprovince comprising Bastar, eastern Singhbhum and Dharwar cratons.During the last 25 years the Central Indian region has received significant attention. The Satpura mobile belt (SMB) or more popularly called as the Central Indian Tectonic Zone (CITZ) has been considered to be a convergent zone between the Bundelkhand Craton in the north and the Bastar-Bhandara Craton to its south. The extensive integrated geophysical studies carried out along a DST sponsored NW-SE trending geotransect passing through the Satpura mobile belt and Bhandara Craton, have revealed a clearly converging pattern of seismic reflectors just beneath the postulated suture, as well as a very different electrical conductivity structure on either side of the postulated suture, coupled with very high near surface conductivity. Although significant geophysical data is available on the SMB/CITZ and adjoining areas, an integration of the data is yet to be attempted. In addition, high precision trace elements (including HFSE, REE, and PGE) and isotopic data on the Supracrustal/greenstone belts in the SMB/CITZ, which are lacking, are essential in order to understand the geodynamic processes involved in generating these Proterozoic greenstone/Supracrustal belts.

We are now aware that orogenic activity of Palaeoproterozoic age is either missing or has not been recognized in the Dharwar Craton. The possibility is that it could have migrated to southern and Central Peninsular India. Most of the Palaeoproterozoic orogenic belts occur to the north and north-west of the Dharwar Protocontinent, within the Bundelkhand and Aravalli Protocontinents. Significant orogenic activity had occurred during Palaeoproterozoic around the Bastar, Chotanagpur, Bundelkhand, Singhbhum etc., in the central and north Indian regions. Some of the well known Palaeoproterozoic sequences of this region are the Nandgaon, Sausar, Dongargarh, Bhandara, Bijawar, Mahakoshal, Betul, Gwalior and other belts/groups. In the present work, detailed characterization of the less studied but important Mahakoshal supracrustal/fold belt has been investigated.The Central Indian region has widespread and extensive occurrence of supracrustal belts/mobile belts/fold belts and have deserved significant attention in recent times. These belts are considered as greenstone belts of a typical continental rift set up. Detailed multi-element geochemistry on the volcanic rocks of Mahakoshal belt will lead in understanding either role of arc-plume interaction in their generation or their derivation by other petrogenetic processes. Also the geodynamic setting of Mahakoshal group appears to be still uncertain (rifted basin, back arc, island arc, ocean floor). It is certain that the Mahakoshal belt needs more precise data generation and interpretation for a better understanding of the Proterozoic plate tectonic processes. Since the Mahakoshal belt is the locus of welding of the Dharwar and Bundelkhand Protocontinents, this belt provides an excellent opportunity to understand the changes which might have occurred otherwise across the Archaean-Proterozoic Boundary (APB). In addition to the above, prevailing uncertainties regarding the presence of an oceanic crust between the Dharwar and Bundelkhand Protocontinents could be settled by a geochemical/isotopic study of the volcanic rocks from the Mahakoshal Group in Central India.

In view of the above tectonic and geodynamic significance, the basic-ultrabasic volcanics from Agori and Chitrangi Formations of the Mahakoshal fold belt (MKB) are investigated in the present work. The metabasalts occurring in the western part of the MKB at Jabalpur-Narsingapur-Sleemnabad areas (Agori Formation) as well as in the eastern part at Sidhi-Thapna-Chitrangi areas (Chitrangi Formation) were studied in the present work. The metabasalts of the western part are melanocraticand highly porphyritic in nature and show ignimbrite and volcanic breccia structures. Whereas the eastern metabasalts exhibit characteristic pillow lava-pahoehoe toes, pyroclastic and volcanic agglomerate structures. Petrographically,the metabasalts from Agori Formation at Sleemnabad-Kusera section contain abundant amphiboles, actinolite, tremolite and serpentine and unusual dark blue variety of chlorite which has inclusions of epidote and quartz. The metabasalts of Narsingapur section (western part) are porphyritic in nature and consists of amygdales of chert and agate and zeolites. At places glass fragments are also noticed. The metabasalts of Sidhi- Chitrangi areas (Eastern Part of MKB) contain abundant amphiboles (actinolite and tremolite) and chlorite. The associated metapyroxenite sills consist of altered olivines, cpx, amphiboles and serpentine. The basic tuffs are noticed at Gopad River section, NW of Devsar in the central part of the MKB, are fine-grained and show fine laminations and characterized by cordierite and staurolite porphyroblasts which are post-tectonic in nature. All these basic-ultrabasic variety of lavas are metamorphosed/ recrystallised to low-grade metamorphism such as upper green schist facies metamorphism.

The metabasalts of MKB show contrasting geochemical characteristics across the belt. The Mahakoshal basic-ultrabasic volcanic rocks from Western region are discussed here and they plot exclusively in the field of thoeliites and exhibit compositional variations from high Fe-thoeliites and komatiitic basalts in the Jensen cation plot. Both thoeliitic basalts and komatiitic basalts are characterized in these suites. REE patterns are characterized by two groups such as LREE enriched (Type-I) and LREE depleted (Type-II) patterns [$(La/Sm)_N$ = 1.20 – 1.40] with flat to depleted HREE patterns [$(Gd/Yb)_N$ = 1.15 – 2.58]. The primitive mantle (PM) normalized distribution patterns show LILE enrichment, negative Th, Nb & Pb anomalies as well as both positive and negative Sr, Eu, P and Ti anomalies indicating the fractionation of mineral phases such as plagioclase-apatite and Ilmenite during partial melting. The tectonic discrimination diagrams suggest normal MORB to dominantly island-arc basalt (IAB) affinity.These metabasalts display geochemical characteristics transition between normal MORB and island-arc basalts.These western basalt lavas also show Nb/Th, Zr/Hf, Nb/Zr, Zr/Y, Nb/Y and Nb/Yb ratios similar to the island arc lavas of back-arc basalts affinity.Apart from this, the metabasalts of the Eastern region in MKB (Sidhi-Chitrangi areas) exhibit thoeliitic basalt characteristics with strong iron enrichment trends. They show compositional variations from High Fe thoeliites, komatiitic basalt and komatiites in the Jensen plot. REE patterns of these matavolcanics show highly fractionated patterns with LREE enrichment [$(La/Sm)_N$ = 1.39 - 4.04] mild negative Eu anomalies ($Eu/Eu^{\star}$ = 0.55 – 0.97) and HREE depleted patterns [$(Gd/Yb)_N$ = 1.56 – 3.35] . LREE enriched over HREE. The PM normalized patterns exhibit LILE enrichments, strong positive Nb + Ta, negative Th, Sr, P and Ti patterns. These eastern basaltic lavas show high levels of HREE enrichment whereas Ni& Cr are depleted relative to MORB. Spidergrams show troughs at K, Th and peaks at Ba, Nb compared to P-MORB. The Tectonic discrimination plots suggest mostly Ocean Island Basalt (OIB) as well as some in CRB + OIB affinity. The metabasalts of the eastern region in MKB exhibit dominantly Ocean Island Basalt (OIB)/OIT geochemical characteristics. The total PGE contained in these selected samples vary from 105 to 360 ng/g. The PGE abundances and their ratios such as Pd/Ir (4.3 to 12.9) and Pd/Rh (4.3 to 11.6) indicate that they have been derived from an evolved Komatiitic melt. The primitive mantle normalized PGE pattern display characteristics Rh positive anomaly and Pt negative anomaly with an enrichment of PPGE over IPGE. The concentrations of PPGE (75 to 334 ng/g) are almost three times more than that of the IPGE (23 to 64) in all the samples. The fractionation of PPGE over IPGE also indicates participation of sulfide phase in platinum group mineral crystallization. Relatively strong

positive correlation between Au and Pd (r2 = 0.72) and Au and Ir (r2 = 0.61) indicate participation of chloride and carbonate enriched fluids in the system during magmatism. The data presented above indicate a tentative model involving plume-arc interaction processes for the derivation of the metavolcanic rocks of the both Chitrangi and Agori formations of the MKB respectively.

ATTENUATION CHARACTERISTICS OF SEISMIC CODA WAVES AND HIGH FREQUENCY BODY WAVES IN THE GARHWAL-KUMAON HIMALAYA, INDIA.

Sivaram K[1*], Dinesh Kumar[2], S.S.Teotia[2] and S.S.Rai[3]

[1]CSIR-National Geophysical Research Institute, Hyderabad, India

[2]Department of Geophysics, Kurukshetra University, Kurukshetra, India

[3]Earth and Climate Science Program,Indian Institute of Science Education & Research (IISER), Pune, India

[*]sivaramk@ngri.res.in

We study the frequency dependent attenuation characteristics of the crust in the Garhwal-Kumaon Himalaya using seismic coda waves and high frequency body waves, obtained from about250high quality 3-component local earthquake waveforms.The quality factor (Q) is inversely related to the attenuation or the decay of seismic wave amplitude during its propagation in the crust.In the assessment of regional seismic hazard, the study of attenuation of seismicwaves facilitatesthe understanding the physical processesand structural heterogeneity of the crust. Due to geological diversity in the Himalayan region, we parameterized the region in three blocks along the latitude to study their attenuation properties.

We compute the crustal attenuation ($Q= Q_0 f^n$)properties using different approaches. The single backscattering model of Aki and Chouet (1975) is used for the estimation of the quality factor of seismic coda waves (Q_c)while the coda normalization andYoshimoto's extended coda normalization methodsare used for the estimation of the quality factors of direct S-waves ($Q_\square$) and direct P-waves ($Q_\square$)respectively. These computations are made in the frequency range 1-20 Hz.We observe variations in attenuation mechanisms, indicated both in the attenuation parameters Q_c, $Q_\square$ and $Q_\square$and variation of frequency dependence parameter 'n'.There is also an increasing trend of estimates of Coda Q with lapse times of 20s, 30s, 40s, 50s, 60s and 80s. The estimated values of body wave $Q_\square$and $Q_\square$are in general, low and highly variable. $Q_\square$varies from 21.95±2.76 to 146.01±3.71. $Q_\square$varies from 58.49±1.92 to 101.07± 6.48.

Many researchers treat Q_c as a tectonic parameter and the regions with high tectonic activity are characterized by low Q_c values. Further, a strong correlation between 'n' and the level of tectonic activity of the study regions has been observed by several investigators. This indicates that the three blocks in our study are active tectonic regions.

It is well known that attenuation of seismic waves can be separated into two main types: scattering (or redistribution of energy) and intrinsic (or loss of energy).Using the multiple scattering formulation of Wennerberg (1993), the instrinsicattenuation(Q_i^{-1}) and scattering attenuation (Q_s^{-1}) are separated.Our work provides a first order understanding of the predominantattenuation mechanism existing for the upper crust in the region.

For the threestudy blocks considered, following observations are made related the seismic attenuation property: (i) Q_c is more than $Q_\square$, which seems to adhere to the *Zeng's* (1991) theory; (ii) due to the complex structure of crust in the three blocks, there is a mixed effect of the scattering attenuation and intrinsic attenuationacross the transect consisting of the three blocks, for the considered

frequency range (1–20 Hz); (iii) the ratio $Q_{\square}/Q_{\square}$ is not the same for the three study blocks over the whole frequency range. The studies undertaken in this workindicate the presence of varying levels of rock saturation, possible fluids in the crustal depths near MCT zone and strong lateral variations in the shallow crustal structure beneath Garhwal-Kumaon Himalaya. These observations and a growing body of other investigations suggest that fluids(water, magma, and gases such as CO_2, SO_2, etc.)are intimately linked to a variety of earthquake faultingprocesses and propagation effects.

GROUNDWATER OVEREXPLOITATION IMPLICATION ON NATURAL GROUNDWATER RECHARGE RATE

R. Rangarajan, V. Venkatesam and D. Muralidharan
CSIR-National Geophysical Research Institute, Hyderabad-500007
rangarajanngri@gmail.com

Groundwater is the principal source of dependable water supply in India. The primary source of recharge to groundwater is by percolation of fraction of rainfall through unsaturated zone. The secondary source of recharge includes seepages from surface water bodies such as rivers, streams, lakes / tanks / ponds, canals, return flow from irrigation fields etc. The dependence of groundwater for domestic, industrial and irrigation sectors in the Indian subcontinent has increased several folds during last two decades. The overexploitation of groundwater resources has resulted in sharp decline in water level and quality deterioration.

The exploitation of groundwater resources is predominant particularly over hard rock covered granite areas of semi arid southern India, where the average annual rainfall is about 500-700 mm. Due to poor groundwater potential of this region, the increase in groundwater exploitation in rural region mainly for agricultural sector and domestic needs in urban region has resulted significant water level decline in many areas. The pre monsoon static water level occurred at depth range of 7-10 m below ground level (bgl) in 1984-87 has declined to a level of more than 30- 40 m bgl in recent years over granitic terrain. Intensive rice and wheat cultivation (double crop rotation) mainly through groundwater resources has led to declining trend of groundwater level and there is a growing concern of agricultural sustainability in the large part of Indo-Gangetic Alluvial covered Central Punjab region. Irrigation return flow due to surface and groundwater applied irrigation is a major source of groundwater recharge over this region. Static water level measurements in several observation wells using loggers at Punjab Agricultural University (PAU) campus, Ludhiana, in Central Punjab region has indicated steady groundwater level decline at the rate of about 0.8 m/y. Integrated studies for assessing irrigation return flow and water balance calculation in the PAU campus area indicated that overexploitation of groundwater for intensive cultivation of paddy and wheat is the main reason for continuous water level decline.

The overexploitation of groundwater resources has caused de-saturation of shallow aquifer and resulted in increase of unsaturated zone. Rainfall data analysis carried out for the last 100 years for selected stations indicate that the mean annual rainfall is not likely to increase in future. The increase in unsaturated zone implies increase in amount of rainfall required for soil moisture deficit caused by evaporation or evapo-transpiration every year. Rainfall-Recharge relationship was established in 1997 based on natural recharge data obtained using injected tritium tracer technique in several watersheds and basins located in different hydro geological provinces of India with characteristics regression equations. The regression relations indicated 240 mm as a minimum amount of rainfall (threshold level) required for initiating deep percolation and recharge to the aquifer system over granite terrain. Due to increase in thickness of vadoze / unsaturated zone, the threshold amount of rainfall required

for initiating recharge has increased and thereby annual precipitation recharge has significantly reduced. The tritium profiles observed at the natural recharge sites in two areas having similar geomorphological and hydrogeological conditions for two different times scale with a gap of 20 years shows reduction in tracer migration peak as the vadoze zone depth increases, resulting in low to negligible recharge rates. The low to negligible recharge rate in recent years even during normal monsoon years shows that the precipitation recharge component decreases steadily and may require attention of water planners.

The trend of increase in groundwater exploitation for domestic and agricultural sectors is likely to continue forever where surface water resources are not available. In view of increase in population growth and expansion of agricultural and industrial sectors and domestic requirements, there will be a severe stress on available groundwater resources in the coming years. The natural groundwater recharge may reduce with time but wont increase. Assuming that necessary financial and technical resources do become available, following water management practices may be implemented for arresting decline of water level and revitalizing the groundwater potential to achieve water security at least for drinking needs in the low to moderate rainfall semi arid regions.

i) For hard rock Granite terrain

- Rejuvenation of percolation/ minor irrigation tanks in rural areas and lakes in urban areas
- Recycling of water
- Minimizing the area of paddy cultivation in hard rock semi arid areas
- Strict regulation on drilling deep bore wells for irrigation purposes near drinking water sources

ii) For Indo-Gangetic Alluvium, Central Punjab

- Shifting the paddy transplanting date to period of low evapotranspiration, i.e. in the month of July instead of June
- Puddled Transplantation Rice (PTR) can be replaced by Dry Seeded Rice (DSR)
- Growing paddy only in alternate years
- Farm ponding for recharge in large irrigated fields
- Community Well irrigation practices

STATUS OF GROUNDWATER IN KURUKSHETRA DISTRICT: A GIS BASED EVALUATION

SK Goyal[1], Dheeraj Thakur[1] and B S Chaudhary[2]

[1]RKSD College, Kaithal

[2]Dept of Geophysics, Kurukshetra University, Kurukshetra

sanjayktl@gmail.com

Abstract: Groundwater is one of the precious natural resource which is essential for sustenance of human activities and for the social and economic progress of a region. The present study examines the spatio-temporal changes in groundwater depth and quality in Kurukshetra district of Haryana State. Pre- and Post-monsoon data pertaining to depth of water level below ground level (bgl) and electrical conductivity (EC) were attained from Groundwater Cell, Department of Agriculture; Kurukshetra (Haryana). Spatial distribution maps for depth and EC were prepared in GIS environment for 2001 and 2012. Change detection maps were generated using Raster Calculator in Arc GIS 10.1 for the identification of critical areas in the study region. The study revealed a decline in average ground water depth from 18.0 m bgl in June 2001 to 31.3 m bgl in June 2012. The post-monsoon levels were also found to decline from 18.26 m bgl in October 2001 to 32.44 m bgl in October 2012. Average EC of groundwater was observed to havedegraded from 243μS/cm in June 2001 to 645μS/cm in June 2012

and from 318μS/cm in October 2001 to 646μS/cm in October 2012. Total 94.2% area in the district has been identified as critical area, where depth to water level has increased from 12 mbgl to 17 mbgl in last 11 years. From the analysis of EC values from change detection map, it was observed that there was increase in average EC values but is still within the permissible limits.

MAGNETIC POLARITY STRATIGRAPHY OF THE MIDDLE JURASSIC BATHONIAN SECTION AT PATCHAM ISLAND, KACHCHH BASIN, INDIA

M. Venkateshwarlu[1], B. Pandey[2],D. B. Pathak[2] and Jai Krishna[2,]

[1]Geochronology (TIMS) and PalaeomagneticStudies, CSIR-National Geophysical Research Institute, Uppal Road, Hyderabad-500 007.

[2] Department of Geology, Banaras Hindu University, Varanasi-221 005.

Magnetic Polarity Stratigraphy studies were initiated in Kachchh basin by collecting 40 oriented block samples of limestones from 12 sites covering Late Bajocian -Bathonianintervalat Goradongar Dome of Patcham Island, Western Kachchh, Gujarat. The samples of Goradongar exhibited moderate to weak magnetizations with intensities range from $8.98x10^{-2}$ to $1.26x10^{-4}$. Systematic alternating field and Thermal demagnetization experiments were conducted on sediment samples. Thermal demagnetization results have shown good clustering of the directionsfrom intermediate to steep temperatures. The mean declination and mean inclination obtained from this section is Dm=349, Im=41 with α_{95}=9.68. This mean direction indicate that the Mesozoic sediments in this part of Kachchh have not been affected by the Deccan Volcanism (Dm=345; Im=-45). Magnetostratigraphy of the Goradongar section samples show both normal and reverse polarities indicating that this section has recorded reverse polarity of the Earth's magnetic field during Bathonian period (168.3-166.1 Ma). This section is correlated with the Geological Time Scale of Ogg et al. 2010 from M41 and below.

ON THE PRESENT TECTONIC SCENARIO OVER THE MYANMAR OFFSHORE USING HIGH-RESOLUTION SATELLITE GRAVITY DATA

R. Bhattacharyya[1] and T. J. Majumdar[2*]

[1]Centre of Excellence for Energy Studies, Oil India Ltd, Guwahati – 781022, India

[2]Space Applications Centre (ISRO), Ahmedabad – 380 015, India

** tjmajumdar@rediffmail.com*

Myanmar has 17 hydrocarbon-bearing sedimentary sub-basins but many of them are largely unexplored. The major petroliferous basins to date are the Central Basin, Irrawaddy Delta Basin, Pegu Yoma Basin, Gulf of Moattama Basin and Rakhine Coastal Basin. Many petroleum companies are holding acreages in Myanmar and doing exploration/ production operations. The majority of gas from Zawtika are being used to meet Thailand's growing gas demand while gas from Shwe is being exported to markets in southwest China. One-third of Myanmar's total perimeter of 1,930 kilometers (1,200 miles) forms an uninterrupted coastline along the Bay of Bengal, the Andaman Sea and the Gulf of Moattama. The exploration and production of oil in Mayanmar has been reported from Oil seeps and hand-dug wells in the Yenangyuang area in way back thirteenth century.

Myanmar is one of the world's oldest oil producers, exporting its first barrel in 1853. Rangoon Oil Company, the first foreign oil company to drill in the country, was created in 1871. Between 1886 and 1963, the country's oil industry was dominated by Burmah Oil Company (BOC), which discovered the Yenangyaung field in 1887 and the Chauk field in 1902. Both are still in production.

The Myanmar offshore exploration has started since 1965 and drilled some exploration wells in Rakhine and Moattama Offshore. The Myanmar Offshore can be geologically divided into three basins e.g. Rakhine Offshore Basin, Moattama Offshore Basin and Tanintharyi Offshore Basin, which have specific tectono-stratigraphy and petroleum systems. The youngest source rocks (Miocene) found in the Gulf of Martaban and northern Andaman Sea. The Myanmar offshore exploration was revived in 1982, with discovery of Yadana gas field about 70 km offshore in the Irrawaddy Delta fan at a water depth of 45 m. Exploration strategies designed to find larger commercially viable gas fields offshore are driving this trend toward deeper drilling. In order to meet the forecasted growth in domestic/ international gas demand, Myanmar Oil and Gas Enterprise (MOGE) is keen for development of new gas reserves both onshore and offshore. Offshore gas reserves as estimated are encouraging but participation will mainly depend on the Myanmar's regulatory regime and the fiscal policy.

The rapid assessment of offshore sedimentary basins has been the need of the present day geophysical exploration, for which satellite altimetry has emerged as a powerful reconnaissance tool, in recent years. With the advent of more and more altimetry missions with increasing accuracies and varying orbital configurations, it has been possible to generate large-scale altimeter-derived residual/ prospecting geoid and gravity anomaly maps over the oceans. Satellite altimetry (mainly in Ku and C bands) offers as an inexpensive and rapid reconnaissance tool for the sparsely surveyed Indian Ocean region. It can be used to infer subsurface geological structures analogous to gravity anomaly maps generated through ship-borne survey. The basic concept of the technique 'Satellite Gravity' lies in the fact that the surface of any water body, in absence of external forces, forms an equipotential surface. The sea surface height measured by satellite altimeter when corrected for atmospheric propagation delays and dynamic oceanic variabilities conforms to the equipotential surface, known as the geoid. The geoid contains information regarding mass distribution inside the entire earth including those due to variations in sea bottom topography. Geoid is used to compute residual and prospecting geoids - hypothetical surfaces related to the mass distribution in various lithospheric zones. Geoid is also converted to gravity using a simple technique. Sedimentary structures containing lighter materials than the surrounding igneous rocks/basement should be characterized by lower geoid/gravity signatures. The satellite-derived gravity has emerged as a new tool for sparsely surveyed western Myanmar offshore region.

An attempt has been made to identify the Arakan Yoma trend which forms the southern part of the Indo-Burman Ranges and in the south the NNE striking west vergent folds parallel the west coast. NNE striking west vergent folds parallel the west coast. At about 19°N the strike of the Arakan Yoma changes from NNE to NNW due, apparently, to the extension of a NW-SE lineament approaching from the southeast. No lateral movement has been observed on this lineament in the Arakan Yoma, the western and southern Myanmar basin is proven to be oil and gas reserve. Various exploration blocks have been announced by MOGE. In this study an attempt have been made to explore the coastal and deepwater areas of Myanmar in conjunction with satellite gravity and source rock and maturity data as available. The high resolution satellite gravity have been generated over the western Myanmar offshore depicting the present day tectonic scenario as correlated with known tectonic features such as the Sagaing fault. Various NE-SW trending lineament have been identified and the result suggests that the offshore Martaban basin to be a prolific basin. The Yadana, Itagun in the south are of Type-3 kerogen and the Mya and Shew field in the south western are also shows Type-3 kerogen. The north south trends of lineaments/features are parallel to Sagaing faults. However, NNE-SSW trending features can be correlated with broad tectonics of the area with anticlockwise movement of Burmese plate. The accumulation of flysch sediments in the offshore and ophiolite had happened due to rotation and allowed more sediment to deposit and thereby enriched the area by marine sediments and carbonates. Figure 1 shows the high-resolution satellite gravity image over the Myanmar offshore

and its surroundings after superimposition of tectonic and structural features. Thus, satellite gravity image over the study area has been found suitable for exploration of the Myanmar offshore.

Related References:

Curray, J.R., Emmel, F.J., Moore, D.G., 2003, The Bengal Fan : morphology, geometry, stratigraphy, history and processes. Marine and Petroleum Geology 19 (2003) 1191-1223.

Esser, R., 2001, Discoveries of the 1990s: were they significant? : Chapter 3 in AAPG Memoir 74: Petroleum Provinces of the Twenty-first Century, Eds. M.W. Downey, J. R. Threet, and W. A. Morgan, pp. 35-43.

Haxby, F., Karner, G.D., La Brecque, J.L. and Weissel, J.K., 1983, Digital images of combined oceanic and continental data sets and their uses in tectonic studies. EOS Trans., American Geophysical Union (AGU), 64 , 995-1004.

Mahmood, A., et al., 2003, An overview of the sedimentary geology of the Bengal Basin in relation to the regional tectonic framework and basin-fill history. Sedimentary Geology, 155, 179–208.

Majumdar, T.J., Mohanty, K.K., Mishra, D.C., and Arora, K., 2001, Gravity image generation over the Indian subcontinent using NGRI/EGM96 and ERS-1 altimeter data. Current Science, 80(4), 542-554.

Majumdar, T.J., and Bhattacharyya, R., 2004, An Atlas of very high resolution satellite geoid/gravity over the Indian offshore. SAC Tech. Note No. SAC/RESIPA/MWRG/ESHD/TR-21/2004, Nov. 2004, 46 p.

MOGE Reports, Myanmar Petroleum Geology and Hydrocarbon Potential, Myanmar.

Roy, S., 1999, Energy from gas hydrates. Science Tribune, Chandigarh, June 17, 1999.

Sandwell, D.T., and Smith, W.H.F., 1997, Marine gravity anomaly from Geosat and ERS-1 satellite altimetry. Journal of Geophysical Research, 1997, 102, 10039 – 10054.

Wandrey, C.J., 2006, Eocene to Miocene Composite Total Petroleum System, Irrawaddy-Andaman and North Burma Geologic Provinces, Myanmar, Chapter E in Wandrey, C.J., ed., Petroleum systems and related geologic studies in Region 8, South Asia: U.S. Geological Survey Bulletin 2208-E, 26 p.

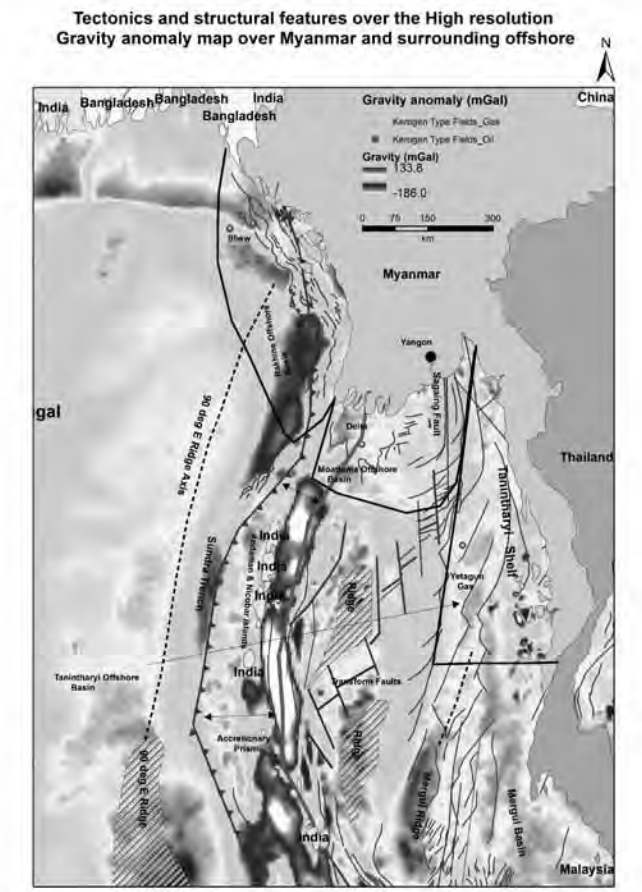

Fig. 1

INTEGRATED MAGNETOTELLURIC AND SEISMIC MODEL OF THE DEEP CRUSTAL AND LITHOSPHERIC STRUCTURE OF THE SIKKIM HIMALAYA

A. Manglik[1*], G. Pavan Kumar[2] and S. Thiagarajan[1]

1. CSIR- National Geophysical Research Institute, Uppal Road, Hyderabad

2. Institute of Seismological Research, Raisan, Gandhinagar

**ajay@ngri.res.in*

We present the results of a broadband magnetotelluric (MT) survey along a 200-km-long profile across the Sikkim Himalaya in conjunction with a seismic model of the region. The MT data were acquired at average station spacing of 5-6 km and transfer functions of 31 sites in 0.01-1000s period range have been used for 2-D joint inversion of TE and TM modes. Since the impedance tensor decomposition analysis revealed the presence of transverse geoelectric strike [Manglik et al., 2013, Tectonophysics, 589:142-150] in the Main Central Thrust Zone (MCTZ) bounded between two thrusts,the MCT-1 and the MCT-2, we prepared a hybrid dataset for joint inversion by incorporating two dominant strike directions, one coinciding with the strike of the under-thrusting Indian plate and the other representing the transverse strike.This hybrid dataset was inverted and several diagnostic tests were performed. The final composite model reveals several conductive and resistive features between the Ganga foreland basin and the High Himalayan Crystallines. Here, we focus on the deep crustal and lithospheric structure beneath the Sikkim Himalaya by integrating the present MT results with the seismological model of Singh et al. [2010, Tectonics, 29:TC6021].

The integrated model reveals the Moho offset of about 14 km at the southern boundary of the MCTZ separating the moderately conductive southern segmentfrom the highly resistive northern segment. The Moho jumps sharply from about 44 km depth to 60-62 km depth within a profile distance of about 30 km across the MCT-2. The sharp resistivity change across the MCT-2 implies the presence of a steep deep crustal fault. Occurrence of earthquakes down to 50-60 km depth in this region supports the presence of such a fault.The dominant strike-slip nature of the earthquakes could be used to infer that the deep crustal fault is probably a terrain boundary between two geological blocks, having contrasting crustal structures, which has got activated due to the convergence of the Indian and the Eurasian plates. The present integrated model reveals the difference in the nature of the crust and mantle lithosphere across this boundary. The southern segment of the mantle lithosphere has moderate resistivity whereas the northern segment has very high resistivity. Such a contrast is not seen in the seismic velocity model. Shear wave velocities of both segments are around 4.7 km/s. Within the crust, the seismological study has delineated a Moho doublet related to partialeclogitization of the Indian lower crust in the crustal block north of the MCT-2 which is missing in the southern segment. MT results also reveal the difference in the resistivity structure of the deep crust across the MCT-2. Within the northern block, a change in the resistivity from moderate to very high values at the depth of 42-45 km correlates with the top of the doublet.

In order to understand the cause for high resistivity of partially eclogitized crust, we analyze our integrated model in light of the laboratory measurements of the resistivity and P-wave seismic velocity on the drill core samples from the 5140 m deep Chinese Continental Scientific Drilling Main Hole at the southern part of the Sulu ultra-high pressure metamorphic belt [Salim et al., 2008, J. Applied Sciences, 8:3593-3602]. The measurements carried out on rutile eclogites and retrograde eclogitesrevealed that the seismic velocity for rutile eclogites (6.52±0.26 km/s) does not significantly change from that for retrograde eclogites (6.6±0.13 km/s) whereas the resistivity changes are remarkably large (14338.08±2920.2 Ωm for rutile eclogitesvers. 455.76±169.6 Ωm for retrograde eclogites). Therefore, the high resistivity of the partially eclogitized lower crustal layer may be explained in term ofeclogitesthat have not undergone retrograde metamorphism.

MATHEMATICAL ANALYSIS OF THE HALL EFFECT ON TRANSIENT HARTMAN FLOW ABOUT A ROTATING HORIZONTAL PERMEABLE SURFACE IN A POROUS MEDIUM

M. Suresh* **and A. Manglik**
CSIR- National Geophysical Research Institute, Hyderabad-7
**suresh.mantriki@gmail.com*

This work proposes the exact solution for unsteady flow of a viscous incompressible electrically conducting fluid past an impulsively started infinite horizontal surface, embedded in the saturated porous medium, rotating with an angular velocity. The medium is under the influence of a strong magnetic field with the Hall effect. Our study concentrates on analyzing the effect of the change in the direction of the external magnetic field on the change in the flow behavior and skin frictional forces at the boundary. A system of flow and magnetic field equations is solved by using the Laplace transform method and applying the theory of residues. First, we have studied a special case of the absence of permeability of the porous medium and inclination of the magnetic field to validate our solution with the published results of Rao et al. (J. Appl. Fluid Mech., 2012, 5:105-112). The results are in good agreement. Next, the effects of control parameters; the Hartman number, rotation parameter, the Hall current parameter, inclination of the magnetic field, and the Darcy number, on the primary and secondary velocities have been analyzed. Generally, the magnetic field has tendency to retard the flow velocity. However, the change in the direction of the applied magnetic field and the Hall current parameter (m) only marginally affect the primary flow whereas the secondary flow enhances for small values of m ($m \leq 1$) and decreases for large values of m ($m > 1$) within the thin boundary layer.

DISTORTION AND GEOELECTRIC STRIKE ANALYSES OF MAGNETOTELLURIC IMPEDANCE TENSORS FROM THE SIKKIM HIMALAYA

G. Pavan Kumar[1*] and A. Manglik[2]
1. Institute of Seismological Research, Raisan, Gandhinagar
2. CSIR- National Geophysical Research Institute, Uppal Road, Hyderabad
**pavan.ngri@gmail.com*

Observed magnetotelluric (MT) impedance tensors are generally affected by inductive and galvanic distortions, especially in tectonically complex regions. Minimization of these effects is needed before a meaningful interpretation of MT data can be carried out. This is even more important when the data are interpreted in terms of two dimensional (2-D) models by decomposing the data into respective electric and magnetic polarization modes. The Himalayan Collision Belt is a tectonically complex region where regional structures are disturbed by transverse features necessitating detailed distortion and geoelectric strike analyses. We present detailed distortion and directionality analyses of the broadband MT data acquired along an approximately north-south profile cutting across various major geotectonic domains of the Sikkim Himalaya. Impedance tensors of 31 sites in the period range of 0.01-1000s have been analysed for regional directionality and to understand possible presence of 3-D effects by using Groom-Bailey (GB) decomposition method, phase tensor (PT) analysis, LaTorraca(LT) decomposition technique, andBecken and Burkhardt (BB) method based on the ellipticity criteria of telluric vectors. The principal directions estimated by the GB and the PT approachesindicate the existence of transverse tectonic trend in the north-central segment of the profile which is further reinforced by the analyses employing the LT and the BB approaches. Distortion indices like high skew angle estimatedby the PT and the LT methods; nonvanishingellipticities of telluric vectors by the BB approach, and E and H polarization ellipses by and the LT approach suggest possible presence of 3-D effects/2-D inductive distortions of telluric currents at deeper levels. Localised current channellingis inferred at sites showing anomalous phases exceeding 90^{o}.

3-D SEISMIC VELOCITY STRUCTURE OF KUMAON-GARHWAL HIMALAYA: INSIGHT IN TO QUARTZ RICH ROCKS AND EARTHQUAKE OCCURRENCE

***P. Mahesh[1], Sandeep Gupta[2], S. S. Rai[3] and Ajay Paul[4]**

[1] *Institute of Seismological Research (ISR), Raisan, Gandhinagar*
[2] *CSIR- National Geophysical Research Institute, Hyderabad*
[3] *Indian Institute of Science Education and Research, Pune*
[4] *Wadia Institute of Himalayan Geology, Dehradun - 248001, India*
pmahesh.isr@gmail.com

We present a detailed three-dimensional *P-* wave velocity (V_p) and *Vp/Vs* structure for the Kumaon-Garhwal Himalaya generated by inverting arrival times of 1180 local earthquakes recorded by a seismic network of 50 broadband stations operated during April 2005 - June 2008. The upper crust (< 20 km) show heterogeneous structure in this region. In the near surface (upper 5 km), south of Main Frontal Thrust (MFT) is characterised by low V_P (~5.2 - 5.4 km/s) and low V_P/V_S (~1.67 - 1.72) that could be impression of unconsolidated sediments. We observe that the earthquakes are localized in the regions of low V_P (~ 5.3 - 5.7 km/s) and low V_P/V_S (~1.6 - 1.72) in the upper crust (< 20 km) possibly due to the presence of quartz-rich rocks, e.g., granites, granitic gneisses, schists and quartzites. To the north of Main Boundary Thrust (MBT) a low velocity (V_P ~5.7 km/s) layer is observed at 10-15 km depth. This could be signature of the Main Himalayan Thrust (MHT) in this region. At the depth of 18 - 25 km beneath the Main Central Thrust (MCT) zone an isolated zone of anomalous V_P ~5.7-6.0 km/s and V_P/V_S ~1.75.1.85 is observed. This is just below the maximum concentration of seismicity and also the 1999 (Mb 6.3) and 2005 (Mb 5.3) Chamoli earthquakes; and coincides with the low resistivity zone reported by magneto telluric studies. This could be interpreted as possible presence of fluids due to metamorphic dehydration reaction during underthrusting of the Indian crust. The presence of fluids around and below the seismogenic zone can influence the activity of the fault system; it can affect the long-term structural and compositional evolution of the fault zone, and can alter the fault-zone strength and local stress regime. As fluids enter the active faults in the crust (such as the MCT zone), fault zone friction decrease facilitating the stress concentration in the seismogenic layer leading to mechanical failure. We, speculate that the earthquake occurrence in the Kumaon-Garhwal Himalaya is not only due to stress caused by collision tectonics, but also associated with the lithology of the region.

STATISTICAL TECHNIQUES OF GEOPHYSICAL SIGNAL ANALYSIS

Sunjay and M. Banerjee

Geophysics , Banaras Hindu University,Varanasi – 221005,India
sunjay.sunjay@gmail.com , manasgp@yahoo.com

Geophysical Signal Processing is of paramount importance for precisely imaging subsurface geological features. My research work assigns to delve deep into so many methods, techniques and tools for statistical non stationary geophysical seismic signal processing and imaging - Wavelet Analysis, Principal Component Analysis (PCA), Factor Analysis, Independent Component Analysis (ICA), Blind Source Separation, spectral analysis and Singular Value Decomposition(SVD), Azimuthal Seismic Processing, Subsurface imaging by seismic diffractions, Nonlinear Seismic Imaging, etc. The central idea of principal component analysis (PCA) is to reduce the dimensionality of a data set, which consists of a large number of interrelated variables, while retaining as much as possible of the variation present in the data set. Reducing the complexity of a data set reveals the sometimes hidden, simplified structure that often underlies it, and is therefore, a powerful tool for analyzing data. The principal components are given by an orthogonal linear transformation of a set of variables, such that in the new coordinate system, the greatest variance by any projection of the data comes to lie on the first coordinate (called

the first principal component). This technique has a wide range of applicability such as dimension reduction, patterns recognition, seismic stratigraphy, seismic geomorphology and image processing. PCA and ICA use the statistical properties inherent in data ,extracting useful information which is used for noise suppression and blind deconvolution. In PCA, traces are transformed linearly and orthogonally into an equal number of new traces that have the property of being uncorrelated, where the first component having the maximum variance is used to produce the image. SPSS is employed for statistical geophysical data analysis .

TECTONICS AND TOPOGRAPHIC CONTROL OVER EROSION IN THE EASTERN HIMALAYA

Vikas Adlakha[1*], James Pebam[2], R.C. Patel[3], A.K. Jain[4], and Nand Lal[3]

[1] Wadia Institute of Himalayan Geology, Dehradun 248001, India
[2] Geological Survey of India, Kolkata-700016, India
[3] Department of Geophysics, Kurukshetra University, Kurukshetra 136119, India
[4] Central Building Research Institute, Roorkee 247667, India
vikas.himg@wihg.res.in

Evolution of landscapes in actively deforming orogens is controlled by internal tectonic and external surficial processes together. Is it "Tectonics" or "Climate" which dominate in modulating topographies and exhumation rates of active deforming regions is still a matter of debate (e.g. Whipple, 2009; Herman et al., 2013; Godard et al., 2014). To address this issue, long-term erosion rates at millennial time scale have been derived using 37 new apatite and zircon fission track (FT) Thermochronological dataset in the Eastern Himalaya (Fig. 1), the area which has undergone intense deformation during its evolution (Kumar, 1997) and is strongly affected by monsoon climate since Miocene (Dettman et al., 2003; Bookhagen and Burbank, 2010). The apatite FT ages range from 2.0 ±0.3 to 12.1±1.2 Ma and zircon FT ages vary between 3.3±0.3 and 13.2±0.7 Ma. To understand the role of structures and climate on long-term erosion, apatite and zircon FT ages have been plotted with respect to tectonic sections and precipitation swath profiles derived from Tropical Rainfall Monitoring Mission (TRMM) mean annual precipitation 2B31 post processed data (Bookhagen and Burbank, 2010) calculated from 1998 to 2013 at 5×5 km resolution respectively. Regional slope and relief of the study region have been accessed using ASTER 30m DEM data to understand the interaction between tectonics and topographic changes resulting in the changing pattern of long-term erosion. Our study indicates that long-term erosion appears to mimic the topographic pattern but is unrelated to the distribution of present day precipitation. The mean 1D modeled exhumation rate calculated from all datasets within delineated low slope-zone is 0.40 mm/yr which gets doubled (i.e. 0.82 mm/yr) in the high slope zone. The structural window zones are found to be the zones of focused erosion in the Eastern Himalaya which were developed due to folding of MCT at ~ 8 Ma. Here we propose that the spatial and temporal erosion pattern in the active orogenic settings is strongly governed by the local tectonics of the area rather than the climatic variations on local scales.

References:

Bookhagen, B., Burbank, D.W. (2010). Journal of Geophysical Research, 115, F03019.
Dettman, D.L., Fang, X., Garzione, C.N., Li, J. (2003). Earth and Planetary Science Letters, 214, 267–277.
Godard, V., Bourlès, D. L., Spinabella, F., Burbank, D. W., Bookhagen, B., Fisher, G. B., Moulin, A, Léanni, L. (2014). Geology, doi:10.1130/G35342.1.
Herman, F., Seward, D., Valla, P. G., Carter, A., Kohn, B., Willett, S. D., Ehlers, T., (2013), Nature, 504, 423-426.
Kumar, G. (1997). Geological Society of India Publication, Bangalore, 217p.
Whipple, K. X. (2009). Nature Geoscience, 2, 97-104. 2

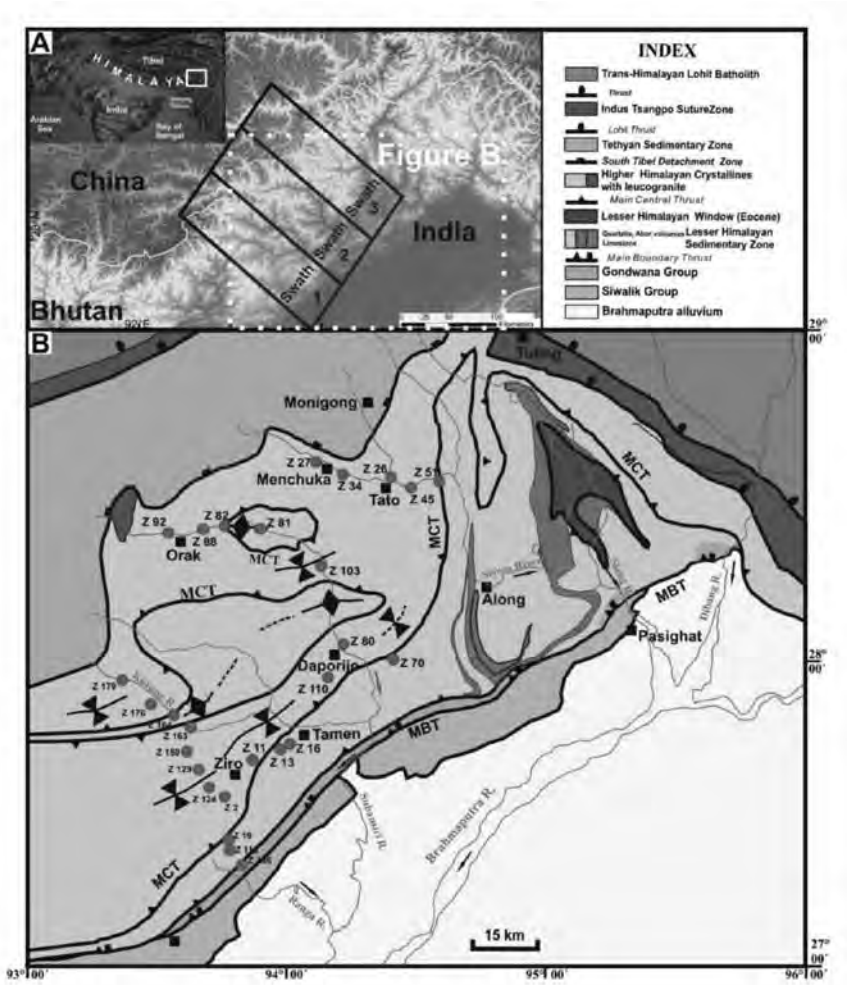

Fig. 1. *A. Overview map indicates location of study area and country borders on ASTER 30m DEM image along with map area in B (dashed rectangle) and swath locations for precipitation analysis. B: Geological map of Eastern Himalaya with locations of collected samples for FT thermochronological analysis.*

DEVELOPMENT OF CRUSTAL SEISMIC EXPERIMENTS IN INDIA – A TIME LINE

DipankarSarkar

CSIR- National Geophysical Research Institute,Hyderabad 500007

12345dip@gmail.com

Crustal seismic experiments in India, commonly known as Deep Seismic Sounding (DSS), started in the late seventies. Since then several dozens of scientific papers havebeen published depicting pictures of the velocity models and/or structural fabric ofdifferent parts of the Indian crust and also of a number of sedimentary basins. Theseresultshave beenwidely used toderive important geological conclusions. Validity and accuracy of deepseismic results in India varied with time, with gradual improvement in data acquisition, processingand interpretation technologies. The early results were primarily the outcome of narrowband seismic data collected with analog recording equipments. The processing andinterpretation tools, mostlyindigenously developed, also had their limitations.With thestarting of digital data acquisition and wide availability of forward modeling techniques,the newer results became better in terms of quantification as well as in quality. Still,modeling procedure remained primarily kinematic, with amplitude information beingqualitatively used on occasions. Also, the modeling process

has been a purely twodimensional approach.Themultifold deep reflection profiling (DRP) studies that wereinitiated in the nineties mostly adopted commercial oil industry data processing packages. Such conventional approaches do have their limitations in extracting the best possibleinformation from thedatapertaining to deeper depths. Since seismic data acquisition requiresgreat humanand financial inputs, there is necessity to reduce the subjectivity in the results byreprocessing the data with more suitable algorithms. This presentation intends todemonstrate the chronological progress in DSS data analysis and recent trends inimproved data processing in obtaining more realistic images of the crust.

POTENTIAL OF NON-CONVENTIONAL ENERGY IN HIMALAYA REGION

***A. M. Dayal, D. J. Patil, M. S. Kalpana and G M Bhat**

CSIR-National Geophysical Research Institute, Uppal Road, Hyderabad -700007, India
dayalisotope@ngri.res.in
Dept. of Geology, University of Jammu, Jammu
bhatgm@jugaa.com

Non-conventional energy source:

Natural gas, primarily methane, from the shale rock formations is emerging rapidly as an unconventional energy resource globally and also in India. Geochemical attributes of the shale source rocks, namely the total organic carbon (TOC) content, thermal maturity and kerogen type are controlling parameters in generation of shale gas. A reconnaissance study was carried out in the Jammu, Kashmir and Ladakh region of Western Himalaya, India in which shale samples were collected from the exposed formations ranging in age from Proterozoic to Cenozoic. The objective of the study was to obtain a preliminary data for the organic richness and kerogen properties in the shales to assess their gas generation potential. In the present work, carbonaceous shales along with coals from the Subathu Group of Jammu & Kashmir (J&K) have been studied for their organic richness and maturity based on the programmed pyrolysis method of Rock Eval (RE) VI. In the Himalayan Foot Hill belt, the Cenozoic and Proterozoic shales were samples for the organic matter characterization.

About seventy samples were collected from the shale horizons exposed in the outcrops and mines fromKalakot, Kotla, Mahogala, Salal, Kanthan and Kalimitti areas of Jammu belonging to the Tertiary Subathu Group, Proterozoic Sirban shales were collected from the Tattapani area, Jammu and Fourteen shale samples from the Permian –Triassic Boundary were collected from the outcrops near Guryul Ravine Section and Baru Spur, and Pahlgam region in Kashmir. The Paleozoic shales were collected from the exposed horizons near Lamayur, Diskit and Sukur in Ladakh.

These samples were analysed in Rock Eval for their organic characterization. A total of thirty carbonaceous shales and coal samples collected from the outcrops present around Kalakot, Kotla, Mahogala, Salal, Kanthan and Kalimitti areas of Jammu showed quite high Total Organic Carbon (TOC) content ranging between 3-65%. For the shales, the S1 (thermally liberated free hydrocarbons) values range between 0.1 -2.6 mgHC/gRock (milligram hydrocarbon per gram of rock sample) and are characteristic of 100% of the sample. The S2 (hydrocarbons from cracking of kerogen) show an elevated value between 0.5 -15.5 mgHC/gRock. The Tmax (temperature at highest yield of S2) ranges between 490-515 °C suggesting an over mature phase for the hydrocarbons. The hydrogen index (HI) is low ranging in values between 10-50 mgHC/gTOC, whereas the oxygen index for all studied samples is near to zero. Largely, the organic matter in majority of samples contains Type III kerogen and has generation potential for the gaseous hydrocarbons.

The Karewa lignites from the Nichoma area are rich in organic matter with the TOC content upto 29.4%. The Tmax ranges between 399-427°C suggesting a mature phase for the hydrocarbons. The hydrogen index (HI) is high ranging in values between 109-278 mgHC/gTOC. The organic matter in majority of samples contains Type III kerogen. The samples from the Permian-Triassic boundary in Kashmir are lean in organic matter with TOC<1%. The HI values for these shales are extremely low suggesting an immature stage for these shales. The Paleozoic shales from Ladakh has low TOC content of <0.5%. These shales have high oxygen index compared to the Hydrogen index, suggesting weathering/metamorphosed stage.

The Rock Eval pyrolysis data form the shales of Himalayan region appears to be varied ranging from excellent to very good to poor. With a high TOC containing type III kerogen and suitable gas generation potential, initiatives taken towards detail studies from viewpoint of shale gas prospect in Subathu Group should prove to be rewarding. The lignites from Karewa Formation show a Type III kerogen and a near mature stage for the hydrocarbons. Estimations on expelled and retained gas inferred from the geochemical properties of the Subathu Group of shales can be made by the taking into account the generation potential, source rock thickness and porosity of the shale formations.

TIME DOMAIN ELECTROMAGNETIC INVESTIGATIONS IN THE AHMEDABAD REGION,CENTRAL CAMBAY BASIN, GUJARAT

G. Pavan Kumar*, Virender Choudhary, Kapil Mohan and B.K.Rastogi
Institute of Seismological Research, Raisan, Gandhinagar
gayatripavankumar@gmail.com

We present the preliminary results of time domain electromagnetic (TDEM) surveycarried out in the Bhavla region, Ahmadabad district located in central part of the Cambay basin to delineatesubsurface resistivity image of the region. Fixed in-loop TDEM soundings were made at 12 selected locations along N-S and E-Wlineswith 100 m sided transmitter loop. For each loop, the transmitter is operated for a sequence of data repetition frequencies ranging from 32 Hz to 1 Hz. Rate of change of secondary magnetic fields produced due to the induced eddy current in the subsurface have been measured at every TDEM sounding site using a receiver coil. The data were processed to get apparent resistivity as a function of decay time.The subsurface electrical resistivity image obtained by combining the results of 1-D smooth inversion for 8 locations along the 2.5 km long the N-S lineindicating in-general three layered structure upto 160m. A 20-30m thick conductive channel of resistivity ~10 Ω.mat a depth of 20-25m interpreted as saturated/unconsolidated rock is overlain on another saturated rock (with possible content of sulfides, clay etc.) of comparably low resistivity. Alocalized fractured resistivity zone (20-25Ω.m) at a depth of 20m extending toentire depth section is observed at north central part of the line. The results could be integrated with hydrogeophysical information for further characterization of the aquiferand the fractured zoneobserved in region.

DELINEATION OF DEEP AQUIFERS ALONG THE AGRA – HALDWANI PROFILE IN THE GANGA PLAINS BY MAGNETOTELLURICS

S. Thiagarajan*, Ankur Kumar, A. Manglik and M. Suresh
CSIR- National Geophysical Research Institute,Hyderabad-7
**sthiagarajan@ngri.res.in*

Groundwater is one of the major sources of water supply for drinking, agricultural, and industrial purposes. Agriculture in India very heavily relieson the monsoon rains. Any deficit in the monsoon precipitation or its failure has serious implications for the country's economy. In the Ganga plains,

groundwater drawn from shallow aquifers (< 30 m or 100 ftbgl) is extensively used for agricultural purposes in non-monsoon months. Monsoondeficit also has impact on the recharge of these shallow aquifers leading to groundwater availability problem for agriculture in the near future. In order to mitigate groundwater shortage, it is essential to delineate deep aquifers which may be judiciously tapped for agricultural purposes during monsoon deficit. Artificial source electrical and electromagnetic (EM) methods are best suited to map aquifer zones in sedimentary environment.

In some cases, natural source EM methods such as magnetotellurics (MT) may also be used to image the near-surface structure, especially in the conducting environment if very high frequency high quality data are available. In our recent MT survey along a profile between Agra and Haldwani, aimed at delineation of the basement structure of the western Ganga basin, we could acquire excellent very high frequency MT data (100 – 10,000 Hz) at many sites along the profile. We have analyzed these dataand could delineate the electrical conductivity structure of the near-surfacebetween 25 to 250m. Our results reveal the presence of an aquifer at about 40-50m (130-160 ft) depthbgl. In this area, agricultural pump sets have been drawing water from 70-80 ft. Sites falling between the Yanuma and the Ganga rives reveal a prominent low resistivity zone (<5 Ωm) of about 50-60m thickness at an average depth of 70-80m bglwhichmay be related to a clay/silt dominated layer. The conductivity structure at this depth is different north of the Ganga river.Our results indicate the presence of deep aquifers in the Ganga plains. Detailed electrical and artificial source EM surveys may help in fine-tuning the depth and thickness of deep aquifers.

MAGNETIC ANOMALIES IN DELINEATION OF GROUNDWATER POTENTIAL ZONES IN A TYPICAL HARD ROCK GRANITIC TERRAIN OF MEDAK DISTRICT, INDIA.

***B.Madhusudhan Rao, S.Venkata Rama Lingam, B.V.S.Murthy and R.Sandya**
Department of Geophysics, Osmania University, Hyderabad – 500 007
**profmadhurao@gmail.com*

In hard rocks, groundwater occurs mainly in secondary porosity zones developed due to weathering, fracturing, faulting, etc., which are highly variable. Systematic and synergistic approaches would be suitable for groundwater prospecting in such regions. A magnetic survey in the eastern a part of Medak District, Andhra Pradesh, India (between northern latitudes $17^0$35′-$18^0$18′ and eastern longitudes $78^0$25′-$79^0$10′),where the dominant rock type in Peninsular granitic gneiss was carried out. The surveys helped studying structural features and the associated intrusives like dolerite dykes besides marking weathering and lithological variations. The data facilitated estimating thickness of weathered layer and the underlying fractured and fissured zone. Results from this study are presented herein and discussed in relation to groundwater occurrence in the study area.

GEOLOGICAL AND PETROLOGICAL STUDIESOFACIDIC ROCKS FROM DEVSARANDKHANAKAREA, BHIWANIDISTRICT, HARYANA, INDIA: A PRELIMINARY REPORT

Naresh Kumar[1], Radhika Sharma[1], A. K. Singh[2]
1*Department of Geology, KurukshetraUniversity,Kurukshetra - 136119 (Haryana)*
[2]Wadia Institute of Himalayan Geology, Dehradun – 248001 (Uttarakhand)
radhika8822@gmail.com;sagwalnaresh@gmail.com

Acidicrocks of DevsarandKhanakareasinsouthwesternHaryanaare part of NeoproterozoicMalani Igneous Suite (MIS) which covers an area of 55,000 sq. km in Northwestern Indian Shield. The MIS represents the largest acidicmagmatism in India and owes its origin to hot spot tectonism

(Kochhar, 1984; Bhushan, 1985; Vallinayagam, 2003). The representatives this A-type anorogenic acid magmatismare well exposed in Jhunjhunu, Jodhpur, Pali, Barmer, Jalor, Jaisalmer districts of Rajasthan and Bhiwani district (Haryana) and also occur at Kirana hills of Pakistan.The MIS predominantly consists of acidic volcanic (rhyolite, trachyte, dacite) with acidic plutonic (granite of various types), mafic volcanic (basalt, andesite), mafic intrusives (gabbro, dolerite) and minor amount of pyroclasts. The present study Devsararea(Survey of India topographic sheet no. H43W1, 1: 50,000, 28^0 46′-28^0 47′30′′ N; 76^0-76^0 05′30′′ E)mainlyconsists of granitic rocks ofvarious colour (dark brown, pink, grey) and quartz porphyry. These different varieties of granite are showing sharp contacts to each other and also with quartz porphyry. In the Khanakarea (Survey of India topographic sheet no. H43V13, 1: 50,000, 28^0 53′-28^0 55′ N; 75^0 50′ 30′-75^0 53′ E) granite porphyry is the main lithology with minor biotite granite and quartz porphyry. The granite porphyry shows various shades of colour viz.dark steel grey, dark grey, purple, light brown and coarse grained porphyryetc. Numerous dykes of microgranite and xenoliths intruded within the granite porphyry. The successive phases of intrusions and variable contacts are observed in the Khanakarea. At places, the contacts are very sharp that normal texture of two variations are also observed in one hand specimen. In some instances,the normal contact zone between two phases of granite porphyry is confused by the incorporation and partial mechanical disintegration of xenoliths of the host granite porphyries.Within few meters of the contact, pegmatitic knots and aplitic veins were also developed. These pegmatitic knots and aplitic veins are mainly observed in the steel grey porphyry type. The contact of quartz porphyry with the biotite granite is sharp and vertical in attitude. Occurrence of quartz porphyry at periphery of granitic massif indicates the absence of clear cut boundary within the upper crust between volcanic and plutonic phenomenon. The present preliminary study suggests that the rocks of Devsar and Khanak areas of the southwestern Haryana are closely similar to the rocks of the MIS. Detail petrological and geochemical studies of these rocks are being carried out to understand tectonic environment and petrogenesis.

References

Bhushan, S.K., 1985. Malani volcanism in Western Rajasthan. Indian Journal of Earth Sciences 12, 58-71.

Kochhar, N., 1984. Malani Igneous Suite: Hot-spot magmatism and cratonization of the Northern part of the Indian shiled. Journal of Geological Society of India 25, 155-161.

Vallinayagam, G., 2003. Basic magmatism of NeoproterozoicMalani Igneous Suite, Western Indian Craton: Petrological and Geochemical Modelling. Indian Journal of Geochemistry 18, 1-18.

REMOTE SENSING AND GEOPHYSICS BASED STUDY ON THE MICRO-EARTHQUAKES OF MARPALLY MANDAL, RANGAREDDY DISTRICT, TELANGANA STATE, INDIA

P. Chandrasekhar and K. Seshadri

Hydrogeology Group, RSAA, National Remote Sensing Centre (NRSC),
ISRO/DOS, Govt. of India, Hyderabad – 500 037
chandrasekhar_p@nrsc.gov.in

The hard rock terrain or the shield areas are supposed to be relatively safer from earthquake point of view as they are placed in zones 2 and 3 respectively of the 'seismic zonation map' of India. However, microearthquakes which are very low intensity earthquakes of magnitude less than 2 on the Richter scale are becoming a common phenomena in the above areas in recent times. A number of such microearthquakes had rocked the surroundings of Damasthapur village in Marpally mandal, Rangareddy district of Telangana state during September-October 2013 creating panic among the residents by causing cracks on a number of houses, dismantling cattle-shelters, etc. In order to understand the reasons for the above, satellite-based remote sensing data pertaining to IRS P6 - LISS-IV sensor was

interpreted and supported by the published gravity data. Intensive ground truth and well inventory were carried out. It is observed that the area was occupied with basalts and enveloped with laterite capping bearing a thickness ranging from 30-40 m. The fractures / faults passing through these rock units were examined on the ground and the water level fluctuations within the area were established. A few electrical resistivity traverses were also run across these fractures and in the weathered zones of basalts and laterites. It is observed that in view of the excess rain fall, shallow water table conditions were increased in both basalts and laterites. The fractures distributed over basalts were influenced by the excess accumulated water coming from the horizontally bedded basalts and also from the weathered lateritic zones. This hydro-loading had resulted into hydro-pressure in the surrounding areas and thus manifested in the form of microearthquakes. Similar type of microearthquakes were also reported earlier in the other parts of Rangareddy district (Vanasthalipuram area) which were caused due to intrusive rocks (dykes) of the granitic terrain whereas the present micro-seismicity was understood as due to the extrusive rocks (basalts).

NEW SEISMIC HAZARD ZONING MAP OF INDIA

B. Ramalingeswara Rao
Scientist 'F' (Ret), CSIR-NGRI & USERS DST- Scientist
brrao_buddha@yahoo.com

After studying 513 historical earthquake descriptions reported in the book entitled 'Seismic Activity - Indian Scenario' (Ramalingeswara Rao, 2014), selected some of the earthquake moment magnitudes, M_w and intensities, MSK assigned based on the observed felt reports, which are plotted along with the Z-factors as a range of effective peak ground acceleration or well known as Zero Period Acceleration (ZPA). We have considered here the combination of both Intensity (MSK) based Seismic Zoning Map of India and Zero Period Accelerations (ZPA) Map of India for 2% probability of exceedance for 50 years design period with 5% damping and 2475 years return period of the maximum considered earthquake. It is also comparable with International Building Code (IBC-2009) standards. Both the parameters of Intensity MSK and moment magnitude M_w are plotted and correlated with the maximum considered earthquake in a zone, which can generate effective peak ground accelerations as ≤ 0.1, 0.16, 0.24 and 0.36 for each zone of II, III, IV and V, respectively (Ramalingeswara Rao, 2014b) which are same as that of Z-factors of IS code 1893-2002.

Thus, the new Seismic Hazard Zoning Map of India is generated by the combination of 45000 MSK intensity based map and map of seismic hazard estimated by NDMA (2011) for 9500 grid points for entire India (Iyengar, Personal Communication). The 2% probability of exceedance for 50 years design period with 5% damping and 2475 years return period been considered by NDMA (2011) to estimate accelerations at bed rock level.

Validation of New Seismic Hazard Zoning Map of India

The New Seismic Hazard Zoning Map of India is tested and verified by considering the spectral accelerations computed by different authors for different regions of India as follows: Chandrasekharan and Das (1992) have prepared spectral accelerations for four recent earthquakes occurred in different regions of NE India. It is found to be 0.4 g to 1.0 g at zero periods, which are comparable with the New Seismic Hazard Zoning map of India as Zone V whereas Raghukanth and Somala (2009) have also found zero period accelerations for NE India is about 1.9 g due to soil amplification (Vs = 1.97 km/ sec).

Due to Koyna earthquake of 1967, the ZPA is about 0.51 g. The work in respect of spectral accelerations of Jai Krishna (1992) has also been compared. Mandal et al., (2013) have computed the spectral acceleration (ZPA) for Sonata belt of about 0.18 to 0.23 g at B-type soil which is comparable with the present new zoning map of India. Seeber et al., (1999) computed for Maharashtra, ZPA is of about 0.33 g for B-C type soil, whereas Raghukanth and Iyengar (2006) have computed for B-type special, ZPA is 0.28 g. Sitharam and Anbazhagan (2008) have computed spectral ZPA value at about 0.11 g for Bangalore region. Sitharam et al., (2012) have also computed by using deterministic method for Karnataka region and they got ZPA values for Bangalore, Belgaum, Bellary, Gulbarga, Hubli, Kaiga, Mangalore and Mysore at 0.18 g, 0.63 g, 0.11 g, 0.081 g, 0.054 g, 0.031 g, 0.114 g and 0.63 g, respectively. Most of these major cities in Karnataka are comparable with the present new zoning map of India.

Shukla and Choudhary (2012) computed ZPA as 0.79 g and 0.48 g for Mundra and Kandla ports, respectively for Gujarat. Further, they have computed the spectral accelerations by using the deterministic spectra which have been prepared for each major city for maximum considered earthquake (MCE) for 5% damping. The most vulnerable site is Bhuj city as it is very close to the most active faults in the state of Gujarat. It has also been observed that the calculated hazard is sensitive to the *b*-value. The variation in hazard computed with respect to *b*-value is highest for Ahmedabad city and lowest for Bhuj city. Based on the present study, the recommended PGA values for the cities studied are 0.13 g, 0.15 g, 0.64 g, 0.14 g and 0.2 g for cities of Ahmedabad, Surat, Bhuj, Jamnagar and Junagadh, respectively.

The computed values for 0.2 sec and 1 sec are also compared well. Likewise, Menon et al., (2010) have also carried out studies on probabilistic macrozonation of Tamil Nadu for entire districts of the Nilgiris, Krishnagiri and Chennai and large parts of Coimbatore, Theni, Erode, Salem, Dharmapuri, Vellore, Kancheepuram, Tiruvannamalai, Villupuram, and Tiruvallur districts lie in zones where the expected PGA for the 2475 yr return period can be 0.14g or more whereas Kalyan et al., (2009) have reported horizontal acceleration for Chennai city as 0.187g. We have considered 0.2 sec for normal residential buildings and 1 sec for monumental like structures. The ZPA critical value should not exceed 0.15 g, otherwise a special seismic design of the structure is essential. Utilization of the updated seismic hazard zoning map of India is needed.

References

Ramalingeswara Rao, B. (2014a). A book on "Seismic Activity- Indian Scenario". Buddha Publishers, Hyderabad, T.S., India.

Ramalingeswara Rao, B. (2014b). Looking for New Earthquake data from 900 AD and Alternate Seismic Activity in Indian Regions. 50th Annual Convention and Meeting on "Sustainability of Earth System - The Future Challenges" held on 8-12 January 2014, at NGRI, Hyderabad, 123-124. IBC-2009.

Chandrasekharan, A.R. and Das, J.D. (1992). Strong Motions Arrays in India and Analysis of Data from Shillong Array - Special Issue Seismology in India: An Overview. Current Science, 62 (1&2), 233-250.

National Disaster Management Authority (NDMA) (2011). Development of Probabilistic Seismic Hazard Map of India. Technical Report, 1-114.

Jai Krishna (1992). Seismic Zoning Maps of India - Special Issue Seismology in India: An Overview. Current Science, 62 (1&2), 17-23.

Mandal, H.S., Shukla, A.K., Khan, P.K. and Mishra, O.P. (2013). A New Insight into Probabilistic Seismic Hazard Analysis for Central India. Pure and Applied Geophysics, 170 2139–2161.

Raghukanth, S.T.G. and Iyengar, R.N. (2006). Seismic Hazard estimation for Mumbai city. Current Science, 91(11), 1486-1394.

Raghukanth S.T.G. and Somala S N, Modeling of strong motion data in Northeastern India: Q, stress drop and site amplification (2009), Bulletin of the Seismological Societyof America, 99(2A):705-725.

Seeber, L., Armbruster, J.G., and Jacob, K.H. (1999), probabilistic assessment of earthquake hazard for the state of Maharashtra, Report to Government of Maharashtra Earthquake Rehabilitation Cell, Mumbai.

Shukla, J. and Choudhury, D. (2012). Estimation of seismic ground motions using deterministic approach for major cities of Gujarat. Natural Hazards Earth System Science, 12, 2019–2037.

Menon, A., Ornthammarath, T., Corigliano, M. and Lai, C.G. (2010). Probabilistic Seismic Hazard Macrozonation of Tamil Nadu in Southern India. Bulletin of the Seismological Society of America,100 (3), 1320–1341.

Kalyan, G., Sreedhar, U. and Dodagoudar, G.R. (2009). Probabilisticseismic Hazard assessment for Chennai. IGC Geotide, Guntur, AP, India, 517-521.

ASSESSMENT OF CONDITIONAL PROBABILITIES OF TSUNAMI OCCURRENCES IN TEN MAIN TSUNAMIGENIC ZONES OF THE PACIFIC OCEAN

R.B.S. Yadav*[1], T.M. Tsapanos[2] and G. Ch. Koravos[2]

[1]*Department of Geophysics, Kurukshetra University, Kurukshetra 136119, India*

[2]*Aristotle University of Thessaloniki, School of Geology, Geophysical department, Thessaloniki 54124, Greece.*

**rbsykuk@gmail.com; rbsybhu@rediffmail.com*

Pacific tsunamigenic rim is one of the most tsunamigenic regions of the world which has experienced large catastrophic tsunamis in the past, resulting huge loss of lives and properties. In this study, probabilities of occurrences of large tsunamis with tsunami intensity (Soloviev–Imamura intensity scale) I≥1.5, I≥2.0, I≥2.5, I≥3.0, I≥3.5 and I≥4.0 have been calculated during next 10, 20, 50 and 100 years in ten main tsunamigenic zones of the Pacific rim area using a homogeneous and complete tsunami catalogue covering the time periods from 1500 to 2011. In order to evaluate probabilistic tsunami hazard, we applied the conditional probability method in each tsunamigenic zone by considering the inter-occurrence times between the successive tsunamis generated in the past that follow the lognormal distribution. Thus, we assessed the probability of the next generation of large tsunamis in each tsunamigenic zone by considering the time of the last tsunami occurrence. The a-posteriori occurrence of the last large tsunami has been also assessed, assuming that the time of the last occurrence coincides with the time of the event prior to the last one. The estimated a-posteriori probabilities exhibit satisfactory results in most of the zones in study area, revealing a promising technique and reliable tsunami data used. Furthermore, the tsunami hazard in different tsunamigenic zones is also expressed in terms of spatial maps of conditional probabilities for two levels of tsunami intensities I≥1.5 and I≥2.5 during next 10, 20, 50 and 100 years. Estimated results reveal that the conditional probabilities for South America and Alaska-Aleutian zones for larger tsunami intensity I≥2.5 are in the range of 92-93%, much larger than the Japan (69%), for a time period of 100 years, suggesting most vulnerable tsunamigenic zones in the study area. The spatial maps provide brief atlas of tsunami hazard in the Pacific rim area.

SENSITIVITY ANALYSIS OF FAULTPARAMETERSON TSUNAMI MODELING

Swapna Mulukutla and Kirti Srivastava

CSIR-National Geophysical Research Institute, Hyderabad, India.

swapna.geophysics@gmail.com

Tsunamis in the Indian ocean originate in the sunda arc covering Sumatra and Java and in the west by makran subduction zone. These two are active subduction zones which can generate tsunamigenic earthquakes in the Indian ocean. The 26th December 2004, tsunami from the Andaman-Sumatra subduction zone created a large scale devastationand killedthousands of people in 11countries around the Indian Ocean. The 27th November 1945, a tsunami which occurred in the Makran subduction zone brought large scale devastation and destruction in the cities and villages lying along

the west coast of India. These mega events of Indian Ocean tsunami stressed the need for assessing tsunami hazard in vulnerable coastal areas.Tsunami wave heights can be estimated accurately if we know the fault parameters of source accurately. The fault parameters include epicentre, magnitude, fault length and width, slip, strike, dip, rake and focal depth. However, in reality most of the earthquake fault parameters can be obtained soon after the occurrence of an earthquake.Hence it is important to understand how these parameters effect the tsunami wave height prediction.

In this study the sensitivity of source parameters on tsunami wave heights is obtained by changing the fault parameters in tsunami simulation. Numerical modeling of tsunami results shows that the tsunami wave heights are sensitive to variation in slip, strike and focal depth but not to rake and dip.

EFFECT ON THE STRENGTH OF GEOMAGNETIC FIELD DUE TO VARIATION IN THE AXIAL SPEED OF EARTH

Mayank Dixit
Institute of Seismological Research, Gandhinagar (Gujarat)
caimera2007@gmail.com

The Magnetic Field of earth is associated with the rotation of partially melted liquid in the outer core. The strength of Geomagnetic Field declined about 10% over the past century. This field is constantly changing & varied in nature. It is not easy to predict the effect of the decrease. The rotation of partially melted liquid in the outer core affects the magnetic field and its rotation is directly related with the axial speed of Earth. The Earth rotates once in about 24 H or currently 23 H 56 m 4 s. Earth rotation is slowing slightly with time. This has resulted in the modern day extending by about 17 ms. In this study a relationship between strength of Geomagnetic Field and axial speed of Earth is presented.

Methodology

Let the Earth be a perfect sphere. A person standing at ISR (Institute of seismological Research) travels along circumference in approx. 24 H. Let circumference of Earth be 'Ci'

So, $Ci = 2 \prod r$

$r = Ci / 2 \prod$

or $c = Ci / 2 \prod$ (see Fig 1) (1)

If we want to find the speed at particular latitude, we need to find the circumference of the circle formed when a plane parallel to the equator intersect the sphere.

Fig. 1: Considering this figure as Earth, r is the radius of Erath, B is the position where a person is standing at ISR, L is the latitude angle, and O is the centre of Earth,

If we want to find the speed at position B, we need to find the circumference having radius a, formed when a plane parallel to the equator intersect the sphere.

Let B be the position of ISR

In Δ OCB
Cos L = BC / BO
BC = BO (Cos L)
or , a = c Cos L
or , a = (Ci Cos L) / (2 ∏) (From 1) (2)

Circumference at ISR = 2 ∏ a

or, Circumference at ISR = 2 ∏ (Ci Cos L) / 2 ∏

or, Circumference at ISR = Ci Cos L

So, Speed at ISR = (Circumference of ISR) / 24

or, S = (Ci Cos L) / 24

S = (40192 Cos L) / 24 = 1674.66 Km/h

or, S = (24902 Cos L) /24 = 1037.58 M/h

The best accepted theory available today to explain the origin of the Earth's magnetic field is the "dynamo effect" theory. In the earth's interior the fluid will play an important role.

If a particle of charge 'q' moves with velocity 'V', then the force will be

F = q (E + VXB) (Lorentz Force Law)

Where E is Geoelectric Field, B is Geomagnetic Field

VXB = V.B Sin θ

Where θ is the angle between V and B

If θ = 90°, then Sin θ = 1

So, F = q (E + V.B)

The particle of Ni & Fe in outer core moving in circular path, which is directly related with the axial speed of Earth.

So, F = Kinetic energy of Earth in circular motion

i.e., F = (I ω^2) /2

Where I is the moment of inertia and ω is angular speed of Earth

or, q (E + V.B) = (I ω^2) /2

or, B = (I ω^2/2qV) – (E/V)

Now, 'V' is the velocity of Ni & Fe particle moving with the same linear speed as the Earth is moving on its axis and by the relation between angular and linear speed $v = r\omega$, so my equation becomes

$$B = \{(I\ S)/(2qr^2)\} - (E/S)$$

Here the second term on R.H.S. is small, so can be neglected it and in the remaining term I,q and r are constants, so it can be written as

$$B \alpha S$$

Result

From above study, it is clear that the Magnetic field of Erath i.e. the Geomagnetic Field is directly proportional to the linear axial speed of Earth. Earth rotation is slowing slightly with time and the modern day extending by about 17 ms, which means that the rotation of Ni and Fe particles in the outer core is also slowing down slightly with time.

SOURCE DEPTH REPRESENTATION OF GRAVITY DATA OVER BIHAR MICA BELT BY CONTINUOUS WAVELET TRANSFORM

Arvind Singh* and Upendra K. Singh

Department of Applied Geophysics, Indian School of Mines, Dhanbad-826004

**arvindsinghgps@gmail.com*

Main complications in interpretation of potential field data are caused due to the insufficient information about the geology of the area. To get rid of such complications there are many method have been developed in order to better interpretation. Wavelet transform method is one of them. Wavelet transform is a well-known method to characterize the potential field anomaly. The continuous wavelet transform (CWT) is used to interpret the source and its location by shifting the information into a secondary space. This method has been verified on various synthetic sources (cylindrical and spherical) anomalies and applied to gravity data of Bihar mica belt and surrounding areas. To find depth of causative sources satellite gravity data has been used.

Results shows that there is a maximum source depth is about 4.5km in northern side while 3.9km in southern side of for profile AA'. Maximum depth of profile BB' ranges 2.5km - 2.9km western and eastern side of the profile respectively. Moreover the source depth is about 2.0km of the profile CC' using satellite gravity data, it is concluded that mean depth of causative sources decreases slowly from south to north over this profile which directs thickness of sediments. The method contributes an important role to locate mean depth of the causative sources without any priori information which can be used in interpretation of potential field data as an initial model in any inversion algorithm.

Methodology

Wavelet Transform method for potential filed has been established by Moreau et al. (1997, 1999). This method previously used for homogeneous, isolated and extended potential field sources (Sailhac et al., 2009). Chamoli (2006); Goyal and Tiwari (2014) used wavelet transform method on various synthetic as well as on field data. Method allows Poisson group of wavelets as a mother wavelet in order to interpret the potential field data. To analyze the signal by mother wavelet, a wavelet domain signal is decomposed into the orthogonal wavelets of finite duration.

The CWT coefficient W_t of a measured potential t(x) is defined as the convolution product.

$$W[\psi,t](p,o) = \int_{R^n} \frac{1}{o^n} t(x)\psi\left[\frac{p-x}{o}\right]dx \quad (1)$$

$$W[\psi,t](p,o) = (D_o\psi * t(p) \quad (2)$$

where ($x \in R^n$) is the wavelet to be analysed; x denotes the abscissa along the particular profile line; t(x) indicates the potential field (gravity or magnetic anomaly); ($o \in R^+$) and p are the dilation and position parameter respectively. Dilation operator D_o can be termed as

$$D_o\psi(x) = \frac{1}{o^n}\psi\left(\frac{x}{o}\right) \quad (3)$$

Moreau (1997) explained the relationship between wavelet coefficients at two altitudes and for any wavelets of homogeneous sources.

$$W^\gamma(x,o') = \left(\frac{o'}{o''}\right)^\gamma \left(\frac{o''+z_0}{o'+z_0}\right)^{-\beta} W^\gamma\left(x\frac{o''+z_0}{o'+z_0}, o''\right) \quad (4)$$

Where indicates the holder exponent o' and o'' denote different altitudes while Z_0 signifies the depth of the causative source. Selection of ideal mother wavelet is main task in wavelet transform. Wavelet transform method provides a reliable path (Moreau et al., 1999) to handle the noises as well as non-stationary data in the case of magnetic field anomalies.

Application on Synthetic data

This methods simply executed on computer program and verified on synthetic gravity data over the cylindrical as well as the spherical source models. Here there is only cylindrical model has been demonstrated. Synthetic gravity anomalies from two cylinders (along 200m long profile) located at the distance six times their depth has been shown in the figure1. CWT shows the estimated source depth is about 15m.

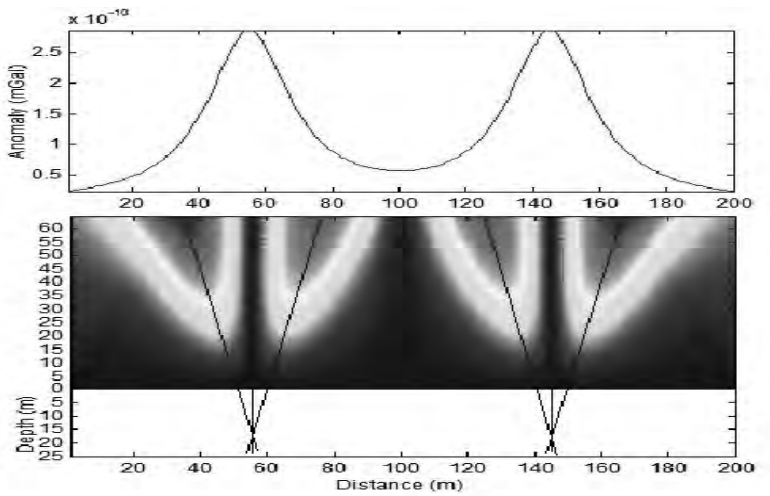

Figure 1

: Gravity anomaly of two cylinders placed at positions of 55m and 145m. The cylinders locates the depths of 15m with density contrast of 1kg m-3.

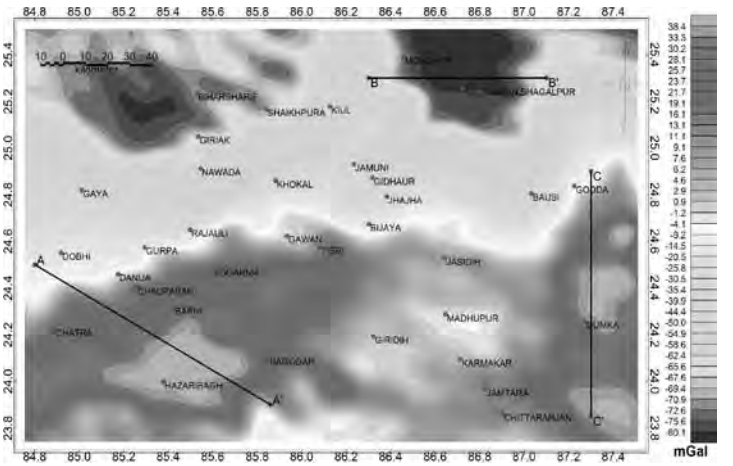

Figure 2: Observed anomaly map of Bihar mica belt and Hazaribag plateau.

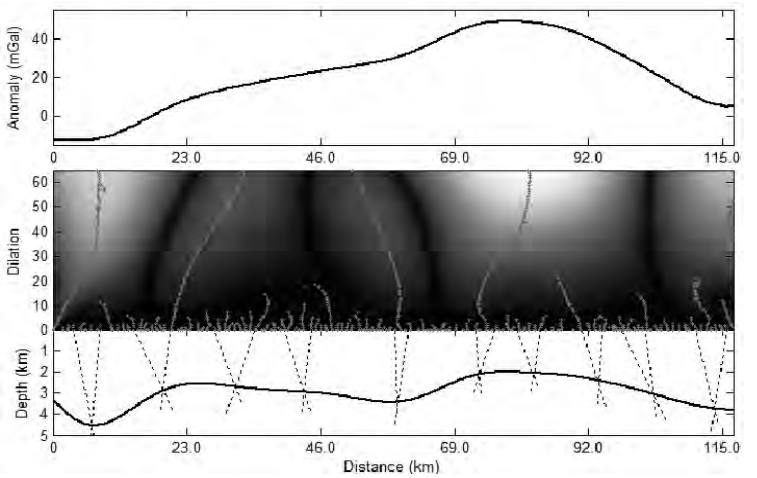

Figure 3: Gravity anomalies from Profile AA', where red lins shows the maxima lines and solid black line relates to the causative source depth. wavelet coefficients calculated using a Poisson wavelet with intersections of modulus maxima lines.

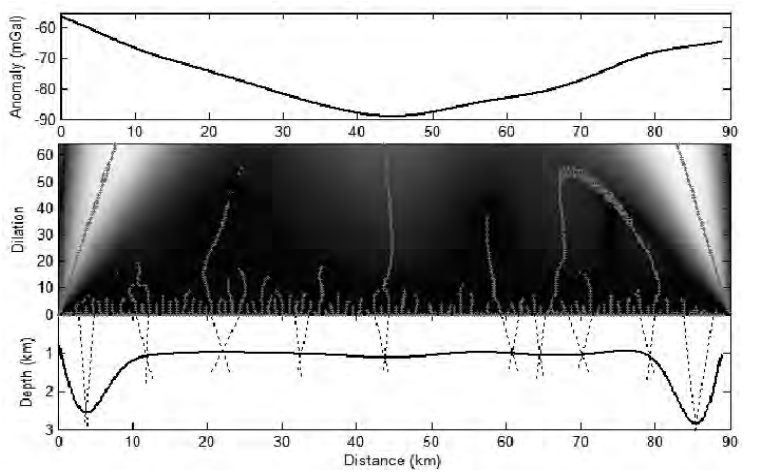

Figure 4: Gravity anomalies from Profile BB', where red lins shows the maxima lines and solid black line relates to the causative source depth. wavelet coefficients calculated using a Poisson wavelet with intersections of modulus maxima lines.

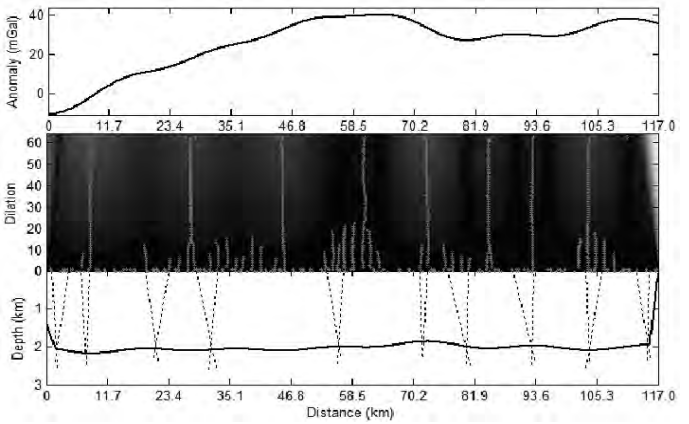

Figure 5: Gravity anomalies from Profile CC', where red lins shows the maxima lines and solid black line relates to the causative source depth. wavelet coefficients calculated using a Poisson wavelet with intersections of modulus maxima lines.

Application on field data

Bihar Mica belt previously studied by many researchers (Guha and Chakravarty, 1983; Ghose, 1983; Ghose et al., 1973); Mahadevan et al., 1967; and Verma et al. 1988) for different prospectus by different methods. The gravity high has been observed southeast and southwest while a gravity low appears in the northeast and northwest of the study region. The three profiles namely AA′, BB′ and CC′ has been drawn over the different parts of the study region where there a maximum anomaly contrast.

Profile AA′: this profile passes across the gravity high along east of the Hazaribag plateau southwest part of the study area. The profile (fig.3) shows the nature of gravity high across this profile and low to west of the Dobhi. An explanation of gravity high and low in terms of two dimensional structure is also shown in this figure. The model suggests that the Hazaribag plateauis underlain by massive body to a depth of about 4.5 km in western side. the low west of Dobhi cannot be explain in terms of a large thickness of alluvium, since alluvium thickness is known to be small (Verma et al., 1988). These low anomaly can be described in terms of granite rocks of 3 km.

Profile BB′: this profile runs north of the Sultanganj and south of the Monghyr. Near surface rocks in the area exhibits a flat nature which may be mica schists and granites. The gravity low along both end of the profile cannot be described in terms of mica schists but can be described in terms of V-shaped granite intrusive underlying the mica schists as seen in figure 4.

Profile CC′: this profile runs N-S direction (east of the Godda and Chitranjan) in the eastern most region of the study area (fig. 5). This profile shows that gravity increases gradually from north to south. High gravity indicates the mica schists and quartzites with granite outcrop. Depth of the causative source is about 2.0 km as shown in figure 5.

Conclusions

The present study demonstrates that the wavelet transform method can explain the locations and sources of potential field data. Extrema lines of the wavelet transform deliver a sufficient and relevant information essential to improve the important parameters of the causative body. The application of the method to the synthetic and satellite gravity data of the Bihar mica belt proves that the method is quick and easy to use. The results shows that causative sources of potential field can be interpreted both qualitatively and quantitatively. Also, CWT method provides the shape of causative body without any prior knowledge within very short time of execution that can be additionally used as a priori model in inversion with better accuracy.

References

Bhattacharyya, B.P., 1982: Tectono-metamorphic effect of granite and pegmatite emplacement in the Precambrian of Bihar Mica Belt. Proc. Symp. On Metallogeny of the Precambrian. Geological Society of India, Bangalore p.45-56.

Blakely, R. J., 1995: Potential theory in gravity and magnetic applications, Cambridge Univ. Press, New York.

Chamoli, A., Srivastava, R. P., and Dimri, R. P., 2006: Indian Journal of Marine Sciences v. 35(3), p.195-204.

Ghose, N.C., 1983: Geology, tectonics and evolution of chhonagpur granite-gneisses complex eastern India, Recent Researches in Geology, v.10, p.211-247.

Ghose, N.C., Shanakin, B. M., and Smirnov, V. N., 1973: Some geochronological observation on the Precambrians of Chhotanagpur, Bihar, India. Geol. Mag. v.110, p.481-484.

Goyal, P., Tiwari, V.M., 2014: Application of the continuous wavelet transform of gravity and magnetic data to estimate sub-basalt sediment thickness, Geophysical Prospecting, v.62, p.148–157.

Guha, P. K. and Chakravari, S., 1983. Identification of target area for mica pegmatites in Eastern India using photo interpretation. ITC Journal, p.1376.

Sailhac P., Gibert D. and Boukerbout H. 2009: The theory of the continuous wavelet transform in the interpretation of potential fields: A review, Geophysical Prospecting v.57, p.517–525.

Mahadevan, T.M., and Maithani, J.B.P., 1967 Geology and Petrology of the mica pegmatites in parts of Bihar mica belt, Mem. Geol. Serv. India, v.93, p.1-114.

Moreau, F., Gibert, D., Holschneider, M., and Saracco, G., 1997: Wavelet analysis of Potential fields, Invers Problems, 23 p.165-178.

Moreau, F., Gibert, D., Holschneider, M., and Saracco, G., 1999: Identification of sources of potential fields with continuous wavelet transform: basic theory, Journal of Geophysical Research, 104, p.5003-5013.

Verma, R. K., Mukhopadhyay, M., Asraf, M. H., Nag, A. K., and Satyanarayana, Y. 1988. Analysis of gravity field over Chotanagpur Plateau and Bihar Mica Belt. Geological Society of India, Memoir 8, p.185-198.

NATURE OF CRUST AND LITHOSPHERIC MANTLE OF SOUTHERN PART OF THE VINDHYAN BASIN AND ITS THERMO-GEODYNAMIC EVOLUTION

***O.P.Pandey, R. P. Srivastava, N. Vedanti, SatyajitDutta**

CSIR-National Geophysical Research Institute, Hyderabad 500007

**om_pandey@rediffmail.com*

Mid to late Proterozoic period is characterised by several intracratonic basins in india that includestectonically active sickle shapedVindhyan basin, which is one of the largest Protrozoic basins of the world, covering an exposed area of about 60,000 sq.km in east-west direction, north of Narmada Son Lineament (NSL). The basincame into existence as a result of continued rifting and subsidence of the central part of the Indian peninsular shield. In order to assess hydrocarbon potential of the Vindhyan Basin, large number of geological and geophysical investigations have been carried out by various agencies, specilly in its southern part, where sediment thickness is maximum. Thus, in this paper, an attempt has been made to combine these data, which provide a totally new picture of the prevailing crustal configuration, thermal regime and its geodynamic evolution.

In past, this region hasbeen subjected to continued uplift and exhumation, magmatism, crustal extension, rifting and subsidence due to thermal perturbations causedby the hot underlying mantle. 5 to 6 km thick layer of sediments, sitting directly over the Bijawar /Mahakoshal group of mafic rocks or exhumed mid-level crust,is expectedinthe deep faulted Jabera basin. High heat flow of 78 mW/m^2,extremely high Moho temperatures (exceeding1000^0C) andmantle heat flow (56 mW/m^2) besidesonly 50 km lithospheric thickness,has beenestimated for this basin. Some regions of the southern Vindhyan basins arethickly magma underplated, with almost missing granitic upper crust due to deep crustal exhumation of as much as 13 km.At around mid to lower crustal level,a 5 to 8 km thick metasomatized zone has also beendelineated, where velocities are considerably lower

than the top and bottom.Further, this region may have been under the influence of a super mantle plume, which was active around 1.1 Ga.Also, there appears a possibility that the southern vindhyans may extend furtherin the southbeyond NSL rift.

IMAGING THICK SEDIMENTS AND THEEOCENE SHELF BREAK OF THE WEST BENGAL BASIN, INDIA, FROM TRAVELTIMETOMOGRAPHY OF REFRACTION DATA

V.Vijaya Rao, KalachandSain*, N. Damodara and ASSSRS Prasad
CSIR-National Geophysical Research Institute, Hyderabad 500007, India.
** kalachandsain@yahoo.com*

Velocity images were derived using first arrival traveltime tomography along four profilesin the West Bengal sedimentary basin. Tomographic images depict smooth velocity variations of Recent, Quaternary and Tertiary sediments of velocity 1.8-4.3 km/s deposited over the Rajmahal trap of 4.8 km/s velocity and the basement (5.8 km/s) down to a maximum depth of 16 km. The upper Jurasic-lower Cretaceous Rajmahal volcanism and outpouring of basaltic lava related to the breakup of East Gondwana due to Crozet / Kergulean hotspot activity has profound influence on the structure and basin configuration of the region. 3-D configuration of the basin is well understood using fence diagram generated from the results of datasets from all the four profiles. The present study indicates a south-easterly dip as evidenced by the sedimentary thickness. The basement depth along the seismic profiles varies from 1km to 16 km depending on its location in the basin. It is shallow in the north & west and deep in the east and south. The depth of the basement on the stable shelf of the basin in the west gently increases to about 8 km and dips to a maximum depth of 16 km in the deep basin part in a short distance in the east. The present study using the data from all the profiles clearly imaged the abrupt increase in sedimentary thickness representing the Eocene Hinge zone / shelf break of the West Bengal basin. The basaltic Rajmahal traps identified in the present study may be related to the mantle plume activity, which is responsible for the breakup of East Gondwana during the Cretaceous. The Eocene shelf break could be related to the Himalayan orogeny during the same period. Velocity models are assessed for their reliability using χ^2 estimates, rmstraveltime residual fit; velocity uncertainity using ray-density and spatial resolution by checkerboard tests.

SEISMICITY PATTERNS OF ANDAMAN-SUMATRA AND MAKRAN SUBDUCTION ZONE- IMPLICATION TO TSUNAMI GENERATION

***Deepak Maurya, Farveen Begum and Kirti Srivastava**
CSIR-National Geophysical Research Institute
**deepakbhu.bhu@gmail.com*

Tsunamis in the Indian Ocean are generated from two subduction zones namely Andaman – Sumatra subduction zone and Makran subduction zone. Our aim is to study the seismicity pattern in and around of Andaman- Sumatra and Makran subduction zones to quantify the earthquake source mechanism in the subduction zones and rule out non tsunamigenic earthquakes. The focal mechanism plot in the Andaman–Sumatra subduction zone shows that most of them are seen to be thrust earthquakes like the 2004 Sumatra, 2005 Nias, 2007 Bengkulu etc which are tsunamigenic. Seismicitiy away from the subduction zone show a strike slip mechanism. Similarly from the focal mechanism plot of the Makran subduction zones we have seen that most of the earthquakes in the subduction zone are thrust type mechanism i.e. 1945 Tsunami. Where as the Murray ridge system which lies in the close vicinity shows strike slip mechanism. As the source mechanism plays a very important role in tsunami generation it is essential to study the under sea earthquakes which are of thrust/strike slip mechanism. After the April 11, 2012 a tsunami warning was given but later it was

withdrawn as it was strike slip earthquake. The seismicity patterns in the Indian ocean would help in identifying based on the epicenter location if they fall under the tsunamigenic or non tsunamigenic earthquakes.

SIMULATION OF STRONG GROUND MOTION IN KANGRA REGION USING EMPIRICAL GREEN'S FUNCTION TECHNIQUE

Babita Sharma
Ministry of Earth Sciences, New Delhi
babita_s@rediffmail.com

Earthquakes are deadliest among all the natural disasters. The areas which have experienced great/large earthquakes in the past are the probable candidates for the next big event. In this study, we have simulated Kangra Earthquake (1905, Mw 7.8) in the North West Himalaya using Empirical Green's Function (EGF) technique. Recordings of Dharamsala Earthquake (1986, Mw 5.4) are used as Green function with a heterogeneous source model and an asperity. It has been observedthat the towns of Kangra and Dharamsala can expect ground accelerations close to 1g during 1905 Kangra Earthquake repetition. The entire studied region can expect acceleration in excess of 100 cm/sec^2 in case of Mw 7.8.Thesites located near the rupture initiation point can expect accelerations in excess of 1g for the magnitudes simulated. For validation, the estimates of the PGA for Mw 7.8 simulation are compared with isoseismal studies carried out in the same region after the Kangra earthquake of 1905by converting PGA values to intensities. It was found that the results are comparable. The obtained PGA values have provided an idea about the level of accelerations experienced in the area during 1905 Kangra Earthquake. Future construction in the area can be regulated and built environ can be strengthened using PGA values obtained in the present analysis.

PRESENT-DAY SLIP RATES ESTIMATION FOR MAJOR ACTIVE FAULT OF NORTH EASTERN REGION OF INDIA DERIVED FROM GPS DATA

***Sanjay K Prajapati[1] and Ashok Kumar[2]**
1 Geosciences Division, Ministry of Earth Sciences, New Delhi
2 National Geophysical Research institute, Hyderabad
go2sanjay_p@yahoo.com

Space geodetic data can provide valuable information about fault slip rates and seismic potential of major active faults. We interpret Global Positioning System (GPS) measurements in the northeastern region and adjacent parts to describe relative motions of crustal blocks, locking on faults and permanent deformation associated with convergence between Indian-Eurasian-Bumra plates. To better constrain the kinematic parameters necessary for quantitative seismic hazard assessment, we invert GPS data together with uplift rates, fault slip azimuths and rates with a kinematically consistent block model of the region to estimate fault slip rates and spatially variable slip deficit rates on the Dauki fault, Eastern thrust fault, MCT, Kopili, Mishmi thrust, CMF fault and sagging fault. We also determine the degree to which faults are either creeping aseismically or, alternatively locked on the block-bounding faults. The Eastern thrust fault is locked mainly at the surface whereas other active major faults of northeast region are partially locked. Most of fault bounded block rotating clockwise relative to Eurasia at a rates of ~ 0.5 to 1.8° /Ma. The current slip rate using block model approach is varies from 1.0 to 14.2 mm/yr along major fault on northeast region. To estimates the robustness of the block velocities and rotations, we also calculated an alternative model with freely slipping faults. We tested two models, one where faults are 100% coupled and one where faults are freely slipping. These models provided the uncertainties on the fault slip rates.

RECONNAISSANCE GROUND MAGNETIC SURVEY FOR IRON ORE IN BAYYARAM AREA, KHAMMAM DISTRICT, TELENGANA, INDIA

***B. Nagaraju, B. Madhusudan Rao, BVS. Murthy, K. Lohith Kumar[1], R. Sudarshan and R.Sandya**

[1] CSIR-NGRI, Department of Geophysics, Osmania University, Hyderabad, 500007.
**rajubhattu84@gmail.com*

Magnetic method is a powerful tool that can be successfully applied in mineral exploration, since magnetics provide a relatively direct mapping of the abundance of magnetic minerals. It also serves as a useful indicator of lithology, structure, weathering and alteration processes. Even though geological prospecting methods can provide valuable information in iron ore exploration and the abundance and shallow depth occurrence of the ore, geophysical methods are necessary to resolve, distribution, grade and geometry of the deposit at depths. Umpteen number of successful application of magnetic method are available in literature. Here we present a report on the first hand reconnaissance magnetic anomaly conducted by us over Bayyaram Iron ore deposits of Khammam district, Telangana.

The Bayyaram Iron ore belt is situated in between Sripuram in the south of Khammam district to Kothagudem in the north of Warangal District. It extends in a NNW-SSE direction over a strike length of 50km along the western contact of Pakhals with the rocks of Khammam Group and Peninsular Gniesses complexThe Major geological units exposed in the area are Khammam Group of Archean, Peninsula Gneissic Complex of Archean to Paleoproterozoic and Pakhal Supergroup of Mesoproterozoic sediments. Amphibole, quartzite-chlorite schist, quartzite and banded hematite magnetite quartzite belong to the Khammam Group occurs as enclaves in the PGC. Dolerite Dikes of Paleoproterozoic age and gabbro of Mesoproterozoic traverse the Granitoids of Gniessic complex are observedin the area. The Pakhal Supergroup of sediments overlie the PGC and Khammam Group of rocks.

All the major geological units of the area trend NNW-SSE with gentle to moderate easterly dips. The Pakhalscould have been affected at least by three periods of folding. The western contact of the Pakhals is partly faulted by NW-SE, SE-NW and WNW-ESE trending fault.

The Iron ore is mainly occurring in two stratigraphic horizons. The First Horizon is Khammam Group, which is in the form of banded hematite magnetite quartzite and low grade iron ore. The Second horizon is within the Gunjeda and Pandikunta Formation of Mallampalli Group of Pakhal Supergroup as detached lens shaped bodies of hematite and high grade iron ore.

Ground geophysical total field magnetic survey has been carried out by us in part of the western contact of Pakhal series with Archean gneissic complex of Bayyaram field area. Total field magnetic data was recorded along five traverses at 505 total numbers of stations;the area covered is about 40 sq. km.The field data was qualitatively and quantitatively interpreted, utilising the magnetic and density property values measure on field samples.

The measured magnetic data was reduced to pole before interpretation because the total magnetic field incorporates the geometric effect of the earth's magnetic field. So, it was necessary prior to interpretation to remove this effect from the data. The process of reducing total magnetic field data to the pole simplifies interpretation and makes the location of the anomaly more accurate. Reduction to pole and upward continuation map was prepared for various heights to facilitate analysis of magnetic data.

The first vertical derivative calculations were used to enhance the effect of near surface sources at the expense of those due to deep seated sources, these calculations also sharpen up anomalies over bodies allowing a clear imaging of the causative structures. Horizontal derivatives were alsostudied for data to enhance the boundaries of the causative body and Analytical signal of the total magnetic intensity map is prepared. This map indicates actual positions of the magnetic sources. The boundaries and contacts among different geological horizons were identified, preparing structural and litho alignment map helpful in the prospecting of iron ores in Bayyaram area. Further analysis of magnetic data to assess the size and dimensions of the iron ore is underway.

A PROBABLE MODEL FOR GENERATING LARGE LOWER-CRUSTAL INTRPLATE EARTHQUAKES IN THE KACHCHH RIFT ZONE, GUJARAT, INDIA

Prantik Mandal
Senior Principal Scientist, CSIR-NGRI, Hyderabad-500007
prantik@ngri.res.in

Through local earthquake tomography, we imaged several zones of reduced seismic velocities and increased Poisson's ratio as well as bulk velocity extending from lower-crustal to sub-crustal depths below the Kachchh rift zone, Gujarat, India. These zones are inferred to be fractured and permeable zones filled with metamorphic fluids and volatile CO_2, which are facilitating the deeper fluid circulation to cause bursts in seismicity in the region. We notice that the 2001 Bhuj, Mw7.7, earthquake also nucleated within the same fluid filled zone. Here, we model the spatial and temporal evolution the entire 2001 Bhuj earthquake sequence as a diffusion process of pore pressure relaxation that generated from the coseismic release of deep circulation of metamorphic fluids or high-pressure CO_2. We propose that the continued occurrences of earthquakes in this rift zone may be driven by the post-seismic (with a permeability of $1.45x10^{-11}$ m^2) release of deep fluid circulation of metamorphic fluids or entrapped volatile CO_2 propagating through damaged zones created by the 2001 mainshock. We also infer that similar episodic mechanisms of deeper fluid circulation would lead to the occurrence of next large intraplate earthquakes in the Kachchh rift zone, Gujarat India.

PALAEOBIOLOGICAL SEDIMENTARY AND GROUNDWATER INDICATORS OF CAUVERY DELTA, INDIA

***V.N.Varma[1], Ben Anita[1], Sivasubramaniam[1] and Sukhija B.S[2]**
[1]Pondicherry Govt. Organisations, India
[2]CSIR-National Geophysical Research Institute, Hyderabad, India
**2varmavel47@gmail.com*

The Vennar-Cauvey river basin forms one of the major coastal sources in Tamilnadu, in South East India for irrigation, domestic and multiuser purposes. Cauvery delta had been developed from the marine depositional system; The O.N.G.C, the geological survey staff, the Central Groundwater Board had conducted surveys in the areas and they explored groundwater development feasibility. According to depositional system it has (1) fluvial continental coarse sand and also fluvial marine muds associated with rich fossiliferrouslimestones; (2) the Shelf platform of carbonates and shales; (3) the deltaic sands and siltsandturbidite fans of Neogene and also the deltaic litterols of Quaternary periods.Thepalaeogeography demonstrates the occurrence of deeper marine conditions in the coastal Karaikakl High. The major delta was reported developed in Miocene time. Karaikal region lies in between Latitudes $10^0$48′ to $10^0$60′ and Longitudes $79^0$40′and $79^0$53′ towards the Bay of Bengal.

In Karaikal region, the hydrogeology is related to the quaternary and tertiary formations. In this region, there are a few paleochannels and levee deposits which act as platform for the potential aquifers in the deeper productive zones. The plio-miocenedeposition are well exposed to the quaternary deposits for hydrogeological purposes. The pliocene bed consists of old marine sediments and this layer is highly saline, unfit for the groundwater development.

The groundwater recharge is pertaining to (1) quaternary alluvium (2) tertiary layer of Lower Miocene layers. The recent and old alluvial layers get recharge from the estuaries and ponds; The pliocene layer is partially get recharge from the alluvial layer and the for the Lower Miocene the outcrop is exclusively from the TanjoreHighlands.Thepalaeomarine settings cause salinity withrich amounts of fossil assemblages.So the Miocene formation is the desirable for groundwater development.

8 groundwater samples of miocene formation except one from the old alluvium sample were collected for chemical analyses including pH and Electrical conductivity tests. The microions constituents for Strontium and iodide ions were also done in selected samples due to the presence of Aragonite mineral and evaporites.For the reference samples for palaeomarine bed and modern marine setting, two samples from Vedaranyam Marine Bed sediment and Arasalaru Estuary samples were collected.All the chemical tests were conducted as per the IARI methods. The Sr^{2+}ion was estimated by the Atomic Spectrophotometer.The iodide analyses was done by Cerium and Arsenous ionic catalytical conversion of Iodate by Sandell methodology using Visible spectrophotometer.

Another essential test for evaluation organic biomarkers for which the Mass Spectroscopic method was used to detect the diagnostic organic compounds. Specific biomarkers of Palmitoleic acid (16:1^9) and Oleic acid (18:1^9) had been eluted as fragmentary ions in the mass arrays at m/z 254 for the first and at m/z 282 for the second compounds.

The stable carbon isotope composition in the Miocene layer were also measured with the help of Mass Spectometer along with the 8 samples taken for chemical tests with reference to PDB limestone standard.. The result accounted for stable carbon isotopes vary from -13 to -5 per mil which are in higher range expressing the heavier carbonaccess in the water samples. The estuary sample expressedresults ofthe immaturedHopanoic acid, a pentacyclic hydrocarbon group plus Vaccenic acid (18:1^11), the latter is a unsaturated fatty acid and isomeric to Oleic acididentifiedthrough the Mass Spectrometer. The higher d^{-13} values of -8 to -5 per milhave the wells located close to the longitudal section of 79° 50′.

Further physical parameters such as H_2S odouremission and hydrothermal water in groundwater samples to maximum of .temperature of 65°C at the time of development were observed. These inputs are viable to determine the groundwater and sedimentary process to thispalaeoenvironment.

On synthesising the above facts; (1) Na-HCO_3-Cl type of wellwater presence in the deeper groundwaters with the dominant accountability of HCO^{3-} anion. The Hydrogen Sulfide and thermal activity had added the inorganic bicarbonate ions. (2) the increased stable carbon isotope composition from -13 to -5 per mil evince the excursion of lighter and organic carbons;

(3) the presence of palmitoleic acid allowed as bioproxy indication for the presence of Sulfur reducing bacteria in the presence of Hydrogen Sulfide emission. (4) The hydrothermal nature may be activated due to radiogenic carbons and by the Sr^{2+}ions. The increased iodide ions are found in

the matured geological sediments and well waters for which I/Cl ratio was employed to discriminate different ages.

The prevoir summary ensures that thispalaeobasin of Cauvey delta is endowed with heterotrophic DesulfotomaculumAcetoxidans hostile towards Eukaroytes in algae as Sulfur Reducing bacteria which is found to be palaeobiologicaldominant species in this environment.

DELINEATION OF GEOLOGICAL STRUCTURES IN AND AROUND CAMBAY BASIN USING GRAVITY AND MAGNETIC SURVEYS

Singh, R.K., VenkateswaraRao, S., Rastogi, B.K., Rahul Kumar, Monika and Komal

Institute of Seismological Research, Department of Science and Technology, Raisan, Gandhinagar -382 009

rksingh57@gmail.com, svenkatgeo@gmail.com

The paper deals with the result of gravity cum magnetic surveys in and around Cambay basin. The gravity and magnetic stations are located over permanent land marks available at an interval of 1 km approximately. The gravity (Bouguer) map and Magnetic (Total field) map show the following features:

1. Eastern and Western boundaries of Cambay basin are well reflected in gravity and magnetic maps.

2. Gravity high along Sami-Harij-Patan-Sidhpur trending NE-SW supported by magnetic high, may be the reflection of Aravali formation within the basin at around 23°49′ 48.77″ N (Patan).

3. A portion of Radhanpur Arch covered in the survey shows gravity high.

4. Radhanpur-Deesa section shows the presence of Deccan traps which is reflected in the form of magnetic high. The gravity low may be either due to lesser thickness of traps along that section or larger thickness of meta sediments.

5. Mehsana basin is reflected in the form of gravity low which is dipping towards east (Visnagar). This gravity low trend towardsVisnagar may be due to largersedimentary thickness.

6. Few plutonic bodies are also reflected at the western boundary of Cambay basin.

7. Several transverse faults trending NE-SW and E-W are well reflected in gravity & magnetic maps of the area.

A significant feature of the map is gravity and magnetic high trending NE near Patan, possibly reflecting the presence of Aravali formation.An other feature is dipping of the Mehsana basin towardseastuptoVisnagar, may be associated with the larger sedimentary thickness having good prospect for oil & gas.

ELECTRICAL IMAGING FOR NEAR SURFACE STUDIES FOR THE MANAGED AQUIFER RECHARGE

Tanvi Arora*and Shakeel Ahmed
CSIR-National Geophysical Research Institute, Uppal Road, Hyderabad
**tanvi@ngri.res.in*

The role of hydrogeophysics is quite relevant for the near surface studies for the better management of aquifer recharge. Over to it, Electrical Resistivity Imaging (ERI) is the most reliable method to decipher the unsaturated zone studies. The important requirement for managing the aquifer recharge are Water Availability (Rainfall); geomorphology; soil and sub-soil conditions; space available; subsurface conditions and much more. A number of experiments are carried out in two different terrenes as well as to answer the different situations leading to the same objective of MAR. ERI was conducted to find out the conducting zones in Karst aquifer systems and testing the efficacy of already proposed recharge structure. This was proposed after continuous vertical electrical soundings along the main drainage system. Leading to the above investigation, the most preferable conducting and resistive zones are marked in the limestone aquifer. Secondly, another experiment of Time Lapse Electrical Resistivity Tomography [TLERT] was carried out to monitor the natural recharge and assess the intervention in dug wells in crystalline aquifer. This work helps in quantifying the recharge to the aquifer and thereby supports the better management scenario in Karst as well as crystalline aquifer systems.

NEW EVIDENCE FOR BURIED PALAEOCHANNEL AND AQUIFER SYSTEMS IN NORTH-WESTERN INDIA FROM HIGH RESOLUTION ELECTRICAL RESISTIVITY TOMOGRAPHY DATASET

Dewashish Kumar[1], R. Sinha[2], A. Densmore[3], S. Gupta[4], S. Mondal[1], V.S. Sarma[1], A. Singh[2], S. Joshi[2], N. Nayak[2], M. Kumar[5], S. Shekhar[5], S.P. Rai[6], W.M. Van Dijk[3] and P.J. Mason[4] and Mrinal K. Sen[7]
CSIR-National Geophysical Research Institute, Hyderabad, India
IIT Kanpur, India
Durham University, UK
Imperial College London, UK
Delhi University, New Delhi India
NIH Roorkee, India
University of Texas, USA
dewashishkumar@ngri.res.in

Mapping the near surface alluvial and fluvial palaeochannel aquifer system of north-western India is of much concern in order to understand the groundwater dynamics and prospects of the alluvial plains of Punjab and Haryana, where groundwater resources are undergoing rapid depletion. Our study is aimed to understand the present groundwater situation, the aquifer geometry and hydrogeological characteristics, and the possible aquifer response to future climate change. We focused particularly on the area around the Ghaggar river, which is partly coincident with a large, incised palaeochannel system. Sediments in the study area consist of stratified, unconsolidated alluvial deposits of Quaternary age. High resolution full waveform electrical resistivity tomography (ERT) investigations were carried out and data acquired at 42 sites covering 33.34 km of line, using a state of the art 4 channel ABEM Terrameter LS. The processed resistivity dataset was inverted using least squares inverse approach with smoothness constraint and with a standard Gauss-Newton optimization technique. This measured dataset produces inverted subsurface 2D resistivity models, which are compared with available lithological data, including core logs. We found that the depths of the major litho facies and dry/

unsaturated sand beds are well identified based on substantial resistivity contrasts. The buried Ghaggar palaeochannel is identified in terms of high resistivity layer and is homogeneous, characterized as a medium to coarse sand sedimentary facies. This layer is confirmed by the resistivity logs as a high resistivity anomaly. The buried palaeochannel (dry/ unsaturated sand) is overlain by silt and clay layers of various thicknesses, which are distinct in the geophysical logs. The thickness of buried sand bodies, correlated with high resistivity layers, varies from 5m to around 35m thick at depths. This is well confirmed by surface resistivity results as well as high positive anomalies from self potential (SP) logs. There are sharp resistivity contrasts in the resistivity models between the sediments deposited in the past and those deposited at younger time. This is confirmed from the resistivity logs as well as low positive anomalies from SP logs. Coarse, medium and fine sand due to their different pore size can be identified based on resistivity contrasts and range of values along with the lithological data vis-à-vis the amount of water saturation of these formations. Alternate bands of multilayer sand along with sand and clay and silty sand are delineated all along the depth profile based on resistivity results with values ranging from ~10 – 500 Ohm.m, although the highest resistivity values at some sites range from 500 to a maximum of 800 Ohm.m. Deeper aquifers mainly contain medium sand, sandy loam and silty sand, which are classified based on the resistivity results and correlation with the lithological and geophysical logs. The aquifer zone lies between ~40m to >131m depth as revealed from inverted resistivity models, which are mainly responsible for heavy production and exploitation of groundwater resources. In general, the water level varies from 24m to 52m below ground level (bgl) in the area of study, which is quite dynamic and show large spatial variations of the saturated part of the aquifer system. The present study and results provide the subsurface geoelectric set up of the aquifer system, mapped the buried palaeochannel layer and the shallow and deeper aquifer, which are utmost required for the conceptualization and preparation of the groundwater flow model.

GEOPHYSICAL APPROACH FOR DELINEATION OF GONDWANA SEDIMENTS BELOW DECCAN TRAP BEYOND THE WESTERN LIMIT OF WARDHA VALLEY COALFIELDS, YEOTMAL AND WARDHA DISTRICTS, MAHARASHTRA

D.C. Naskar and D.K. Saha

Geological Survey of India, Geophysics Division, Eastern Region, Bhubijnan Bhavan, DK-6, Sector-II, 8th floor, Karunamoyee, Salt Lake City, Kolkata-700091.

**dcnaskar@yahoo.com*

Identification and delineation of the hidden sediments under the Deccan trap cover is a difficult problem in geoscientific exploration. The problem of the detection of subtrappean Mesozoic sediments under the volcanic cover can be seen in areas like Saurashtra in India and other similar areas elsewhere including Columbia River Basalt in States and Parana basin in Brazil. Exploration for additional coal measures in the known Gondwana basins and their covered extensions need immediate attention in the present period of energy crisis. In this context, delineation of Gondwana sediments below Deccan trap assumes a greater significance for future exploration. To achieve these objectives, certain areas of southwestern part of the Wardha valley, Maharashtra (Fig. 1) have been selected for electrical survey employing Schlumberger sounding as well as magnetic surveys. The presence of drilling data was an added advantage for correlation of geological litho packages vis-à-vis resistivity data interpretation.

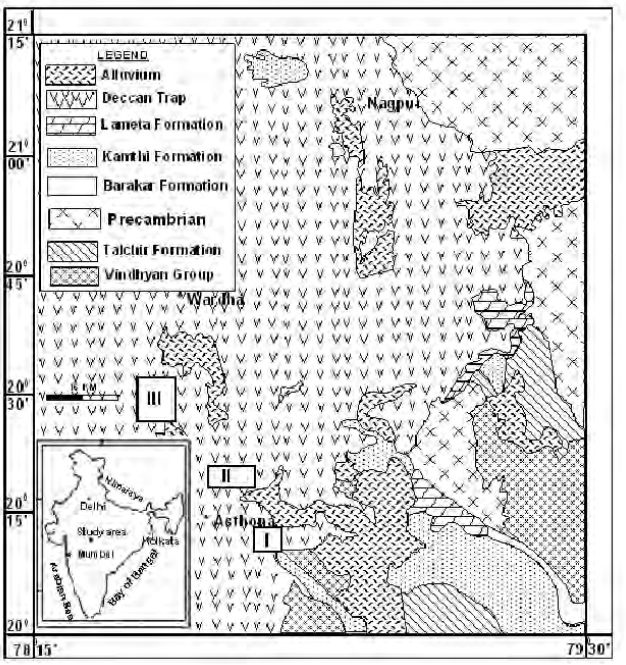

Fig. 1. Geological map of Wardha valley coalfields showing the areas of investigations, Maharashtra

The Wardha valley in Central India, west of Nagpur, Maharashtra state is an important region. The area is represented by a variety of stratigraphic unit's right from the Archaean to Recent alluvium and laterites. The region is gifted with deposits of various minerals like coal, iron etc.

Magnetic survey was carried out in three blocks (I, II, III; Fig. 1). A total of 439 observations were taken. A total of 95 (310 sq km) Resistivity Sounding (RS) was taken using Schlumberger array with a maximum current electrode separation (AB) equal to 4 km.

On correlating interpreted resistivity data with boreholes lithologs drilled by the Directorate of Geology and Mining (DGM) Maharashtra, a relationship has been obtained between range of resistivity and the various subsurface formations and is given below:

Geological Formation	Resistivity (Ohm-m)
1. Alluvium/top soil/Weathered trap	up to 25
2. Deccan trap	50-300
3. Subtrappean formations	15-80
4. Gondwana	6-120
5. High resistivity zone (basement/bedrock)	> 300

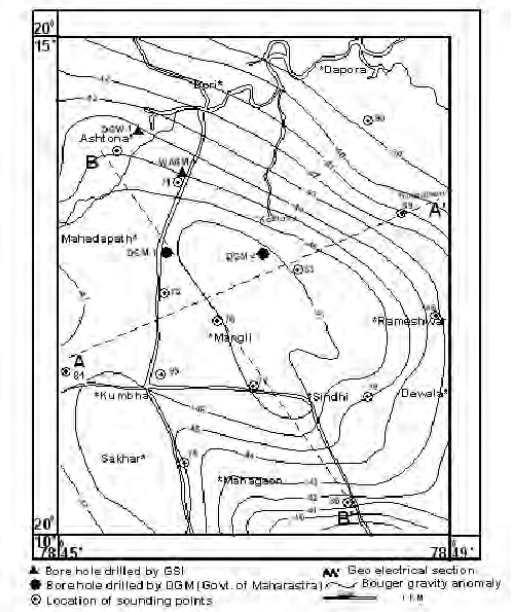

Fig. 2. Location map along with Bouguer anomaly map (after Joga Rao, et al. 1984) in block-I: Kumbha area, Maharashtra

In Block I (Asthona-Kumbha area) location of resistivity soundings along with Bouguer anomaly map is shown in Fig. 2. Some representative sounding curves of the area along with interpreted layer parameters are presented in Fig. 3. The obtained apparent resistivities for half the current electrode separation (AB/2) beyond 100 m show a steep fall in resistivity value. The interpreted resistivity value for this conductive layer at depth varies from 5-18 Ohm-m. This conductive zone may be corresponds to the Talchir formations. In view of obtaining a 2D idea of the area of study, two geo-electric sections (AA′ and BB′) were chosen taking into consideration of gravity response (Fig. 2). The section AA′ is taken from Kumbha in the NW to Khairgaon. The other section, is almost orthogonal to the above has been designated as BB′ (from Asthona to east of Mahagaon).

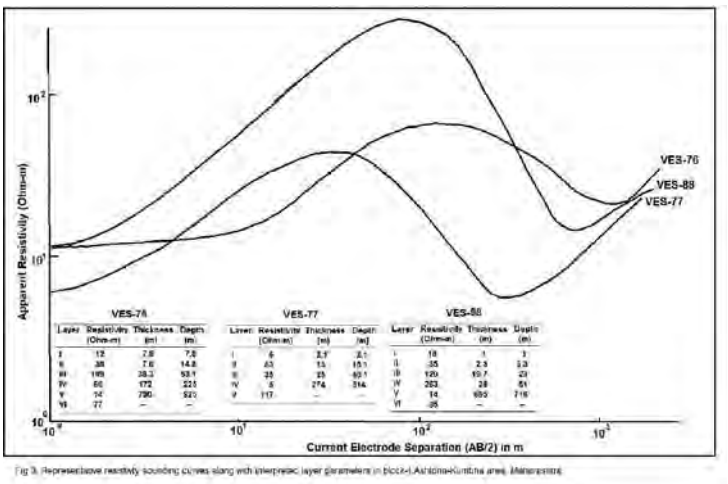

Fig. 3. Representative resistivity sounding curves along with interpreted layer parameters in block-I: Ashtona-Kumbha area, Maharashtra

Along section AA′ (Fig. 4), the top most layer is characterized by resistivity value of 6-15 Ohm-m and thickness varying from 2-15 m corresponds to alluvium/top soil which is underlain by a layer

having resistivity varying from 25-325 Ohm-m and of thickness varying from 50-80 m corresponds to Deccan trap. These are followed by a low resistivity zone 11-104 Ohm-m and of thickness 110-205 m representing sub-trappean formations Motur/Barakar. A thick conductive zone of resistivity varying from 6-18 Ohm-m and thickness varying from 340-700 m representing Talchir is interpreted all along the section. The high resistivity zone (69-500 Ohm-m) representing basement is inferred at deeper level. The results of resistivity soundings are in agreement with the gravity results along the section. Basement depression is found to lie in the central portion of Bouguer anomaly map.

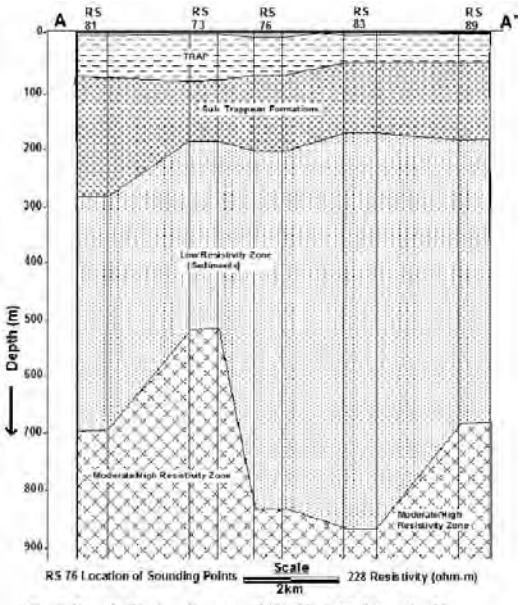

Fig. 4. Geo-electrical section along AA' in block-I: Ashtona-Kumbha area, Maharashtra

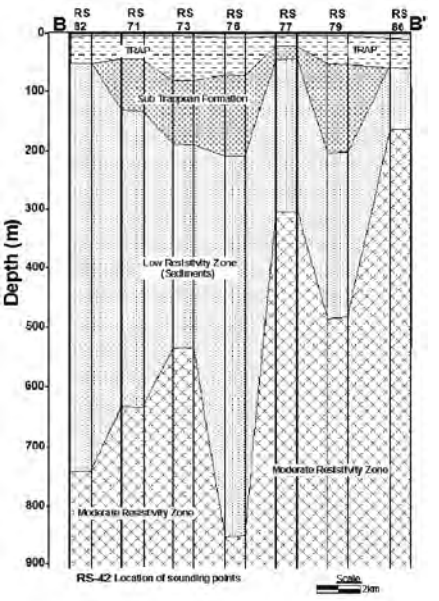

Fig. 5. Geo-electrical section along BB' in block-I: Ashota-Kumbha area.

Along section BB′ (Fig. 5), the top most layer characterized by resistivity value of 4-22 Ohm-m and thickness varying from 2-10 m corresponds to alluvium/top soil. The Deccan trap shows resistivity in the range from 40-203 Ohm-m and of thickness varying from 26-79 m lies below top soil/alluvium. These are followed by a low resistivity zone 22-60 Ohm-m and of thickness 24-143 m representing sub-trappean formations Lameta, Kamthi and Motur. A thick conductive zone of resistivity varying from 5-16 Ohm-m and thickness varying from 106-700 m is inferred all along the section. The basement has been identified below this conductive layer. Interpretation of sounding curves in general reveals that high resistivity basement occurring at greater depth of 871 m in RS 76 in Mangli-Sindhi area, whereas to the south of it (RS 77) the same occurs at a shallow depth of 313 m. The steep gradient could possibly be attributed to a fault zone. However in gravity contour there is no indication of any upliftment of basement. The presence of fault may be due to variation of depth.

In Block II (Wadhona-Pohna area) location of resistivity sounding points is shown in Fig. 6. Some representative sounding curves of the area along with interpreted layer parameters are depicted in Fig. 7. The sounding curves have not indicated any characteristic conductive zone. The details of some soundings along geo-electrical section XX′ across the Wardha river is also given in Fig. 8.

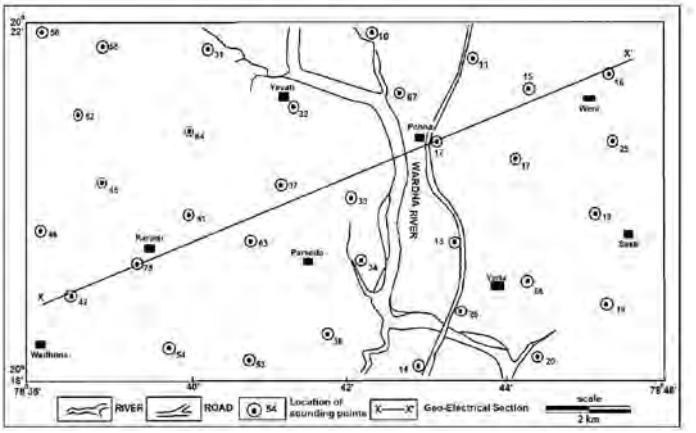

Fig. 6. Location map along with resistivity sounding points and geoelectrical section in block-II: Wadki-Pohna area, Maharashtra

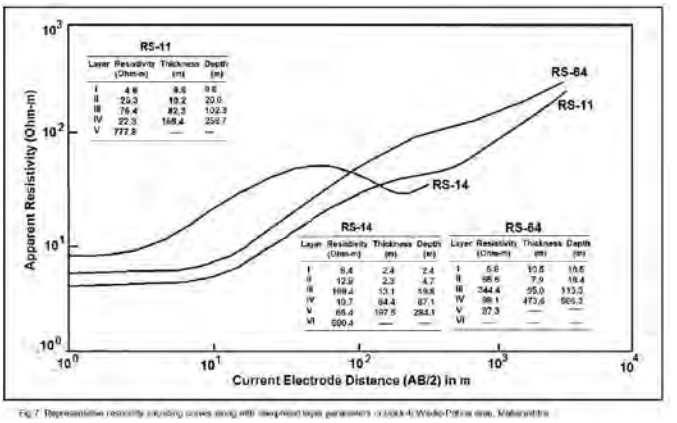

Fig. 7. Representative resistivity sounding curves along with interpreted layer parameters in block-II: Wadki-Pohna area, Maharashtra

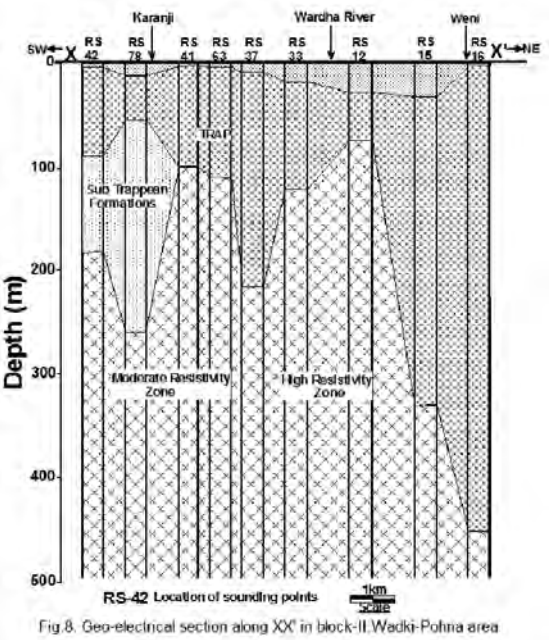

Fig. 8. Geo-electrical section along XX' in block-II: Wadki-Pohna area

The section has brought out a thick zone with variable thickness below the top layer. Thickness of this layer is found to increase towards NE as indicated in sounding number RS 15 and RS 16. A moderate/high resistivity zone (216-1628 Ohm-m) is reflected in the central part (RS 41, RS 63, RS 37) which however could not be correlated with the geological set up. It may be due to the presence of some intrusive body or basement high. The high resistivity basement (461-1628 Ohm-m) at a relatively shallow depth (102-218 m) southwest of Wardha river has been interpreted whereas the same occurs at a greater depth (329-455 m) northeast of Wardha river. The basement has come up to a level of 75 m immediate northeast of Wardha River. The steep gradient could possibly be attributed to a fault zone.

In Block III (Ralegaon-Andori area) location of resistivity sounding points is shown in Fig. 9. Some representative sounding curves of the area along with interpreted layer parameters are depicted in Fig. 10. The details of some soundings along geo-electrical section PP′ and QQ′ are also given in Fig. 11 and Fig. 12.

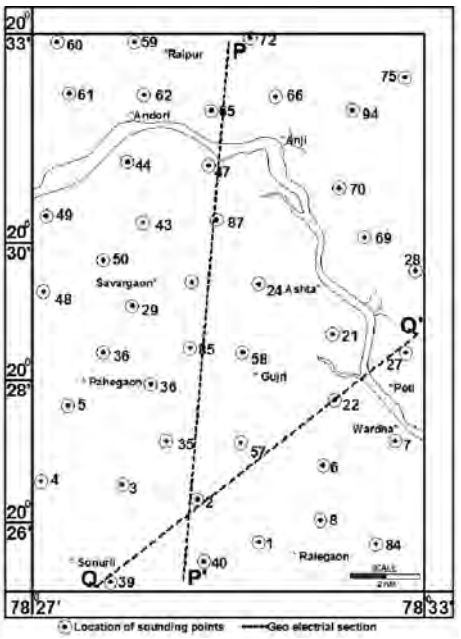

Fig. 9. Location map along with resistivity sounding points and geoelectrical section in block-III: Ralegaon-Andori area, Maharashra

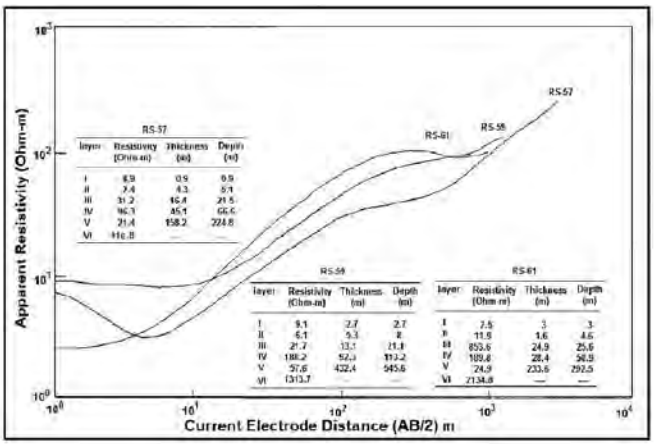

Fig. 10. Representative resistivity sounding curves along with interpreted layer parameters in block-III: Ralegaon-Andori area, Maharashtra

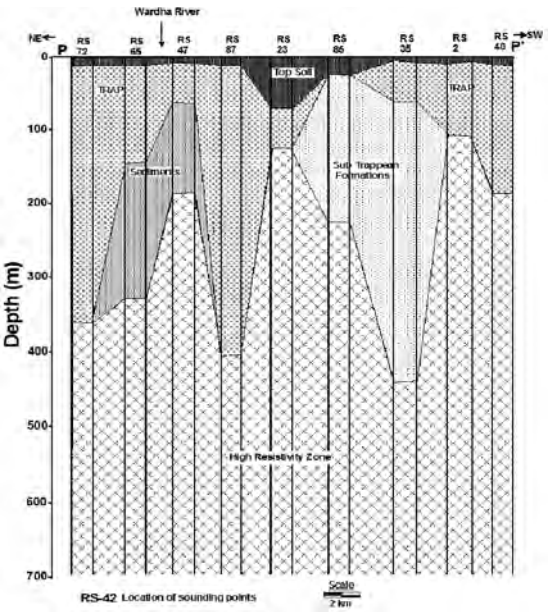

Fig. 11. Geo-electrical section along PP' in block-III, Ralegaon-Andori area, Mahrashtra

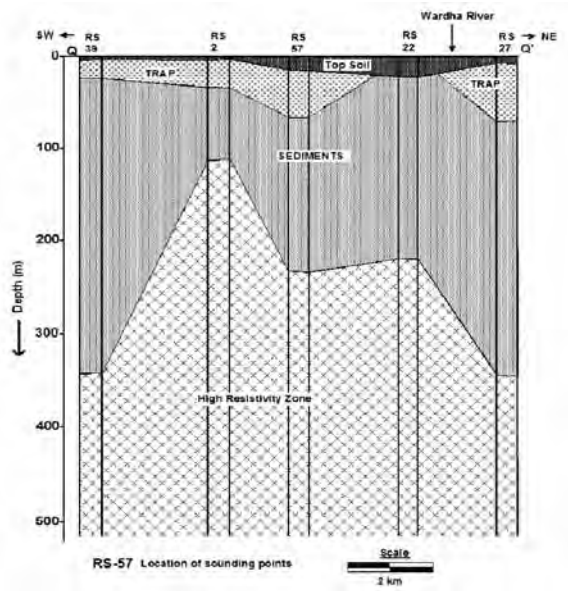

Fig. 12. Geo-electrical section along QQ' in block-III, Ralegaon-Andori area, Mahrashtra

The geo-electric section along PP′ has brought out different subsurface litho interfaces in terms of resistivity and thickness parameters. The variation of resistivity values of subsurface layers/zones indicate that the area is structurally disturbed. At RS 87 the thickness of the second layer is found to be 396 m having resistivity of 150 Ohm-m which is similar to that of trap. However, it is felt that such appreciable increase in thickness is not feasible as per available geological knowledge. Accordingly in all likelihood it is due to the presence of some intrusive body or presence of formation having resistivity equivalent to trap. The increase in thickness may also be due to the presence of faults. Due to overlapping resistivity values, the individual thickness of trap and sedimentary column could not be identified in the area. However, depth to basement could be inferred and is varying from 116 m to 450 m.

The geo-electric section along QQ′ has brought out different subsurface layers characterized by different resistivity values. The first interpreted layer represents top soil/alluvium. This is underlain by a layer having resistivity varying from 91-354 Ohm-m with thickness varying from 22-75 m and is absent at RS 22 attributable to Deccan trap. A low resistivity zone (13-53 Ohm-m) with thickness varying from 86-347 m probably corresponding to sedimentary column is inferred below the trap. A high resistivity zone representing basement revealed all along the section at depth level of 116-370 m.

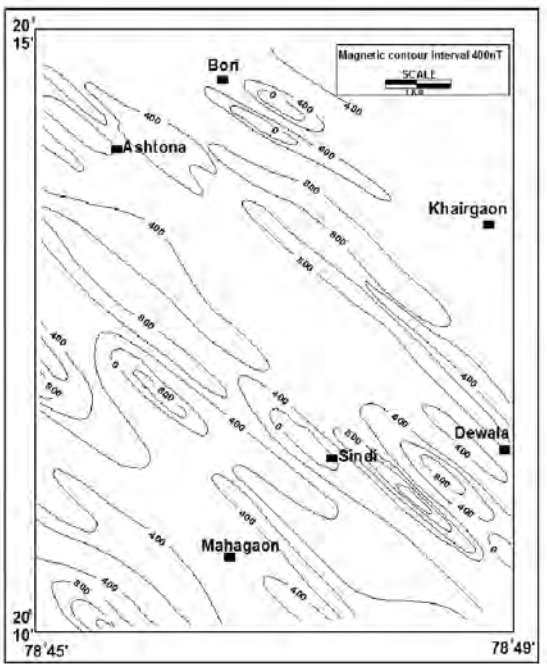

Fig. 13. Magnetic (VF) contour map in block-I: Ashtona-Kumbha area, Maharashtra

In Block I fluctuation of the magnetic anomalies due to the trap layer overlying the Gondwana sediments (Fig. 13). The distinct pattern and orientation of the contours indicate the occurrence of structurally controlled lava flow. The contours show localized anomaly closures of moderate wave number and amplitude (+400 nT) indicative of basement structure. The contour pattern of the magnetic anomalies showing a sharp magnetic gradient indicates a fault zone. This fault zone is running from NW-SE through east and southeast of Sindhi. This fault zone corroborates well with resistivity sounding results.

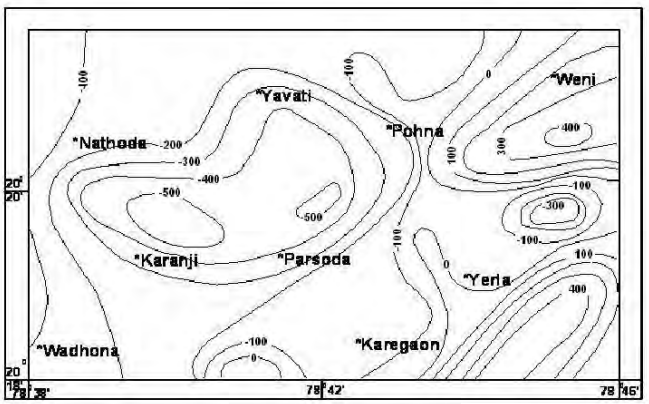

Fig. 14. Magnetic (VF) contour map in block-II: Wadki-Pohna area, Maharashtra

In Block II the contours show localized positive and negative closures associated with low and high wave number and amplitude (Fig. 14). The contour trend varies from NE-SW to E-W which is sympathetic to the Tapti and Narmada lineament. The high gradient of magnetic anomalies in the east suggests occurrence of the Deccan trap at shallow depth. Effects of the basement are not in the magnetic anomaly map. Large amplitude of the magnetic anomaly north of Karanji and Parsoda probably indicates that the trap has gone deeper. Sudden change in magnetic contour pattern running NNE-SSW to the east of Pohna is suggestive of a fault which is well corroborated with resistivity sounding results (Fig. 6 and Fig. 8).

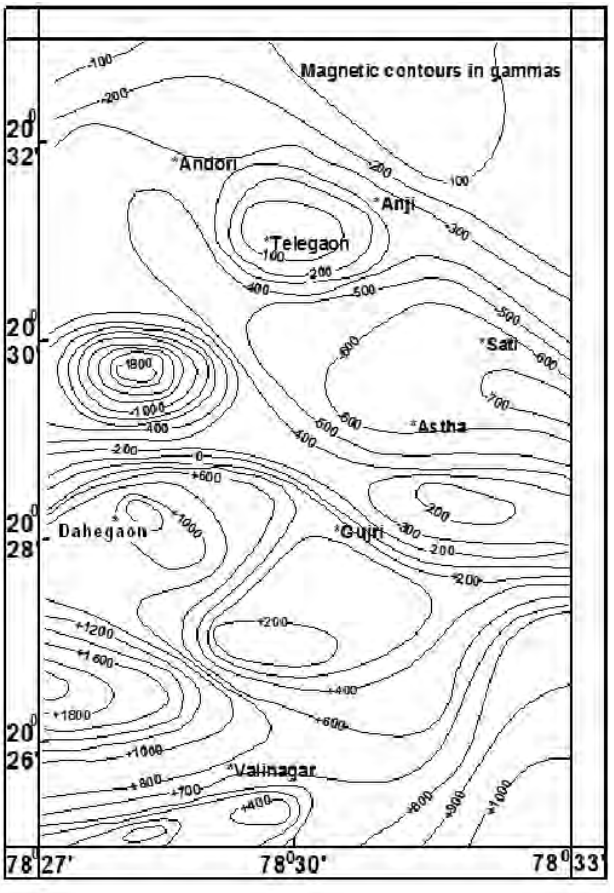

Fig. 15. Magnetic (VF) contour map in block-III: Ralegaon-Andori area, Maharashtra

In Block III magnetic map indicates E-W to NW-SE trend of the contours (Fig. 15). Sharp gradient of contour in west central part suggests occurrence of Deccan trap at shallow depth. Amplitude of the anomaly varies from -1800 nT to +1000 nT, north of Dahegaon (Fig. 15) to the south of it. This high amplitude dipolar anomaly suggests either emplacement of basic bodies along some fault planes or the faults along which concentration of magnetite is a natural phenomenon. Relatively lower amplitude anomalies are observed in the northern, eastern and southeastern part. One significant feature of the map is a sharp change in gradient of magnetic field from western part to the eastern part, NW-SE of Valinagar. Gradient is high in the western part whereas it is small in the eastern and southeastern parts suggestive of deeper disposition of Deccan lava in the eastern part.

INFRASTRUCTURE OF MESO-PROTEROZOIC JUXTAPOSED GABBRO-NEPHELINE SYENITE PLUTONS, EASTERN GHATS MOBILE BELT, INDIA: GRAVITY AND MAGNETIC STUDIES

S. K. G. Krishnamacharyulu and K. Vijaya Kumar
School of Earth Sciences, SRTM University, NANDED – 431 606
skgkchary@gmail.com

Chimakurti-Errakonda-Uppalapadu plutons represent an unusual clinopyroxenite-gabbro-anorthosite-ferrosyenite and nepheline syenite association in the Prakasam Province of the Eastern Ghats Mobile Belt, India. These plutons are co-spatial in nature and intruded into the deep Precambrian continental crust composed of amphibolites, quartzite and khondalite. Geological and geochemical studies suggest that Chimakurti and Uppalapadu magmatic bodies are coeval but possibly derived from two contrasting magmas. The magmatic association of gabbro, ferrosyenite and nepheline syenites is one of the debating issues in this cospatial magmatic set-up.

The co-spatial Chimakurti, Errakonda and Uppalapadu plutons are exposed with ultramafic and mafic rocks including gabbronorites, clinopyroxenite and anorthosite. The Errakonda pluton is made-up of ferrosyenites and their variants and the Uppalapadu pluton essentially consists of nepheline syenite.

Density, and magnetic susceptibility show a wide variation among the lithologies and are correlated with changing mineral assemblages and abundances. The density and susceptibility values show conspicuous intra-pluton, inter-pluton and pluton-country rock contrast.

The interpretation of gravity and magnetic anomalies over these bodies suggest distinct subsurface infrastructures for the Chimakurti and Uppalapadu plutons with a sharp contact between them. Gravity and magnetic modeling also revealed a differential basement set-up beneath nephyline syenite and gabbro. The interpretation also reveal that the anorthosites and ferrosyenites are limited to shallow depth extents only. This geophysical approach provide a detailed subsurface structure of the plutons which helps in understanding the nature of the magmatic processes associated with the Chimakurti-Errakonda-Uppalapadu plutons and other magmatic bodies of similar nature elsewhere.

SEISMIC HAZARD ASSESSMENT AT MICRO LEVEL INGANDHINAGAR, GUJARAT CONSIDERING GEOTECHNICAL PARAMETERS

***Kapil Mohan, B.K. Rastogi,Vasu Pancholi and Drasti Gandhi**
Institute of Seismological Research, Raisan-382009, Gandhinagar, Gujarat (India)
kapil_geo@yahoo.co.in

Gandhinagar City (the Capital of Gujarat) falls under Zone III of seismic zoning map of India where an earthquake of magnitude 6 can be expected that can damage single tomultistorey buildings. It is also a well established fact that site amplification/ shaking and damage is large in soil covered areas. To estimate the effect of soil on ground motion and to estimate the strong ground motion parameters at surface, the soil modeling and the ground response analysis are conducted along uniformly distributed 14 boreholes drilled upto a depth of 50m. The methodology is divided into three parts (i) Estimation of depth of Engineering Bed layer (EBL) (a layer with a shear wave velocity 400m/sec≤Vs≤ 750m/sec, N value >80 and minimum soil variation below it) through soil modeling, (ii) Estimation of Ground Motion at EBL due to scenario earthquake at nearby active fault and (iii) Estimation of surface strong ground motion using 1D ground response analysis through SHAKE 2000 program.The EBL is found

at a depth of 21m to 33m (shallower in central part and deeper in northern and southern part). The scenario earthquake of magnitude Mw6.0 is considered along East Cambay Fault located at about ~ 20km. The Peak Ground acceleration (PGA) of 0.172g to 0.237g and Peak Spectral Acceleration (PSA) of 0.522g to 0.851g with predominant period of ~0.1sec and 0.25sec (corresponding to 1 to 3 storey buildings) are estimated in the city. The PGA is found higher in the Central part of Gandhinagar city (due to low N valuein the shallower depth) as compared to Northern and Southern part (due to high N-value in theshallower depth). The PGA is found increased by 5 to 38% in the first subsurface soil layer in Gandhinagar city (with 11 to 38 % in silty sand and 5 to 28% in clayey sand) having thickness of 1 to 6m. The Spectral acceleration (Sa) values are found higher than BIS suggested values in the period range of 0.1 to 0.4sec (one to four storey buildings).

THICK LITHOSPHERE OF NORTH INDIAN PENINSULAR SHIELD OBTAINED FROM LONG PERIOD SURFACE WAVE DISPERSION.

G. Suresh[1], S.S. Teotia[2] and S.N. Bhattacharya[3]

[1] *Seismology Division, India Meteorological Department, New Delhi-110 003*
[2] *Department of Geophysics, Kurukshetra University, Kurukshetra-136 119*
[3] *23B Nivedita Enclave, A6 PaschimVihar, New Delhi-110 063*
gsureshimd@yahoo.com

We measure the inter-station Rayleigh and Love wave phase velocities across the north Indian Peninsular (N-IP) shield through cross-correlation and invert these velocities to evaluate the underneath crust to upper mantle velocity structure down to 400 km. We consider a cluster of eight stations in the south and another cluster of three stations in the northern tip of the Peninsula. We measure phase velocities along 29 paths for Rayleigh wave and 19 paths for Love wave joining two stations with one from each cluster and using broadband records of earthquakes which lie nearly on the great circle joining the pair of stations. The phase velocities are in the period range of 10 to 275 s for Rayleigh wave and of 10 to 120 s for Love wave. The model obtained through inversion of the phase velocities indicates 194 km thick lithosphere with 3-layered crust of thickness 37.3 km; the top two layers have nearly same velocities and both constitute the upper crust with thickness of 12.7 km. The upper crust is mafic, whereas the lower crust is felsic. In the mantle lid, velocities increase with depth. The velocities of mantle lid beneath N-IP is lower than those beneath south Indian Peninsula showing the former is hotter than the later perhaps due to large Phanerozoic impact on N-IP. The significant upper mantle low velocity zone beneath N-IP indicates high temperature which is likely due to broad plume head at the middle of the Peninsula.

INTRODUCTION

Many cartons are underlain by lithospheric roots which extend to depth > 250 km in contrast to the oceanic area and Phanerozoic continents (Mahadevan, 2013). These deep roots may perturb the surrounding mantle and the mantle convection. However, the loss of these roots beneath Indian cratons might have been caused by the Deccan plume (Lehmannet al., 2010). Thus the topology of Lithosphere-Asthenosphere boundary (LAB) i.e. the bottom of the mantle lid, beneath the Indian Peninsular shield will allow us to model its formation and evolution. So far the upper mantle structure of the northern part of the Indian Peninsular shield is poorly resolved due to limited broadband earthquake records in the northern part of the shield region.With the installation of a few broadband stations recently, we measure inter-station phase velocities of both Love and Rayleigh waves to evaluate the velocity structure of the northern Indian Peninsular shield (N-IP) region down to 400 km.

DATA AND METHODOLOGY

We consider records of broadband seismic stations operated by the India Meteorological Department (IMD) and the National Geophysical Research Institute (NGRI) to measure inter-station surface wave dispersion over broad period range. We consider two clusters of stations: the south cluster is located in Koyna-Warna region in the NW Dharwarcraton(in the western Peninsula) and the north cluster is in the northern tip of the Peninsula (Figure 1). For interstation phase velocity measurement, we consider the records of two earthquakes (Table 1) which lie nearly in the same great circle joining a pair of stations with one from each cluster. The angle between the two great circles (1) joining the two stations and (2) the longer of the two great circles joining each station and the epicenter, is required to be less than 3° (Bhattacharya et al., 2013), in order to minimize the influence of the structure between the earthquake and nearest station; this also minimizes the errors in azimuth arising from refraction would introduce only second order effects in phase velocity. We process28 inter-station wavepaths for Rayleigh waves and 17paths for Love waves (Table 2) after careful examination for good quality records consisting of least scattered waves and only those waveforms having a signal to noise ratio ≥ 2.5. We use vertical components of displacement seismogram for Rayleigh waves and transverse components for Love waves. In this method of measurement of inter-station phase velocity, the group arrival time of period Ti is obtained through frequency time analysis (FTAN) (Bhattacharya, 1983, 2013) for each seismogram, which is further is windowed in time domain centered on this arrival time. Windowed seismogram is filtered in a narrow band centered at frequency 1/Ti. Finally we cross correlate a pair of such filtered seismogram, one from the north cluster and another from the south cluster. The correlated waveform shows maximum amplitude (crest) at a time when the phase difference is zero; this time corresponds to the phase arrival time and is used to compute phase velocity (= inter-station distance/ time) of period Ti.

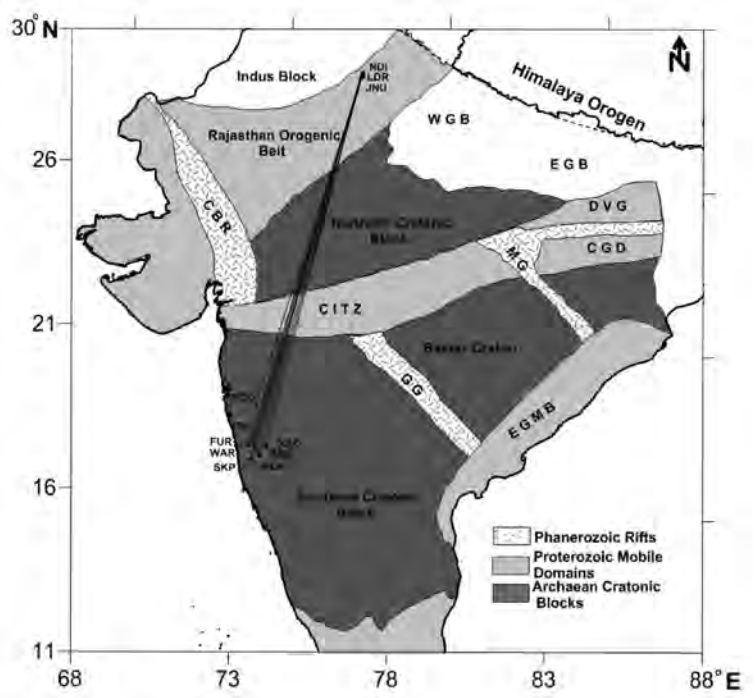

Figure 1. *Precambrian cratonic blocks and associated mobile belts in and adjoining regions of present study. (Figure modified from Mahadevan, 2013). Abbreviations: CBR-Cambay rift; CITZ-Central Indian Tectonic Zone; DVG- Damodar Valley Graben; CGD-Chotanagpur Gneissic-Granitic Domain; EGMG-Eastern Ghat Mobile Belt; GG-Godavari Graben; WGB-West Ganga Basin; EGB-East Ganga Basin. Locations of observatories (triangles) and the inter-station wave paths used in this study are shown.*

Table 1. The hypocentral parameters of the earthquakes used (from NEIC, USGS)

Earthquake number	Date	Origin time (UTC)	Latitude	Longitude	Depth (km)	Magnitude
1	2012 JUN 29	21:07:33.90	43.43	84.70	18	6.3 (m_b)
2	2012 OCT 28	03:04:08.82	52.79	-132.10	14	7.8 (M_W)

Table 2. Station pairs used

Event no. 1	Paths	NDI-ABG	NDI-FUR	NDI-GKL	NDI-KRD	NDI-KOK	NDI-SKP	NDI-WAR				
	Waves used	LR, LQ	LR, LQ	LR,	LR, LQ	LR, LQ	LR, LQ	LR, LQ				
Event no. 2	Paths	NDI-ABG	NDI-FUR	NDI-GKL	NDI-KAD	NDI-KOK	NDI-POO	NDI-SKP	NDI-WAR	LDR-ABG	LDR-FUR	LDR-KOK
	Waves used	LR, LQ	LR, LQ	LR	LR, LQ	LR, LQ	LR, LQ	LR, LQ	LR	LR,	LR	LR, LQ
	Paths	LDR-GKL	LDR-KAD	LDR-POO	LDR-SKP	LDR-WAR	JNU-ABG	JNU-FUR	JNU-GKL	JNU-KAD	JNU-SKP	JNU-WAR
	Waves used	LR	LR, LQ	LQ	LR, LQ	LR, LQ	LR	LR	LR	LR	LR	LR

Note: LR: Rayleigh waves(28 wavepaths); LQ: Love waves(17 wavepaths)

INVERSION AND RESULTS

We perform a non linear iterative search of a model using genetic algorithm (GA) (Suresh et al., 2008). In GA, we obtain a model minimizing the misfit between observed and theoretical phase velocities. We define misfit as

$$\varphi = \max\left(\frac{1}{NR}\sum_i \delta_i^R, \frac{1}{NL}\sum_j \delta_j^L\right)$$

where δ_i^R is the absolute difference between the observed and theoretical phase velocity of a given model at periods $T_i(i=1, 2, \ldots\ldots, NR)$ for Rayleigh wave; δ_j^L are corresponding values of periods $T_j(j = 1, 2, \ldots\ldots, NL)$ for Love wave.

We considered a layered structure down to 400km with 3 layered crust, below which there are 8 layers. The model parameters V_S and V_P/V_S in each of top 10 layers are considered as variable. Thickness of the layers of the crust and a few layers of the upper mantle are considered as variables making total number of variables as 27; we did not consider thicknesses of all layers to restrict the number of variables in GA operation for better convergence to a solution. In the present study, evaluations of upper and lower boundaries of LVZ of upper mantle are important issues; the upper boundary of LVZ coincides with LAB. So we consider the thickness of layers around these two boundaries as variables.

Based on the previous studies on the Indian Peninsula, initially we considered possible LAB depth between 140 and 160km. However a few operations of GA showed that the LAB is below 160 km depth. In view of this we considered limits of thickness in the upper mantle beyond this depth.

With 27 variables, we consider K=150 models during each generation and best solution is obtained after 350 generations. In each GA operation, we get best solution for 27 variables. GA operation is repeated 24 times and mean of the 24 best solutions is considered as the final accepted solution; the standard deviations show broad estimates of deviations of the model parameters. The theoretical curves for this model are in Figure 2.

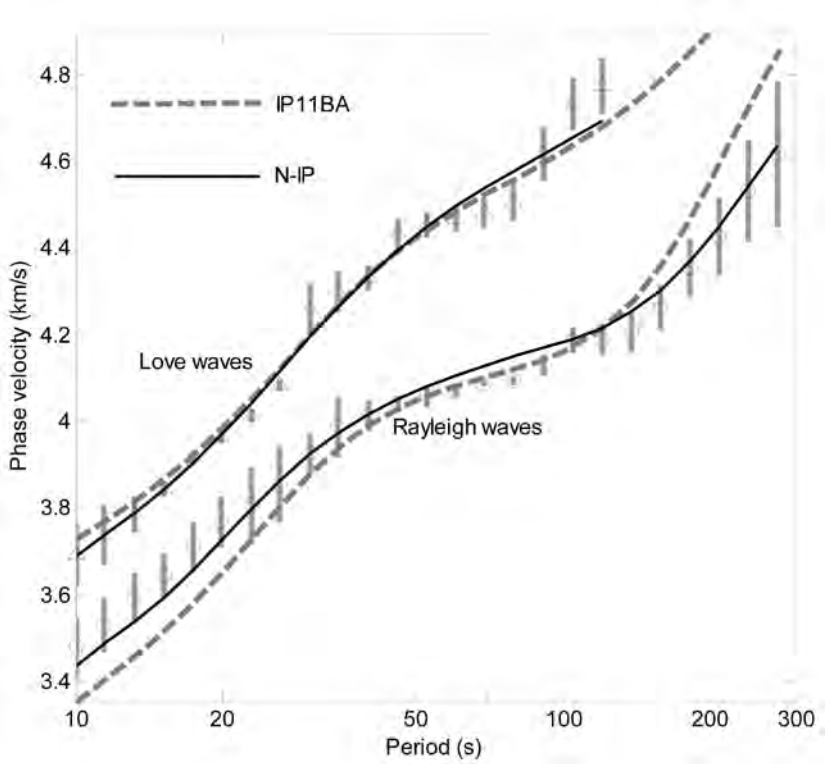

Figure 2. *Observed mean phase velocities of Rayleigh and Love waves are shown by small circles and triangles; vertical grey lines through these symbols show ± one standard deviation. The theoretical curves for crust-upper mantle of Bastar craton (IP11BA, Bhattacharya et al., 2009) and those of north Indian peninsula (N-IP) (Present study) are shown. The theoretical curves of Love waves for IP11BA and N-IP (Present study) are close to each other.*

DISCUSSIONS

The crust of N-IP shows that *Vs* as well as V_P in the top two layers are close to each other; thus considering these top two layers as an upper crust, we find the thickness of this part of the crust as 12.7 km, while the lower crust is 24.6 km. The southern part of the present wave paths are close to those used by Prajapatiet al. (2011) across NW-DVP, where upper crust is 15.2 km thick. In the upper crust of N-IP, the V_P/V_S is between 1.82 and 1.83. Such mafic crust was noted in adjoining West Ganga Basin (WGB) (Mitraet al., 2011). However, at N-IP, the lower crust is felsic ($V_P/V_S \sim 1.68$). This lower crust has V_S (=3.904 km/s) similar to that of NW-DVP (V_S=3.89km/s). Such*Vs* at lower crust is higher than the corresponding values in the adjoining regions like WGB and Indus block crust (Suresh et al., 2008), where the crust is thicker due to sedimentary deposits.

Down to 160km, the mantle lid of N-IP is similar to that of the Bastarcraton (Bhattacharya et al., 2009) (Figure 3). Below this depth there is a slight increase of *Vs* down to LAB, which is at 194km depth. Such increase is consistent with other observations in cratons, where *Vs* reach higher values with depth in the lithosphere (Lebedevet al., 2009). For south-IP (S-IP), a significant high velocity was noted in mantle lid with LAB at 155 km depth (Mitraet al., 2006) (Figure 3). Thus the mantle beneath S-IP is colder than that beneath N-IP. The Phanerozoic impact was feeble in S-IP compared to N-IP making S-IP lighter and colder lithosphere (Mahadevan, 2013). In the western side of Dharwarcraton, gravity data shows LAB is as deep as 165 km (Aroraet al., 2012).Considering maximum negative *Vs*gradient as an indicator of LAB, the velocity structure of the Bastarcraton (Bhattacharyaet al., 2009) shows LAB depth as 160 km beneath this craton. While in N-IP we find LAB is at 194km depth. Thus, we find that the LAB depth is increasing from south to north agreeing with the findings of Priestley andMckenzie (2006).

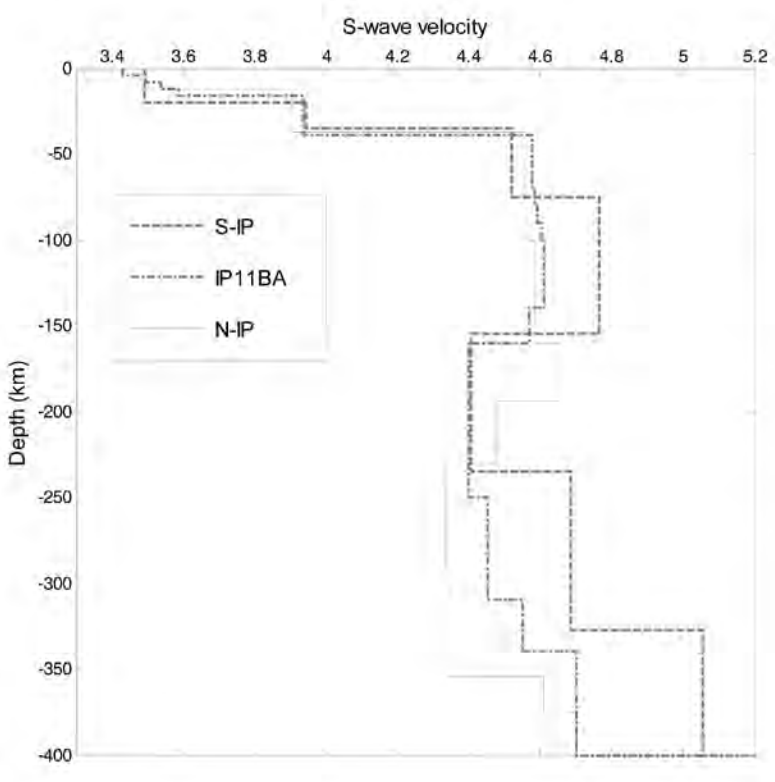

Figure3. *The upper mantle structure of north Indian Peninsula (N-IP) (Present study) compared with those of south Indian Peninsula (S-IP, Mitra et al., 2006) and Bastar craton in east Indian Peninsula (IP11BA, Bhattacharya et al., 2009).*

The partial derivatives show that the measured phase velocities up to 275 s for Rayleigh and 120 s for Love waves allow us to ascertain the radial anisotropy down to 240 km reliably. We observe the radial anisotropy in the shield area is absent at least in the crust and mantle lid since an isotropic model satisfied both the measured Rayleigh and Love wave velocities.

Beneath N-IP, the 161 km thick upper mantle LVZ extend from 194 to 355km depth; in LVZthe lowest velocity is 4.33km/s, which is 6-7% decrease of $V_S$in LVZ. Although the LVZ thickness closely agrees with other cratons but the decrease of *Vs* is slightly larger compared to 4-5% beneath the other cratons (Lebedevet al., 2009).For the Indian peninsular shield, Rao and Lehmann (2011) postulated large plume head of diameter 2000-2500 km centered at the middle of the peninsula. In LVZ of N-IP

we find that V_S has decreased along with V_P. Partial melt only decreases V_S and not V_P (Wang et al., 2008). Thus, we do not consider a presence of partial melt in LVZ, which is hot due to presence of a plume head.

CONCLUSIONS

We conclude the following from the evaluated crust and uppermost mantle structure of N-IP:

1. The 3-layered crust is 37.3 km thick. The top two layers have velocities close to each other and these two layers constitute upper crust, which is 12.7 km thick and is mafic.

2. The theoretical curves of the isotropic upper mantle satisfy the observed data. This indicates that the radial anisotropy either is absent or weak at least in the crust and mantle lid.

3. The lithosphere is 194 km thick and $V_S$increases downward below the crust. Relatively high V_S in mantle lid shows its low geothermal gradient. Comparison of V_S shows that the lithosphere in N-IP is hotter than S-IP perhaps due to large Phanerozoic impact on N-IP compared to S-IP.

4. Strong LVZ is interpreted as positive thermal gradient due to which thermal mantle convection may not occur (Eatonet al., 2009). The high temperature in LVZ is likely due to broad plume head centered at middle of the Indian Peninsula.

5. The important result of crust and uppermost mantle structure obtained here will help to study the evolution and stability of lithosphere and to obtain upper mantle thermal convection model beneath cratons of N-IP.

REFERENCES

Arora, K., Dimri V.M., Singh B., Mishra D.C., and Grevemayer I., 2012. Three dimensional lithospheric structure of the western continental margin of India constrained from gravity modelling: implication for tectonic evolution. Geophys. J. Int., v.198, pp:131-150.

Bhattacharya S.N., 1983. Higher order accuracy in multiple filter technique, Bull. Seismol. Soc. Am.,V.73, pp:1395–1406.

Bhattacharya S.N., Suresh G., andMitraS., 2009. Lithospheric S-wave velocity structure of the Bastarcraton, Indian Peninsula from surface wave phase-velocity measurements, Bull. Seism. Soc. Am., v.98, pp:2715–2723.

Bhattacharya S.N., Mitra S., and Suresh G., 2013. The shear wave velocity of the upper mantle beneath the Bay of Bengal, Northeast Indian Ocean from interstation phase velocities of surface waves, Geophys. J. Int., v.193, pp:1506-1514.

Eaton, D.W., Darbyshire F., Evans R.L., Grutter H., Jones A.G., and Yuan X., 2009. The elusive lithosphere-asthenosphere boundary (LAB) beneath cratons, Lithos, v.109, pp:1-22.

Lebedev S., Boonen J.,and Trampert J., 2009. Seismic structure of Precambrian lithosphere: New constraints from broadband surface-wave dispersion, Lithos,v.109, pp:96-111.

Lehmann B., Burgess R., Frei D.,Belyatsky B.,Mainkar D., ChalapathiRao N.V., and HeamanL.M., 2010. Diamondiferous kimberlites in Central India synchronous with the Deccan flood basalts, Earth planet Sci. Lett.,v.290, pp:142–149.

Mahadevan T.N., 2013. Evolution of Indian continental lithosphere: insights from episodes of crustal evolution and geophysical models. J. Ind.Geophy.Union Soc. India, v.17, pp:9-38.

Mitra S., Priestley K., Gaur V.K., andRai S.S., 2006. Shear-wave structure of the south Indian lithosphere

from Rayleigh wave phase-velocity measurements, Bull. Seismol. Soc. Am.,v.96, pp:1551-1559.
Mitra S., Kainkaryam S.M.,Padhi A., Rai S.S., and Bhattacharya S.N., 2011. The Himalayan foreland basin crust and upper mantle, Physics of the Earth and Planetary Interiors,v.184, pp:34-40.
Prajapati S., Suresh G., and Bhattacharya S.N., 2011. Crustal Structure of the Northwest Deccan Volcanic Province, India, and the Adjoining Continental Shelf from observed Surface-Wave Dispersion, Bull. Seismol. Soc. Am.,v.101, pp:1488–1495.
Priestley K., and MckenzieD., 2006. The thermal structure of the lithosphere from shear wave velocities, Earth and Planetary Science Letters,v.244, pp:285-301.
Rao N.V.C., and Lehmann B., 2011. Kimberlites, flood basalts and mantle plumes: New insights from Deccan Large Igneous Province, Earth-Science Reviews,v.107, pp:315-324.
Suresh G., Jain S., and Bhattacharya S.N., Lithosphere of Indus block in the northwest Indian subcontinent through genetic algorithm inversion of surface-wave dispersion, Bull. Seism. Soc. Am., v.98, pp:1750–1755.
Wang Y., Wen L., and Weidner D., 2008. SH- and P-velocity structures and compositional models beneath southern Africa, Earth and Planetary Science Letters,v.267, pp:596-608.

POSTER

MANUAL AND COMPUTER BASED INTERPRETATION OF WELL-LOG DATA : A COMPARISON

Amita

Department of Geophysics, Kurukshetra University Kurukshetra 136 119 India
amitarohilla11@gmail.com

Well-logging is the branch of Geophysics in which the petrophysical properties of the earth's subsurface are measured as a function of depth. It is subsurface geophysical method in which recording instruments are near to the zones of interest and considered as eye to the subsurface as compare to other geophysical methods. The parameters measured through well logs are used during interpretation process for computing the values of different reservoir parameters such as: effective porosity, clay volume, water saturation, net pay thickness, and hydrocarbon saturation, etc. Well logs are also used to distinguish between oil and gas, or water in a reservoir, and to estimate hydrocarbon reserves.

A comparison between manually and computer based interpretation of well logs have been investigated in the present study. The different logs including GR, Caliper, Neutron, Density and Resistivity from four wells have been used for this purpose. The results have been compared by estimating the average reservoir parameters like effective porosity, volume of clay, pay thickness and water saturation etc. In this process, the intervals having shale content greater than 45% and effective porosity less than 6% are considered as non-reservoirs. The reservoirs with water saturation greater than 75% are water bearing while reservoirs with water saturation less than 75%, shale content less than 45% and effective porosity greater than 6% have been considered as hydrocarbon bearing. The applications of well logs in the accurate estimation of petrophysical parameters leading to identification of hydrocarbon bearing pay zones have been discussed here.

The present study has shown the importance of well logs in reservoir characterization and thus the importance of well logging in the exploration and exploitation of hydrocarbons

ESTIMATION OF ATTENUATION CHARACTERISTIC USING FREQUENCY DEPENDENT CODA WAVE QUALITY FACTOR OF NIIGATA PREFECTURE REGION, JAPAN

Ashvini Kumar[1*], A. Joshi[1],Sandeep[1],Parveen Kumar[2], Azad Kumar[1]
[1]Department of Earth Sciences, Indian Institute of Technology, Roorkee, India.
[2]Graphic Era University, Dehradun.
** ashvini_sharma2006@yahoo.co.in*

In order to evaluate seismic hazards of any given region, it is very important to study the attenuation characteristics of seismic waves. Factors such as geometrical spreading, inelasticity, absorption and scattering result in overall attenuation of the seismic waves. Attenuation characteristic of a medium is defined by anelastic attenuation of seismic waves. This in turn, is characterized by a dimensionless quantity called quality factor *Q* (Knopoff, 1964).In the present study coda wave attenuation characteristic has been investigatedforthe Niigata region, Japan. Single back scattering model given by Aki and Chouet (1975), has been used for estimating the coda $(Q_c(f))$ relationship. The dataset of strong motion waveforms of 50 earthquakes within the Niigata region recorded at five stations has been used in present work. Coda waves of 30 sec window length, filtered at six different frequency bands, centred at 1.5, 3.0, 6.0, 12.0, 20.0 and 28.0 Hz, respectively have been analyzed using the single backscattering method.The frequency dependent coda $(Q_c(f))$relationshiphas been determined for this region using the formula $Q_c = Q_0 f^n$. The frequency dependent $Q_c(f)$ relationship has been obtained as $Q_c(f) = 106f^{0.81}$for this region. The mean value of the estimated Q_c vary from 101±29 (at 1.5Hz) to 1743±349 (at 28Hz). Coda $(Q_c(f))$ has been found to increase with central frequency at all the frequency bands. Further, a comparison of coda $Q_c$obtained in the present work, when made with available values from other parts of the world, indicates that the distribution falls within the range of values justified for the tectonically active regions.

THE ATTENUATION CHARACTERISTICS OF STRONG GROUND MOTIONS OBSERVED IN THE 2011 SIKKIM EARTHQUAKE, NE HIMALAYA

Anjali Sharma, Prince Kamboj, Komal Sharma, and Ritu Chahal
Department of Geophysics, Kurukshetra University, Kurukshetra.
princekambo07@gmail.com, sharma.droneshkomal@gmail.com

The Peak Ground Acceleration (PGA) is one of the important parameters of earthquake strong ground motions.It is considered for the earthquake safe seismic design of engineering structures. The PGA is the single parameter extensively used in the preparation of seismic hazard maps of various regions of the world. It is the simplest way to characterize the earthquake hazard. The Peak Ground Acceleration is determined by the higher frequencies present in the accelerogram. The Peak Ground Acceleration at a site is affected by many factors. These include (i) the size of the earthquake (represented by its magnitude) (ii) distance of the site from the source (iii) site conditions (whether rock or soil) (iv) fault type (strike slip, normal or reverse) and (v) tectonic environment (interplate or interaplate).

Several studies have been done to obtain attenuation relations for PGA as a function of magnitude and distance for various regions of the world. Most of these studies are based on the regression or multiple regression analysis of large data sets of strong motion acceleration records.The strong motion data set obtained thus far for earthquakes of moderate/larger size are not adequate to do multiple regression analysis for obtaining PGA attenuation relation as a function of distance and magnitude.

In the present study, the several available attenuation relations have been used to investigate whether any of available relation is able to predict the observed PGA as a function of distance for the 2011 Sikkim earthquake of NE Himalaya. The relation thus identified can be used to estimate the PGA values for future earthquakes in the region and is also useful for the simulation of earthquake strong motions in the region.

FIELD AND PETROGRAPHICAL STUDIES OF ROCKS OF MEWANAGAR AREA, BARMERDISTRICT, WESTERN RAJASTHAN, INDIA

Naresh Kumar and Naveen Kumar

Department of Geology, Kurukshetra University,Kurukshetra, 136119 Haryana
sagwalnaresh@gmail.com, naveen.nain48@gmail.com

The rocks of Mewanagar area are a part of Malani Igneous Suite (MIS) which covers an area of 55,000 sq. km in Northwestern Indian Shield. In Rajasthan, the rocks of MIS are spreaded from South of Sirohi to North of Pokaran and from East of Jodhpur to the edge of the Thar Desert. Neoproterozoic MIS represents the largest felsic magmatism in India. MIS is the largest A-type, anorogenic acid magmatism in the Western Peninsular India and owes its origin to hot spot tectonism (Kochhar, 1984; Bhushan, 1985; Bhushan and Chandrasekaran, 2002; Vallinayagam, 2003).The rocks of MIS are mainly of felsic volcano-plutonic with fewer amounts of mafic lithounits. The Mewanagar area (Survey of India topographic sheet no. 45C/1; Scale 1: 50,000; 25°47′- 25°48′ N, 72°08′-72°09′ E) which is a part of MIS is located 120 km SW of Jodhpur and 30 km NW of Siwana in Western Rajasthan.Mewanagarconsists of extrusive (rhyolite,trachyte, tuffs and basalts) and dyke phase (basalts and dolerite). Rhyolite shows various shades of colour viz.dark grey, light grey, purple, light brown, dark brown and brick red etc.Mineralogically, bluish trachyte is similar to rhyolite and shows a sharp contact with rhyolite. Basalt is observed in form of flows as well as dyke which cut the different outcrops of the rhyolites. Basalt is fine grained and displays black/dark brown, light greyish brown and dark greyish brown colour. Basalt contains small size vesicles (upto 2 mm) and sometime vesicles are filled by calcite veins. Dolerite dykes (dark greyish, black colour & medium grained) are mainly cutting across rhyolite and trachyte. Petrographically, trachyte flows are showing similar petrographical features as shown by rhyolites and they consist of orthoclase, quartz, riebeckite, arfvedsonite, magnetite and hematite as aphenocrysts or groundmass.Porphyritic, glomero-porphyritic, perthitic& flow textures are observed in rhyolite. Basalt flows consist essentially of plagioclase feldspar (labradorite) and clinopyroxene (augite) in ophitic and sub-ophitic texture. Dolerite dyke contains plagioclase,pyroxene and iron oxides with hypidiomorphic texture. Different shades of rhyolites, volcanic joints, volcanic caves, wall like structure, jointed and fractured appearance in rhyolite are the distinguished features of Mewanagar area. Luniriver is flowing at outer margin of the studied area along Nakora area and taking sudden U turn from West to South direction (Vallinayagam and Kumar, 2007). This indicates the relationship between tectonism and volcanism which can be explained and understand by petrological, petrographical and geochemical studies of the Mewanagar area.

References

Bhushan, S.K., 1985. Malani volcanism in Western Rajasthan. Indian Journalof Earth Sciences 12, 58-71.

Bhushan, S.K., Chandrasekaran, V., 2002. Geology and geochemistry of the magmatic rocks of the Malani Igneous Suite and Tertiary Alkaline Province of Western Rajasthan. Memoirs of Geological Surveyof India 126, 1-129.

Kochhar, N., 1984. MalaniIgneous Suite: Hot-spot magmatism and cratonization of the Northern part of the Indian shiled. Journal of Geological Society of India 25, 155-161.

Vallinayagam, G., 2003. Basic magmatism of NeoproterozoicMalani Igneous Suite, Western Indian Craton: Petrological and Geochemical Modelling. Indian journal of Geochemistry 18, 1-18.

Vallinayagam, G., Kumar, N., 2007. Volcanic vent in Nakora Ring Complex of Malani Igneous Suite, Northwestern India . Journalof Geological Societyof India 70 (5), 881-883.

CHARACTERIZATION OF SHEAR WAVE ATTENUATION IN THE CENTRAL HONSHU REGION, JAPAN FROM THE INVERSION OF STRONG MOTION RECORDS

Parveen Kumar[1*], A. Joshi[2], Dinesh Kumar[3], S. S. Teotia[3], Ashvini Kumar[2] and Sandeep[2]

[1]Graphic Era University, Dehradun, Uttarakhand, India
[2]Indian Institute of Technology, Roorkee, Uttaranchal, India
[3]Department of Geophysics, Kurukshetra University, Kurukshetra, Haryana, India
**sainiparveen.saini@gmail.com*

The Central Honshu Region is one of the seismically active regions of Japan. Frequent seismic activities in this region demonstrate the seismotectonic nature of the region. Present study aims to investigate the attenuation properties of shear wave in the region lying between 35.4° N to 36.4° N latitude and 137.2° E to 138.2° E longitude, by using strong motion data of KiK-net network installed in this area. Attenuation properties of the media govern the amplitude of seismic waves at various distances from an earthquake source. Attenuation can be quantitatively defined by the quality factor (Q). In this work, waveform data from 13 local events recorded at various stations between December 2002 and June 2006 have been used. Records from the borehole sensors installed at different stations have been used in the present work. Thus records are free from site amplifications. This waveform data have been used to obtain the frequency-dependent shear-wave quality factor ($Q_\beta(f)$). This work presents the results of inversion algorithm to find S-wave quality factor for a system of equations using the approach given by Joshi (2006). Both the horizontal components have been used to calculate seismic moment from the source displacement spectra of S wave. The spectra of S phase in the acceleration record along with the average value of seismic moment computed from two horizontal components has been used as an input to the present inversion algorithm. Several values of the corner frequency have been selected iteratively and are used as input to the inversion algorithm. In each iteration, root mean square error is calculated between the obtained and observed data and final $Q_\beta(f)$ is determined corresponding to minimum root mean square error.

In the present work $Q_\beta(f)$ is obtained at different stations. The $Q_\beta(f)$ at each station is determined by using both the North South (NS) and East West (EW) components of acceleration records. The $Q_\beta(f)$ values obtained at each station from both NS and EW component have been used to determine a regional $Q_\beta(f)$ relationship for the central Honshu region, Japan of form $Q = Q_o f^n$ i.e. $Q_\beta(f) = (98 \pm 1.1) f^{(1.0 \pm 0.05)}$. The relation $Q = Q_o f^n$ in general provides Q_o, which represents heterogeneities, and n, represents level of tectonic activity of the region. The Q(f) relation suggests low Q_0 (<200) and high n (>0.8) values, which are characteristics of tectonically and seismically active regions (Kumar et al., 2004). In the present work, the obtained regional $Q_\beta(f)$ relation shows low value of 'Q_o' and high value of 'n' which revealed that the region is seismically active and characterized by local heterogeneities. Comparison of the present relation with other worldwide relations of active region also revealed that it falls within the range of values that are typically found in the tectonically active regions.

The main features in this area are the Median Tectonic Line (MTL) and the Itoigawa-Shizuoka Tectonic Line (ISTL). The Median Tectonic Line is an expression of Japan's longest fault system and it connected with the Itoigawa-Shizuoka Tectonic Line in this study area. The ISTL is a major tectonic structure that divides the Honshu into NE and SW parts (Yabe, 1918; Kato, 1992). The $Q_\beta(f)$ relations have been determined at different stations situated on both the sides of ISTL. The stations lies on the eastern side of the ISTL have high $Q_\beta(f)$ values as compare to the stations which lies on the western side of the ISTL. The higher $Q_\beta(f)$ values are due to thicken pile of sediments in the depression area towards the eastern side of ISTL. The distribution of quality factor values at different stations determined in the present work have been compared with the available probabilistic seismic hazard map of the region and it shows some remarkable similarity with seismic hazard map.

FISSION TRACK ANALYSIS: A TOOL TO RECONSTRUCT THERMAL HISTORY AND EVALUATION OF OIL GENERATION POTENTIAL OF SEDIMENTARY BASINS

Khushboo, Pooja Saini, Akhil Kumar, Mohit Kumar Puniya, RC Patel and Nand Lal
National Facility on Low-temperature Thermochronology, Department of Geophysics, Kurukshetra University, Kurukshetra
khusboo.geologist@gmail.com

The generation of oil in sedimentary basin is largely a function of the extent to which suitable source sedimentary rocks have been heated in 60° to 130°C temperature window. It is thus widely understood that the most important factor in the maturation of these oil source rocks is the temperature history. It is important to know, not only the maximum palaeo-temperature that a rock has experienced, but also how temperature has varied through time.

Fission Track (FT) analysis is an unique technique to the interpretation and quantification of palaeo-temperature with time of sedimentary basins. In sections that have been hotter in the geological past, FT analysis provides estimates of maximum palaeo-temperatures. It is useful for studying the thermal history of sequences containing source rocks and it can provide information critical to the understanding of the timing of oil generation.

The FT analysis technique depends on observation on annealing of fission tracks in apatite. The annealing of fission tracks is temperature and time dependent, as the generation and maturation of oil is a function of temperature and time. The temperature interval over which track annealing occurs in the apatite (a common detrital mineral in sedimentary rocks) is 60° to 120° C. The same temperature range is required for the maximum generation of oil. Fission Track in apatite separated from the sedimentary rocks, thus contain a record of its heating in the oil generation window. The pattern of apatite FT ages, together with detailed analysis of the distribution of track-lengths, provides information on thermal history which cannot be obtained by any other technique. This unique advantage of FT analysis technique is that it can provide information not only about maximum palaeo-temperature, but also about their variation through time.

Fission Tracks in detrital zircon are stable at higher temperature (200° to 300°C) than in apatite. Fission tracks in zircon enables to understand the limits of maximum temperatures the sedimentary basins reached as well as gives the important information on sedimentary provenance.

BASEMENT STRUCTURE OF THE CENTRAL GANGA BASIN BY MAGNETOTELLURICS

L. AdiLakshmi*, A. Manglik, M. Suresh, and S. Thiagarajan
CSIR- National Geophysical Research Institute, Hyderabad-7
lakshmigeo2008@gmail.com

We present the results of a broadband magnetotelluric (MT) study carried out to delineate the basement structure of the central Ganga basin along a 285 km long profile between Hamirpur and Rupadia (Nepal border). The subsurface electrical resistivity image obtained by combining the results of 1-D Occam inversion for 39 sites reveals a significant contrast in the geoelectric structure from south to north along the profile indicating that the crustal structure of the Indian plate beneath the sedimentary cover is heterogeneous. At the southern end, the Bundelkhand massif is delineated as a high resistivity block buried beneath 250-300 m thick sediments. The basement depth gradually increases to about 500-600 m at Kanpur and to about 1.2 km at Lucknow. Here, the basement

depth increases to more than 2.5 km within a profile distance of 20 km. The sudden deepening of the basement could be attributed to the Lucknow fault. The underlying rocks also have moderate resistivity and possibly represent the Vindhyans. The deepening of the basement continues northward. The sedimentary sequence at the northern end of the profile is more than 9 km thick indicating a very deep basement. Integrating the resistivity image with the seismic velocity structure in the area and the lithological information from the 3927 m deep Matera-I well reveals that thetop 4 km section in this areais constituted of Oligocene and younger rocks, and Neogene and recent sediments whereas the underlying >5 km thick section is composed of sedimentary rocks of the Bahraich Group overlying the Achaean basement. We also infer the presence of a graben-type structure coinciding with the Bahraich depression delineated by seismic exploration studies based on the extension of the low resistivity zone below the seismically derived basement around Bahraich. In this region, the sedimentary rocks of the Matera formation, and the Lower and the Middle Siwaliks up to 4 km depth are highly conductive and also have low seismic velocity, as derived by a receiver function analysis at Bisalpur, implying that these are not well consolidated and thus can have high seismic hazard potential. The present results have implications for hydrocarbon exploration, hazard potential scenario of the central Ganga basin, and flexural strength of the Indian plate.

DENSE MINERAL ASSEMBLAGE OF THE LOWER SIWALIK NAHAN FORMATION IN THE TYPE AREA NAHAN IN NORTHWESTERN HIMALAYA AND ITS SIGNIFICANCE IN DECIPHERING THE PROVENANCE OF THE SEDIMENTS

A.R. Chaudhri, Rajesh Ranga, Vikram Sharma and Sarita Mann
Department of Geology, Kurukshetra University, Kurukshetra 136119 (Haryana)
rajeshranga333@gmail.com

The Siwalik sediments extend from Jammu and Kashmir to Assam for more than 2300 km. The dense mineral assemblage of the Lower Siwalik Nahan Formation of the type area Nahan has been analyzed to decipher the provenance of these sediments in the type area. The non-opaque dense mineral assemblage identified in the Lower Siwalik, Nahan Formation of the type area and adjoining regions in the northwestern Himalaya include zircon, tourmaline, rutile, garnet, epidote, chlorite/ chloritoid, biotite and staurolite. Garnet is the most abundant dense mineral. The opaque minerals form a greater proportion of the mineral assemblage and are represented by ilmenite, magnetite, haematite and limonite. The dense mineral assemblage is suggestive of the derivation of a major part of the detritus from the crystalline, metamorphic and sedimentary rocks exposed in the North of the Siwalik foredeep.

ESTIMATION OF SOURCE PARAMETERS AND SITE AMPLIFICATION FUNCTIONS FROM ANALYSIS OF ACCELEROGRAMS OF 2011 SIKKIM EARTHQUAKE, HIMALAYA

Kusham Sandhu and Dinesh Kumar
Department of Geophysics, Kurukshetra University Kurukshetra – 136119 India
kusumsandhu33@gmail.com

The locally recorded earthquake strong ground motions carry rich information about the source parameters, which may be used for testing source models and therefore for the evaluation of seismic hazard of a region. The estimated source parameters are also useful for developing the regional scaling relations.

The recorded accelerograms of September 18, 2011 Sikkim earthquake (M_W = 6.9) have been used in the present study to estimate the source parameters and site amplification functions. The horizontal components of accelerograms are rotated with respect to the hypocenter to obtain transverse component accelerograms. These are assumed to be approximately representing SH waves. The advantage of using SH waves for the analysis is that these waves are minimally affected by the crustal heterogeneities. The displacement spectra were obtained from the SH acceleration waveform by integration. The spectra of high energy packets observed in the SH waves is modeled using Brune'smodel.A two step grid search procedure for the estimation of long period spectral level and Q has been used while keeping the corner frequency fixed obtained independently. The H/V spectral ratio has been used to estimate the site amplification functions for the recording stations.

The earthquake source parameters obtained in this study are- corner frequency(fc) : 0.09 Hz, seismic moment (M0): 2.31×10^{26} dyne-cm, stress drop ($\Delta\sigma$) : 53 bars, and moment magnitude (Mw): 6.86.The values obtained are found to be consistent with those of reported in other studies. This agreement shows the validity of the procedure used in the analysis. The frequency bands of significant site amplification have been identified and are useful for the simulation of earthquake strong ground motions in the region.

MAPPING FOR ARTIFICIAL RECHARGE SITES IN SOME PARTS OF ADILABAD DISTRICT, TELANGANA STATE, INDIA BY ELECTRICAL RESISTIVITY METHOD

D.Vidyasagarachary, *B. Anjaiah and Lohit Kumar

Department of Geophysics, Osmania University, Hyderabad, Telangana State, INDIA

**anjigeophysics2011@gmail.com*

With the increased demand on water resources, the availability of ground water became scanty in arid and semi arid regions. The agricultural activities are purely based on the availability of surface and ground water resources. To augment the demand for ground water, the application of artificial recharge method offers great scope at the time ofshortage of water. The selection of recharge method depends on the geology of area, geomorphology, soil conditions and weathering profile and thickness. The lithology in the area is Basaltic rocks of Deccan Plateau. Successive basaltic lava flows resulted in a layered crystalline rocks with intervening beds of clay , ash etc. The inter-trappean beds form good aquifers in addition to the top weathered and fractured zones.

For this study, an attempt has been made to delineate various lithological conditions by applying electrical resistivity method (VES) in the study area. There are about 50 electrical resistivity soundings conducted, and most of the VES curves were interpreted as A, H, and HA type. Through the electrical resistivity data obtained were interpreted and a lithological map andiso-resistivity map is prepared. The iso-resistivity map became a model in locating recharge zones.The electricalresistivity is found to be more suitable in locating possible sites for artificial recharge.

MEASUREMENT OF AMBIENT SEISMIC NOISE AT SEISMIC OBSERVATORY, KURUKSHETRA UNIVERSITY CAMPUS

***Deepak Kumar, Sourabh, Sushil Kumar and Sunil Kumar**
Kurukshetra University, Kurukshetra
**jangradeepak80@gmail.com*

Ambient seismic noise level at any recording stations plays a vital role in the quality of seismic data recorded by a seismological station. The seismological observatory in Kurukshetra University campus is in operation for the past 4 years and recorded many local, regional and teleseismic events. The observatory is equipped with high dynamic range seismic digitizer (Quanterra Q330S) connected to tri-axial broadband seismometer (Model No. STS-2) with flat 3dB frequency response to ground velocity from 120 sec to 50Hz. The recorded ambient noise spectrum of the station has been compared to the 'minimum' and 'maximum' standard models of the United States Geological Survey (USGS) (Figure 1) for various seasons over a 24hrs period and compared with noise-level at one of the standard seismological observatory of IMD located at Ridge, Delhi. It has noted that a little diurnal variation in the noise-level has been noted at the site. There is more background noise variability in the long period band (periods larger than 10 sec) compared to short-period band, but mostly in the horizontal components. The signal-to-noise ratio of the events for various magnitude ranges occurred within 100km radius of the observatory have been compared. Further, seismic ambient noise acts as an excitation function for the specific resonances of both buildings and subsoil. If the soil resonance frequency is the same as that of a building on that soil, a coupled resonance will be induced. The recorded seismic noise data has been analyzed to estimate the soil resonance frequency to identify such seismic amplification of the buildings close to the observatory.

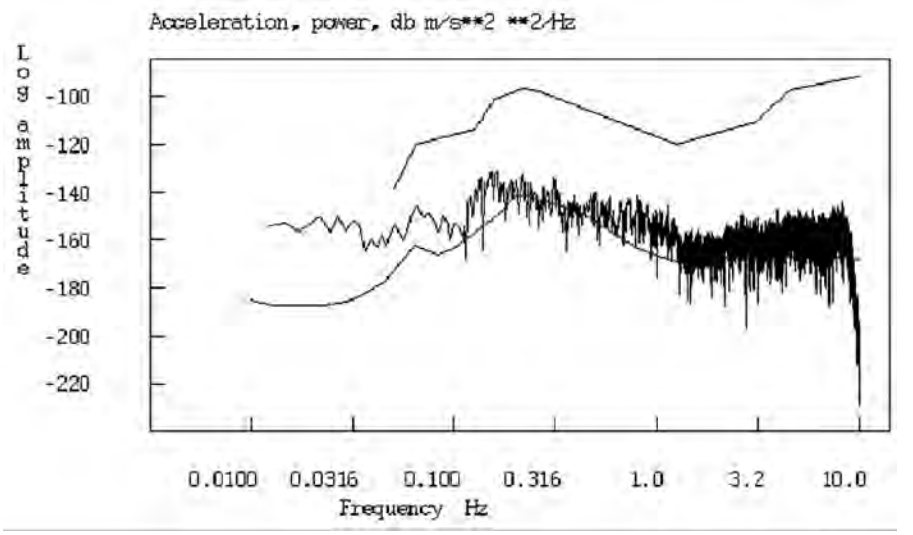

EVALUATION OF THE SITE AMPLIFICATION FUNCTIONS IN DELHI- NCR REGION

Kartik Sharma*, Shruti Malik, Neha Panwar
Department of Geophysics, Kurukshetra University, Kurukshetra, India
connectkartik2007@gmail.com, shrutimalik1603@gmail.com

The National Capital Region (Delhi)is encompassed by the various intra-plate faults that have been responsible for the number of earthquakes in the region. Also, the presence of Himalayan ranges in the near vicinity of the region makes it more vulnerable to the seismic hazards.Being the economic

hub of the country, there has been tremendous development in the region (especially in the estate sector) in the past decade and increasing population density drags the attention of the Administrators as well as the Geoscientists in order to evaluate the seismic hazard of the region. The ground motion recorded at any site has three factors namely- source effect, path effect and the site effect.The site amplification plays an important role in the modifying the upcoming motion at the surface. Thus,site effect accounts for the effect of the surficial layer to the upcoming waves or how it is going to affect the energy approaching towards the surface.

In the present study we have estimated the site amplification at two sites of different geology (i.e one site is at the hard rock and other one is at the soil site) using the Horizontal to vertical Spectral ratio (HVSR) method. The average of the FFT of the NS and EW component has taken to obtain the FFT of the average horizontal component which is then divided by the FFT of the vertical component in order to get the site amplification function. For this purpose we have used multiple events recorded at these sites and then average the estimated value. The results obtained here are useful in the simulation of the ground motion at the sites of the interest where past records are not available and hence are useful to the evaluatethe seismic hazard of the region.

EFFECT OF CLIMATE CHANGE ON SUBSURFACE THERMAL STRUCTURE

M. Ravi*, D. V. Ramana and R. N. Singh
CSIR-National Geophysical Research Institute, Hyderabad, India
**ravi.cgp@gmail.com*

Changing climate has the impact on the subsurface thermal structure. The varying temperature of the air over the surface will affect the subsurface soil temperature. Groundwater flow is another important process, which perturbs the thermal distributioninto the subsurface. To investigate the effect ofclimate change (both the air temperatures and the surface soil temperatures)on the subsurface, one dimensional transient heat conduction-advection equationis solved by using finite element method.A Robin type boundary condition, which relates surface heat flux in terms of both air temperature and surface soil temperature with heat transfer coefficient,is applied on the surface. The initial condition of superimposed linear and exponential function is applied on the subsurface. The numerical solutions are computed for various values of heat transfer coefficient (H) and groundwater recharge or discharge velocities (v) with respect to time. These results reveal that the temperatures are sensitive to frequency and attenuation of the periodic boundary condition. These results would be further useful in understanding the future environmental conditions.

ANALYSIS OF EARTHQUAKE DATA OF NORTH-WEST HIMALAYA FOR THE DETERMINATION OF HYPOCENTRAL PARAMETERS AND FAULT PLANE SOLUTIONS

Prarabdh Tiwari*, Pankaj , Harish
Kurukshetra University, Kurukshetra
pttiwari75@gmail.com

As the Himalayan mountain chain, developed through convergence of Indian and Eurasian plate is seismotectonically active belt of the world. Longitudinally the Himalayan is divided into five main tectonic zones, from south to north, sub-Himalaya, Lesser Himalaya, Higher Himalaya, Tethys Himalaya and the Indus Suture. The main principal thrusts that divided these zones are Himalayan Frontal Thrust (HFT), Main Boundary Thrust (MBT), Main Central Thrust (MCT) and Indus Suture

Thrust (IST) respectively. Several devastating earthquakes of magnitude 8 and above occurred during the last decades. The peninsular India has relatively less seismicity. In this present study, analysis of broadband digital waveform data of local earthquakes recorded by the seismological network in NW Himalaya has been analyzed to study the earthquakes source mechanisms adopting P-wave first motion method. About 30 local earthquakes, recorded during 2007-2012, have been selected for this analysis based on high signal to noise ratio and good azimuthal coverage. Only those earthquakes are selected which are recorded by at least 10 seismological stations. The magnitude of selected earthquakes for this analysis varies within the range 1.0-3.9. The digitizer and recording equipment's are synchronized with GPS timing system. Ultimately Fault plane solution of some earthquake has been prepared using Seisan & GMT Software. So this present study says about the type of focal mechanism present at the NW Himalaya mainly near to the MCT. Mostly Oblique strike slip fault has been found here. Hypocentral parameters are thus calculated and they clearly tells about the sense of shear/stress behind that fault. So this study can be helpful for:

Monitoring of local earthquake such that it can be act as precursor for future earthquake.

For making pre-plan strategy for local earthquake risk management (for Himanchal Pradesh region).

Basically we can know the type of fault present there using fault plane solution so can be act as source of literature of that area.

Hence this study can revels all the facts about the recent earthquake held at NW Himalaya which is very seismically active nowadays and for future also.

INTERPRETATION OF SPHERICAL GRAVITY ANOMALY USING A NON-LINEAR (GAUSS-NEWTON) TECHNIQUE

PrernaGaba*, Charu Kamra and Neha Chaudhary

M. Tech. (Applied Geophysics), Department of Geophysics, Kurukshetra University, Kurukshetra 136119, Haryana, India

**prernagaba02@gmail.com, Charukamra007@gmail.com, nehachaudhary202@gmail.com*

The gravity method of exploration detects variations in density of subsurface materials by measuring gravity at the surface. The interpretation techniques of Bouguergravity anomalies include (i) direct interpretation and (ii) indirect interpretation. The indirect interpretationinclude trial and error method to find the approximate shape and depth of the structures that produce Bouguer gravity anomalies. This method is found to be time consuming and tedious. An inversion procedure can be used instead of making large number of calculations.

This study illustrates the application of a non-linear (Gauss-Newton) inversion technique to interpret the gravity anomaly due to a spherical ore body. In this approach the non-linear problem is linearised about some initial model. For the spherical ore body, the initial model parameters namely depth (Z), dimension (R) and density (ρ) can be estimated using depth rules of gravity interpretation. The values of initial model parameters can be refined further using the Gauss-Newton procedure.

The Gauss-Newton procedure has been applied to the synthetic as well as field data. The published field data has been used for this purpose.

STRONG MOTION GENERATION AREAS MODELING OF THE 2011 TOHOKU EARTHQUAKE USING MODIFIED SEMI-EMPIRICAL TECHNIQUE

Sandeep1*, A. Joshi[1], Kamal1, Parveen Kumar[2] and Ashvini Kumar[1]
1 Department of Earth Sciences, Indian Institute of Technology Roorkee, Roorkee-247667, India
2 Graphic Era University, Dehradun
sandeeparora95@gmail.com

In this work semi-empirical technique of simulation of strong ground motion has been modified to incorporate the effect of strong motion generation areas (SMGAs) in the modeled rupture plane. Strong motion generation areas identified within the rupture plane of the Tohoku earthquake of 11th March, 2011 (Mw=9.0) have been modeled using this modified technique. Two different source models having four and five SMGAs respectively are considered for modeling purpose. Strong motion records using modified semi empirical technique have been simulated at two near field stations located at epicentral distance of 137 km and 140 km respectively using two different source models. Comparison of the observed and simulated acceleration waveforms is made in terms of root mean square error (RMSE) at both stations. Minimum root mean square error of the waveform comparison has been obtained at both the stations for source model having five SMGAs. Various strong motion parameters extracted from observed and simulated records have been also quantitatively to confirm the validation of simulation technique. compared Comparison of waveforms and parameters extracted from observed and simulated strong motion records confirm the efficacy of the developed modified technique to model earthquake characterized by SMGAs.

LATERAL VARIATIONS IN THE MOHO CHARACTER BENEATH THE EASTERN HIMALAYA

Dipankar Saikia*, M. Ravi Kumar and D. Sarkar
CSIR - National Geophysical Research Institute, Hyderabad 500007
**Presently with INCOIS (Ministry of Earth Sciences), Hyderabad*

This study focuses on delineating the lateral variations in the crustal fabric of the Nepal, Sikkim and Bhutan Himalaya regions using P- to-s and S-to-p converted phases isolated from waveforms of 2622 teleseismic earthquakes recorded by 212 broadband stations operated under the HIMNT, Hi-Climb and SIKKIM experiments. A total of 28187 high quality P receiver functions binned and stacked in narrow latitudinal and longitudinal grids reveal distinct variations in the sharpness and depth to the crust mantle boundary (Moho) both along and across the strike of the Himalaya. Interestingly, the Moho seems to be very weak (almost absent) beneath certain segments particularly the Indo-Gangetic foredeep just ahead of the collision front. Clear evidence for low shear velocities in the middle crust beneath certain segments of the Himalaya is revealed in terms of coherent negative polarities of the conversions. Interpretation of this feature in terms of channel flow remains a conjecture in view of the intermittent nature of these LVL's.

DELINEATION OF INTER-TRAPPEAN BASALTS AND POSSIBLE COAL SEAMS OVER BIRBHUM DISTRICT, WEST BENGAL

Piyush Priyam and S. K. Pal*

Department of Applied Geophysics, Indian School of Mines, Dhanbad – 826 004, India
sanjitism@gmail.com

Geoelectrical and Geoelectromagnetic methods have been used worldwide in volcanic areas for structural information, geothermal evaluation and hydrothermal circulation. Magnetotelluric methods proved its effectiveness in investigation in trap covered areas (Gokarn et al.1992) for the delineation of Traps and inter-trappeans. In the present study our aim is to delineate the basaltic flows, inter- trappean sediments in Rajmahal trap, and possible coal seams in Gondawana formation below the Rajmahal trap. Basalt is essential component for building, road and infrastructure developments. Exploration of coal in Gondawana formation in this region is also an economic importance for the nation. These challenges were handled by state-of-the-art geophysical technique Audio Magnetotelluric (AMT).

The study area comes under the region of Rajmahal volcanism which is part of Peri-continental magmatism. Igneous activity in Gondawana period is confined mainly to the phases of Rajmahal volcanism and intrusive activity associated with it. The Rajmahal volcanics is mainly exposed in a large part of Rajmahal hills. The outcrop cover an area about 4300 km2 and show low easterly dips and disappear below the Bengal alluvial tracts on the east. Birbhum coalfied, Birbhum District with reserve of 3795.45 million tons has already been established in this coalfied. In the south-central part of the coalfield in Pachami area, a thick coal seam zone with maximum recorded thickness of 156 m having 118 m of clean coal has been recorded. Exploratory activities in other areas of the coalfield for providing additional resource are being still continued. In both the areas coal occurs at depth of ~150-300 m below the cover of hard basaltic rocks and other sediments (pib.nic.in. 2002).

In General, the study area is characterized by the intra-trappean sediments underlain by weathered and massive basaltic layer. The Rajmahal volcanics together with inter-trappean beds have maximum exposed thickness of nearly 220 meters and the inter-trappean beds may range from few centimeters to as much as 10 meters or more. Borehole studies confirmed 28 numbers of basaltic lava flows whose individual thicknesses ranges from <1 m to a maximum of ~70 m and also presence of inter-trappeans of thickness from few cm to ~17 m (Mukhopadhyay et al. 1986).The inter-trappean are often tuffaceous and contain beds and pocket of bentonite, especially in the northern parts of Rajmahal hills. Pyroclastic deposits comprising tuffs, agglomerates, scoria, pumice, volcanic breccia and ash flows, some of them with plant remains, are reported to range in thickness from a few cm to 17m (Sengupta, 1988; Ghose et al. 1996).

AMT is a passive electromagnetic imaging technique using the earth's magnetic field to map geologic contacts and structure typically to depths of 500 meters or more. With the lower MT frequencies, subsurface imaging can be extended deeper. The ability to identify geologic features varies with depth and depends upon target size, resistivity contrasts and contact geometry. The electrical conductivity is much more sensitive to geochemical changes than other bulk physical properties such as acoustics impedance, density and seismic velocity.

In the present AMT data were acquired for 30 minute duration using state-of-the-art MTU5A Phoenix instrument. Using AMT sounding data, on the basis of dimensionality indicators (tipper magnitude <0.1) it is found that the area in showing mainly 1D features and thus we done 1D inversion of AMT data. Presently we have identified three to four basaltic lava flow layers, two to

three inter-trappean sediment layers and one possible coal seam/inter-trappean sediment layer. We are planning further to record a longer duration data to map the deeper basaltic lava flow and possible coal seam/inter-trappean sediment layer.

References:

Ghose, N.C., Singh, S.P., Singh, R.N. amd Mukherjee, D. (1996). Flow stratigraphy of selected section of the Rajmahal basalts, eastern India. Jour. Southeast Asian Earth Sci., v.13(2), pp.83-93.

Gokarn SG, Rao CK, Singh BP and Nayak PN (1992) Magnetotelluric Studies Across The Kurduwadi Gravity Feature. Phys. Earth Planet Int. 72: 58-67

http://pib.nic.in/archieve/lreleng/lyr2002/rapr2002/15042002/r150420025.html.

Mahadevan, T.M. (2002). Geology of Bihar & Jharkhand. Geological Survey of India, Banglore. Pp.459-461.

Sengupta, S. (1988). Upper Gondawana stratigraphy and palaeobotany of Rajmahal Hills, Bihar, India. Palaeontologica Indica, New series, v.XLVIII, p.182.

PALYNOFACIES AND HYDROCARBON SOURCE ROCK POTENTIAL OF NEOGENE SEDIMENTARY FORMATIONS OF NORTH-WEST HIMALAYA, INDIA

***R.Panwar, R.Rani and Sikander**

Department of Geology, Kurukshetra University, Kurukshetra

**rashmipanwar2009@gmail.com*

Palynofacies analysis vis-à-vis maturation potential of dispersed organic matter of Early Neogene sedimentaries of North-West Himalayas has been attempted in the present investigation, for thermal maturation index of sedimentary organic matter is serving as a reliable tool for hydrocarbon prospectivity the worldover. The palynofacies analysis of Kasauli Formation and co-eval sedimentaries of North-West Himalaya reveals variety of dispersed organic matter dominated by grey amorphous organic matter followed by biodegraded organic matter, spore-pollen, black organic matter, fungal remains and structured terrestrial organic matter in the decreasing order of abundence. The thermal maturation index (TAI value) calculated by visual estimation method falls in the range of 2.0-2.5 in the standard TAI scale of Staplin (1969). The dominance of grey amorphous organic matter in the palynofacies preparation of these sediments and TAIin the range of 2.0 to 2.5 indicate marginal to approaching optimum level of thermal maturation for the liquid hydrocarbon potential of these sedimentaries.

HIGH VELOCITY MANTLE ROOT BENEATH DHARWAR CRATON: A NEW TOMOGRAPHIC MODEL

Sudesh Kumar[1], Sandeep Gupta[1] and S.S. Rai[2]

[1]CSIR-National Geophysical Research Institute, Uppal Road, Hyderabad- 500 007

[2] Indian Institute of Science Education and Research, Pune- 411 008

kumarsudesh77@gmail.com

We present a new tomographic model for P wave velocity beneath Dharwar craton to a depth up of 400 km obtained by inverting travel times of teleseismic wave recorded at 63 broadband seismic stations. The craton is divided into the 2.7-3.36 Ga western Dharwar , and eastern Dharwar with the age of 2.5 Ga. Post cratonization, the region was influenced by the Proterozoic Cuddapah basin evolution, Eastern Ghat, kimberlite explosion at 1100 Ma , Indo-Antarctica separation at ~100 Ma and India Madagascar separation at ~90 Ma.

In order to image the craton, we deployed a station network with an average stations spacing 50-100 km covering Dharwar craton and part of southern granulite trerrain. Stations were equipped with broadband CMG-3T/3ESP sensors with RT30 digital recorder and GPS. We used selected teleseisms in the distance range of 28-100 degree with $M_b > 5.5$ and showing coherence pattern. After visual inspection of waveforms with high signal-to-noise ratio 639 earthquakes recorded at minimum five stations are chosen for tomographic modeling.

We finally selected 8235 P wave traces on which theoretical arrival time are calculated by using the 1-D IASP91 Earth model. Residuals are found by subtracting the theoretical times from the observed ones and are affected by error in hypocenter location, origin time and velocity heterogeneity of path. To minimise the effects of these uncertainties/errors outside the model area, we subtracted mean of the residual of each event from the raw residuals. This resulted in relative residuals that are mainly caused by velocity variations beneath the seismic network.

Our 3D tomographic model reveals coherent high P-wave velocity beneath the WDC extending to ~ 160 and 300 km depth beneath the EDC and WDC respectively. We interpret these high velocity mantle anomalies as the lithospheric root beneath the two geological domains that remain largely unaffected from several tectonic reworking.

CONVERSION OF STRONG MOTION RECORDS FROM SOIL SITE TO ROCK SITE OF THE NANTOU, TAIWAN EARTHQUAKE OF 27TH MARCH,2013

***Piu Dhibar[1], A.Joshi[1],Chun-Hsiang Kuo[2],Kuo-Liang Wen[3]and Che-Min Lin[2]**

[1]Department of Earth Sciences, Indian Institute Technology Roorkee, Roorkee, India.
[2]National Center for Research on Earthquake Engineering, Taipei, Taiwan.
[3]Department of Earth Sciences, National Central University, Taoyuan, Taiwan.
**piu.dhibar89@gmail.com*

Strong motion records identified within the rupture plane of the 27th March 2013Nantou, Taiwan earthquake (Mw=5.9) have been convert from soil siteto rock site in this work. It is seen that available records are all at the surface which include site amplification terms. The site amplification terms in all records have been removed using SHAKE91 program and S-wave velocity profile at each site. The observed records corrected for site amplification terms are further used for comparison with records at the rock and soil for several models. Once the observed records at soil sites are transferred at the bedrock, the next task to show the effect of H/V ratio in soil site and rock site. To show the effect of soil or rock in the strong motion records assume two models in this work. One is two-layer model andthe other is four-layer model.The records are compared with the help of both models at rock site as well as soil site. The strong motion recordsare comparedat different stations. With the help of frequency and amplitudedata of horizontal and vertical records at different stations are compared with the help of two-layer model as well as four-layer model which shows how the records are affected when these records are converted from soil site to rock site.

SPATIO-TEMPORAL ANALYSIS OF FLUORIDE CONTAMINATION IN GROUND WATER USING GIS AND GEOSTATISTICS IN PARTS OF NALGONDA DISTRICT, TELANGANA, INDIA

ManindarPandiri*, Das, I. C. and Subramanian, S. K.
National Remote Sensing Centre, ISRO, Balanagar, Hyderabad
**manindar.pandiri@gmail.com*

Severe health problems are faced in several parts of the world due to the high concentration of fluoride in drinking water. This causes dental and skeletal fluorosis to humans. The main characteristics of excess fluoride in the body shows as staining and pitting of the teeth (dental fluorosis) and bone deformities and brittleness (skeletalfluorosis).Nalgonda district in Telangana, India is one such region where high concentration of fluoride is present in groundwater. This district is rich in minerals like limestone, clay, Uranium deposits and building materials like granites/granite gneisses. Fluoride is generally found in excess quantity in the granitic rocks of late Archaean. The main objective of this research was to study the spatio-temporal variation of F^- in North-Eastern parts of Nagonda district affected by excess fluoride and factors that may be influencing this pattern by using GIS integration. In the present study samples from 40 wells were collected during Pre- and Post-monsoon period for 5 years between 2010-2014. Samples were analyzed for quality parameters like fluorine, chlorine, PH, TDS, alkalinity and hardness. It was observed from the study that pre-monsoon (Mar-Jun) samples are having more fluoride than the post-monsoon (Jul-Oct) date samples. The fluoride concentration in groundwater of this region ranged from 0.23 to 7.0 mg/l with a mean of 0.99 mg/l. 20% of the samples possessed high concentration of fluoride, i.e., above 1.5 mg/l which is not suitable for human consumption. Different factors such as lithology, slope, landuse, geomorphology and soil were considered in the GIS analysis for the high concentration of fluoride. Results showed that the weathering of the granitic rocks and evaporation of groundwater are mainly responsible for high fluoride concentration in groundwater in this area.

SIMULATION OF ACCELEROGRAMS OF 2011 SIKKIM EARTHQUAKE USING A SEMI-EMPIRICAL APPROACH

RenuYadav, Dinesh Kumar and S.S. Teotia
Department of Geophysics, Kurukshetra University Kurukshetra 136119 India
renuyadav_geokuk@yahoo.com

The simulated strong ground motions from earthquakes are required for the specific seismic sources and propagation paths and therefore useful for the detailed evaluation of seismic hazard of a region. It also enhances the sparse data base and helps in improving the understanding of the earthquakes. A number of techniques are available for simulating the accelerograms. These techniques have their own limitations and advantages.

The present study is based on the simulation of strong ground motions from 2011 Sikkim earthquake (M 6.9). A semi-empirical approach has been used for this purpose. The first step of the approach is based on the construction of envelope function of larger magnitude earthquake by the superposition of envelope functions of smaller magnitude earthquakes. The accelerogram of the target event is obtained by combining the envelope function with a band limited white noise. The approach required the parameters like fault area, orientation of the fault, hypocenter, size of the subevents, rupture velocity, duration, source-site distance and attenuation parameter. The Q relation developed for Sikkim Himalaya has been taken into account. The value of 0.048 is used to account the decay

of high frequencies (κ). This is the average value determined from 32 earthquakes occurred in NE region. The attenuation regression which determines the peak of envelope function has been identified by comparing a number of available empirical relations with those of observed values.

The synthetic and observed accelerograms have been compared in terms of peak ground acceleration (pga), the waveforms, and their corresponding Fourier and response spectra. The successful modeling of the empirical accelerograms shows that the semi-empirical approach adopted here can be used for the simulation of strong ground motions from future earthquakes in the region.

LIQUEFACTION HAZARD STUDY OF DAHEJ AND KAMBOI PORT AREA, GUJARAT

Vasu Pancholi*, Rahul Ranjan, Suraj Kumar, Vinay Kumar Dwivedi and B.K. Rastogi
Institute of Seismological Research, Raisan, Gandhinagar- 382009
vasu_pancholi@yahoo.com

Over the past decade we have observed increase in seismic activity all over the world.Seismically active regions cause losses of many lives and properties due to earthquake.So it is a prime requirement of evaluating seismic hazard possibilities.One of the major effects caused by earthquake is Liquefaction phenomenon.Liquefaction leads to large failure of structures and devastatingcollapse in the form of sudden settlements, landslides, lateral spreading etc. Evaluation of Liquefactionbegan to evolve after Great Alaskan earthquake (M=9.2) and 1964 Nigata earthquake (M=7.5), which produced significant liquefaction related damages.

Looking at the recent development and industrial growth on the coastal belt of Gujarat there is a requirement of soil liquefaction study to save losses of so many lives and damages of properties from future earthquakes.

This paper shows liquefaction study of Dahej and Kamboi port area, Gujarat by Seed and Idriss simplified procedure. There are two boreholes drilled upto depth of 40m. Soil samples were collected at every 1.5m depth for which we performed lab tests like Grain size Analysis, Atterberg Test, Density, Specific Gravity and Moisture Content are performed for evaluation of Liquefaction potential. Standard Penetration Test is also carried out at the depth interval of 3m in both boreholes. The N value obtained from SPT test is corrected to get $(N_1)_{60}$ for evaluation of Liquefaction. The overburden correction (C_N) was done using the equation suggested by Kayen et al. (1992), which yields a maximum value of 1.7 for C_N. The other corrections for N values were applied based on NCEER (1997). The area at Dahej site comprises of alternate layers of silt and clay with having some patches of sand at lower depth th

e soil is dense silty sand with some percentage of gravels whereas Kamboi area under study comprises of layers of clay, silt and sand alternatively.At both sites, the surface soils are found to be loose and susceptible to Liquefaction hazard. Hence, Liquefaction potential is determined and factor of safety against it is calculated for each depth.

CODA Q ESTIMATES OF BILASPUR REGION OF HIMACHAL LESSER HIMALAYA

Vandana Ghangas[1]*, S.C. Gupta[1], Ashwani Kumar[1]
[1]Department of Earthquake Engineering, Indian Institute of Technology Roorkee, Roorkee-247667, India
vandana.ghangas@gmail.com

In the present work the quality factor (Q) of Coda waves of Bilaspur region of Himachal Lesser Himalaya has been estimated using the single backscattered model proposed by Aki and Chouet (1975). Coda waves of 94 local events located within 100 km of the region having magnitude (0.15<ML<3.03) has been used to study the attenuation of seismic waves in the frequency range of 1.5 to 24 Hz. These events were recorded on digital station in Sikandera (SKND) during the period from May 2008 to April 2011 employing a five station seismological network in the region. The vertical component records were used in the present study. Hypocenter parameters of these events have been estimated with HYPOCENTER computer program. A MATLAB code has been developed for the estimation for Coda Q (Qc). The code follows the guidelines of CODAQ subroutine of SEISAN. The waveforms whose signal to noise ratio (SNR) is greater than 5 are selected for analysis. Only those Coda Q (Qc) values having correlation coefficient 0.7 or more are considered for the region to obtain the reliable values of Qc. By analyzing the Coda waves at different frequencies from 1.5 to 24 Hz the estimated Qc values varies from 155 at 1.5 Hz to 3781 at 24 Hz for lapse time window of 30 sec. This shows that Qc is function of frequency and its value increases as frequency increases. A Q–f relation is obtained for the entire region as Qc=105 f 1.14 . Qc estimated in this way represents the average attenuation properties of the medium covering an area about 21899 sq. km. having lateral extent of 204 km. and vertical extent of 102 km.The observed Qc relation is also compared with those observed in other seismically active regions of the India and found that the estimated Qc value around Bilaspur region of Himachal Himalaya is highly heterogeneous and seismically active as compared to the other seismically active regions of India.

ESTIMATING THE EFFECT OF NON POINT SOURCE POLLUTION ON GROUNDWATER WITH SWAT MODEL – CASE STUDY ON NALGONDA DISTRICT, TELANGANA, INDIA

***PoojaIngole, Das, I. C. and Subramanian, S. K.**
National Remote Sensing Centre, ISRO, Balanagar, Hyderabad
**ingole.pooja119@gmail.com*

Non-point source groundwater pollution (NPS) has become a major problem in recent years due to more human interactions and disturbances to natural landscapes. The present study wascarried out to examine the applicability of Soil and Water Assessment Tool (SWAT)-a hydrologic-water quality model, for assessing the nitrogen (N) and Phosphorous (P) load inground water. The calibrated SWAT model was used to estimate the water soluble NO3-N, NH4-N, P, organic N and organic P loads being transported as pollutants by runoff and percolated water in the study area. The study area is historically prone to fluoride contamination. The swat model consists of5 steps (1) data preparation (2) sub basin discretization (3) HRU definition (4) parameter sensitivity analysis and (5) calibration and validation.During the basic data preparation stage of the study, land use, DEM, soil and slope maps covering the study area were derived and analyzed with the help if geographic information system (GIS). Weather data have been analyzed to calculate the mean monthly values for each weather parameter. SRTM DEM was usedin the SWAT model to start watershed delineation. With the help of land use data, soil data and slope data hydrologic response units(HRU) were created. Finally, after providing all the inputs for model set up, SWAT model was simulated. SWAT was calibrated and validated for daily discharge and sediment concentration using the observed data. The performance of the model

was evaluated using the statistical measures of coefficient of determination (R2) and Nash-Sutcliffe efficiency (ENS). The results of the study indicated that SWAT is capable of estimating the discharge and sediment yield of the study area and can form an important input for assessing the effect of NPS pollution on groundwater.

DELINEATING THE NEAR SUBSURFACE GEOLOGY USING SEISMIC REFRACTION METHOD

***Anirudh Singh, PKS Chauhan, Gayatri Devi, Zamir Ahmad and Abha Mittal**
CSIR-Central Building Research Institute, Roorkee, Uttarakhand, India
**asgeo7@gmail.com*

Seismic refraction has proven a useful geophysical tool for geotechnical investigations. It is widely used in the fields of engineering geology, geotechnical engineering and exploration geophysics. The methods depend on the fact that seismic waves have differing velocities in different types of soil (or rock): in addition, the waves are refracted when they cross the boundary between different types of soil or rock. The methods enable the general soil types and the depth to strata boundaries, or the bedrock. Seismic refraction surveys are performed using an engineering seismograph, geophones and energy source. Present study has been carried out near the stadium of H.N.B. Garhwal University, Srinagar Uttarakhand. 24 – Channel engineering seismograph Teraloc Pro by ABEM, 14 Hz frequency geophones have been used with 12 pound hammer and polymer strike plate as an energy source. Then data is processed using Reflex 2DQuick and Reflex W softwares. In this paper efforts have been made for delineating the near surface geology and number of layers.

In this seismic refraction study, 5 shot-points have been used inline, to obtain high resolution seismic refraction data. In this test site, the subsurface material was mapped on the basis of velocity of materials along survey line. Results indicate that the area was made up of three main layers, with velocity increases fairly with depth. First layer has velocity range of 334 m/s to ~600 m/s, and the depth of this layer is 3-4m in range. The second layer velocity lying in the range of 1000-1100 m/s, this increase in velocity is due to the alteration in the lithology and the compaction, this zone is having the depth up to 16.5m. The last layer encountered was having higher velocity of the order of >1500 m/s.

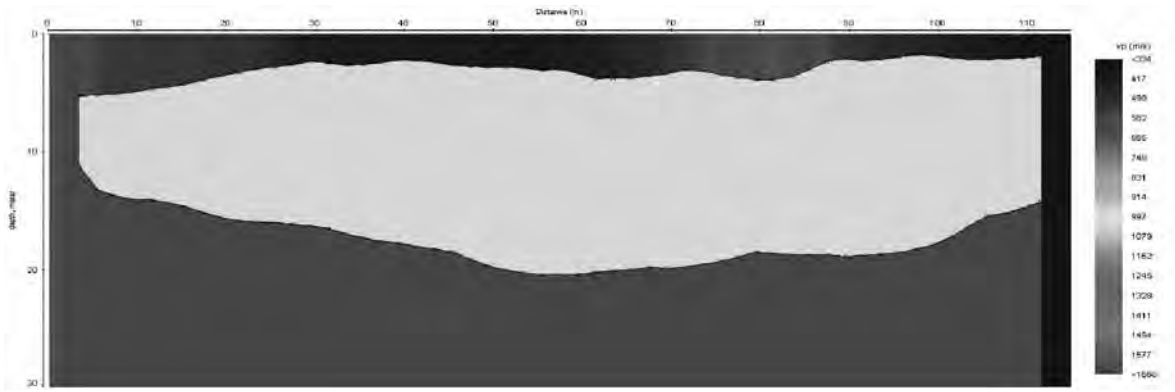

Fig.1 The velocity model of the field site at Srinagar.

TECTONIC GEOMORPHIC SIGNATURES OF ACTIVE DEFORMATION ALONG BAZARI FAULT IN THE FRONTAL SIWALIK HILLS NEAR NAHAN, NORTH WESTERN HIMALAYA

A.R.Chaudhri, Sarita Mann*, Mahavir Ror, Rajesh Ranga, Vikram Sharma and V.K. Verma
Department of Geology, Kurukshetra University, kurukshetra 136119, Haryana
saritasmann01@gmail.com

The Frontal Himalayan terrain is tectonically active due to the continuous northward movement of the Indian Plate. It exhibits deformation of the strata and development of numerous fold/ fault structures which are sympathetically linked to the Himalayan Frontal Thrust (HFT). Satellite imagery of the terrain around Nahan reveals the presence of active deformation. Chaudhri (2008, 2011, and 2012) studied the active deformation in the Frontal Siwalik Hills near Panchkula, Trilokpur and Nahan. In this study a multidisciplinary approach involving IRS LISS MX IV imagery, maps and charts, morphometric analysis, geomorphic analysis along with field investigations are being utilised to identify the active tectonic structural elements in the region.Inthe Kaulawala Bhood region just after the confluence of Majhyar Ki Nadi and Tarapur Ki Nadi the Run Choe exhibits significant stream offset of 455 meters on account of the presence of an active tectonic left lateral strike slip fault with significant oblique slip component. The fault is being named as the Bazari Fault and it shows a surface expression of 9.5 kilometres.Thevalues of more significant tectonic geomorphic indices viz. stream length gradient index, stream sinuosity index, mountain front sinuosity indexand ratio of valley floor width to valley height indexin the affected segment reveal that the terrain is tectonically active.

References:

CHAUDHRI, A. R., 2008. Tectonic geomorphic signatures of active deformation along Gunthala Fault in the Frontal Siwalik Hills near Panchkula, Northwestern Himalaya. Bull. Indian Geol. Assoc., v. 41 (1& 2), pp. 17-23.

CHAUDHRI, A. R., 2011. Assessing Tectonic Character the Terrain in the Frontal Siwalik Hills near Trilokpur, Northwestern Himalaya using Remote Sensing and Tectonic Morphometric Approach. International Journal of Earth Sciences and Engineering, ISSN 0974-5904, Vol. 04, No. 05, pp. 787-795.

CHAUDHRI, A. R., 2012. Tectonic Morphometric Studies as a Tool for Terrain Characterizationin the Himalayan Foothill Region – A Case Study. Journal Geological Society of India, Vol.79, pp.210-218.

ON THE ESTIMATION OF DIMENSIONALITY AND GEOELECTRIC STRIKE DIRECTION FROM MT DATA RECORDED IN GARHWAL HIMALAYAN REGION

Manoj Kumar[1], Israil M.[1], Pravin K. Gupta[1], Sudhanshu Tyagi[1], S. K. Varsheney[2]
[1]Department of Earth Sciences, Indian Institute of Technology Roorkee,
manojkumarnain1993@gmail.com, mohammad.israil@gmail.com,
[2]Department of Science and Technology, New Delhi, India;
skvdst@nic.in

Dimensionality and Geoelectric strike direction have been estimated from magnetotellurics data recorded along Roorkee-Gangotri profile in Uttarakhand, Himalaya, India; using WAL invariants. We calculated WAL invariants for each site and based on the average error in the data threshold for each invariant has been defined. Based on the WAL dimensionality criteria and threshold values of each invariant, dimensionality variation with frequency at each site has been estimated. Dimensionality characteristics of WAL invariants are: the non-zero values of first two invariants (I_1, I_2) and zero values of next four invariants (I_3, I_4, I_5, I_6) indicates the 1D geoelectric structure. If the two invariants (I_3, I_4) are also non-zero, the data represents 2D structure with a strike direction that can be recovered from MT response. The last three invariants (I_5, I_6, I_7) indicates different degrees of three-dimensionality. The analysis demonstrates that southern zone of the profile is represented by 1D geoelectric structure at high frequency. Geologically this zone represents sediments of Indo-Gangetic plain. Deeper part

of the info-Gangetic plain and most of the northern region along the profile is represented by 2D geoelectric structure. A few sites in the low frequency region also indicate 3D structure in Higher Himalayan region. The results demonstrate the spatial and frequency variation of dimensionality of geoelectric structure and geoelectric strike direction along the profile.

CRUSTAL THICKNESS MODELING BASED ON AN ISOSTATIC MODEL AND NON-ISOSTATIC GRAVITY CORRECTION OFSINGHBHUM CRATON

***Archana Jarial[1], M. Bagherbandi[2,3], N. Kumar[1] and A.P. Singh[1]**

[1]CSIR-National Geophysical Research Institute, Uppal Road, Hyderabad-500007, INDIA

[2]Royal Institute of Technology (KTH), SE-10044, Stockholm, SWEDEN

[3] Department of Industrial Development, IT and Land Management, University of Gävle, SE-80176 Gävle, Sweden.

**jarial.archana723@gmail.com*

The orogenic mountains are accompanied by thickening of the crust and buoyancy of these deep crustal roots supports their topography (Airy, 1855).Heiskanen made Airy's theory moreprecise and computed the necessary tables for isostatic reduction, and called Airy-Heiskanen's isostatic model, assuming the topographic mass compensation to be strictly local. The VeningMeineszmodified the Airy-Heiskanenhypothesis by introducing the regional instead of local compensation (VeningMeinesz, 1931). Moritz utilized the VeningMeinesz inverse problem in solving the isostatic gravimetric model for finding the mohodepths (Moritz, 1990) introducing global instead of regional compensation. The VeningMeinesz-Moritz problem (Sjöberg, 2009) is to determine the Moho depth such that the compensating attraction totally compensates the Bouguer gravity anomaly on the Earth's surface, implying that the isostatic anomaly vanishes on the earth's surface. Using VeningMeinesz-Moritz gravimetric-isostaticmodel, we modeled the boundary between crust and upper mantle of the Singhbhumcraton.The EGM2008 global gravity model (Pavlis et al., 2008) and the DTM2006 global topography/bathymetric model (Pavlis et al., 2007) are used to generate the isostatic gravity anomalies. To determine the Moho undulation and the crustal structure, the gravitational contributions of topography, bathymetry and sediments were computed and evaluated their density effects on Moho geometry (Bagherbandi et al.,2013).Further the residuals between the isostatic and seismic Moho depths are then modeled and corrected by applying the gravitational effect of different crust layers' density variation andthenon-isostatic correction(i.e., related to the crust mantle density contrast variation) to the Moho geometry.The results of gravimetric inversion are finally compared with the global crustal seismic model CRUST1.0 (http://igppweb.ucsd.edu/~gabi/crust1.html). The comparison of results shows the better crustal depth after applying non-isostatic correction than before.

References:

BagherbandiM,Tenzer R, Sjoberg, L.E, Novak P., 2013.Improved global crustal thicknessmodelling based on the VMM isostatic model and non-isostatic gravity correction. Journal of Geodynamics 66, 25-37.

Airy, G.B., 1855. On the computations of the effect of the attraction of the mountain masses as disturbing the apparent astronomical latitude of stations in geodetic surveys. Transactions of the Royal Society of London Series B 145.

Moritz, H., 1990.The Figure of the Earth.Wichmann H, Karlsruhe.

VeningMeinesz, F.A., 1931. Une nouvelle methode pour la reduction isostatiqueregionaledeI'intensite de la pesanteur. Bulletin Geodesique 29, 33-51.

Sjöberg, L.E., 2009. Solving VeningMeinesz-Moritz inverse problem in isostasy. Geophysical JournalInternational 179(3), 1527-1536.

Pavlis, N., Factor, J.K., Holmes, S.A. and Simon, A., 2007. Terrain-Related Gravimetric Quantities Computed for the Next EGM. Presented at the 1st International symposium of the International Gravity Service 2006,

August 28- September 1, Istanbul, Turkey.
Pavlis, N., Holmes, S.A., Kenyon, S.C. and Factor, J.K., 2008. An Earth Gravitational model to degree 2160: EGM08. Presented at the General Assembly of the European Geosciences Union2008, April 13-18, Vienna, Austria.

CHARACTERIZATION OF SHALLOW STRUCTURE BY MASW TECHNIQUE USING MULTIMODE SURFACE WAVE DISPERSION

Sunny Kr Ranjan and S. K. Pal*
Department of Applied Geophysics, Indian School of Mines, Dhanbad – 826 004, India
**sanjitism@gmail.com*

High resolution velocity spectrum showing frequency versus phase-velocity (f-v) plot has been generated for a typical 24-channel seismic trace recorded by 4.5 Hz vertical component geophones with 2m geophone spacing, 1ms sampling interval and 1 second record length. The generated velocity spectrum has been utilised to enhance fundamental mode (1st) and different higher modes (2nd, 3rd and 4th mode). Initially a velocity profile has been generated considering only the fundamental mode. Further another velocity profile has been generated considering the fundamental mode and all possible higher modes. The velocity profile generated by considering the entire modes has improved the accuracy and resolution of the inverted S-wave section.

Introduction:

Surface wave dispersion is very important for geotechnical problems and seismic hazards studies. Surface wave techniques are generally used for seismic site characterization because they are both economically and time convenient when compared to borehole seismic methods. Generally we use surface wave mainly because of six fold reasons: i) surface wave amplitude attenuates according to $\sqrt{R}$ and not directly to R, ii) it is a high amplitude wave and contains around 67% of total energy, iii) surface wave dispersion does not suffer from LVL(Low velocity layer) problem, iv) it is not affected by blind zone (hidden layer) problem, v)it is easy to generate, and the final result is the vertical shear-wave profile which is highly valuable for subsurface geological interpretation, vi) it is of dispersive nature and helps in delineation of vertical subsurface heterogeneity.

It is normally assumed in these applications that the fundamental mode of Rayleigh waves dominates the recorded wave field and higher modes can be ignored (Park et al., 1998, Xia et al., 1999 and Zhang et al., 2003a). However, in recent years utilization of multimode surface waves has been getting more and more attention and researches have shown that higher modes of Rayleigh waves can be exploited to improve the accuracy and resolution of the inverted S-wave velocity profile (e.g.,Gabriels et al., 1987, Beaty et al., 2002, Beaty and Schmitt, 2003 and Xia et al., 2003). Other researches on surface wave techniques further demonstrate that higher modes possess significant amounts of energy at higher frequencies and contribution of higher modes tends to become more significant in the presence of a low-velocity layer (such as a roadbed structure or pavement) (Tokimatsu et al., 1992, Foti et al., 2002, Forbriger, 2003a, Forbriger, 2003b and O'Neill et al., 2003; and Ryden et al., 2004). When surface wave propagates it contain the entire mode. Manually we cannot separate the higher modes from the fundamental mode. Conventionally, only fundamental mode is considered which lead to severe error when dispersion curve is generated. As comparisons to direct borehole measurements are normally good, but erroneous results arise for detection of some complex structures with velocity reversals. A couple of reasons are likely responsible for discrepancies. The first is that misidentification of normal modes (Zhang and Chan, 2003b and O'Neill and Matsuoka, 2005), which

leads to wrong results. The second reason is that insufficient resolution of the fundamental mode data results in the fact that the fundamental mode is insensitive to fine changes in S-wave velocities (Xia et al., 2003), which will lead to the ambiguity of uniqueness of the deduced model. The third reason is that the limited resolution of the wavefield transformation in a lower frequency range (McMechan and Yedlin, 1981 and Forbriger,2003a) and contamination of the fundamental mode by significant amount of higher modes in a higher frequency range (Xia et al., 2003) lead to a larger reading error for the fundamental mode over the corresponding frequency range.

Results and discussion:

A typical 24-channel seismic trace using 4.5 Hz vertical component geophones with 2m geophone spacing, 1ms sampling interval and 1 second record length is shown in Fig1. High resolution velocity spectrum showing frequency versus phase velocity (f-v) is shown in Fig. 2. Fundamental mode (1st) and different higher modes are enhanced (2nd, 3rd and 4th mode). Velocity spectrum and dispersion curve considering only the fundamental mode is shown in Fig.3 (a) and corresponding misfit value plot for fundamental mode with respect to generation is 3(b). Velocity spectrum and dispersion curve considering the fundamental mode and all possible higher modes is shown Fig.4 (a) and corresponding misfit value plot with respect to generation is shown in Fig4(b). A velocity profile has been generated considering only the fundamental mode as shown in Fig.5 (a). Further, another velocity profile has been generated considering the entire possible modes as shown in Fig.5(b).

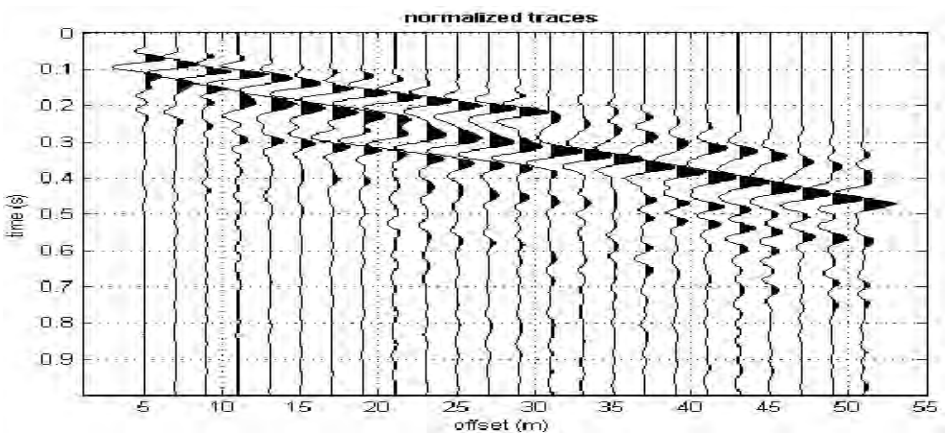

Fig.1 A typical 24-channel seismic trace using 4.5 Hz vertical component geophones with 2m geophone spacing, 1ms sampling interval and 1 second record length.

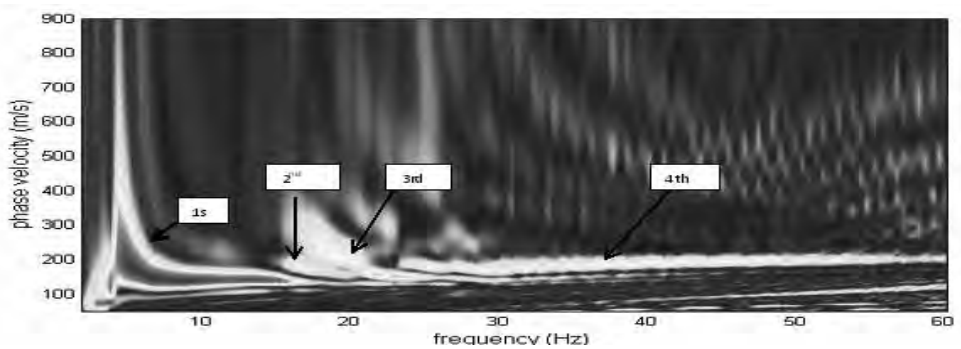

Fig. 2 High resolution velocity spectrum showing frequency versus phase velocity (f-v). Fundamental mode(1st,) and different higher modes are enhanced (2nd, 3rd and 4th mode).

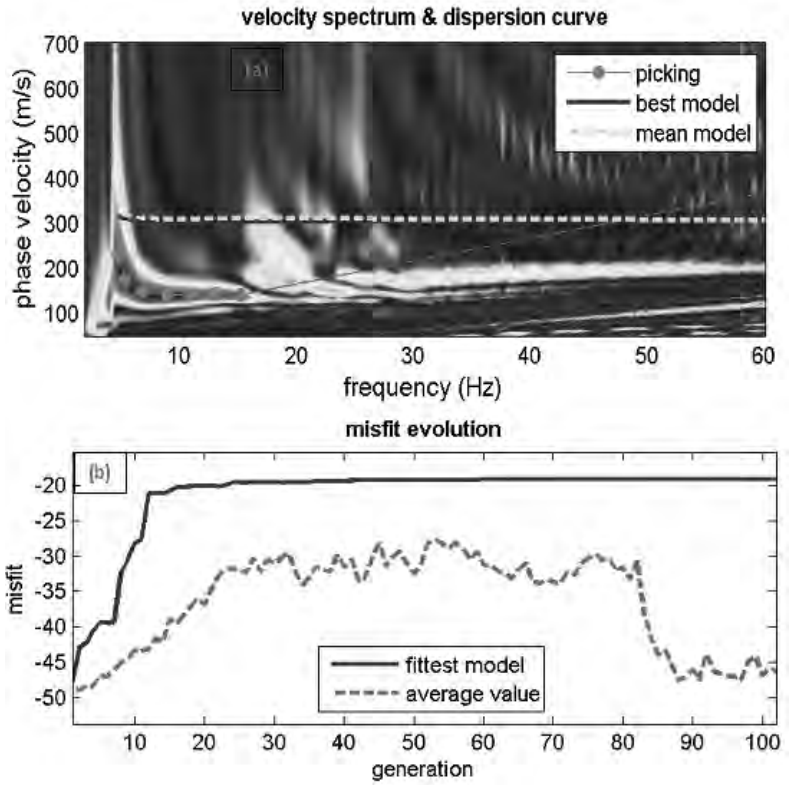

Fig.3 (a)Velocity spectrum and dispersion curve by considering only the fundamental mode. (b) Misfit value plot for fundamental mode with respect to generation.

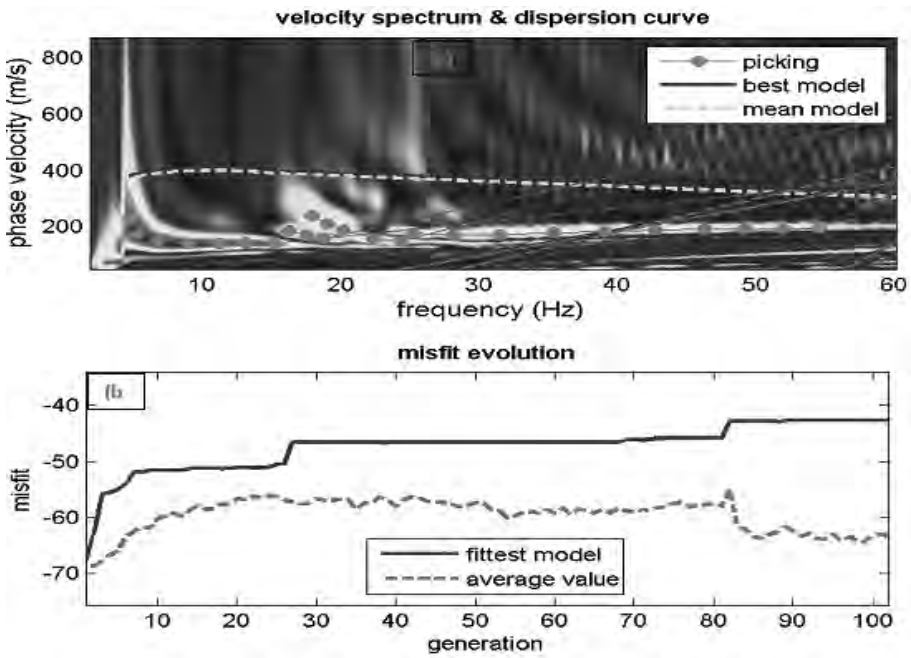

Fig.4 (a)Velocity spectrum and dispersion curve by considering the fundamental mode and all possible higher modes. (b) Misfit value plot for the fundamental mode and all possible higher modes with respect to generation.

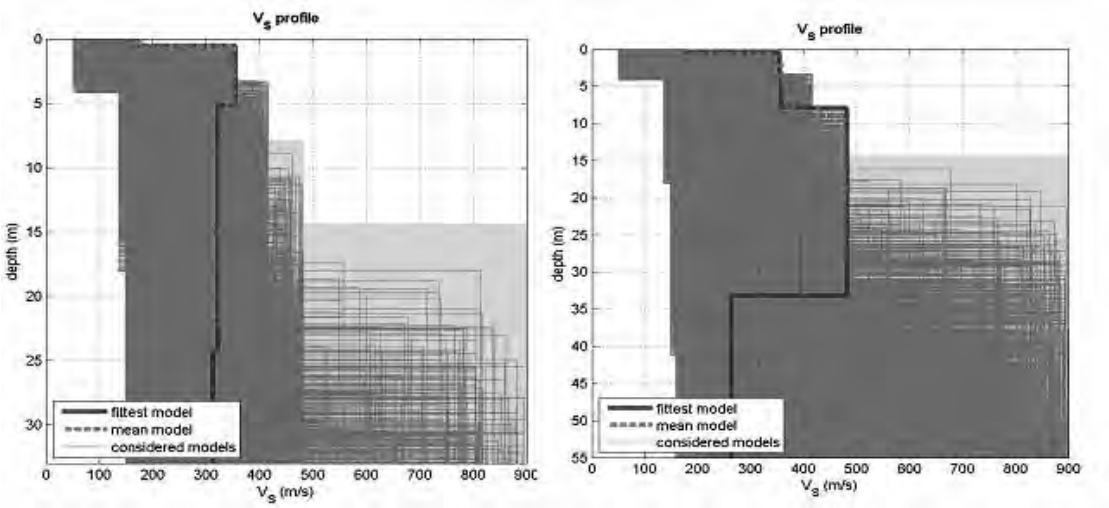

Fig.5 (a)Velocity profile considering only the fundamental mode. (b) Velocity profile considering the fundamental mode and all possible higher modes.

Conclusions:

The generated velocity spectrum has been utilised successfully to discriminate fundamental mode (1st) and different higher modes (2nd, 3rd and 4th mode). The velocity profile generated by considering the entire modes provide improved S-wave section with better accuracy and resolution than that of generated only considering the fundamental mode. The present study reveals that all the higher modes along with fundamental mode is of prime interest for accurate mapping of subsurface using MASW techniques.

Acknowledgements:

The authors wish to thank to the Director, ISM and HOD, Department of Applied Geophysics, ISM, Dhanbad for their keen interest in this study. Authors are thankful to DST for funding the project (SB/S4/ES-640/2012) on geotechnical characterization of Jharia coal field area using Geophysical techniques.

References:

Beaty, K.S., Schmitt, D.R., Sacchi, M., 2002. Simulated annealing inversion of multimode Rayleigh-wave dispersion curves for geological structure. Geophysical Journal International, 151, 622–631.

Beaty, K.S., Schmitt, D.R., 2003. Repeatability of multimode Rayleigh-wave dispersion studies. Geophysics, 68, 782–790.

Dal Moro, G., Pipan, M., Forte, E., Finetti, I., 2003. Determination of Rayleigh wave dispersion curves for near surface applications in unconsolidated sediments. In: Proceedings SEG (Society of Exploration Geophysicists) 2003, 73rd Annual Meeting, Dallas, Texas, October 26–31, 2003, pp. 1247–1250.

Forbriger, T., 2003b. Inversion of shallow-seismic wave fields: II. Inferring subsurface properties from wave field transforms. Geophysical Journal International, 153,735–752.

Gabriels, P., Snieder, R., Nolet, G., 1987. In situ measurements of shearwave velocity in sediments with higher-mode Rayleigh waves. Geophysical Prospect, 35, 187–196.

McMechan, G.A., Yedlin, M.J., 1981. Analysis of dispersive waves by wave field transformation. Geophysics 46, 869–874.

Miller RD, Xia J, Park CB, Ivanov J. Multichannel analysis of surface waves to map bedrock. Leading Edge 1999;18,1392–6.

O'Neill A, Dentith M, List R. Full-waveform P-SV reflectivity inversion of surface waves for shallow engineering applications. Exploration Geophysics, 34,158–73.

Park CB, Miller RD, Xia J. Multichannel analysis of surface waves. Geophysics 1999;64(3):800–8.

Ryden, N., Park, C.B., Ulriksen, P., Miller, R.D., 2004. Multimodal approach to seismic pavement testing. Journal of Geotechnical and Geoenvironmental Engineering, 130 (6), 636–645.

Tian, G., Steeples, D.W., Xia, J., Miller, R.D., Spikes, K.T.,Ralston, M.D., 2003. Multichannel analysis of surface wavemethod with the autojuggie. Soil Dynamics and Earthquake Engineering,23 (3),243–247.

Tokimatsu K, Tamura S, Kojima H. Effects of multiple modes on Rayleigh wave dispersion characteristics. Journal of Geotechnical Engineering ;118,1529–1543.

Xia J, Miller RD, Park CB. Estimation of near-surface shear-wave velocity by inversion of Rayleigh wave. Geophysics, 64(3),691–700

Xia J, Miller RD, Park CB, Hunter JA, Harris JB, Ivanov J.Comparing shear-wave velocity profiles from multichannel analysisof surface wave with borehole measurements. Soil Dynamics and Earthquake Engineering ;22(3),181–90.

Xia J, Miller RD, Park CB, Ivanov J, Tian G, Chen C. Utilization of high-frequency Rayleigh waves in near-surface geophysics. Leading Edge 2004;23(8),753–759.

Zhang SX, Chan LS. Possible effects of misidentified mode number on Rayleigh wave inversion. Journal of Applied Geophysics,53,17–29.

MINERAL MODELLING OF PARIWAR FORMATION OF JAISALMER BASIN, RAJASTHAN THROUGH WELL LOG ANALYSIS

Sanskar Srivasthava and Kedareswarudu Utla
University of petroleum and Energy Studies, Dehradun
kedareswarudu@yahoo.com

Lithology determination and mineral identification using well log analysis are the initial processes of formation evaluation. These two processes together are known as Mineral Modelling and are essential to characterize the reservoir and predict the nature of pore fluid. This paper aims to discuss the results of Mineral Modelling of Pariwar formation of Jaisalmer Basin, Rajasthan. Mineral Modelling is done through two approaches. The first approach is Deterministic Modelling to predict the lithology using Cross-Plots. The main Cross-Plot used for lithology determination is Neutron-Density Cross-Plot which also determines porosity. The presence of Clay in the formation is determined using Thorium-Potassium Cross-Plot. This approach uses a limited number of Logs and Components. The second approach is Probabilistic Modelling which uses computer aided numerical modelling techniques and confirm the lithology. Mineral identification is done in three steps using an Interactive Mineral Solver algorithm. The first step is to set values for various formation parameters mainly, volume of Quartz, Water, Gas, Clay, Pyrite and Glauconite. The second step is framing response equations of logging tool and reconstruction of Logs. The third step is comparison of the constructed logs with the actual logs and generation of "incoherence" function. The incoherence is a measure of the fit between the two sets of logs. An iterative method minimizes the incoherence and output the result when the given convergence criterion is satisfied. Pariwar Formation is encountered at two depths differ approximately by 200 m and designated as zone-1 (shallow) and zone-2 (deeper). Effective porosity of Pariwar formation varies from 0.17 to 0.30 and 0.15 to 0.26 in zone-1 and zone-2, respectively. The corresponding values of Sw varies 0.55 to 0.95 and 0.60 to 0.99. Pariwar formation is found to be clastic and cleaner than other formations in the site of investigation.

SUBSURFACE RESISTIVITY IMAGING FOR GEOTECHNICAL INVESTIGATION IN KURUKSHETRA UNIVERSITY KURUKSHETRA, HARYANA

Sushil Kumar* and Peush Chaudhary
Department of Geophysics, Kurukshetra University, Kurukshetra-136119
**sushil_gp24@yahoo.co.in*

Kurukshetra is the District headquarter of Kurukshetra District of Haryana State. Haryana state forms a divide between the Ganges and Indus water catchments. More than 98% area of the state is covered by the alluvial plain including western desertic terrain of sand dunes. A large part of the

Haryana plains constitutes a widely spaced topographic depression between Shivalik and Aravalli hills which has almost a flat topography on regional level and poor drainage system. The Kurukshetra district is located between 29°36′ to 3°18′ N latitudes and 76°10′ to 77°19′ E longitudes. It is bounded on the north by Ambala district, on the west by Patiala district of Punjab, on the south-west by Kaithal district, on the south by Karnal district and on the east by Yamuna Nagar. The district covers a total area of 1217 sq. km. Kurukshetra University lies in the latitude 29°52′ N to 76°25′ E.

Geoelectrical resistivity surveys were conducted in the Kurukshetra University campus, Haryana, India to investigate subsurface resistivity. The focus is to understand the subsurface lithology for better understanding from geotechnical perspective. A total of 15 sites were selected inside and in the neighborhood of the Kurukshetra University Campus. Vertical Electrical Sounding (VES) survey was carried out by using Wenner Array with electrode spacing 5m. Expected depth of investigation is approximately 20m. The average resistivity values of the region is about100 ohm-m. The survey was conducted by using Syscal Kid resistivity meter and the measured resistivity profiles were interpreted using 2D resistivity inversion programme (RES2DINV). The resistivity structures from VES yields significant information about the resistivity of the area and provide a clear view of the thickness and distributions of various lithological units.

3D CHARACTERIZATION OF SEISMIC B-VALUE IN THE ARAKANYOMASUBDUCTION BELT

Aditya Kumar*, SumitBhuin, Vishal Rathi and Monika Bhatia
mehtaaditya786@gmail.com

The Arakansubduction belt is seismically one of the most active regions of the world, which has experienced several large to great earthquakes in its past history. It is bounded by Himalayan seismic belt and Eastern Syntaxis in the north, Burmese plate in the east, Andaman subduction belt in the south and Indian plate in the west. High seismicity in the region is attributed to the subduction tectonics between the Indian plate in the west and the Bermese plate in the east. Majority of the earthquakes occur in the depth range of 30–60 km and define an eastward gently dipping seismicity trend surface that coincides with the Indian slab. The dip of the slab steepens in the east direction and earthquakes occur down to a depth of 150 km. Subduction is still continuing in this region, which is evidenced by the intermediate to deep focus earthquakes in this range.

The seismicity in the Arakan-Yomasubduction belt is assessed by frequency magnitude recurrence relation. The spatial mapping of seismic b value is performed for this purpose. According to the frequency-magnitude relation, the b value is obtained by the relation log10N = a - bM, where N is the cumulative number of earthquakes, and a and b are constants related to the activity and earthquake size distribution, respectively. These variations in b-value are related to differences in stress, pore pressure, and material heterogeneity and therefore can give important constraints when analyzing the seismotectonics and hazard potential of a region. High b values are often correlated with the low stress field and vice-versa. In the present study, 2D and 3D seismic b-value is mapped in the study region using a homogeneous and complete seismicity database during the period 1964-2012. These maps are directly correlated with differential stress filed in the region and hence important for the seismic hazard assessment.

SEISMIC AND ELECTRICAL TOMOGRAPHY SURVEYS FOR THE SAFETY OF DAM STRUCTURES

M.S. Chaudhari, M. Majumder, J. Roy, V. Bagade, S. Ranga and R.S. Ramteke
Central Water and Power Research Station, Pune 411024, India
mukund_chaudhari@yahoo.co.in

The ageing and degradation of dam structures is an inevitable problem whose consequences on the safety of the structure are important. Presently, site characterization using geotechnical engineering has some limitations to adequately describe these subsurface ground conditions. All geotechnical tests provide information from point to point and the values are interpolated in between places. These tests grossly under sample the subsurface and are frequently inadequate (Sarman & Palmer, 1990). The use of seismic tomography and electrical resistivity imaging in the assessment of dam structure is of primary importance. Geophysical methods are useful as non-destructive tools that can provide information over large volumes as compared to point measurements. In the Manikdoh masonry dam, seismic tomography survey was carried out in five horizontal and two vertical planes and also one electrical resistivity imaging profile was taken on the top of the dam. The travel time data for tomography analysis was collected by placing geophones on the downstream face and hammer points on the upstream face of the dam. The velocity distribution between each consecutive pair of source line and receiver line of the plane was computed using Simultaneous Iterative Reconstruction Technique. The weak zones, if present, are represented by low velocity values and hence can be delineated. The reliability of travel time data is ensured by comparing the travel times at the point of intersection of common source to receivers pairs in horizontal and vertical planes. The weak zones obtained from the horizontal planes matched well with that in vertical tomograms. An attempt was also made to corroborate the weak zones obtained in seismic tomography survey with the low resistivity zones in electrical resistivity imaging section.

Introduction

Assessing the quality of dam structure is important to ensure its integrity and stability. Seismic transmission tomography can be a valid tool to detect mechanical discontinuities and the decay in structures and to aid rehabilitation (Cardarelli, 2000). Seismic tomography can generate a cross sectional picture of an object detecting the inner defects or material properties of the rock and filled materials (Hu Chih-Hsin et al, 2012). Seismic Tomography has been used extensively in geophysical work (Dines and Lytle, 1979), e.g. for a dam site on Reunion Island (cotton et al., 1986), for research on buried voids, for shafts and tunnels (Lytle and Dines, 1980) and for Pre-and Post-excavation studies for a nuclear power plant (Wadhwa et al., 2005). In tomographic reconstruction, measurement of some energy which has propagated through a medium is made and from this energy, internal distribution of the medium's character is obtained by inversion process (Redington and Berninger, 1982; Jackson and Tweeton, 1994). Acoustic tomograms can be made using amplitude, phase shift or travel time observations. Generally, seismic tomographic surveys use travel time data (Kevin, 1988) because of ease and convenience. Subsequently after the impoundment of the Manikdoh dam, constructed on River 'Kukadi' in Junnar Taluka of Pune District in the year 1984, heavy leakages were observed through the masonry in both the galleries as well as in the downstream face of the dam. In view of this, seismic straight ray travel time tomography of the structure was carried out to suggest possible weak zones which are susceptible for seepage. Seismic tomography survey was carried out along five horizontal and two vertical planes in the month of may when the water level in the reservoir was minimum. The quality of in-situ masonry is an important parameter and can be assessed by seismic wave method as the compressional wave velocities evaluated by this technique give an idea of the strength of the masonry. The advantage of the tomographic studies is that it yields in- situ velocity distribution of the sampled area at much lower cost and in much shorter time. The velocity distribution, in turn

helps in delineating the lateral and vertical extent of weak zones. The weak zones, if present, will be represented by low velocity values and hence can be delineated. One profile using Electrical Resistivity Imaging using 48 electrodes with 2 m spacing was also taken.

Data Acquisition

A 10 Kg sledge hammer, 10 Hz vertical Geophones and a 24-channel signal enhancement seismograph model McSeis SX were used for data acquisition. The survey was conducted along five horizontal planes at elevations 705 m, 700 m, 695 m, 690 m, 685 m and two vertical planes at chainage 463 m and 443 m (Fig. 1). For horizontal and vertical planes, geophones were placed on the downstream face of the dam while the hammer points were located at the same elevation but on the upstream face of the dam. In horizontal planes 24 geophones spaced 2 m apart were placed on the downstream face of the dam and 47 hammer points spaced 1 m apart were used for generating acoustic waves on the upstream face of the dam yielding 1128 ray paths. Typical ray paths between different positions of the transmitter of the source line on the upstream face and geophones of the receiver line on the downstream face of the dam is shown in Fig. 2. The first plane was at RL 705 m and other planes were at 5 m elevation difference. In vertical planes 24 geophones spaced 1m apart were placed on the downstream face of the dam and 24 hammer points spaced 1 m were used for generating acoustic waves on the upstream face of the dam yielding 576 ray paths. The geophones were planted vertically on the tip of the metallic rod inserted at the desired location by drilling small drill hole for maximum sensitivity.

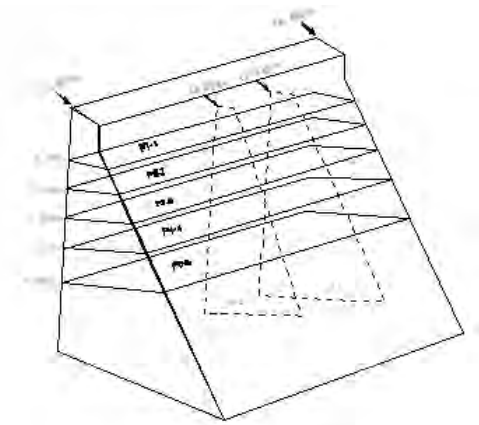

Fig. 1 Schematic diagram showing horizontal and vertical planes covered by Seismic Tomography Survey

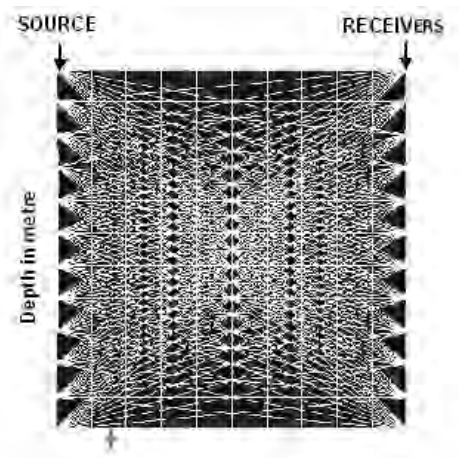

Fig. 2 Typical ray diagram for various positions of source and receiver

The electrical resistivity imaging survey was conducted by ARES automatic resistivity imaging system manufactured by M/s GF Instruments, Czech Republic. In the present studies, Wenner-Schlumberger array is deployed. Electrical Resistivity Imaging (ERI) profile was taken on the top of the dam using Wenner Schlumberger electrode configurations from chainage 432 m to 526 m. For ERI survey, 48 electrodes in a line at 2.0 m interval were deployed. The apparent resistivity values thus measured are inverted using RES2DINV software package to obtain true resistivity depth section.

Data Analysis

In the seismic tomography of the dam, the zone between the receiver line on the downstream face and source line on the up-stream side of the dam is divided into small cells. The choice of number of cells depends on the total number of P-wave arrivals recorded in the field experiment. The two dimensional plane 1-1 at elevation 705 m between source line and receiver line was descretised on square grid points, 14 across the width of the plane (0.552m) and 47 along the plane (1.0 m). In the procedure adopted for data collection, there were 1128 rays and hence 1128 travel time equations. The number of pixels for this plane was 658. This means 658 unknowns against 1128 equations. Therefore, for this type of set-up, where the number of equations is much larger than the number of unknowns, a near unique inversion is possible. Once the cell size is decided, tomographic inversion begins with an assumption of initial model of the compressional wave velocity between source line and receiver line. With these initial average velocities, first arrival times of the rays for all possible positions of sources and receivers are calculated using straight ray tracings. These synthetic travel times are compared with the field measured travel times and the differences or residuals are inverted to obtain perturbations to the velocity model using algorithm of Jackson et al. (1992). The procedure is repeated and the velocity model is perturbed until, either there are no differences between the model travel times and the measured arrival times or RMS error is within the set limit (Singh and Singh, 1991). Travel time data for tomographic analysis was collected one plane at a time. The seven tomograms depicting P wave velocity distribution were obtained by inverting the arrival times. The reliability and uniqueness of the velocity tomograms were improved by putting the lower (1000 m/sec) and upper (4000 m/sec) limits on the velocities. Analysis of synthetic model studies suggests that upper and lower velocity limits are helpful in obtaining a velocity distribution that is unique and matches more closely with the model data (Ghosh et al., 2000).

The dominant frequency observed in the compressional waves on most of the records was about 450 Hz. By taking compressional wave velocity of masonry about 3000 m/sec, yields a dominant wavelength of the waves to be about 6.6 m. The maximum allowable resolution is quarter of the wavelength i.e. 1.6 m.

Results and Discussion

The five horizontal and two vertical tomograms depicting lateral and vertical variations of P-wave velocities for the planes between source lines on the upstream side and receiver lines on the downstream side were obtained by inverting the arrival times using algorithm of Jackson et al. (1992).

Fig. 3 and Fig. 4 shows contoured image of the P-wave velocities for the plane 2-2 and plane 3-3. From the P- wave velocity distribution for Plane 2-2 at 700 m elevation appears to have a velocity above 2500 m/s. An isolated low velocity zone (W-2) with velocity ranging from 1500 to 2500 m/sec can however be spotted from chainage 463 m to 468 m on the upstream side and extending from 0 m to 2 m across the width of the plane.

From the P- wave velocity distribution for plane 3-3 at 695 m elevation, a very prominent low velocity zone (W-3) with velocity ranging from 1500 m/sec to 2500 m/sec is observed from chainage 462 m to 469 m extending from 0 m to 4 m (Fig. 4). This low velocity zone can be correlated with the low velocity zone W-2 in plane 2-2 (Fig. 3) occurring within chainage 463 m to 468 m. The remainder of the plane has velocity above 2500 m/s indicating good quality masonry.

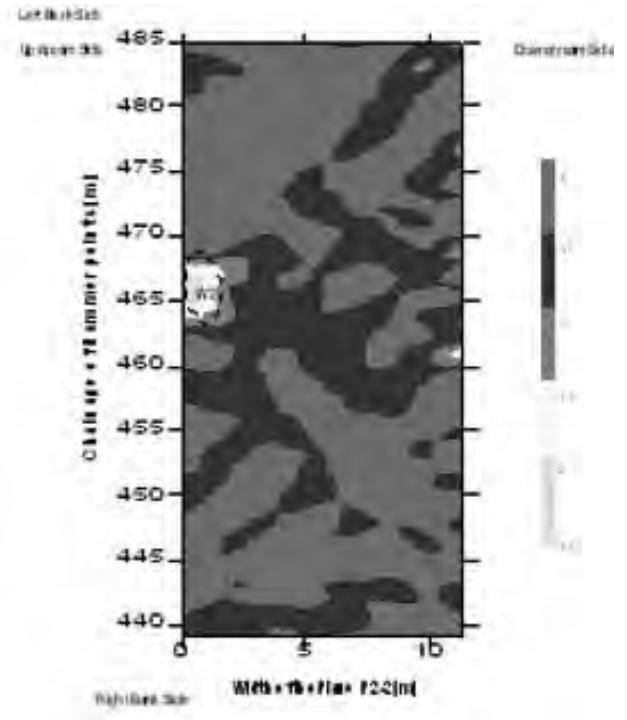

Fig.3 P- wave velocity distribution along plane P 2-2 (700-700)

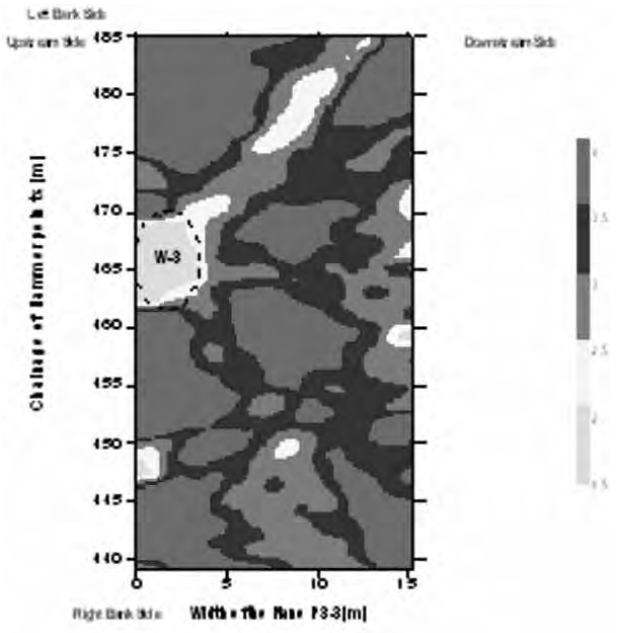

Fig. 4 P- wave velocity distribution along plane P 3-3 (695 – 695)

Fig. 5 depicts the P - wave velocity distribution of vertical plane VP 2 at chainage 463 m extending from elevation 685 m to 708 m. Two low velocity zones with velocity ranging from 1500 m/s to 2500 m/s are seen on the upstream side. The first low velocity zone (W-5) is spotted from EL 700 m to 703 m on the upstream side dipping down towards downstream and tapering off at EL 697.5 m, 8 m downstream of the upstream face. The second low velocity zone (W-6) is observed from elevation 693 m to 698 m at upstream face dipping down towards downstream and tapering off at elevation 692 m extending 8 m from downstream to upstream face. These two low velocity zones W-5 and W-6 may be correlated with the low velocity zones (W-2 & W-3) observed in plane P 2-2 and plane P 3-3.

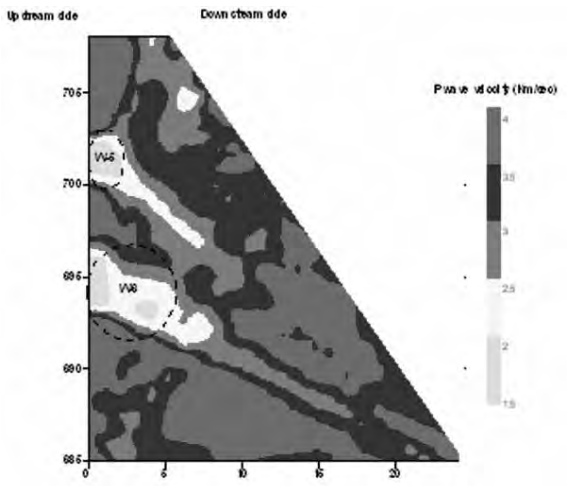

Fig. 5 P- wave velocity distribution along vertical plane VP 2 at chainage 463 m

Electrical resistivity imaging section of 94.0 m length taken on the top of the dam at elevation 714.3 m from chainage 432 m to 526 m using Wenner-Schlumberger electrode configuration is shown in the Fig. 6. From the section it is seen that one low resistivity zone with resistivity ranging from 129 Ω m to 829 Ω m exists from chainage 462 m to 474 m at elevation from 700 m to 696 m. This low resistivity zone corroborates with the low velocity zone W-3 obtained in horizontal plane 3-3 at elevation 695 m.

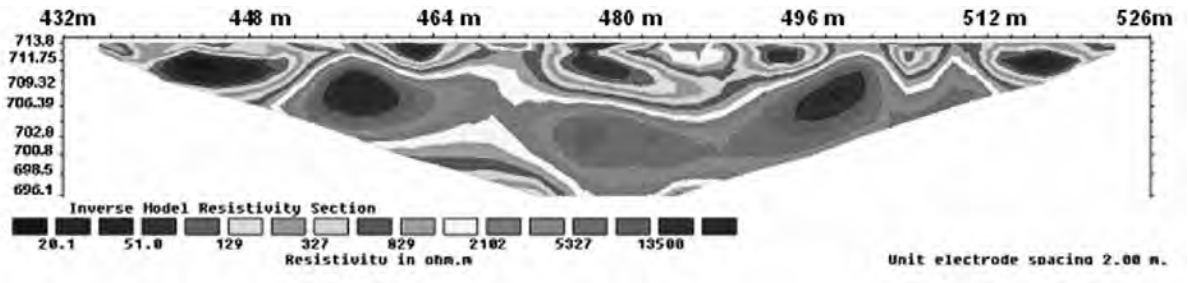

Fig. 6 Electrical Resistivity Imaging Section from chainage 432 m to 526 m

Conclusions

The tomography survey results suggest that the possible low velocity zones are between elevation 695 m to 705 m. Two low velocity zones (W-2 & W-3) in the horizontal plane P 2-2 and P 3-3 is further supported by the low velocity zone W-5 and W-6 obtained from vertical section VP 2 at elevation 700 m to 703 m and 693 m to 698 m. Therefore the existence of a prominent low velocity zone extending

from elevation 695 m to 703 m from chainage 462 m to 469 m is inferred as weak zone. From the Electrical Resistivity Imaging section it is seen that one low resistivity zone with resistivity ranging from 129 Ω m to 829 Ω m exists from chainage 462 m to 474 m at elevation from 700 m to 696 m which corroborates with the low velocity zone W-3 obtained in horizontal plane 3-3 at elevation 695 m. It is recommended that proper treatment of these weak zones should be carried out to strengthen the masonry of the Manikdoh dam for reducing leakage.

Acknowledgements

Authors are grateful to Shri S.Govindan, Director, Central Water and Power Research Station (CWPRS), Pune for constant encouragement and for permission to publish this paper. The help and co-operation extended by project authorities during collection of data is thankfully acknowledged.

References

Bregman, N.D., Hurley, P.A. and West, G.F., 1989. Seismic Tomography at fire-flood site; Geophysics, 54, 1082-1090.

Cotton, J.F., Deletie, P., Jacquet – Francillon, H., Lakshmanan, J., Lemeine, Y. & M., Sanchez, 1986. Curved ray seismic tomography: Application to the Grand Etang Dam (Reunion Island), First break, 4, 25-30.

Dines, K.A. & R.J. Lytle, 1979. Computerized geophysical tomography, IEEE Proc., 67, 1065-1073.

Jackson, M.J., Tweeton, D.R. and Fridel, M.J., 1992. Approaches for optimizing the use of available information in cross-hole seismic tomographic reconstruction, Proc. Geotech.Geocomputing Conference, Denver, 130-143.

Lytle, R.J. & Dines, K.A., 1980. Iterative ray tracking between boreholes for underground image reconstruction, IEEE Trans, Geosci, Remote Sensing, V.GE -18, 234-240.

Nolet, G., 1985. Solving or resolving inadequate and noisy tomographic system. Journal Computational Physics, 61, 463-482.

Redington, R.W. & Berninger, W.H., 1982. Medical Imaging Systems, Physics Today, 34(8), 36-46.

Singh, R.P. and Singh, Y.P., 1991. RAYPT A new inversion technique for geotomographic data, Geophysics, 56, 1215-1227.

Wadhwa, R.S., N. Ghosh, M.S. Chaudhari, Ch. Subbarao and Raja Mukhopadhyay, 2005. Pre-and Post-excavation cross-hole seismic and geotomographic studies for a nuclear power project; Journal of Indian Geophysical Union, 9 (1), 137-146.

GROUND PENETRATING RADAR STUDIES FOR LOCATING SUBSIDENCE ZONES AND BURIED BOAT WRECK

M.S. Chaudhari, Ch.Subbarao, V.Chandrasekhar, J. Roy and R.S. Ramteke

Central Water and Power Research Station, Pune 411024, India

cwprs@yahoo.com

GPR is used in a variety of geological media and structures to detect objects, changes in material properties, voids, cracks and other inhomogeneities. Mapping the dielectric permittivity and electrical conductivity is an effective tool to locate buried objects, cavities and similar anomalies. The propagation of the radar signal depends on the frequency-dependent electrical properties of geological materials which in turn are governed primarily by the water content, minerals and clay. Data collected during GPR surveys conducted in January 2010 at village Kambal Danga, J & K and in March 2013 at Kosi barrage, Bihar were used to demonstrate the application of GPR technique in delineating subsidence zones above a railway tunnel in a paleo channel and to locate a buried boat wreck under the Kosi river sands respectively. Results from the studies show that GPR can provide useful information on shallow subsurface anomalous objects and conditions.

GPR studies for locating subsidence zone

Excessive seepage was observed into a tunnel of the Udhampur-Katra railway line dug through the Shivalik range of lower Himalayas near village Kambal Danga, J&K. The tunnel passes through thickly bedded sediments of recent age. A part of the tunnel passes through the aquifer of an old buried channel comprising boulders embedded in sandy/silty matrix which is under water charged condition with very heavy water discharge (upto 1000 ltr/sec in monsoon) observed in the tunnel. The thickness of the overburden in the area varied from 10 m to over 100 m. The bed rock is pebbly sandstone but it is not exposed in the surveyed area.

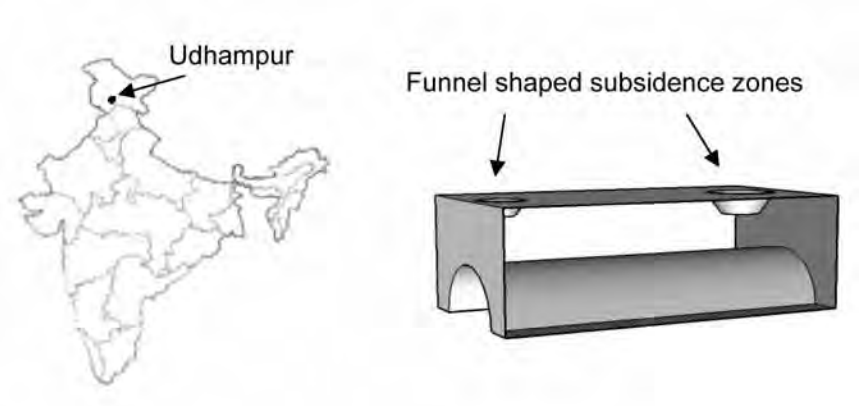

Fig.1 Index map of site and schematic sectional view of the tunnel

Two funnel shaped cavities extending up to the ground surface were formed above the tunnel (Fig.1). Depth of the funnel (cavity) on the eastern end was around 12 m but a few more zones prone to caving were suspected between the crown of the tunnel and ground surface at other locations. The maximum depth of the crown of the tunnel below the ground level was about 31 m. To locate hidden voids/zones prone to subsidence below the ground surface, formed during the tunneling operation, GPR survey above the tunnel on the ground along and across the tunnel orientation were carried out.

Data were acquired using GPR System equipped with a 100 MHz shielded antenna in close vicinity of the tunnel alignment on the ground surface in East-West direction between tunnel RD (Reduced Distance) 12780 m and 13440 m along 3 traverses viz., L1 (along the central line), L2 (~ 2.5 m South of the central line), L3 and L10 (~ 2.5 m North of the central line). In addition, many GPR traverses of varying lengths both parallel and perpendicular to the central line L1 were also conducted in the available space. A few traverses were conducted very close to the existing open cavity on the eastern side to establish the GPR signature above cavities in the area. In all, 43 GPR profiles of varying lengths were taken to detect the subsurface cavities. Fig. 3 shows the layout plan of GPR traverses on the ground surface with reference to the tunnel alignment on the ground.

The GPR was operated in distance mode with distance triggering interval of 0.1 m and ground velocity of 100 m/μsec. Processing sequence like DC shift, frequency filtering, linear and exponential gain, subtracting mean and f-k migration, velocity analysis of hyperbolic reflections were applied on the raw data to enhance the true anomalies.

The GPR records obtained revealed a few clearly visible anomalies in the form of hyperbolic reflections. The velocity analysis of these reflected events revealed a velocity of 57 to 70 m/μsec, much lower than that of the host medium i.e. sedimentary strata. From the velocities, orientation and

areal extent of the hyperbolic reflections, the events are inferred to be emanating from subsidence zones prone to caving. The locations of these zones were corroborated by conducting additional GPR traverses in the close vicinity of the anomalies. Figure 2 shows a typical GPR record from traverse L3.

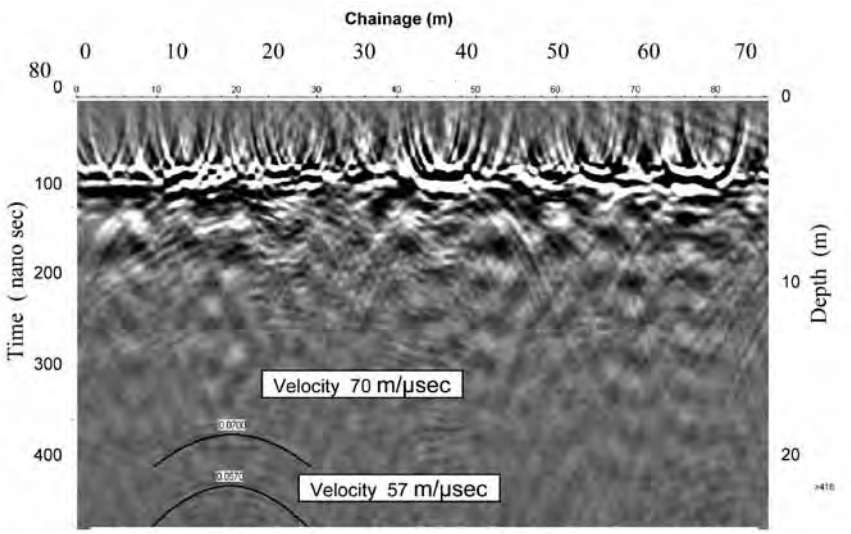

Fig. 2 GPR record along Profile L3 showing subsidence zone prone to caving

In this figure the hyperbolic signature observed was interpreted as subsidence zone prone to caving, the location of which was determined from the vertex of the hyperbolic arc. Similar anomaly was observed in GPR records of profiles L1 and L2 around the same tunnel RD and this subsidence zone is marked as S-7 in the location plan (Fig.3). In all 10 subsidence zones prone to caving were inferred in the area investigated.

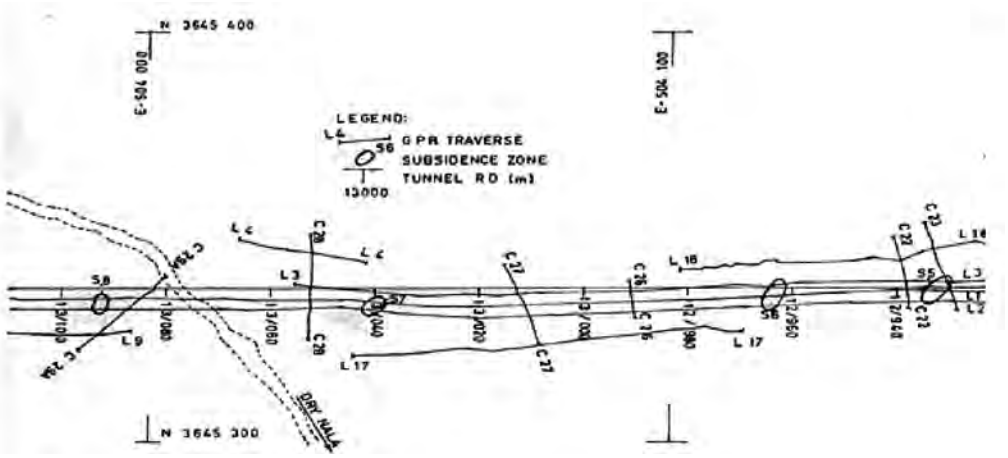

Fig.3 Location plan showing GPR traverses and few subsidence zones

GPR studies for locating a buried boat wreck

A dredger deployed for extracting silt from the sand bar in the downstream of Kosi barrage, Bihar encountered sudden floods during August 2011. It could not be brought to the river bank and had to be abandoned due to the severity of the flood. It was observed later that the dredger drifted in the water current about a kilometer and a half downstream and was last seen close to a shoal with a small portion of the dredger popping out above the water surface. It eventually disappeared and

presumably got buried at the same location. GPR studies were conducted in March 2013 when the water level was at its lowest (to ensure dry surface sand conditions) to locate the dredger.

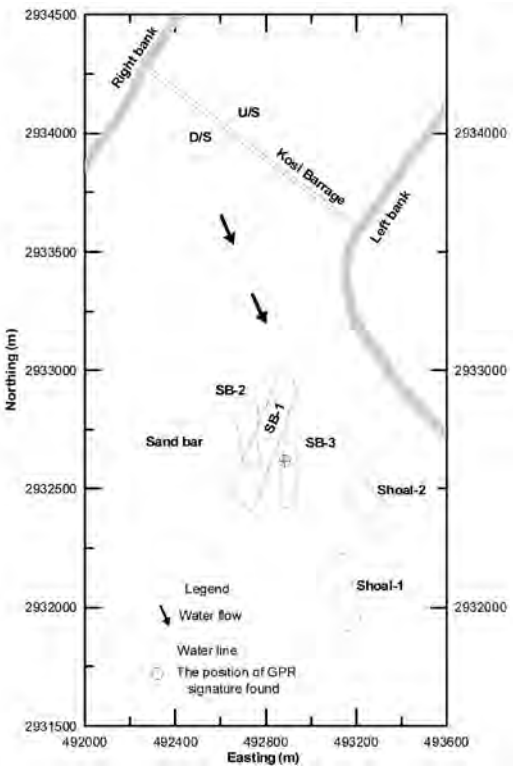

Fig.4. Layout map of the area covered by GPR studies downstream of Kosi Barrage, Bihar

The geology of the area downstream of the Kosi Barrage constitutes the alluvial plain of the late Paleogene-Neogene times. The sand bars in the Kosi river are made up of sandy/silty layers and are saturated with fresh waters.

The GPR was operated in distance mode with distance triggering interval of 0.1 m and a ground velocity of 80 m/μsec for sand for collecting data.

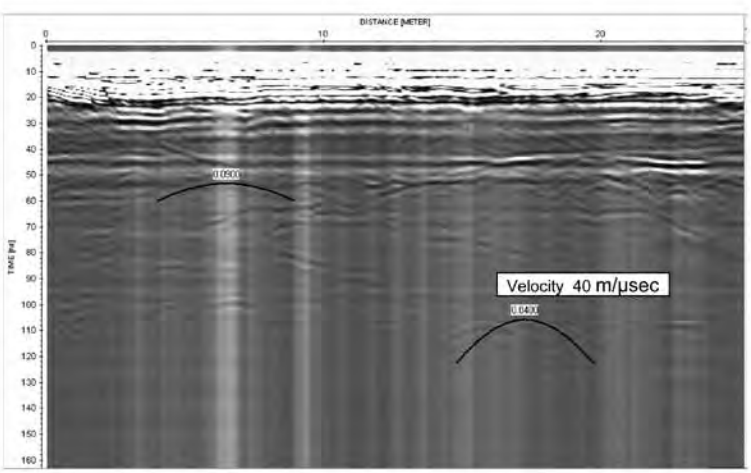

Fig.5 GPR record showing signature of buried boat wreck along with velocity estimation

Initially, a rectangular area (SB-1) of dimensions of about 550 m X 100 m (Fig. 4) was marked around the speculated location and the survey was carried out in the area along several small profiles. No significant signatures were encountered in these profiles. Thereafter, studies were carried out in a similar fashion in an area adjacent to the previous one on the west side along another rectangular area (SB-2) of size 400 m X 100 m (Fig. 4). All these profiles showed a sequence of silt layers of varying levels of compaction without any discernible signature of a buried object.

Suspecting that the dredger might have drifted further, surveys were carried out in two shoals d/s of the former one. For this, two rectangular areas of sizes 300 m X 60 m and 280 m X 50 m were marked in shoal-1 and shoal-2 respectively (Fig. 4). Here too, the GPR records revealed a similar geological sequence of stratified silt without any significant anomaly of any buried object.

At the end, the rectangular area (SB-3) of size 330 m X 60 m, east of the first rectangle (SB-1) in the sand bar was investigated by taking several smaller profiles as previously done. In one of the profiles, a signature of a buried object which was different from that of the silt layers was found at a depth of approximately 5-6 m (Fig. 5). The velocity analysis of the hyperbolic reflections showed a velocity of 40 m/μsec for the buried object. This was interpreted as the remnant of the boat wreck and its location was marked. To approximately mark the orientation of the buried object, the area was closely investigated by taking several smaller profiles with a close spacing of 2 m between successive lines using a 250 MHz antenna for better resolution (Fig. 6).

Similar signatures in the form of hyperbola were found in these profiles also revealing a signature of a buried object. The UTM coordinates of the location where the GPR signature was obtained were noted as 2932607 N and 492881 E.

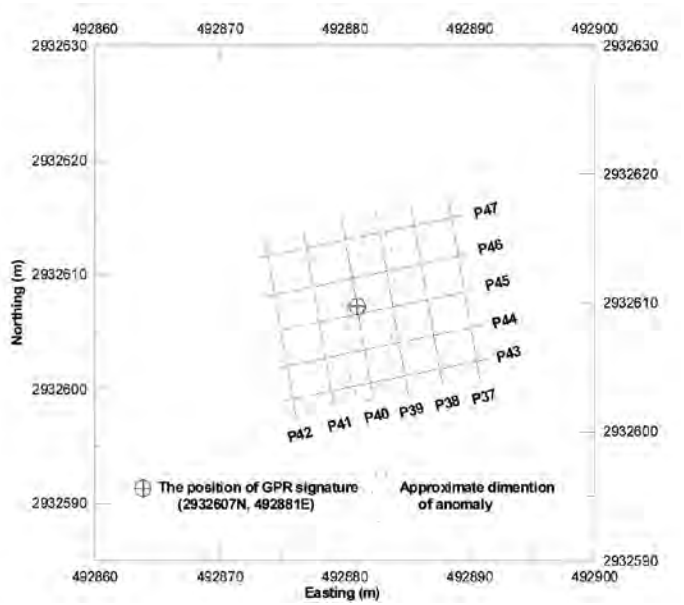

Fig.6 Detailed layout of survey lines inside rectangle SB-3 (Inferred location of buried Dredger)

Conclusions

GPR is a versatile technique to map the areal extent of near-surface objects or changes in the surface material and eventually produce images of those materials. Subsidence zones resulting from the tunnel excavation in paleo channel comprising small boulders in sandy/silty matrix were delineated.

A vast area of river sands and shoals downstream of Kosi river was rapidly scanned and located the buried boat wreck of the dredger. These case studies demonstrate the efficacy of the GPR technique in the near surface environment.

Acknowledgements

Authors are grateful to Shri S.Govindan, Director, Central Water and Power Research Station (CWPRS), Pune for constant encouragement and for permission to publish this paper. The help and co-operation extended by project authorities during collection of data is thankfully acknowledged.

REFERENCES

Annan,A.P. and Davis,J.L. 1976. Impulse radar sounding in permafrost. Radioscience, 11, p.383-394

Daniels, J.J., J. Bower, and F. Baumgartner, 1998. High resolution GPR at Brookhaven National Lab to delineate complex subsurface structure. Journal Environmental and Engineering Geophysics, 3, Issue 1, p.1-6.

Daniels, J.J., R. Roberts, and M. Vendl, 1995. Ground penetrating radar for the detection of liquid contaminants. Journal of Applied Geophysics, 33, p.195-207.

Davis, J.L., and A.P. Annan, 1989. Ground penetrating radar for high resolution mapping of soil and rock stratigraphy. Geophysical Prospecting, 37, p.531-551.

Haeni, F.P., 1996. Use of ground penetrating radar and continuous seismic-reflection on surface-water bodies in environmental and engineering studies. Journal of Environmental & Engineering Geophysics, 1, No. 1, p.27-36.

Mala Geoscience, 2002. RAMAC/GPR Operating manual: Mala Geoscience, Skolgatan, Sweden.

CHEMICAL QUALITY OF GROUNDWATER AND SOIL IN PARTS OF TOSHAM AREA (HARYANA) IN RELATION TO HUMAN HEALTH

Savitha and Naresh S

Department of Geology, Kurukshetra University, Kurukshetra- 136119 Haryana
sagwalnaresh@gmail.com, savi_geokuk@yahoo.com

Tosham Ring Complex (TRC) (Survey of India topography sheet no..44P/13;Scale 1.50,000);(28° 46′-28°55′ N;75° 50′-75°58′) is located 160 KM WNW of Delhi.TRC area is about 205sq Km which is a part of Malani Igneous Suite (MIS) and composed of acid volcanic and the associated granites The rocks of MIS are andesite ,pyroclasts ,basalt ,gabbro ,dolerite and are well exposed in the Bhawani district (at Tosham area of Haryana). High incidence of cancer have been reported from many district of southwest Punjab and adjoining areas of Haryana,(Kochhar and Dadwal,2004;Kochhar et al.,2007). The probable cause of cancer may be the presence trace elements like Th,U,Cr,Sr,As,P,F in the soil and water of area .The chemical analysis of Water and soil sample of surrounding areas of TRC has revealed that the concentration of some of these elements were higher than the permissible limits prescribed by the Bureau of Indian Standards and World Health Organization(WHO). The dominant lithology of TRC consists granite ,quartzite,and felsites. Granite is an intrusive felsic igneous rock and is relatively high in minerals containing U,Th and K. The chemical reactions of ground water with the rocks of buried Aravali –Delhi ridge ,high heat producing Tosham granite (Malani) , and quartzite a might have been the cause of high values of elements recorded in ground water (Kochhar et al., 2006). The weathering process like hydration ,hydrolysis ,solution,abrasion ,attrition may be the cause of change in soil and water chemistry of particular area and which in turn affects the lives of surrounding areas Therefore Soil water interaction in relation to human being is a dynamic rather than static process. It describes the means by which soil, rocks and minerals are changed by physical and chemical processes into other soil components. Weathering is an integral part of soil water interaction and reflects the weathering processes associated with the dynamic environment .

References

Bhushan, S.K., 1985. Malani volcanism in Western Rajasthan. Indian Journal of Earth Sciences 12, 58-71.

Kochhar, N., 1983. Tosham Ring Complex,Bhiwani, India.Porceedings of Indian Natural Science Aczdemy 49A. pp.459-490 shiled.

Kochhar, N., 1984. Malani Igneous Suite: Hot-spot magmatism and cratonization of the Northern part of the Indian shiled. Journal of Geological Society of India 25, 155-161.

Vallinay Granite is an intrusive felsic igneous rock, meaning that it solidifies from magma below the surface, and is relatively high in minerals containing silicon and aluminium. The interaction of ground water with the rocks of buried Aravali –Delhi ridge ,high heat producing Tosham granite (Malani) and basement rocks (Delhi Quartzite) in the region might have been the cause of high values of agam, G., 2003. Basic magmatism of Neoproterozoic Malani Igneous Suite, Western Indian Craton: Petrological and Geochemical Modelling. Indian journal of Geochemistry 18, 1-18.

Bhushan, S.K., Chandrasekaran, V., 2002. Geology and geochemistry of the magmatic rocks of the Malani Igneous Suite and Tertiary Alkaline Province of Western Rajasthan. Memoirs of Geological Survey of India 126, 1-129.

Vallinayagam, G., Kumar, N., 2007. Volcanic vent in Nakora Ring Complex of Malani Igneous Suite, Northwestern India . Journal of Geological Society of India 70 (5), 881-883.

AN INVESTIGATION OF THE RESPONSE OF THE MESOSPHERE-LOWER THERMOSPHERE-IONOSPHERE REGION TO EARTHQUAKE OVER A TROPICAL STATION ALLAHABAD

Susheel Kumar and N. Parihar

Indian Institute of Geomagnetism, Navi Mumbai 410 218, India

susheel@iigs.iigm.res.in

It is now well known that the crustal deformations and earthquakes induce certain changes in the mesosphere-lower thermosphere-ionosphere (MLTI) region viz. the changes in electric and magnetic field prevalent at ionospheric heights, the changes in critical frequency of F-layer, the perturbations in ionospheric plasma/electron density, the reduction in electron temperature in ionosphere before earthquake etc.. During April 2009 – May 2010, ground-based measurements of several nightglow features from the MLTI region were carried out at Allahabad (25.5^{o} N, 81.9^{o} E), India using an all sky imaging system. During this period, several earthquakes measuring 5 – 8 in Ritcher scale occurred in and around the Indian subcontinent (latitude ~ 0 – 35^{o} N and longitude 65 – 100^{o} E) during April 24 – 29, 2009, June 20 – 22, 2009, October 23 – 25, 2009, April 06 – 17, 2010, and May 09 – 18, 2010. A detailed investigation of different nightglow features in context of earthquake activity was performed. Herein, a comprehensive report of the events has been presented.

NATURAL FRACTURE AND BREAKOUT DELINEATION FROM FMI AND PREDICTION OF SHEAR WAVE VELOCITY USING MULTIPLE REGRESSION MODELS USING WELL LOG DATA IN KRISHNA-GODAVARI BASIN

***Dip Kumar Singha and Rima Chatterjee**

Department of Applied Geophysics

**dip28kolkata@gmai.com*

Introduction

The Formation Micro Imager (FMI) log is a resistivity imaging tool consisting of two perpendicular pairs of caliper arms, with the end of each arm hosting a pad andattached flap. The pads and flaps contain a number of resistivity sensors (typically 24 on each pad or flap), the data fromwhich can be processedto build up a "picture" of thewellborewall based on resistivity contrasts (Ekstrom et al.,

1987; Rajabi et al., 2010).Two main types of processed resistivity image logs are available: static and dynamic in FMI log. Static images are those which have had one contrast setting applied to the entire well. Theyprovide useful views of relative changes in rock resistivity throughout the borehole. Dynamicimages, which have had variable contrast applied in a moving window, provide enhanced viewsof features such as fractures, bed boundaries.By convention, low resistivity features, such as shales or fluid-filled fractures, are displayed asdarkcolors whereas high resistivity features are displayed as shades of brown, yellow and white. The FMI tool also collects information on theshape of the wellbore cross-section and the hole geometry, in addition to the resistivity image data.

Formation Micro-image (FMI) data are available for selected depth intervals in wells KD and KL. Regression models for prediction of S-wave velocity have been estimated using five well data where P-wave and S-wave data are available in selected depth interval.Shear wave velocity is important in the study of seismic inversion and petrophysical evaluation, particularly for evaluation of formation geomechanical properties.

Natural Fracture

A fracture is a surface along which a loss of cohesion in the rock texture has taken place.A fracture is sometimes called a joint and, at the surface, is expressed as cracks or fissures in therocks. Generally fractures are grouped into various types such as crack, fissure, joint, gash,Fault. The orientation of the fracture can be anywhere from horizontal to vertical. The roughsurface separates the two faces, giving rise to fracture porosity. The surfaces touch at pointscalled asperities. Altered rock surrounds each surface and infilling minerals may cover part or allof each surface. Minerals may fill the entire fracture, converting an open fracture to a healed orsealed fracture.In our study we divided natural fractures in a different way such open fracture, partially openfracture and resistive fracture. Typical example of natural fractures from wells KD and KL: open, partially open and closed fractures are displayed in figure 1.

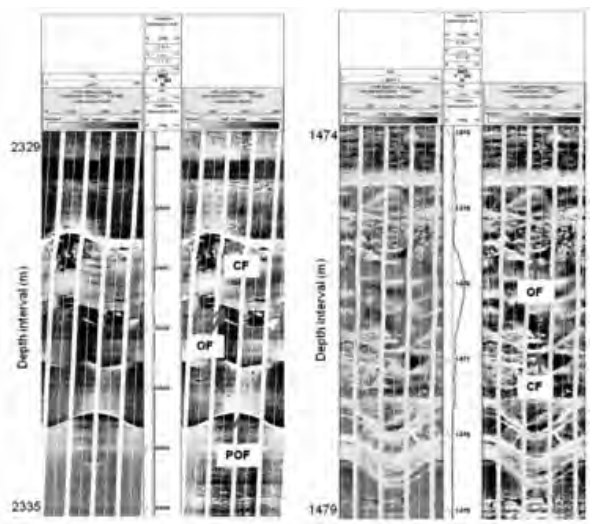

Figure 1: Typically example of natural fracture from well KD and KL

Breakout

Figure 2 shows the typically breakout signature in the several depth intervals of two wells. The well KDin EastGodavari sub-basin has penetrated the oldest sediments in the K-G basin. The breakouts

are observed in this well at depths between 2395-2632 m; corresponding to a total length of breakout for 114 m. This depth range is characterized by mean S_H orientation of N19.01^{0}E. The well KL has breakouts for total length of 6 m for a depth interval of 1101-1350m characterizing N19.24^{0}E in the Oligocene sediments.

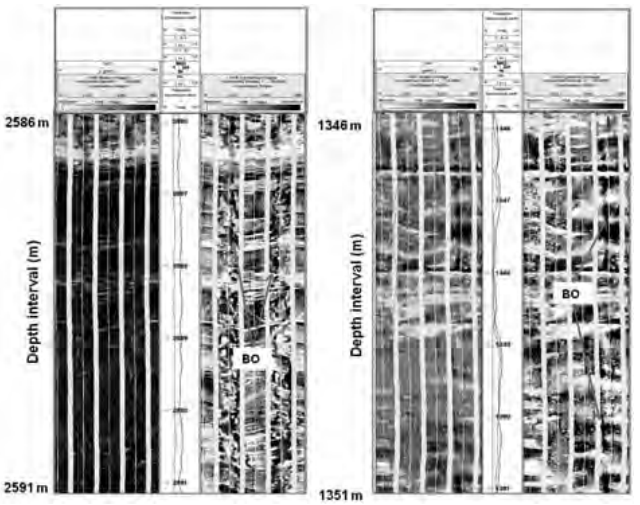

Figure 2: Breakout observed at selected depth interval for wells KD and KL

Drilling Induced Fracture

DIFs are created when the stresses concentrated around a borehole exceed that required to cause tensile failure of the wellbore wall (Aadnoy, 1990). DIFs typically develop as narrow sharply defined features that are sub-parallel or slightly inclined to the borehole axis in vertical wells and are generally not associated with significant borehole enlargement in the fracture direction. FMI images has been used to interpret drilling-induced fractures (DIFs)which areoriented parallel to the in-situ S_H orientation (Bell, 1996) as displayed for well KL. The drilling induced fractures have only been noticed for a length of 14m within depth interval of 1101-1565m in well KL shown in figure 3. DIF in well KL has indicated the S_H orientation towards N21.84^{0}E in sediments of Oligocene to Miocene age.

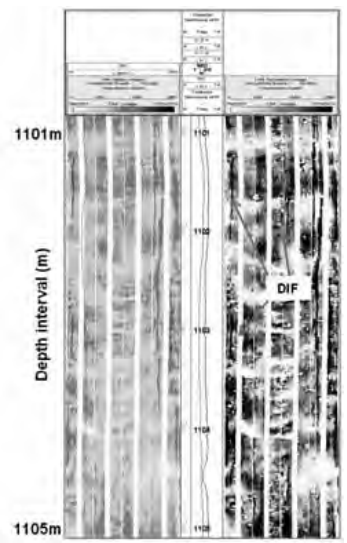

Figure 3:Drilling induced fracture (DIF) for well KL in depth interval 1101-1105m

Regression Model for prediction of S wave Velocity

The information on density, sonic P and S wave velocities are to be known in order to determine the rock mechanical properties from well log data. The P and S wave velocities and density have been used to estimate the elastic moduli in a petrophysical evaluation, which are helpful in determination of maximum and minimum horizontal stresses. However, the absence of the dipole shear sonic logs imposes severe limitations to such applications. We propose regression models for computation of S wave velocity from four wells namely; KA, KG, KK and KE under the study area. Sandstones, shaly sandstones and shales comprise a major component of K-G basin and are of significant relevance to hydrocarbon reservoir. It is known that the elastic velocities of rocks are related to mineralogy, pore geometry, degree of consolidation, cementation, confining pressure, pore fluid, pore pressure and temperature (Han et al., 1986). Many theoretical/experimental models exist considering the effects of porosity, clay, pore shape, fluid, and matrix moduli on the elastic properties of rocks (Gassmann, 1951, Biot, 1956, Castagna et al., 1985). Therefore, in order to establish the predictive models among parameters such as: Vp, shale/clay content (Vsh) and porosity (ϕ) obtained in this study, simple regression between Vp and Vs has been performed in the first stage of analysis. The linear regression relation between Vp and Vs with R^2 of 0.92 resembles the relation given by Castagna et al., 1985. Multiple regression analyses have been carried out to correlate the Vs with Vp, Vshas well as withVp, Vsh, ϕ for four above mentioned wells. The models are validated with the Vs log for wells KR Figure 5. The models predicted results are seen to match reasonably well with the observed Vs log for these wells.

These are the model equation constructed from Vp and Vs data

Model 1: Vs predicted = 0.69Vp – 544.82 with R^2 = 0.92
Model 2: Vs Predicted = 0.71Vp - 202.20Vsh – 559.75 with R^2 = 0.95
Model 3: Vs Predicted = 0.68Vp – 376.22Vsh – 783.87ϕ – 257.709 with R^2 = 0.96

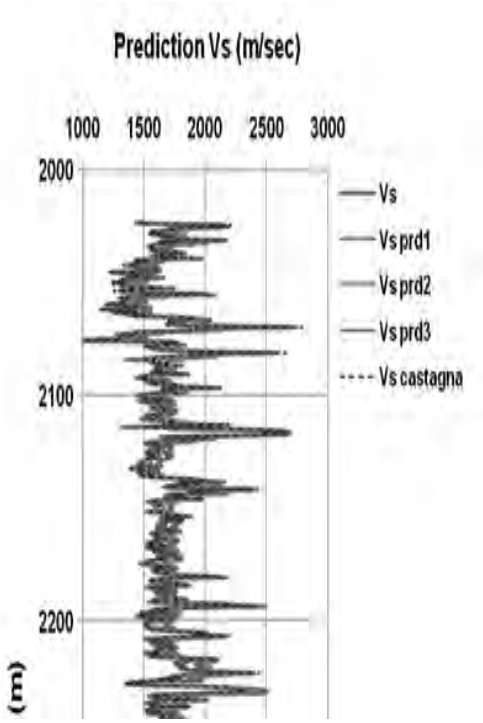

Figure 5: Validation of three models for well KR

Conclusion

The breakout and DIF are carefully identified from well KD and KL. The mean S_H orientation of N18.6^{0}E determinedherein is still broadly consistent with theorientation calculated previously and confirms a NNE-SSW maximum horizontal stress orientation. The natural fractures are also noticed from different depth interval in geological formation.The orientations of open fractures at various depth intervals are estimated from FMI log are in close match with the estimated S_H from breakout. The predicted Vp and Vsare closed match with Castagna" s equation. Then this developed model can be utilised for those wells where no Vp and Vs data are available. The prediction of Vs considering the effect of clay and porosity without discriminating lithology will be helpful for estimation for other rock mechanical parameters.

Acknowledgements

Authors are very much thankful to ONGC, Deharadun for providing us log data and geological information.

References

Aadnoy, B.S., 1990, Inversion technique to determine the in-situ stress field from fracturing data, Journal of Petroleum Science and Engineering, 4, 127-141.

Bell, J.S., 1990, The stress regime of the Scotian Shelf offshore eastern Canada to 6 kilometres depth and implications for rock mechanics and hydrocarbon migration. - In: Maury, V. and D. Fourmaintraux, eds., Rock at Great Depth, Rotterdam, Balkema, 1243-1265.

Biot, M. A., 1956, Theory of propagation of elastic waves in fluid saturated porous solids, Journal of the Acoustical Society of America, 28,168-178.

Castagna, J.P., Batzle, M. L. and Eastwood, R. L., 1985, Relationships between compressional-wave and shear-wave velocity in clastic silicate rocks, Geophysics, 50(4), 571-581

Ekstrom, M.P., Dahan, C.A., Chen, M.Y., Lloyd, P. M. and Rossi, D. J., 1987, Formation imagingwithmicroelectrical scanning arrays, Log Analyst, 28, 294–306.

Gassmann, F. 1951. Elastic waves through a packing of spheres. Geophysics 16 (4): 673–685.

Rajabi, M., Sherkati, S., Bohloli, B. and Tingay, M., 2010, Subsurface fracture analysis and determination of in-situ stress direction using FMI logs: An example from the Santonian carbonates (Ilam Formation) in the Abadan Plain, Iran, Tectonophysics, 492, 192-200.

IDENTIFICATION OF SUITABLE AQUIFER ZONES USING ELECTRICAL METHODS IN CENTRAL PART OF THE ADILABAD DISTRICT, TELANGANA, INDIA.

K.Lohith Kumar1, B.Nagaraju, R.Sudarshan, *K.Upender and B. MadhusudanRao

1. CSIR- National Geophysical Research Institute

Centre of Exploration Geophysics, Department of Geophysics,OsmaniaUniversity, Hyderabad-500007

lohithkumarkgeophy@gmail.com

Groundwater surveys are carried out in Adilabad district of Telangana though is bounded by perennial reverse like Godavari in the south and Penganga in the north and Pranahita in the east has its problem of scarcity of water, in lean seasons especially in the central part of hard rock region.The increasing demand for fresh water has necessitated the exploration for new sources of groundwater, particularly in hard rock terrain, where groundwater is a vital source of fresh water, a fast, cost effective and economical way of exploration is to study and analyze geophysical resistivity survey data, the hard rock begin with the volcanic Deccan traps on the top and the peninsular granitic complex at the base with the quartzites etc. on the pakhal group lying in between. The infra trappeans sedimentary layer at the bottom of trap rocks, the dolomitic and phylytic shale and sandstones in the pakhal appear for

the favourable of ground water occurrence .Besides their litho groups the NW-SE treading lineaments and the NW-SW lineaments cutting across which appear to represents structural faults might be helping occurrence and movement of ground water flow. It is in this context an area near by 250sq. km has been related in the Deccan trap covered area located east of Utnoor.

DC electrical methods are among the most popular tools for groundwater exploration in both porous and fissured media a methodology has been developed to estimate the hydraulic conductivity and transmissivity of hard rock granite and basaltic aquifer from geo electrical parameters. New approach has been developed to refine and improve Vertical Electrical Soundings (VES) interpretation which helps in sorting theresults in various categories of varying reliability. In the present study atotal150 VES were conducted by us with random distribution of locations with the main aim of locating bore-well points for irrigation, drinking water supply. The maximum spread of current electrodes in the Schulumberger survey is 120(AB/2)m, have in general revealed A&H type curves, and indicated 3or4 layers in the subsurface.

Further, for the analyses of the pseudo section advanced software methods of interpretation was adopted ,Resistivity and thickness values of VES points are different for each layer and it is observed that resistivity value varies from 3 ohm-m to 30 ohm-m with the thickness of 1.5m to 15m for the first layer and the second varies from 20ohm-m to 200ohm-m with the thickness of 6m to 30m and final layer varies from with the thickness of 30m to60m.On the basis of the resistivity and depth values together with local geology, more number of points are suggested for drilling in the study area, where high yielding bore wells were observed at low resistivity zones within the intratrappeans beds. The study has revealed that the Deccan traps and granites may provide groundwater high-potential zone, the majority of drilled bore-wells are of 1000 -1500 GPH yield used for irrigation and drinking purpose.

GEOMORPHOLOGY AND TECTONICS OF NORTHEAST TAMILNADU: A REMOTE SENSING STUDY

S.Aravind Bharathvaj and S.Lasitha

Department of Earth Sciences, Pondicherry University, Puducherry-605014
aravi13@gmail.com

The use of satellite remote sensing in delineating the structural trends has been proved beyond doubt owing to its spectral, spatial and temporal capabilities. Most of the tectonic activities that take place deep inside the surface of the earth, however have its own surficial implications, which enable the remote sensing tool to be used to identify those regions. The

Precambrian-Archaean rocks of Peninsular India show evidence of polyphase metamorphism, multiple deformations, repetitive folding and intense fracturing (Balaji, 2009). These highly fragmented and widely disseminated rock types show contrasting fold styles,multi-variate linear and planar features. A part of northernTamilNadu which exhibit a complicated tectonic history has been selected for the present study, which extends from 78°56′22″ to 79°54′36″ in the East and 12°30′to 11°31′32″ in the North. The major Districts in the study area are Villupuram, Tiruvannamalai, Cuddalore,Kanchipuram and the U.T of Puducherry. The study area is comparatively a flat terrain, except for the inselbergs present. The major rivers of Sankarabarani and Ponnaiar flow through the area.The Landsat 8 data product is used for interpreting Geomorphology of the area and ASTER elevation data is used to understand the terrain topography and most of the lineaments are identified from the DEM.

Majority of the selected area is covered by deep pediments. Alluvial plains are seen all over the region, indicating the drainage flow of the area. Even though delta is formed, they are not very prominently developed, as the region is evidently an eroding or submerging coast (Ramasamy et.al., 1987; Ramasamy&Balaji., 1995a). Also the delta is evidently marginated by a major graben that extends from Cumbam into the Bay of Bengal in NE-SW direction. Mio-Pliocene uplands are major features in the region. Other than this only the GingeeIntrusive are the denudational features that are totally contrast to the generally seen fluvial and weathered sediment plains. The lineaments are majorly aligned in three orientations. NW-SE, NE-SW, NWW-SEE and the small magnitude intraplate earthquake occur in the region are seen as associated with shear zones, which is suggestive of neo-tectonic activity. The Gangavalli shear zone (GSZ) passes through the study area, which coincided with the variation in the structural trend associated with lineaments and shear zones, which suggest that it can be responsible for the major changes in the directions of Sankarabarani and Ponnaiar River. The Geomorphic features such as the valley fills,intermontane valley show that the region is highly eroded than the surrounding regions. The Intermontane Valley is sure evidence that there is an active fracture or a fault. Linear depositional features associated with drainages show the deep seated fractures. Also deflected drainages are indications of presence of fractures. The eyed drainages along Ponnaiarare result of local uplift of the terrain. In the event of the upliftment is being small, it appear as sandbar deposit as in the case of Sankarabarani. The absences of a delta even in the presence of two rivers suggest that the area may be under submergence.The shoreline erosion patterns also indicate there is dominant erosion than deposition in the absence of any manmade structures. Overlapping lineaments and geomorphic anomalies indicate that this region is subjected to recent tectonic activities.The anomalies are mainly controlled by the NE-SW trending lineaments. The NE-SW trending dykes also seen prominently to the east of GSZ, and the SE-NW dykes are seen to the east. Dash et al (2013) suggested the dyke in the region shows distinctly different pole positions and magnetic orientation. It can be suggested that the GSZ may be acting as a major structural divide between the two types of dykes, which shows different trends to the east and west of the shear.This study is yet to be substantiated with a detailed geophysical study.

WEIGHT OF EVIDENCE MODELLING FOR LANDSLIDE SUSCEPTIBILITY ZONATION MAPPING IN GARHWAL HIMALAYA.

Pardeep K. Guri, P.K. Champati Ray, Ramesh Chandra Patel
guri.pradeep@gmail.com

Garhwal Himalaya is one of the most prominent hot spots of landslide occurrences in India. Many religion and tourists sites located in the region; therefore every year lakhs of tourists visited the area. Recently the area suffered by rapidly growing population and increasing number of hydropower projects, and unplanned infrastructure enhance the overall risk due to landslide occurrence significantly. Therefore, an attempt was made to assess landslide susceptibility using weights of evidence (WofE) bivariate statistical modelling techniques in Geographical Information System(GIS). This methodology has dual advantage as it demonstrates how to derive critical parameters including preparation of landslide inventory in spatio-temporal domain in one of the data scare region of the world. Secondly, it allows to experiment with various combination of parameters to assess their cumulative effect on landslides. Total 15 parameters and two different landslide inventories (prior to 2007 and 2007-2011) were prepared from satellite data analysis supported by field investigation used as inputs for model built and validation. Several combinations of parameters were carried out and finally best model have combination of 8 parameters predicted the overall 76.5% of landslide in 24% of total area demarcated as high and very high susceptibility zones. The study has highlighted that using such methodology landslide susceptibility assessment can be carried out in vast stretches of Himalaya currently affected by landslides.

EFFECTOF DEPTH OF BASEMENT TOPOGRAPHY ON GROUND MOTIONCHARACTERISTICS

Vinay Kumar, Kamal, Luxman Kumar and J.P. Narayan
Department of Earthquake Engineering, Indian Institute of Technology Roorkee, Roorkee- 247 667
vinaytomar23@gmail.com

The effects of basement topography (BT) on the characteristics of seismic waves have been receiving increasing interest after 1994 Northridge earthquake during which unique damage pattern in the cities of Santa Monica and Sherman Oaks was inferred. The effects of depth of BT on ground motion characteristics in both the quantitative and qualitative manners are recognized in this paper. Seismic responses of various BT models have been computed using a 2D fourth order accurate staggered-grid finite-difference algorithm for SH- wave propagation simulation in viscoelastic medium. In order to accurately quantify the depth of BT effects on the spectral amplification of ground motion, a frequency dependent damping in time-domain FD simulation is implemented based on rheology of generalised Maxwell body, widely known as GMB-EK rheological model. The analysis of simulated results revealed a drastic change in ground motion characteristics and generation of new seismic phases. The curves for average spectral amplification are not so smooth and symmetrical as was that of amplitude amplification of SH-wave because of presence of diffractions from the bottom and corners of the BT.Results of this study depict that consideration of BT effect is as much important as that of surface hills/ridges during seismic hazard assessment.

UPPER CRUST OF THE ARCHEANDHARWARCRATON IN SOUTHERN INDIA AS REVEALED BY SEISMIC REFRACTION TOMOGRAPHY AND ITS GEOTECTONIC IMPLICATIONS

N. Damodara, V. Vijaya Rao and Kalachand Sain
CSIR-National Geophysical Research Institute, Uppal Road, Hyderabad 500007, India.
naradamu@gmail.com

Imaging shallow crustal structure is essential to extend the geological information from surface mapping to a depth and to develop tectonic models. Seismic refraction data acquired along a 200-km-long line in the Dharwar craton of the Indian shield are used to derive the crustal velocity structure using seismic tomography. The structures have been assessed through checkerboard tests to demonstrate the reliability of the final velocity model. Further, the final model is tested for its reliability by synthetic modeling and to identify the probable presence of artifacts, if any. Upper-crustal velocities vary between 5.7-6.4 km/s and are determined to a depth of 10 km, probably due to very low-velocity gradients in the upper crust. Undulating high and low velocities in the top layers of the crust are terminated at a depth of 7-8 km, indicative of a probable detachment. We interpret the undulating upper-crustal velocity layers to represent a fold-thrust belt structure that developed during a collision in a transpressional tectonic regime, consistent with the model of Chadwick et al. (2000; 2007), which suggests oblique convergence and accretion of two crustal blocks in the region. The velocity structure also correlates reasonably well with the distinct geological units. We interpret the steepness of the undulating layers as representative of faults that bound various tectonic domains.

THE LG SEISMIC WAVE ATTENUATION IN GUJARAT STATE, WESTERN INDIA

Sandeep Kumar Aggarwal[1] and Prosanta Kumar Khan[2]
[1]*Institute of Seismological Research, Gandhinagar, Gujarat, India*
sandeep12480@gmail.com
[2]*Department of Geophysics, Indian School of Mines, Dhanbad, Jharkhand, India*
pkkhan_india@yahoo.com

The Gujarat State of Western India, concern of the present study, lies between latitude 20 - 25°N and longitude 68 - 75°E, and mainly covers the Kachchh, Saurashtra, Cambay and western segment of Narmada geo-fracture (Fig. 1). During the break-up of Gondwana in the Jurassic, this area was affected by rifting with a roughly west-east trend. During the collision with Eurasia the area has undergone shortening, involving both reactivation of the original rift faults and development of new low-angle thrust faults (Naini and Talwani, 1983; Biswas, 1987; Storey et al., 1995). The three failed rifts: Kachchh, Cambay and Narmada and several active faults are located in these regions. During post-collision, the Kachchh and Narmada rifts became zones of compression giving strike-slip and thrusting tectonic environment. The two rifts have E–W trending major faults that are active, while the Cambay basin has N to NNW trending marginal faults which are less active at present. The Saurashtra region occurs as a horst bounded by these three rifts in the east, south and north, and was evolved during main tectonic phase in the late cretaceous. Thus, the region has witnessed various tectonic activities such as inter-continental splitting, episodic rifting, reactivation of the ancient fault zones and Deccan volcanism due to Reunion plume activity.

The above description clearly demonstrates that the region is one of the most seismically active intra-continental regions of the world, and was suffering from the flurry of large earthquakes since historical times (Rajendran and Rajendran, 2001). The largest historical earthquake occurred in the region on June 16, 1819, has created a ~E-W-striking 100 km long highland, known as Allah Bund (Johnston, 1996; Bilham, 1998; Rajendran and Rajendran, 2001). Another damaging earthquake of Mw 6.0 with maximum intensity of IX in MM Scale occurred near Anjar, Gujarat in 1956. The recent one is the 26 January 2001 Mw 7.7 strong Bhuj earthquake jolted the entire Gujarat State. This earthquake was the strongest ever happened in Western India, over last more than 175 years, and took more than 12,000 human lives. Different parts of the state occasionally records moderate to great earthquakes, and interestingly there exist all the four seismic zones V, IV, III and II in Gujarat under seismic zoning map of India (BIS 2002). The Kachchh and adjoining region along the Pakistan border falls under zone V (highest seismic zone). A narrow fringe of the northern Kathiawar peninsula and remaining part of Kachchh falls under zone IV. The rest part of Gujarat region falls under zones III and II. The rapid growth of industrialization as well as the cities makes the Gujarat more prone to seismic risk. The region houses one of the world's largest oil refineries, numbers of chemical industries, large maritime facilities, etc. Gujarat is also in the process of developing number of Special Economic Zones and Special Investment Regions. All these information indicate that the incidences of even a moderate magnitude earthquake may cause higher hazard potential in larger areas due to dense population, non-engineered structures and efficient transmission of wave energy.

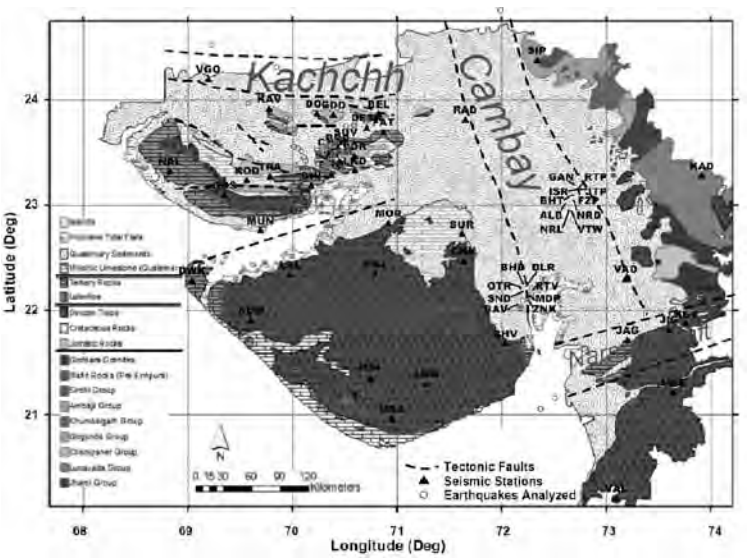

Figure 1. The geology map describes the seismograph stations and locations of epicenters of earthquakes in the State of Gujarat.

We carry out the analysis of Lg seismic wave attenuation over the Gujarat region through generalized inversion at various frequencies between 0.5 and 10 Hz, and the selected frequency band is seismically hazardous. The inversion at these frequencies results average frequency dependent attenuation structure of the entire Gujarat region. The input dataset consist of 40 Kachchh, 18 Saurashtra and 2 Mainland crustal earthquakes recorded at 60 sites in Gujarat. A total of 60 earthquakes have 400 travel paths recordings in geographical region Gujarat at a distance ranges ~ 200 to 600 km. The magnitude size M 3.6 to 5.1 and best quality waveforms were used to estimate average Q_{Lg} of Gujarat region. We found the relationships for average frequency dependent attenuation as $Q_{Lg}(f) = 357f^{0.17}$ for frequency range 0.5-2.0 Hz and $Q_{Lg}(f) = 250f^{0.65}$ for frequency range 2.0 to 10 Hz for Gujarat region. For complete frequency band 0.5-10 Hz, the relationship is found to be $Q_{Lg}(f) = 333f^{0.45}$ (Fig. 2, Table 1).

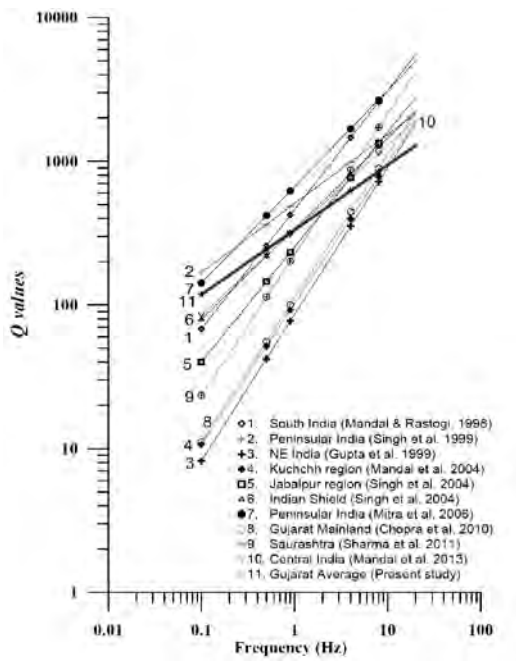

Figure 2. Comparison of Q values between Gujarat (present study) and other regions of India.

The results are compared with other tectonics regions of India as well as from other studies for Gujarat (Fig. 2, Table 1). The results are comparable with local geological condition and agree with estimates of site amplification by other researchers. This study is the first attempt to determine Q_{Lg} for Gujarat region using Gujarat earthquakes and provide understanding of attenuation of Lg waves required for the prediction of ground motions during future earthquakes.

Table 1. Various seismic wave's attenuation relationships as $Q= Q_0 f^n$ for different parts of India.

Sl. No.	Study area	Average $Q=Q_0 f^n$	References
1	South India	$Q_c=460f^{0.83}$	Mandal and Rastogi(1998)
2	India Shield	$Q_{Lg}=508f^{0.48}$	Singh et al.(1999)
3	North East India	$Q_c=86f^{1.02}$	Gupta et al.(1999)
4	Kuchch region	$Q_c=102f^{0.98}$	Mandal et al.(2004)
5	Indian Shield	$Q_{Lg}=800f^{0.42}$	Singh et al.(2004)
6	Jabalpur region	$Q=339f^{0.63}$	Singh et al.(2004)
7	Peninsular India	$Q_{Lg}=665f^{0.67}$	Mitra et al.(2006)
8	Kachchh,India	$Q_s=121f^{0.92}$	Chopra et al.(2010)
9	Saurashtra, Gujarat	$Q_c=224f^{0.98}$	Sharma et al.(2011)
10	Central India	$Q_s=332f^{0.59}$	Mandal et al. (2013)
11	Gujarat	$Q_{Lg}=333f^{0.45}$	Present Study

References

Bilham, R., Slip parameter for the Rann of Kachchh, India, 16 June 1819, earthquake, quantified from contemporary accounts, *Geol. Soc. Spec. Publ*., 1998, **146**, 295-319.

Biswas, S. K., Regional tectonic framework, structure and evolution of the western marginal basins of India. *Tectonophysics*, 1987, **135**, 307–327.

Chopra, S., Kumar, D. and Rastogi, B. K., Attenuation of high frequency P and S waves in Gujarat region, India. *Pure and applied Geophysics,* (2010), **168**, no. 5, 797-813.

Gupta, S. C. and Kumar, A., Seismic wave attenuation characteristics of three Indian regions: A comparative study. *Current Science*, (1999), vol. **82,** no. 4, 407-413.

Johnston, A. C., Seismic moment assessment of earthquakes in stable continental regions – II. Historical seismicity, *Geophys. J. Int*. 1996, **125**, no.3, 639-678.

Mandal, H. S., Khan, P. K. and Shukla, A. K., Shear wave attenuation characteristics over the Central India Tectonic Zone and its surroundings. *Journal of Asian Earth Sciences*, (2013), vol. **73**, 440-451.

Mandal, P., Jainendra, Joshi, S., Kumar, S., Bhunia, R. and Rastogi, B. K., Low coda Qc in the epicentral region of the 2001 Bhuj earthquake of Mw 7.7. *Pure and applied Geophysics,* (2004), **161**, 1635-1654.

Mandal, P. and Rastogi, B. K., A frequency dependent relation of coda *Qc* for Koyna-Warna region, India. *Pure and applied Geophysics,* (1998), **153**, 163-177.

Mitra, S., Priestley, K., Gaur, V. K. and Rai, S. S., Frequency dependent Lg attenuation in the Indian platform. *Bull. Seismol. Soc. Am*., 2006, **96,** no. 6, 2449-2456.

Naini, B. R. and Talwani, M., Structural framework and the evolutionary history of the continental margin of western India. *AAPG Mem.,* 1983, **34**, 167–191.

Rajendran, C. P. and Rajendran, K., Charactristics of deformation and past seismicity associated with the 1819 Kutch Earthquakes, noth-western India. *Bull. Seismol. Soc. Am*., 2001, **91**, 407-426.

Sharma, B., Kumar, D., Teotia, S. S., Rastogi, B. K., Gupta, A. K., Prajapati, S., Attenuation of coda waves in Saurashtra region, Gujarat (India). *Pure and applied Geophysics*, (2011), doi: 10.1.007/s00024-011-0295-1.

Singh, S. K., Garcia, D., Pacheco, J. F., Velenzuela, R., Bansal, B. K. and Dattatrayam, R.S., *Q* of the Indian shield. *Bull. Seismol. Soc. Am.*, 2004, **89,** 1620-1630.

Singh, S. K., Ordaz, M., Dattatrayam, R.S. and Gupta, H. K., A spectral analysis of May 21, 1997, Jabalpur, India earthquake (Mw = 5.8) and estimation of ground motion from future earthquakes in the Indian shield region. *Bull. Seismol. Soc. Am.*, 1999, **89,** 1620-1630.

Storey, M., Mahoney, J. J., Saunders, A. D., Duncan, R. A., Kelley, S. P. and Coffin, M. F., Timing of hot spot related volcanism and the breakup of Madagascar from India. *Science*, 1995, **267**, 852–855.

3D SEISMIC MODELING : AEFFECTIVE TOOL FOR THE DESIGNING OF SEISMIC SURVEY

Luxman Kumar[1],Prasanna kumar[2] and Dinesh Kumar[3]

1 – Department of Earthquake Engineering, Indian Institute of Technology Roorkee.
2 - Oil and Natural Gas Corporation Limited, Dehradun.
3 - Department of Geophysics, Kurukshetra University, Kurukshetra.
kumarluxman90@gmail.com

The success of a seismic survey depends on its planning. Seismic modeling plays an important role in the planning of seismic survey. It is also useful for seismic processing, interpretation, and reservoir characterization which makes the results more effective and reliable. Seismic forward modeling reduces the risk in seismic exploration by providing quantitative information to design 3D seismic surveys in a better way.

The present study illustrates the applications of 3D Seismic modelling for seismic survey planning. The models have been generated with the help of the horizons, velocity volume, and well log data. A few survey geometries have also been generated with the help of MESA software. Different parameters of seismic acquisition have been tested and used in these survey geometries. A 3D seismic modelling (Ray tracing) has done with the help of generated model and geometries using the NORSAR Software. The study shows the importance of 3D seismic modellingto design the survey geometry and to know how different survey geometries are helpful to illuminate the area of interest in the subsurface or to illuminate the different horizons of interest. This has been found to be useful to finalize the geometry of seismic survey.

DELINEATION OF CHANNEL COMPLEX WITHIN MIOCENE FORMATION USING MULTI ATTRIBUTE ANALYSIS AND SPECTRAL DECOMPOSITION TECHNIQUES

K.Ramachandran*, Santosh Dhubia and P.H.Rao

Gujarat Energy Research and Management Institute, Gandhinagar
ramachandran.K@germi.res.in

Channels play an important role in exploration for Oil & Gas. Delineating channels and the sediment fill within the channels is vital for identification of channel prospects. 3D Seismic data when subjected to multi attribute analysis will pave way for delineation of channels and the sediment filled within the channels. Multi attribute analysis using amplitude attributes and spectral decomposition are found to be best tools. In this paper an effort was made to delineate the channels by using the spectral decomposition technique and Multi attribute analysis, to demarcate the extension of a meandering channel complex in an area falling in Tarapur block of Cambay Basin. Multi attribute analysis suggest possibly the channel is filled with sand and a good candidate for exploration.

ENHANCEMENT OF STRATIGRAPHIC FEATURES USING SELECTIVE VOLUME SEISMIC ATTRIBUTES

Radhika Arora and Kedareswarudu Utla
University of Petroleum and Energy Studies, Bidholi, Dehradun, Uttarakhand
kedareswarudu@yahoo.com

Seismic Attribute Analysis is a way to describe and quantify the inherent characteristics of Seismic Reflection Character in seismic data. Seismic attributes enhance structural, stratigraphic and depositional environment hidden in the seismic data. Attributes derived from the phase content of seismic data improves the continuity of seismic reflectors and is an important attribute for the interpretation of seismic startigraphy and depositional regimes. However, multi-attribute analysis is preferred to improve the quality of interpretation andamplify the subtle changes in lithology.An understanding of the working of attributes is required to rightly set the user defined parameters inorder to avoid any geostatistical errors. This paper aims to figure out a set of attributes that can be specifically applicable to enhance the sequence stratigraphicfeatures in any 3D seismic cube of a region using PETREL software.A cluster of attributes are available under the Geophysics option in the models paneof Petrel for enhancing the structural as well as the stratigraphic features present in the 3D seismic data. However, only a few of them are helpful in amplifying the stratigraphic features. Attributes such as RMS Amplitude, Envelope, Structural Smoothening, Instantaneous Phase, Chaos, Variance and Cosine of instantaneous phase from the volume attribute library in Petrel are generally applied on the original seismic cube. The same attributesare used varying the user defined parameters to have a clear understanding of the functioning of these attributes.It is observed that a few of them are only able to give the expected results. Among them Instantaneous Phaseand Cosine of Instantaneous Phase gave the best results in enhancing the stratigraphic features because of the invariant nature of the attributes in terms of amplitude and also both the weak and strong seismic events are enhanced equally. Amplitude peaks and troughs remained at the same position but strong as well as weak events exhibited equal strength. Structural smoothening also well demarcated the stratigraphic boundaries by reducing spatial noise present in the dataand increased the continuity of reflectors. RMS Amplitude and Envelope are not of much help as they are basically used to distinguish the lithology due to the difference in the energy content of the various porous and non-porous media.

INVERSION OF WELL LOG DATA FOR BETTER DETERMINATION OF PETROPHYSICAL PARAMETERS

Ajay Malkoti
JRF at AcSIR-NGRI
CSIR – National Geophysical Research Institute, Hyderabad 500007
ajmalkoti@gmail.com

In this work, an attempt has been made to invert the well log data using precise estimates of average mineralogical composition for different lithologies. The method has been verified by using synthetic data then, applied to well log data of a decining oil field operated by the Oil and Natural Gas Corporation of India (ONGC). Available logs were used for determination of petrophysical parameters viz. porosity, shale volume, sand volume andsaturation in different zones of reservoir.

The forward modelling technique,whichuses standard well log response equation, is based on the mineralogical composition. It includes, determination of lithologiesthatare present in the reservoir with the help of some priori data, determination of an average mineralogical model corresponding to eachlithology,computation of the lithology response by summing the responses ofminerals present in

the lithology.Based on available information,suitable models for the average mineral composition of rock (e.g. shale) have been selectedin this work. The method was applied to Gamma Ray, SP, Density, Porosity logs that exhibit linear response.It is known that Resistivity logs have nonlinear nature which could be attributed to shale and presence of more than one fluid. Hence, to deal with non-linearity we used Genetic algorithm for optimization. The inversion results for ankleshwar well data showed an average error of about 5.27 % between the synthetic and real logs.

COLLOIDAL GREEN QUANTUM DOTS AS GROUNDWATER PARTICLE TRACERS

Lopamudra Bhattacharjee[a], R. Rangarajan[b] and Rama Ranjan Bhattacharjee[a]

[a]PSG Institute of Advanced Studies, Coimbatore, Tamil Nadu 641004

[b]CSIR-NGRI, Hyderabad

Tracer test methods can be applied in vadoze / unsaturated zones and saturated / groundwater zones for determining transport parameters such as transport velocity, porosity, dispersivity etc. These are important parameters to study hydrogeology of any region. Conventional radioactive chemicals, gases or molecular tracers have been used to study hydrogeology for decades in order to qualitatively or quantitatively measure how water flows through a reservoir, as well as being a useful tool for estimating residual water saturation [1-7]. However, use of radioactive elements as tracers has potential hazardous effects on the environment. Although some gamma radiotracers are good for hydrological studies, they cannot be used because of high radio toxicity and without prior permission from atomic energy regulatory board (AERB) to use in laboratory and field conditions. Tritium is already considered to be a good tracer as one can easily get permission from AERB, but it cannot be put in large quantities in the aquifer medium. Conventional tracers requires large quantum of tracer material. Large quantum of tracer material will change the hydraulic characteristics of the medium. Other main issues with non- radioactive molecular tracers is their molecular dimensions and hence very high diffusion coefficient [1,2,8-11]. In the case of laminar flow with very low velocity (0.00001-0.001m /d), diffusion coefficient will be very high for ionic and tritium tracers due to concentration gradient. Due to high diffusion coefficient of the conventional molecular tracers, it is very difficult to determine actual groundwater flow velocity. Retrieving these tracers from bore-well experiments take long times (100 days to 2 years) depending on the dimensions of the bore-well and injection/arrival path lengths. Also due to dilution effect and large mixing, the clear peak signal from the tracers may not be picked under field conditions. Lot of important information regarding hydrogeology is hence lost and cannot be easily retrieved.

Under these conditions, we propose that nano-dimensional tracers will give reliable information for hydrogeological studies. This is due to the controlled dimensions and smaller diffusion coefficients of these systems necessary for easy and quick retrieval from reservoirs that help geologists to analyze the flow behavior of reservoir water more accurately. Thus, known glitches associated with conventional tracer materials, has turned geologist's attention on nanomaterials because they have low diffusion and uniform flow in fluid channels [11-13]. Thus it will help in determining hydraulic connectivity across geological barriers, estimation of flow velocity and aquifer parameters, preparation of groundwater flow maps, selection of sites for artificial recharge, waste disposal etc. Nanoparticles due to their unique electronic and optical properties have been used for sensor applications in various fields especially in biology [14-18]. Researchers have used nanoparticles tagged with bar codes of different fluorescent color, for providing the information about fluid movements in vivo as well as cell imaging applications. Recent literature shows extensive work has been done in the area of MRI and other imaging techniques using nanoparticles as tracers. There are very few reports on using nanoparticles in geological studies. Zhao and coworkers have shown that iron nanoparticles can be transported like a tracer without significant

retardation thorough porous media. Recently, Subramanian and coworkers has reported the carbon quantum dots (CQDs) as potential tracer to explain the exact manner of preferential flow with respect to chemical tracer [11] though the quantum dot used in their studies have very low quantum yield values reported. But there is no report on comparative tracer studies through packed sand column where conventional radiotracer and chemical tracer is simultaneously injected with CQD and the arrival times were compared.

In the current work, we report the synthesis of highly fluorescent and size controllable CQDs and their flow behavior in a packed sand column. In the column study under controlled condition, it is possible to measure exactly the input water used for every time interval, output water collected, stored water at any point of time very accurately as the dimensions of the column is known. Hence the column study provides scope to analyze the performance of different tracers and to select the suitable and better tracer for water movement through different type of formation to estimate reliable hydraulic parameters. The porous media used in the present column experiment is medium to fine sand. The sand samples are from various regions of the Indian peninsula including Indo Gangetic Alluvial Plains, Punjab Agricultural University campus, Ludhiana and Punjab. We have studied comparative flow behavior between the CQDs with conventional tracers such as tritium and chloride within the column. The column studies indicated that nano-tracers arrived together with the conventional tracers. It also indicated that these studies required small quantity of nano-tracer material with reliable output signal. The parameters estimated through column studies using the material of the field area can be unique and more reliable. The CQD systems used as nano-tracers are highly fluorescent and can be easily detected using fluorescence microscope at very low dilutions (0.01 wt%). The CQDs are polymer stabilized and can be easily dispersed in water. The dispersion stability in water has been studied at various pH, temperature and pressure using the fluorescence property of the CQDs. This is important so as to determine the robustness of the material and its future applications as geological tracers. The photostability of the CQDs was also tested which is important for its application in natural environments. The fluorescence property of the CQDs was compared with that of humic acid, a natural contaminant found in ground water having fluorescence properties, for realistic screening of the tracer behavior for field studies. Finally we showed that the CQDs can be coated with magnetic iron oxide for easy separation and detection of the CQD tracer from bore-well excavations. That will be paving the pathway for new generations of hybrid nano-tracres.

References:

C. Leibundgut, Tracer technologies for hydrological systems, 1995.

S. N. Devis, G. M. Thompson, H. W. Bentley, G. Stiles, Ground water tracer a short review, *Ground water*, 1980, **18**, (1) 14-23.

L. Maurice, J. A. Barker, T. C. Atkinson, A. T. Williams, P. L. Smart, A tracer methodology for identifying ambient flows in boreholes, *Ground water*, 2011, **49**, (2) 227–238.

P. G. Cookas, D. K. Solomonb, Recent advances in dating young groundwater: chlorofluorocarbons, $^{3}H/^{3}He$ and ^{85}Kr, *Journal of hydrology*, 1997, **191**, 245-265.

W. Drost, D. Klotz, A. Koch, H. Moser, F. Neumaier, W. Rauert, Point dilution methods investigating ground water flow by means radioisotopes, *Water resources research*, 1968, **4**, (1), 125-146.

W. E. Sanford, R. G. Shropshire, D. K. Solomon, Dissolved gas tracers in groundwater: simplified injection, sampling, and analysis, *Water resources research*, 1996, **32**, (6), 1635-1642.

F. Winter, Using tracer techniques to investigate groundwater recharge in the Mount Carmel aquifer Israel, Ph.D Thesis, *Albert ludwing university*, Freiburg, 2006.

N. M. Antovic, N. Svrkota, I. Antovic, R. Svrkota, D. Jancic, Radioactivity in Montenegro beach sands and assessment of the corresponding environmental risk, *Isotopes in environmental and health studies*, 2013, **49**, (2), 153-162.

G. Yuce, M. Gasparon, Preliminary risk assessment of radon in groundwater: a case study from Eskisehir, Turkey, *Isotopes in environmental and health studies*, 2013, **49**, (2), 163-179.

W. E. Sanford, W. A. Hertig, A. L. Herczeg, Preface: Insights from environmental tracers in groundwater systems, *Hydrogeology Journal*, 2011, **19**, 1–3.
S. K. Subramanian, Y. Li, L. M. Cathles, Assessing preferential flow by simultaneously injecting nanoparticles and chemical tracers, *Water resources research*, 2013, **49**, 29–42.
Tcherniak, A. Prakash, J. T. Mayo, V. L. Colvin, S. Link, Fluorescence correlation spectroscopy of magnetite nanocrystal diffusion, *J. Phys. Chem. C.*, 2009, **113**, 844–848
H. S. Salim, Applications of nanoparticle image velocimetry in nanofluids, Master's Thesis, *University of Tennessee*, 2011.
Y. Kim, R. C. Johnson, J. T. Hupp, Gold nanoparticle-based sensing of spectroscopically silent heavy metal ions, *Nano letters*, 2011, **1**, (4), 164-167.
P. Sharma, S. Brown, G. Walter, S. Santra, B. Moudgil, Nanoparticles for bioimaging, *Advances in colloid and interfacescience,* 2006, **123**, 471–485.
Y. L. Hung, T. M. Hsiung, Y. Y. Chen, Y. F. Huang, C. C. Huang, Colorimetric detection of heavy metal ions using label-free gold nanoparticles and alkanethiols, *J. Phys. Chem. C.*, 2010, **114**, 16329–16334.
C. T. Yavuz, A. Prakash, J. T. Mayo, V. Colvin, Magnetic separations: From steel plants to biotechnology, *Chemical engineering science*, 2009, **64**, 2510–2521.
S. R. Kanel, R. R. Goswami, T. P. Clement, M. O. Barnett, D. Zhao, Characteristics of surface stabilizedzero-valent iron nanoparticles inporous media,*Environ. Sci. Technol.* 2008, **42**, 896–900.

EARTHQUAKE ACCELERATION RECORDS AND DIGITAL FILTERING

Alka Rani, Sonia Devi and ShivaniBaliyan
Department of Geophysics, Kurukshetra University Kurukshetra 136119 India
alkaggoswami@gmail.com

The digital recording of earthquake waveforms provides an opportunity to view the waveforms in a different way and perform advance signal processing techniques. One of the important applications with digital data is to correct the data for the effect of the instrument and to view the signals (time or frequency domain) as ground displacement, velocity or acceleration within the bandwidth where they have a signal level above the background noise. The most common operation on earthquake waveforms is to filter the earthquake waveforms to enhance some features like arrival times of different phases and suppress others. A number of studies have discussed the problem of applying different causal and acausal filters for processing earthquake accelerograms.

The present study illustrates the effects of digital filtering on the acceleration records from earthquakes. The different types of digital filters have been used for this purpose. This includes Butterworth filters, Chebyshev and Bessels filters of different orders. The acceleration records of the earthquakes occurred in Himalaya has been used for this investigation. The effects of types of different filters have been shown on displacement, velocity and acceleration records. The effects of digital filters on different parameters like peak ground displacement, peak ground velocity and peak ground acceleration, Arias intensity and Fourier amplitude spectrum have been examined here. The study will help to select the appropriate filters for the processing of earthquake records.

A COMPARATIVE STUDYOF DEPTH TO BED ROCK DERIVED FROM MASW AND SEISMIC REFRACTION METHODS FOR SITE CHARACTERIZATION OF CHENNAI CITY

P.Prabhakara Prasad., Trupti.S., PavanKishore.P., Srinivas GS and Seshunarayana.T.
CSIR-National Geophysical Research Institute, Hyderabad-500 007
pvsspp@ngri.res.in

Multichannel analyses of surface waves (MASW) and seismic refraction surveys were carried out in Chennai region for determining the variation of shear wave velocity and depth to bed rock to use in site- characterization studies at Chennai. Primary-wave velocity (V_P), shear wave velocity (V_S) are estimated by using Refraction and MASW seismics at 204 selected locations situated in and around Chennai city. From refraction seismics the sub surface layering andits primary wave (Vp) velocities and depths were determined. From MASW studies thevariation of shear wave velocity(Vs)with depth and depth to Bedrock wasestimated. Comparative study has been made on the bedrock depth Contour maps prepared from MASW and Refraction seismics.It can be seen from the depth counter maps that the depth to bedrock is shallow in the southern part and deeper bedrock in the northern part of Chennai region. Bed rock depth values are varying from5-35m from south to North throughout Chennai region. The Vp and Vs values obtained from these studies shows better resolution with depth. It is concluded from the results that the Bed rock depth values obtained from MASW and Refraction studies are also in good agreement.

AN OVERVIEW ON DEVELOPMENT OF SEISMIC ZONING MAPS OF INDIA

Neeraj Chaudhary*, NehaTanwar and AshwaryaRana
Department of Geophysics, Kurukshetra University, Kurukshetra – 136119
neerajchoudhary035@gmail.com

India is one of most earthquake vulnerable countries in the world which has experienced four great earthquakes (1897 Shillong Plateau, 1905 Kangra, 1934 Bihar-Nepal and 1950 Assam) within about fifty years of the short time interval. The level of seismic hazard in India is expressed in terms of 'seismic zoning maps' prepared by Bureau of Indian Standards (BIS). The seismic zoning process is referred as the geographical delineation of areas having different potentials for hazardous effects from future earthquakes. The purpose of this poster presentation is to describe the history of development of seismic zoning maps of India through chronological order including the limitations on its uses. It also discusses the progressive development of the seismic zonation map of India and how it was reviewed, revised and modified periodically with the availabiity of more data and with better understandings of dynamics of the earthquake. The seismic zonation is a process which provides information about any decision making for urban, regional planning or for earthquake design in earthquake prone areas. Therefore, such observations points out that there is a clear cut and urgent need for updating the seismic zonation of vulnerable areas for bedrock motion thus becomes important, so that the planners and administrators can make use of it after applying appropriate amplification factors to take into account the local soil conditions,for better land use planning and safety development.

DIGITAL IMAGE ENHANCEMENT OF SINGHBHUM SHEAR ZONE AND SORROUNDINGS USING LANDSAT ETM+ DATA

Sandeep Kumar Gupta*, S K Pal
Department of Applied Geophysics, Indian School of Mines, Dhanbad-826004

For optical remote sensing spatial and spectral resolution are highly correlated factors. For design constrains of sensors, there is an inverse relation between these parameters. General sensors with high spectral resolution, characterised by capturing the radiance from different land covers in a high number of bands of em spectrum and do not have the optimal spatial resolution, and vice-versa. However the high spectral and spatial resolution is desirable when undertaking the complex morphological studies. A high spectral resolution eases the discrimination of land cover types on the other hand spatial resolution delineate the area covered by each land cover type as well as to locate the terrain features and structures. Thus the fusions of two band images have become a promising technique to obtain images with high spatial and spectral resolution. For the purpose of image enhancement I have taken Landsat ETM+ data and fused two and more band data to obtain the enhanced images by the IHS fusion technique, Wallis filtering technique and Wavelet resolution merge techniques. Image is clearly enhanced and different morphological features are easily depictable by visual interpretation technique.

References:

Pal S. K., MajumadarT. J., Bhattacharya A.K., 2007, ERS-2 SAR and IRS 1-C LISS-III data fusion: A PCA approach to improve remote sensing based geological interpretation. ISPRS journal of Photogrammetry and Remote sensing 61,281-297.

Welch R., Ehlers M., 1987, Merging multi resolution SPOT HRV and Landsat TM data. Photogram. Eng. Remote Sens., vol. 56, pp. 301-303.

Wilson T. A., Kabrisky M., 1997, Perceptual-based image fusion for Hyperspectral data, IEEE Trans. Geosci. Remote Sensing, vol. 35, pp. 1007-1017.

QUANTIFICATION OF GAS HYDRATES FROM SEISMIC DATA IN FRACTURED SHALE IN KRISHNA-GODAVARI BASIN IN THE EASTERN INDIAN MARGIN

Vivekanand Pandey* and Kalachand Sain
CSIR-National Geophysical Research Institute, Hyderabad - 07
* *mr.vivekanandpandey@gmail.com*

Gas hydrates have been recovered in vertically fractured shale by the drilling and coring of Indian National Gas Hydrates Program (NGHP) Expedition-01 at the drilling site 10 in Krishna- Godavari (KG) basin of the eastern Indian margin. The log data have been used to estimate the saturation of gas hydrates in such an anisotropic media. Here we estimate the saturation of gas hydrates from seismic data along a line passing near the site 10 and apply two methods for assessing the results. In both methods, we have calculated the acoustic impedance from seismic data using the Hampson-Russel Seismic (strata) software. In the first method, we establish an empirical relation between the acoustic impedance and the porosity from well log data to obtain the porosity from acoustic impedance derived at each CDP of seismic data. The porosity derived from seismic data and the modified Archie's constants are then used to estimate the saturation of gas hydrates along the seismic line with a constraint from log data. The result shows gas hydrates as laterally varying up to 25% of pore space.

In the second method, gas hydrates have been estimated by rock physics transform. Saturation of gas hydrates from sonic velocity at site 10 is estimated assuming anisotropy from fracture filling gas hydrates. Then the ratio of true acoustic impedance to acoustic impedance of water bearing formation

(RAI) is calculated at the drilling site. Empirical relation from cross plot of saturation at site 10 from sonic velocity and ratio of acoustic impedance (RAI) is then used to estimate the saturation of gas hydrates from seismic data, which laterally vary up to 25% of pore space. Gas hydrates estimated by both methods match reasonably with the saturation obtained by pressure core at the well site, and provide a good assessment of results.

Data:

From the twelve lines (six in-lines and six cross-lines) high resolution MCS data around site 10 in KG basin was provided to NGRI from ONGC under the NGHP for the assessment of gas-hydrates, we have used Line-a (NW-SE) passing through nearby the site 10. The seismic data processing is performed in amplitude preserving manner. PSTM should be used for AVA analysis because it collapses the diffraction to the target depth to be smaller than the Fresnel zone and hence increases the lateral resolution (Brekhout, 1985; Mosher et al. 1996). PSTM is preferred to pre stack depth migration (PSDM) for AVA analysis because PSTM preserves amplitude better than PSDM (Per Avseth; 2010).

The post stack inversion is the classical seismic inversion to give acoustic impedance (AI) but it is not sufficient for estimation of fluid content. AVO attributes can support post stack AI inversion most of the issues related to fluid content, however during the post stack inversion we ignore the fact that Vp and Vs are related to each other. Pre-stack AI inversion can fix these problems. Pre-stack AI inversion involves modified Fatti-smith version (Fatti et al. 1994) Aki-Richards's AVA equation. We have used the same PSTM gather and well log data (P-wave velocity, S-wave velocity and density) at site 10 as input for pre-stack AI inversion in STRATA (CGGVeritas Hampson-Russell) software, Fig. (1) Shows inverted AI along the line.

Saturation estimation of gas-hydrates using Acoustic Impedance (AI):

Presence of gas-hydrates in sediments makes it highly resistive than the background water bearing sediments. Assuming pore spaces are filled with water and gas hydrates Archie's law Equation (1) can give water saturation and hence the gas hydrates saturation.

$$S_h = 1 - \left(\frac{R_0}{R_t}\right)^{\frac{1}{N}}$$

$$\text{where } R_0 = a\emptyset^{-m}R_w \qquad .1$$

R0 is resistivity of water saturated sediments, Rt is the true resistivity of formation, is density porosity and Rw is the formation water resistivity while a, m, n, are derived imperially. Simple Archie's law gives a=3.2, m=0.5 and n=2 and equation (1) over estimates the gas hydrates saturation obtained from pressure core data at site 10. Lee and Collett [2009] have modified these Archie's constants (a=3, m=2, and n=3) to get saturation comparable to that of estimated by pressure core data, that is still showing some deviation from pressure core data. to overcome this problem we have used saturation exponent n=3 and equation (2) and (3) for R0 and Rt for gas hydrates zone. Where a0=3.2, m0= 0.5 are the Archie's constant for the sediments saturated with water, and a=3, m=3 are Archie's constant for sediments having gas hydrates.

$$R_0 = a_0\emptyset^{-m_0}R_w \qquad .2$$

$$R_t = a\emptyset^{-m}R_w \qquad .3$$

Estimation of gas-hydrates saturation using the resistivity method needs true porosity of the formation. Porosity along the seismic line can be obtained from AI, using AI and porosity relation equation (4) from well log at site 10.

$$\emptyset = 239.5(AI)^{-1.27} \quad .4$$

Fig. (2) Shows porosity derived from AI along the line using above relation and hence gas hydrates saturation along the seismic line.

Under natural compaction, relation between seismic parameter (VP, density and P-wave acoustic impedance) and sediment parameter (porosity and saturation) can be established using rock physics. Estimation of gas hydrates from seismic data is a two-step procedure: (i) inversion of seismic data to acoustic impedance and (ii) estimation of gas hydrates saturation from acoustic impedance using rock physics model (Zhang et al., 2011).

Using the three phase model for hydrate bearing sediments, Zhang et al. (2011) have quantified gas hydrates in the eastern Green Canyon Area, Gulf of Mexico based on seismic inversion and rock physics transform. By using the cross plot of RAI and gas hydrates saturation in sand with 35-45% porosity and in clay with 35-45% porosity, they obtained similar relation except in case with high gas hydrates saturation.

Zhang et al. (2011) used the theoretical model of gas hydrates for isotropic formation. However, gas hydrates in KG basin have been found in vertical fracture in shale formation, which makes the medium anisotropic. To introduce the fracture induced anisotropy, Lee and Collett (2009) have used a two-step procedure and estimated the gas hydrates saturation at well location. Obtained saturation shows good agreement with saturation obtained from pressure core data at the site 10. We have normalized the AI value with AI of water bearing sediments we get the ratio of acoustic impedance at well site 10. We have used the cross plot of AI and gas hydrates saturation SH to establish a relation between saturation and RAI.

$$Sh = -0.15 * RAI^3 + 0.58 * RAI^2 - 0.27 * RAI - 0.049 \quad .5$$

Using this relation we have estimated gas hydrates saturation from acoustic impedance (AI) along the seismic line Fig. (3).

Results:

Acoustic impedance of seismic data provides useful information for the quantification of gas hydrates over a larger area with a constraint from well log data at one site. Acoustic impedance along a seismic line in KG basin was estimated using the pre-stack as well as post-stack inversions of seismic data. We have employed two different approaches to translate the seismically derived acoustic impedance to the saturation of gas hydrates. Using the resistivity method, we have transformed the acoustic impedance into the porosity from which we have estimated the saturation of gas hydrates using the modified Archie's law, valid for anisotropic media as has been used by Lee and Collett (2009) for the estimation of gas hydrates from sonic log data. The acoustic Impedance and rock physics transform involves a relation between the ratio of acoustic impedance and gas hydrates saturation that has been derived from the well log data by assuming fracture filling gas hydrates occurrence with fracture orientation of 900. Both the approaches yield consistent results with lateral variation of gas hydrates along the seismic line up to 25%. The results also match with the saturation measured from the pressure cores at the specified depths.

References:

Archie, G.E., 1942. The electrical resistivity log as an aid in determining some reservoir characteristics. Transactions of The American Institute of Mining, Metallurgical, and Petroleum Engineers 146, 54–62.

Avseth P., Mukerji T and G Mavko 2010, Quntitative Seismic Interpretation: Applying rock physics tools to reduce interpretation risk, Cambridge University Press.

Berkhout A. J. 1985, Seismic Migration: Imaging of Acoustic energy by wave field extrapolation A theoretical Aspect, 3rd edn. New York : Elsevier Science.

Fatti, J. L., Smith, G. C., Vail, P. J. Strauss, P. J. and P. R, Levitt, 1994, Detection of gas in sandstone reservoirs using AVO analysis: A 3-D Seismic case history using geostack technique. Geophysics, 59, 1362-1376.

Lee, M.W., Collett, T.S., 2009. Gas hydrate saturations estimated from fractured reservoir at Site NGHP-01-10, Krishna-Godavari Basin, India. Journal of Geophysical Research, 114, B07102, 1-13.,

Zhang, Z.J., Han, De-hua, Qiuliang, Y., 2011. Quantitative interpretation for gas hydrate accumulation in the eastern Green Canyon Area, Gulf of Mexico using seismic inversion and rock physics transform. Geophysics 76, 4, B139–B150.

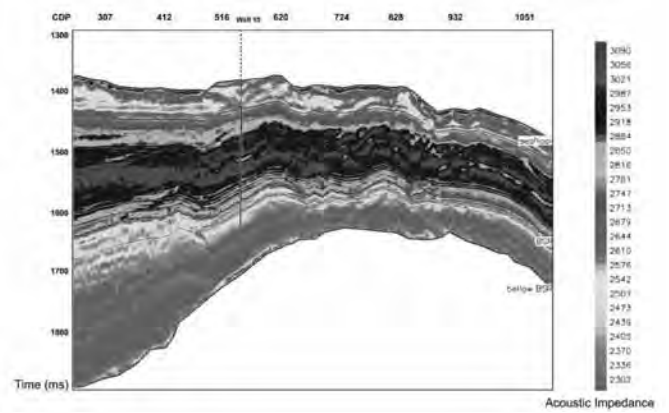

Fig. 1 Acoustic impedance (AI)

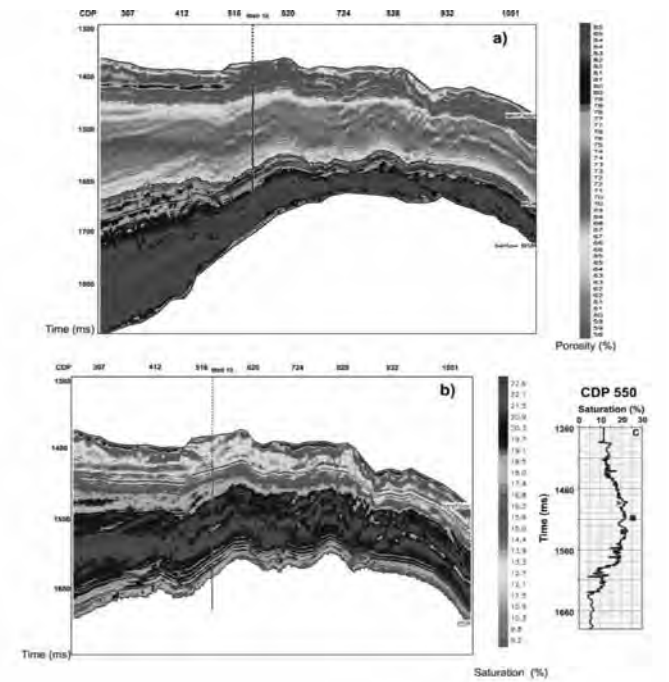

Fig. 2 Porosity and Saturation

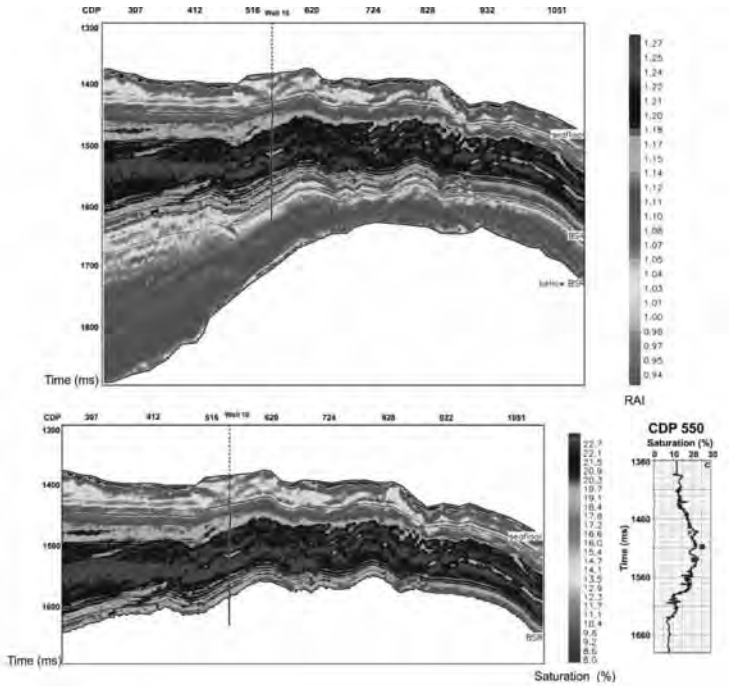

Fig. 3 Ratio of acoustic Impedance (RAI) and Saturation

A PICTURE OF ATTENUATION TOMOGRAPHY IN ALMOST CONTINUOUS FREQUENCY BAND OBTAINED FROM INVERSION OF STRONG MOTION DATA

Monu Tomer and A. Joshi
Department of Earth Sciences, IIT Roorkee, Roorkee
monutomer3@gmail.com

In thepresent work three dimensional frequency dependent S wave (Q_β) quality factor for central Honshu region of Japan has been estimated using the inversion of strong motion data. The inversion method was proposed by Hashida and Shimazaki (J Phys Earth. 32, 299–316, 1984) and has been used and further modified by Joshi (Curr Sci. 90, 581–585, 2006; Natural Hazards. 43, 129–146, 2007) and Joshi et al. (J. Seismol.14, 247–272, 2010).In this work this method has been further modified by incorporating the Kriging Interpolation technique to find the spectral acceleration values at points where data is not available. Grid size control in x and y directions are made available as a modification in this technique. The algorithm is now able to handle the data of any number of earthquakes. Further the technique has been modified to calculate the attenuation coefficients for different frequencies simultaneously. Depending upon the above modifications the results have been calculated for different grid sizes and at different frequencies. The results have been compared with the geological features of the study area which show good resolution and association with geologic features.

ANALYSIS OF SEISMIC NOISE PRECEDING KACHCHH, INDIA EARTHQUAKE OF 19 JUNE 2012 FOR ADVANCE WARNING – ENCOURAGING RESULTS

Indra N Gupta[1], David P. Schaff[2], Bal K Rastogi[3], P Mahesh[3] and Robert A Wagner[1]

[1]Array Information Technology, Greenbelt, Maryland, USA,
[2]Lamont-Doherty Earth Observatory, Columbia University, Palisades, New York, USA,
[3]Institute of Seismological Research, Gandhinagar, India

A significant fraction of the ambient short-period seismic noise at a given site may be attributed to P, S, Rayleigh and Love waves with spectral characteristics strongly dependent on the geological structure underlying the recording station. Unlike an underground nuclear explosion, a large earthquake is generally preceded by intense activity within the hypocentral region. This pre-earthquake activity canbe extremely complicated and may occur at several places at various depths mostly within the hypocentral region and may last over short and/or long periods of time. Thiscauses significant temporal variations in the geological environment and leads to significant variations in the spectral characteristics of ambient seismic noiseobserved at nearby recording stations.

The Kachchh, India Mw 5.1 Earthquake of 19 June 2012 was well recorded at several three-component broadband stations at various epicentral distances. Analysis of limited data from two stations has indicated two distinct premonitory variations in the low-frequency (less than 0.5 Hz) spectral characteristics of noise, initiating several days before the earthquake: (1) systematic shift of peak frequencies to lower values and (2) significant changes among the three components (vertical V, radial, R and transverse, T) of ground motion, evidenced by spectral ratios such as T/R. These results for premonitory variations in the composition of seismic noise are similar to those observed for several earthquakes in the United States. Although these preliminary results need to be confirmed by analyzing considerably more data from several additional recording stations, they appear to suggest an entirely new methodology for obtaining advance warning of a few days or more before a large earthquake.

NCAOR

The Indian gateway to polar regions

Maitri - Indian Research Base in Antarctica

National Centre for Antarctic and Ocean Research **(ESSO-NCAOR) - an autonomous R&D Institution under Ministry of Earth Sciences - is the nodal agency coordinating and implementing the Indian Polar (Arctic, Antarctic and Southern Ocean) Programs. It is the only institute in the country that has the capability to raise, archive & process ice cores from polar regions. India has successfully launched 33 scientific expeditions to Antarctica and 08 expeditions to Arctic and 07 to Southern Ocean till now. Apart from *Maitri* and Bharati in Antarctica, India has another research Base – *Himadri* – in the Arctic.**

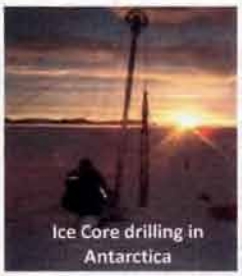

Ice Core drilling in Antarctica

Indian Team at South Pole

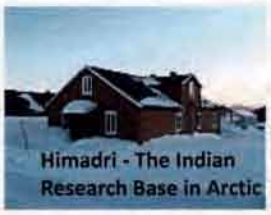

Himadri - The Indian Research Base in Arctic

Bharati –New Indian Research Base in Antarctica

Research

- Ice Core Studies
- Polar Limnology
- Remote Sensing
- Climate Change Studies
- Southern Ocean Processes
- Environmental Impact Assessment
- Microbial Biodiversity & Biogeochemistry
- Geoscientific studies of the EEZ
- Exploration for polymetallic hydrothermal sulphides
- Continental Shelf Mapping

Facilities

- National Antarctic Data Centre
- Earth Station - Satellite Link with *Maitri and Bhararti*
- Ice core processing and repository complex
- Digital repository for Antarctic publications
- State of the art laboratory and library facilities
- Oceanographic Research Vessel - *Sagar Kanya*

National Centre for Antarctic & Ocean Research
Earth System Science Organisation-(ESSO)
(Ministry of Earth Sciences)
Headland Sada, Vasco-da-Gama, Goa 403 804, India

ESSO

Phone: +91-(0) 832-2525600/601, Fax: +91-(0)832-2520877, info@ncaor.org , http://www.ncaor.gov.in